



**HAL**  
open science

# Reversal strategies within the lateral habenula to ameliorate depressive-like behaviors

Anna Tchenio

► **To cite this version:**

Anna Tchenio. Reversal strategies within the lateral habenula to ameliorate depressive-like behaviors. *Neurons and Cognition [q-bio.NC]*. Université Pierre et Marie Curie - Paris VI, 2017. English. NNT : 2017PA066301 . tel-01722820

**HAL Id: tel-01722820**

**<https://theses.hal.science/tel-01722820>**

Submitted on 5 Mar 2018

**HAL** is a multi-disciplinary open access archive for the deposit and dissemination of scientific research documents, whether they are published or not. The documents may come from teaching and research institutions in France or abroad, or from public or private research centers.

L'archive ouverte pluridisciplinaire **HAL**, est destinée au dépôt et à la diffusion de documents scientifiques de niveau recherche, publiés ou non, émanant des établissements d'enseignement et de recherche français ou étrangers, des laboratoires publics ou privés.

# Université Pierre et Marie Curie

Ecole doctorale n°138  
« Cerveau Cognition Comportement »

Doctoral thesis title:

## Reversal strategies within the lateral habenula to ameliorate depressive-like behaviors

Presented by Anna Tchenio  
Directed by Dr. Manuel Mameli

Team « Synapses and pathophysiology of reward »  
Institut du Fer à Moulin

Presented the 08th decembre, 2017

### Members of the jury:

Dr. Philippe Faure – président  
Pr. Paul Slesinger – rapporteur  
Pr. Stephan Lammel – rapporteur  
Dr. Alberto Bacci – examinateur  
Pr. Manuel Mameli – directeur de thèse



Except where otherwise noted, this work is licensed under  
<http://creativecommons.org/licenses/by-nc-nd/3.0/>

## Abstract

---

Prolonged exposure to aversive stimuli leads to cellular and circuit adaptations that contribute to the emergence of neuropsychiatric disorders such as depression. Interactions between the dopaminergic (DA) and the serotonergic (5HT) systems have been implicated in these pathological adaptations ultimately influencing motivated behaviors. Interestingly, the lateral habenula (LHb), an ethologically well-conserved epithalamic region, directly and indirectly controls DA and 5HT systems, and its activity is modulated by aversive events in both humans and animals. Moreover, the activity of the LHb increases in animal models of depression and depressed human patients. Conversely, strategies that locally target the LHb have been shown to reverse depressive-like symptoms both in animal models and in humans.

Altogether, this led to the hypothesis that LHb dysregulation could play a role in the emergence of depressive like symptoms. However, little is known about the early cellular and molecular adaptations that occur within the LHb after exposure to aversive events. Moreover, most of the animal models employed to interrogate the LHb role in depressive states used acute painful stimuli; whether LHb function becomes aberrant after chronic exposure to painless stressors remain elusive. In my thesis work, I explored the precise cellular and molecular adaptations of LHb neurons following exposure to different kind of unpredictable aversive experiences, and their importance for the expression of depressive like symptoms.

More precisely, I will present the results of an initial work aiming to identify early cellular and molecular adaptations within the LHb following unpredictable stimuli and their importance for the emergence of depressive symptoms. This study shows that unpredictable foot-shocks lead to decreased surface expression and function of the gamma-aminobutyrate receptor (GABA<sub>B</sub>R), a metabotropic receptor that hyperpolarizes LHb neurons through the activation of the G protein-coupled inwardly-rectifying potassium channels (GIRKs). This decrease of GABA<sub>B</sub>R-GIRK signaling went along with an upregulation of the activity of the protein phosphatase 2 (PP2A), which is a well-known down-regulator of GABA<sub>B</sub>-GIRK complex surface expression. GABA<sub>B</sub>R-GIRK signaling tightly controls LHb activity, and its downregulation consequently leads to aberrant hyperexcitability of LHb neurons. Using specific strategies to restore the GABA<sub>B</sub>R-GIRK signaling within the LHb, such as GIRK overexpression, or local pharmacological inhibition of PP2A activity, we were able to ameliorate depressive like states following unpredictable foot-shocks.

The second study allowed instead to establish the cellular adaptations within the LHb following a chronic non-painful aversive experience and during a critical developmental

period. I showed that exposure to maternal separation in childhood (MS mice) also leads to depressive like symptoms together with a hyperexcitability of LHb neurons. This stress-driven increase in LHb activity was causally linked to a decrease of the GABA<sub>B</sub>R-GIRK signaling. Moreover, using diverse reversal strategies such as chemogenetics or a therapeutically-relevant intervention such as Deep Brain Stimulation (DBS), we could selectively decrease LHb neuronal activity and consequently ameliorate the depressive like symptoms, suggesting a causal link between these two phenotypes.

Altogether, the work presented in this thesis suggests that LHb neuronal hyperexcitability could represent a common substrate necessary for the expression of certain aspects of the depressive like state and further supports its relevance as a potential target in the treatment of this disorder.



## Résumé

---

L'agression de l'organisme par un agent physique, psychique ou émotionnel déclenche une réponse physiologique et comportementale qui permet à un individu de se prévenir du danger et de maintenir sa survie. Le système nerveux central a depuis longtemps été identifié comme un majeur acteur de cette réponse adaptative. Cependant, une exposition prolongée au stress conduit à des adaptations cellulaires et des réadaptations de circuits neuronaux qui contribuent à l'émergence de troubles neuropsychiatriques. L'interaction entre le système dopaminergique (DA) et sérotoninergique (5HT) a été impliquées dans ces réarrangements physiologiques et pathologiques qui influencent les comportements motivationnels de l'individu face à une menace. Fait intéressant, l'habenula latérale (Hbl), une région du cerveau très conservée entre les espèces, contrôle directement et indirectement les systèmes DA et 5HT, et son activité est modulée par des stimuli aversifs chez les humains et les animaux. De plus, l'activité de la Hbl est augmentée chez des modèles animaux de la dépression ou lors de l'induction d'un épisode dépressif chez des patients humains. Inversement, l'emploi de stratégies ayant pour cible la Hbl permettent d'améliorer certains symptômes dépressifs à la fois chez les modèles animaux de dépression et chez l'homme. Ainsi, la dérégulation de l'Hbl pourrait jouer un rôle dans l'apparition de symptômes dépressifs. Cependant, les changements moléculaires et cellulaires précoces qui se produisent au niveau de Hbl suite à l'exposition continue à un environnement aversif restent peu connus. De plus, la plupart des modèles animaux utilisés pour interroger le rôle de Hbl dans l'état dépressif implique une exposition répétée de l'animal à des stimuli douloureux. Si la fonction de l'Hbl est aberrante lors d'une exposition chronique à d'autre type de stress reste méconnu. Dans mon travail de thèse, je me suis intéressée aux adaptations cellulaires et moléculaires au niveau des neurones Hbl suite à l'exposition de différents types d'expériences aversives et leurs relatives importances pour l'expression de symptômes dépressifs.

Plus précisément, je présente dans ce manuscrit, les résultats d'un premier travail qui vise à identifier les adaptations cellulaires et moléculaires de Hbl suite à l'exposition de souris à des chocs électriques et leurs rôles dans l'émergence de symptômes dépressifs. Cette étude montre que l'exposition à de brefs aléatoires chocs électriques entraîne une diminution de l'expression de surface de récepteur métabotropiques gamma-aminobutyrate B (GABA<sub>B</sub>Rs), et par conséquent une diminution de leur fonction au niveau des neurones de l'Hbl. GABA<sub>B</sub>R est un récepteur métabotrope couplé à la protéine Gi, il hyperpolarise les neurones de l'Hbl

par l'activation du canal potassique GIRK. La diminution de la signalisation GABA<sub>B</sub>R-GIRK est accompagnée par une augmentation de l'activité de la protéine phosphatase 2 (PP2A), reconnue pour induire l'endocytose du complexe GABA<sub>B</sub>R-GIRK. GABA<sub>B</sub>R-GIRK contrôle étroitement l'activité Hbl, et par conséquent une diminution de leurs fonctions conduit à l'hyperexcitabilité des neurones de l'Hbl. En adoptant des stratégies visant à restaurer spécifiquement la signalisation GABA<sub>B</sub>R-GIRK dans l'Hbl, telle que la surexpression GIRK, ou l'inhibition pharmacologique locale de l'activité PP2A, nous avons observé une amélioration de certains symptômes « dépressifs », établissant ainsi un lien causal entre l'aberrante diminution du signal GABA<sub>B</sub>R et certain aspect de l'état dépressifs.

La deuxième étude permet d'établir l'effet d'une expérience aversive chronique non douloureuse sur la fonction Hbl. Dans ce travail, la séparation de petits et de leur mères (souris MS) conduit à posteriori au développement de symptômes dépressifs accompagnés par une hyperexcitabilité des neurones de la Hbl. Cette augmentation d'activité est, au moins en partie, expliquée par une diminution de la signalisation GABA<sub>B</sub>R-GIRK. De plus, prenant avantage de la technologie chimio-génétique ou des récentes avancées en terme thérapeutique telle que la stimulation cérébrale profonde (DBS), j'ai été en mesure de réduire localement l'activité de l'Hbl des souris MS. D'autre part, l'utilisation de ces diverses stratégies étaient suffisante pour améliorer les symptômes dépressifs des souris MS, suggérant un lien de causalité entre ces deux phénotypes.

Dans l'ensemble, ces travaux suggèrent que l'hyperexcitabilité des neurones Hbl pourrait représenter un substrat commun nécessaire à l'expression de symptômes dépressifs et ainsi constituer une cible potentielle pour traiter certains aspects de la dépression.

## Acknowledgements

---

At the end of this research, I am convinced that the thesis is far from being a lonely work. Indeed, I could never have carried out this doctoral work without the support of several people whose generosity, good humor and interest in my research allowed me to progress and learned a lot throughout these 3 years.

In the first place, I am grateful to my thesis supervisor, Manuel Mamei, for the trust he has given me despite my limited knowledge in his field when I started. I would like to thank him by accepting to supervise this doctoral work, for its multiple advices and challenges that make me progress and advance, for all the hours he has devoted to directing this research. I would also like to tell him how much I appreciated his high availability not only by providing an indispensable support and good ideas in my research over almost 3 years, but also for all the hours devoted to re-reading this thesis, for his abundant advices and its emotionally support through the rough road to finish this thesis. Thank you for listening and understanding. As he could say, “work hard/play hard”, I thank him for the amazing energy and dynamism that he brings in the lab and the care that he has for his people. I greatly enjoy these 3 years in the team and dedicated to this work. Thank you for this great and memorable opportunity.

I want to thank also my friends and colleagues: Frank (the professor) which try to teach me Dutch proverbs although I must confess to have forgotten every word since... Kristina (the mum) which often made sure none of us starved, Salvatore (the sailor) which made sure none of us went thirsty (or sober) and Massimo (the “geek”) that kept us entertained with his huge repertoire of anecdotes and funny video. Guys, I could thank you in many way, you are amazing people, and it is a pleasure to work in a so crazy/funny lab... Among everything, thank you for all this discussions inside or outside the lab, around a barbecue or a glass of wine, for sharing with me your knowledge and experience, and your unlimited support in the good and bad moments, that pushed me and help me a lot during these years. Thanks also for all the nice moments spent together, celebrations, dinners, travelling and also to share the motivation to “try” to stay healthy (swimming/ running / badminton/ climbing and hiking)... not always simple...

I also like to thank all the Fer a moulin, starting by its director, Jean-Antoine Girault, that maintain a wonderful atmosphere in his department, full of conviviality, creativity and exchanges which create a perfect environment to growth as a young scientist. Of course, it will be nothing without all the people that composed it, so thank to all the “feramoulinos” people. A particular thank to Sana, Emily, Jessica, Ferran, Marie, Fanny, Benoit... among many others, that not only permit to have some nice constructive scientific discussions, but also with who I shared a lot of fun in gypsy concert, jazz swinging, driving bike in the middle of the night in Paris ....

I also would like to thank the help of Megan Creed for her tips for the DBS and the researchers of the IFM for their scientific advice and helpful discussions.

Finally, I would like to thank my family, for their love and unrestricted support, which have permit me to achieve this work. In particular, I would like to thank my mother Sylvie and my grandmother Jeanine, as well as my brothers and sister Jonathan, Gwenael, and Chloe (and also Aylan, Reda and Sophie) for their love and their skills to always find the good word (or smile for Aylan) to motivate and guide me. Last but not least, I would like to thank my father Paul, that transmit me his love for science, to always have trust in me, and always understanding the things that I said or not.

It is impossible to summarize what all these people have done for me and how much they contribute to this work, so THANK you.

# Contents

Abstract .....	1
Résumé .....	3
Aknowledgements .....	5
Contents.....	6
Table of figures .....	7
List of abbreviations .....	8
Introduction .....	10
Depression .....	11
I. A brief history of depression .....	11
II. Treatment of major depressive disorder .....	13
III. Studying depression in laboratory animals.....	15
A. Learned helplessness model .....	17
B. The chronic mild stress.....	18
C. Social defeat .....	19
D. Maternal separation .....	20
Neural circuits of depression .....	21
Emerging role of LHb in depression .....	23
I. Lateral habenula as a node to control midbrain regions .....	24
II. Lateral habenula function in processing negative information.....	26
III. Lateral habenula modifications in depression .....	28
GABA <sub>B</sub> receptors: master of the neuronal activity.....	30
I. GABA <sub>B</sub> receptor structure and function .....	30
II. GABA B receptors trafficking.....	32
III. GABA <sub>B</sub> receptor regulation.....	33
Methodological section .....	37
Experimental subjects and stress paradigms .....	37
Behavioral tests .....	38
Drug/intervention .....	39
Surgery .....	40
Electrophysiology.....	40
Analysis and drugs. ....	42
Context and objectives of the study I: GABA <sub>B</sub> receptors trigger LHb hyperactivity, an early marker of depressive like symptoms.....	43
Context and objectives of the study II: LHb hyperactivity as a long term adaptation underlying MS-driven depressive like symptoms.....	68
Discussion .....	90
I. Stress-driven mechanisms underlying GABA <sub>B</sub> receptor plasticity in the LHb.....	90

II. Induction mechanism of GABA <sub>B</sub> receptor plasticity following different kind of stress .....	93
III. Circuit specificity of GABA <sub>B</sub> receptor regulation in the LHb .....	95
IV. What is the functional relevance of GABA <sub>B</sub> receptor dependent hyperexcitability for the emergence of depressive like symptoms .....	96
V. Targeting LHb hyperexcitability to treat depression? .....	97
A. Caveat of DBS intervention: .....	97
B. PP2A inhibitors as potential antidepressant drugs .....	98
C. Consequences of LHb hyperexcitability on downstream circuitries .....	99
Conclusion.....	102
Publications and contributions .....	104
References .....	105

## Table of figures

Figure 1 Epidemiology of depression .....	12
Figure 2 Depression treatments .....	14
Figure 3 Rodent models of depression and behavioral assay to assess the depressive phenotype .....	16
Figure 4 Simplified schematic of neural circuits implicated in depression .....	22
Figure 5 Lateral habenula anatomy: a hub between forebrain structures and neuromodulatory nuclei .....	25
Figure 6: Lateral habenula encodes of aversive information and drive motivated behaviors .....	27
Figure 7 Cellular and molecular adaptations within the habenula in a rodent model of depressive-like states. ....	29
Figure 8 GABA <sub>B</sub> R subunits and functions.....	32
Figure 9 GABA <sub>B</sub> R regulations.....	35
Figure 10 Potential mechanisms underlying LHb GABA <sub>B</sub> R-GIRK reduction in rodent model of depression.....	94

## List of abbreviations

---

<b>5HT</b>	5-hydroxytryptamine
<b>AMPAR</b>	$\alpha$ -amino-3-hydroxy-5methyl-4-isoxazolepropionic acid receptor
<b>AMPK</b>	adenosine monophosphate-activated protein kinase
<b>Ca<sup>2+</sup></b>	calcium ion
<b>(<math>\beta</math>)CaMKII</b>	(beta)-calcium calmoduline-dependent protein kinase type II
<b>ChR2</b>	channel rhodopsin 2
<b>CMS</b>	chronic mild stress
<b>DA</b>	dopamine
<b>DBS</b>	deep brain stimulation
<b>DREADD</b>	designer Receptor Exclusively Activated by Designer Drugs
<b>DSM</b>	Diagnostic and statistical manual of mental disorders
<b>ECT</b>	electroconvulsive treatment
<b>EPN</b>	entopeduncular nucleus
<b>FS</b>	foot-shock
<b>FST</b>	forced swim test
<b>GABA</b>	gamma-aminobutyric acid
<b>GABAA R</b>	gamma aminobutyric acid type A receptor
<b>GABAB R</b>	gamma aminobutyric acid type B receptor
<b>GABAB<sub>1a,b/2</sub></b>	gamma aminobutyric acid type B receptor subunit 1a,1b,or 2
<b>GIRK</b>	G-protein inwardly-rectifying potassium channel
<b>GIRK1-4</b>	G-protein inwardly-rectifying potassium channel subunit 1 to 4
<b>GluA1-4</b>	glutamate AMPA receptor subunits type 1-4
<b>GPCR</b>	G-protein coupled receptor
<b>GRIN-lenses</b>	Graded-Index lenses
<b>HPA</b>	Hypothalamic–pituitary–adrenal
<b>I-baclofen</b>	current evoked by baclofen application
<b>KCTD</b>	potassium channel tetradimerization Domain containing proteins
<b>KO</b>	knock-out
<b>LDT</b>	laterodorsal tegmentum
<b>LH</b>	lateral hypothalamus
<b>LHb</b>	lateral habenula

<b>LHp/(cLHp)</b>	learned helplessness / (congenital learned helplessness)
<b>LTD</b>	long term depression
<b>LTP</b>	long term potentiation
<b>MAOI</b>	monoamine oxidase inhibitor
<b>MS</b>	maternal separation
<b>MHb</b>	medial habenula
<b>mPFC</b>	medial prefrontal cortex
<b>NA</b>	noradrenaline
<b>NAc</b>	nucleus accumbens
<b>NDRI</b>	noradrenaline and dopamine reuptake inhibitors
<b>NRI</b>	noradrenaline reuptake inhibitors
<b>NSF</b>	N-ethylmaleimide-sensitive fusion
<b>NMDA</b>	N-methyl-D-aspartic acid
<b>PFC</b>	prefrontal cortex
<b>PKA</b>	protein kinase A
<b>PKC</b>	protein kinase C
<b>PP1</b>	protein phosphatase type 1
<b>PP2A</b>	protein phosphatase type 2
<b>RMTg</b>	rostromedial tegmental nucleus
<b>RGS</b>	regulator of G protein signaling
<b>S</b>	serine residue
<b>SD</b>	social defeat
<b>SNX 27</b>	Sorting nexin 27
<b>SSRI</b>	serotonin reuptake inhibitors
<b>TCA</b>	tricyclic antidepressant
<b>TST</b>	tail suspension test
<b>VGCC</b>	voltage-gated calcium channel
<b>VP</b>	ventral pallidum
<b>VP<sub>pv</sub></b>	parvalbumin- neurons in the ventral pallidum

## Introduction

---

Physiological and behavioral adaptations of an individual facing a real or potential threat are required for the well-being or the survival. This highly adaptive response depends on the orchestration of several neuronal circuits ultimately allowing to assign specific negative valence to an event and subsequently guide optimal behaviors such as avoidance. Monoaminergic systems have been implicated in this immediate encoding of aversive event. Indeed both serotonergic (5HT) neurons of the raphe and dopaminergic (DA) neurons of the ventral tegmental area (VTA) have been described to physically respond to acute aversive stimuli and influence negative reinforcement or avoidance learning both in human and animal studies (Brischoux et al., 2009; Cohen et al., 2015; Crockett et al., 2009; Deakin and Graeff, 1991; Hayes et al., 2014; Matsumoto and Hikosaka, 2009a; McCutcheon et al., 2012; Puglisi-Allegra and Andolina, 2015; Schweimer and Ungless, 2010; Ungless et al., 2010). In contrast, exposure to severe or chronic aversive stimuli, particularly when coupled with a lack of predictability or lack of control (Maier and Seligman, 1976; Short and Maier, 1993), elicits detrimental, long-lasting effects on brain function, that could precipitate the emergence of neuropsychiatric disorders, including mood disorders (Anisman and Matheson, 2005; Kessler, 1997; de Kloet et al., 2005). Mood disorders are associated with deficits in both rewarding and punishment encoding, leading to the assumption that dysfunction in neural circuits including the DA and 5HT systems may underlie depressive-like symptoms (Nestler and Carlezon Jr, 2006; Owens and Nemeroff, 1994; Russo and Nestler, 2013). However, although the role of DA and 5HT in depression have received particular attention, these systems are interconnected and tightly controlled by a much broader circuit (Ogawa et al., 2014; Pollak Dorocic et al., 2014). Considering that persistent negative events have deleterious effect in both DA and 5HT system (Owens and Nemeroff, 1994; Russo and Nestler, 2013) it is likely that dysregulation of common upstream structures may be critical for the development of neuropsychiatric disorders. I therefore became interested in studying the potential modifications within neuronal circuits that directly control monoaminergic nuclei.

The lateral habenula (LHb) is an epithalamic region that directly and indirectly controls DA and 5HT neurons (Lammel et al., 2012; Pollak Dorocic et al., 2014; Stamatakis and Stuber, 2012; Weissbourd et al., 2014). Interestingly, a clinical study reported the potential therapeutic benefit of deep brain stimulation (DBS) in the LHb for the treatment of depression in a single case in human (Sartorius et al., 2010). This work was one of the first of a long series of studies supporting the hypothesis of the potential role of LHb in depression (Lecca et



al., 2014; Li et al., 2011, 2013; Seo et al., 2017; Shabel et al., 2014). Despite this growing body of evidence, whether LHb dysfunction can be a common substrate underlying specific aspects of depressive-like state independently of the events that trigger it remains unknown.

In my thesis work, I will first introduce the complexity of the depressive disorder, then I will briefly summarize key pathological reorganization of the mesolimbic system in depressive-like state to give a general context of how aversive and reward-related circuits can underlie certain aspect of this disease. Next, I will present how LHb can control the mesolimbic system and I will discuss the current literature around the cellular properties - from the GABA<sub>B</sub>R to the hyperactivity - of the LHb, which can be instrumental for the expression of depressive like symptoms.

## Depression

### I. A brief history of depression

Historical documents throughout the ages point to the long-standing existence of depression as a health problem for human beings. Already in the ancient Greeks, the Hippocrates school described the “Melancholia”, a condition associated with “aversion to food, despondency, sleeplessness, irritability, restlessness”. Although they believed that an excess of black bile in the spleen caused depression, the similarities between the Greek descriptions of depression and those of the modern age are striking. The following centuries led to a dark period of obscurantism where notably the religions refuted the natural cause of mental illness and associated it to witchcraft or demonic possession. Indeed, it was not until the XIXth century, that mental illness was reevaluated and successively considered to have psychological and social causes or to be an inherited disease. The industrial revolution notably led to the building of psychiatric institution, and the brain became the focus of efforts to understand the pathophysiology of this disorder. The Second World War marked a turning point, where the mental illness started to be considered as a real problem of society. Along with the evolution of the psychiatry, the discovery of the first antidepressants greatly ameliorated the condition of the depressed patients. Moreover, a new manual categorizing the various mental problems were established in the United States, the Diagnostic and statistical manual of mental disorders (DSM) (Frader, 1987).

In a new version of this manual, the major depressive episode is characterized by a persistent, unreactive low mood and a loss of interest in pleasure. These symptoms are associated with a range of other symptoms such as significant weight loss, insomnia or hypersomnia,

psychomotor agitation or retardation, fatigue or loss of energy, feelings of worthlessness or excessive or inappropriate guilt, diminished ability to think or concentrate, or indecisiveness, as well as recurrent thoughts of death or suicide (Diagnostic and statistical manual of mental disorder, 5th edition). However, depression is recognized to be a highly heterogeneous disease, with the presence of variable set of symptoms across individuals. Due to this complexity, clinicians and scientists are still trying to discriminate and study specific aspects of the disease, ranging from anhedonia, behavioral despair, and social withdrawal to learning deficits. This different endophenotypes point out to the diversity of functional alterations: the anhedonia, is a dysfunction in reward encoding, which leads to the loss of motivation for natural rewards such as food or sex. Alternatively, behavioral distress or hopelessness imply impairments in aversive-stimuli encoding, leading to the inability to cope with a negative situation. This diversity of symptoms suggests that discrete neural circuits could be implicated in different aspects of the disease.

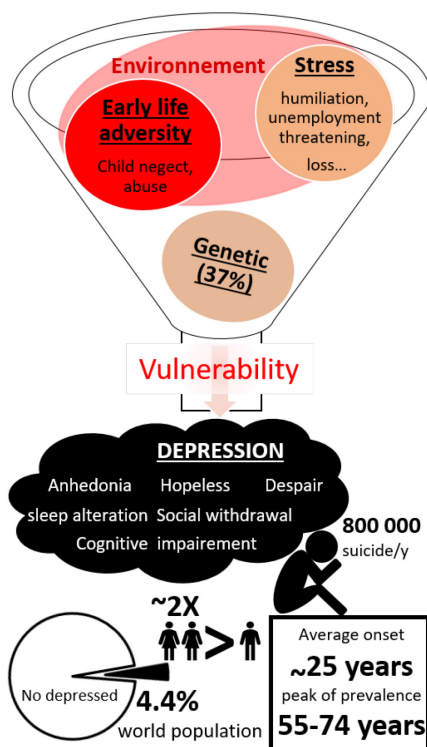


Figure 1. *Epidemiology of depression*

A large part of high individual vulnerability can be explained by interactions between genetic predisposition which has been estimated at 37% (Sullivan et al., 2000), and environmental factors (Anisman and Matheson, 2005; Kendler et al., 1999; Kessler, 1997). Epidemiologic studies provide evidence that early life adversity increases the risk to develop depression (Agid et al., 1999; Norman et al., 2012) as well as stress in adulthood. Indeed, major adverse life events such as humiliation, threatening or loss (Farmer and McGuffin, 2003; Paykel, 2003; Slavich et al., 2010) as well as accumulation of chronic stressful events (Brown and Harris, 1978; Hammen et al., 2009) precipitate depression.

Depression is among the most important cause of disability according to a report of the WHO (2017), it is a complex disorder characterized by a diversity of symptoms that can be categorized in “endophenotype” such as anhedonia, behavioral despair, hopelessness, sleep disturbance, social withdrawal and cognitive impairment. In its most severe conditions depression can lead to suicide. It affects around 4.4 % of the global population and it is twice more common in females than males. The prevalence globally increases with the age and the average age onset is the middle of 20s’ years old with a peak of prevalence at 55-74 years old.

Considering the heterogeneity of etiology and symptoms, a general therapeutic treatment taking into account all the variables is difficult to achieve.

In the next chapter, I will summarize the currently available treatments and their limitations as well as newly emerged interventions offering potential promising improvements for treatment.

## II. Treatment of major depressive disorder

Antidepressant treatment emerged by serendipity in 1950 with the finding that the antitubercular agent iproniazid (a monoamine oxidase inhibitor (MAOI)) and that the imipramine (tricyclic antidepressant (TCA)) arising from antihistamine research were very efficient in relieving depressive symptoms (Kuhn, 1957; Loomer et al., 1957). MAOIs inhibit the breakdown of 5HT, noradrenaline (NA), and DA thus increasing the availability of these neurotransmitters. TCAs increase the synaptic concentration of 5HT and NA by inhibiting their reuptake. These discoveries were concomitant with the finding that reserpine (that irreversibly blocks the vesicular monoamine transporter (VMAT)) induces depressive-like symptoms (Muller et al., 1955). Overall, these data led to the monoaminergic theory of depression, suggesting that an imbalance, mainly in 5HT, NA and DA neurotransmission, is at the core of the pathophysiology of depression (Bunney and Davis, 1965; Delgado, 2000; Hirschfeld, 2000; Schildkraut, 1965).

This theory led to the development of new several classes of antidepressants with similar way of action, aiming to correct the monoaminergic deficiency. Among them the selective serotonin, noradrenaline, and/or dopamine reuptake inhibitors, such as citalopram or fluoxetine (SSRI; NRI; NDRI) that are still nowadays the most prescribed antidepressants (O'Leary et al., 2014, 2015). Modern antidepressant molecules differ from the older drugs as they aim to reduce their deleterious side effects and narrow the neurochemical targets. However, even if their tolerance has improved, little ameliorations have been reported in terms of the slow onset of clinical effect or their efficacy (Baghai et al., 2011; Holtzheimer and Mayberg, 2011a). Indeed, standard treatment still presents a high percentage of pharmacological resistance ( $\pm 30\%$ ) or relapse ( $\pm 50\%$ ) (Al-Harbi, 2012; Holtzheimer and Mayberg, 2011a; Trivedi et al., 2006). Furthermore, the mechanism of action of such molecules on brain wiring, neuronal activity or plasticity remains still elusive. Thus, the monoaminergic theory appears to be too restrictive, and it looks obvious that the therapeutic effects of antidepressants cannot be solely explained by the facilitation of 5HT and NA neurotransmission (Hindmarch, 2002; Massart et al., 2012).

Other alternative strategies of the drug treatments have been developed, and are prescribed notably in treatment resistant patients such as the electroconvulsive therapy (ECT). This procedure showed a remission of 75% in resistant depression with the advantage of its immediate effect (Sienaert, 2011). However, the action of ECT is broad, its mechanism is poorly understood, and it presents side effects such as confusion and memory loss (Bolwig,

2011; Ingram et al., 2008). Alternatively, DBS of the prefrontal cortex (PFC) (Mayberg et al., 2005), Nucleus Accumbens (NAc) (Bewernick et al., 2010; Schlaepfer et al., 2007) or more recently LHb (Sartorius et al., 2010) also have reported amelioration in groups of treatment resistant depressed patients. All these structures were primarily selected based on neuroimaging studies showing their aberrant activities in depressed patients and/or their important role in reward circuits correlated with anhedonia (one of the prominent symptoms of depression) (Delaloye and Holtzheimer, 2014). Despite their promising therapeutic interest, these studies remain still preliminary. Indeed, the way of action of the DBS is nowadays still enigmatic. The observation that DBS and lesions could have similar behavioral effect led to the theory that DBS inhibits neuronal activity. However, mixed pattern of neuronal excitation and inhibition have been described following DBS in certain brain regions and also raise the question of a local effect (Maks et al., 2009; McIntyre et al., 2004; Vitek, 2002). Further studies, looking at the effects of DBS in particular brain regions are thus warranted to refine and better understand this intervention.

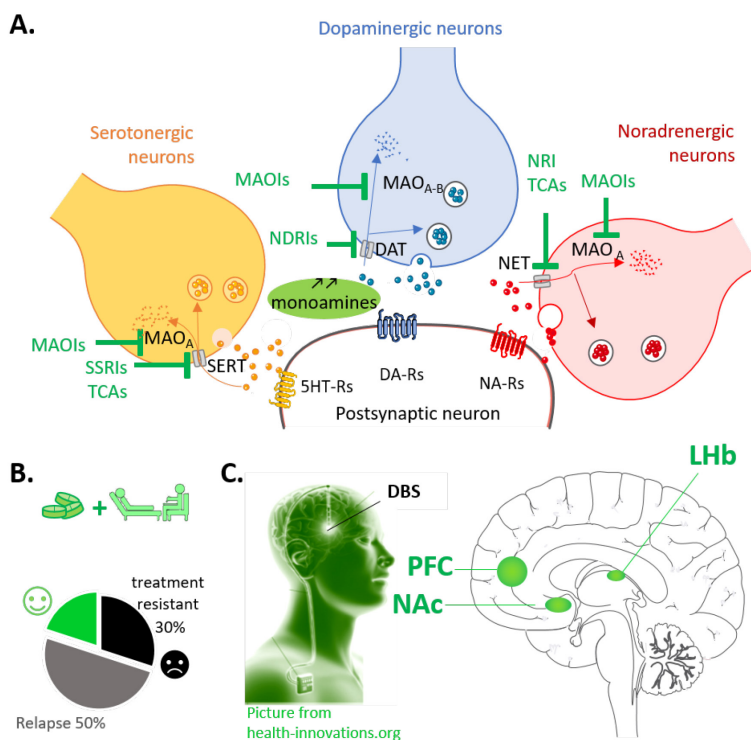


Figure 2. Depression treatments

**A. Main action of pharmacological therapies:** Antidepressants aim to restore "imbalanced" brain chemistry. They boost monoaminergic neurotransmitters by blocking their reuptake (tricyclic antidepressants -TCAs-, Selective serotonin reuptake inhibitors -SSRIs-, Norepinephrine–dopamine reuptake inhibitors -NDRI-, Norepinephrine reuptake inhibitors -NRI-) or by preventing their metabolism (monoaminoxidase inhibitors (MAOIs).

**B. Current treatments** consist of psychological treatments (such as psychotherapy) and/or antidepressant medication (such as selective serotonin reuptake inhibitors [SSRIs] and tricyclic antidepressants [TCAs]). However 30% of patients exhibit treatment-resistant, and less than the half shows remission.

**C. Deep Brain Stimulation (DBS) as alternative strategy to treat depression.** DBS is a promising alternative intervention in the case of treatment-resistant depression. This approach involving the bilateral placement of electrodes at specific neuroanatomical sites. The prefrontal cortex (PFC), the Nucleus accumbens (NAc) and the lateral habenula (LHb), are nowadays the target of clinical trials. These regions have been selected based on previous neuroimaging studies that report their aberrant metabolic activity as well as loss of brain volume in treatment resistant patients.

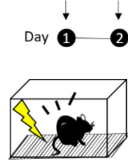
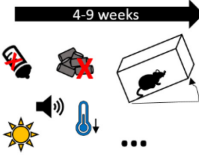
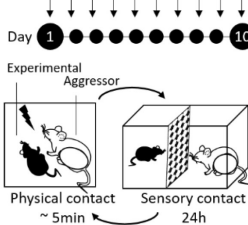

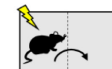




Overall major depression affects more than 300 million people according to a recent report by the World Health Organisation, (*WHO 2017-GENEVA*). It is a leading cause of disability worldwide, with a total annual cost estimated at 118 billion euro in Europe (Sobocki et al., 2006), and 210 \$-billion per year in US (Greenberg et al., 2015). Given the public health

significance of this pathology, novel treatments are needed. Indeed, current available treatments fail to provide significant improvement nearly half of the time (Al-Harbi, 2012; Holtzheimer and Mayberg, 2011a; Trivedi et al., 2006). One explanation is still the lack of understanding of the specific brain circuits and molecular changes underlying depressive symptoms. The focus on particular symptoms and novel treatment interventions is a necessary step to permit a better understanding of the neurobiology of the illness and achieve larger improvements.

### III. Studying depression in laboratory animals

Using brain imaging approaches and neuroendocrine responses in humans provided valuable information about the brain circuitry implicated in mood disorders. Nevertheless, the detailed investigation of physiological responses and molecular modifications in the human brain are limited by obvious practical and ethical difficulties. To circumvent these limitations, animal models have emerged as an alternative and valuable tool to understand the pathophysiology of depression. Three sets of criteria have been proposed for assessing animal models of human mental disorders: construct validity, face validity, and predictive validity (Nestler and Hyman, 2010; Willner, 1984). Construct validity refers to the relevance of the mechanism in which the model is based. So far, no genetic strong determinants were found for depression (Dunn et al., 2015) limiting genetic model in replicating multifaceted phenotype and strong pharmacology validity. Hence, the main animal models of depression are based on the epidemiological evidence that severe or chronic stress and adverse psychosocial experience often precede the depressive episode. The face validity corresponds to whether the model resembles depression in respect to the presence of ethological similarities and biomarkers. Even if symptoms such as guilt, suicidality, and sad mood are typical human features, other endophenotypes can be reproduced and measured in laboratory animals. These include notably the helplessness (referring to hopelessness in human), anhedonia, social withdrawal and behavioral despair, respectively indicated by the increased failure and latency in the shuttle box test, decrease in sucrose preference and social interaction, and increased immobility in forced swim test or tail suspension test (see Fig. 3). Finally, the predictive validity is when the animal model exhibits symptoms' amelioration with pharmacological and non-pharmacological treatments for depression. Here, I will give examples of different models currently used in the literature:

## Models of depression

	Learned helplessness	Chronic mild stress	Social defeat	Maternal separation
	 <p>Day 1 → Day 2</p> <p>Repetitive uncontrollable shocks</p>	 <p>4-9 weeks</p> <p>Several hours random stressors</p>	 <p>Day 1 → ... → Day 10</p> <p>Experimental Aggressor</p> <p>Physical contact ~ 5min</p> <p>Sensory contact 24h</p>	 <p>24h OR 1-2 weeks</p> <p>Several hours/days the first 2 weeks after birth</p>
Behavioral Tests				
 <p>Shuttle box test</p>	<p>* <i>Adrien et al., 1991; Sherman et al., 1982; Vollmayr and Henn, 2001; Chourbaji et al., 2005; Song et al., 2006; Winter et al., 2011; Li et al., 2011; Li et al., 2013</i></p>			<p><i>Lukkes et al., 2017</i></p>
 <p>Sucrose preference</p>	<p>under operant condition or after challenged with footshock</p> <p><i>Vollmayr et al., 2004; Enkel et al., 2010; Christianson et al., 2008</i></p>	<p>* <i>Tye et al., 2013; Willner et al., 1987; Grønli et al., 2004; Strekalova et al., 2004; Grønli et al., 2005; Garcia et al., 2009; Bessa et al., 2013; Lim et al., 2015; Erburu et al., 2015; Venzala et al., 2013</i></p>	<p><i>Krishnan et al., 2007; Covington et al., 2010; Chaudhury et al., 2013; Friedman et al., 2014</i></p>	<p><i>Franklin et al., 2011; Gracia-Rubio et al., 2016; Aisa et al., 2007</i></p>
 <p>Tail suspension test</p>		<p><i>Tye et al., 2013</i></p>	<p><i>Krishnan et al., 2007</i></p>	<p><i>Gracia-Rubio et al., 2016</i></p>
 <p>Force swim test</p>	<p><i>Li et al., 2011; Li et al., 2013</i></p>	<p><i>Strekalova et al., 2004; Chang and Grace, 2014; Bessa et al., 2013; Lim et al., 2015</i></p>	<p><i>Kudryavtseva et al., 1991; Friedman et al., 2014</i></p>	<p><i>Franklin et al., 2011; Lajud et al., 2012; Llorente et al., 2007; Lee et al., 2007; Aisa et al., 2007; MacQueen et al., 2003; Couto et al., 2012</i></p>
 <p>Social interaction</p>	<p><i>Christianson et al., 2008; Short and Maier, 1993</i></p>	<p><i>Erburu et al., 2015</i></p>	<p>* <i>Berton et al., 2006; Krishnan et al., 2007; Covington et al., 2010; Cao et al., 2010; Chaudhury et al., 2013; Friedman et al., 2014; Christoffel et al., 2011; Tanaka et al., 2012; Venzala et al., 2013</i></p>	

Behavioral impairments described by the literature for the each model

\* Current test to screen depressive like phenotype in the model

**Figure 3: Rodent models of depression and behavioral assay to assess the depressive phenotype**

Schematic representing the main models of depression describe in this thesis, and their associate phenotype.

Different assays used to assess the depressive phenotype are listed below:

**Shuttle box test:** The subjects are place in a box with 2 compartments. The test consists of several trials where mice are exposed to escapable foot-shocks, as soon as they escape in the opposite compartment the shock stop. If the animal is not escaping after a pre-determined period, it is considered as failure. Latency to escape and number of failures are the two parameters measure in this paradigm. This test is routinely used to screen learned helplessness vulnerable mice (Chourbaji et al., 2005; Vollmayr and Henn, 2001)

**The tail-suspension test (TST)** (Steru et al., 1985) and **the forced-swim test (FST)**, (Porsolt et al., 1977): Rodents are exposed to an acute, unescapable, short-duration stress: suspend by the tail or placed in an transparent tank filled with water respectively. Time spent performing active "escaping"-behavior (struggling/swimming) is quantified relative to time spent immobile. Higher immobility has been interpreted as a sign of behavioral despair or passivity. Although this interpretation can be debated (Nestler and Hyman, 2010), these tests have the advantage to permit a rapid, easy screening of potential antidepressant drugs, or depressive-like behavior in rodent (O'Leary and Cryan, 2013).

**The sucrose preference test** is one of the most common test to assess anhedonia. This test evaluated in a two-bottle choice paradigm the consumption of a sucrose solution in respect to the water consumption. Decreased consumption of sucrose is assumed to be indicative of a reduction in the motivation for the rewarding solution. This sucrose preference is attenuated by a diversity of chronic stressors, notably the chronic mild and unpredictable stress and it is commonly accepted to reflect anhedonia (Willner et al., 1987).

**Social interaction/avoidance test:** This test consists to place an unfamiliar congener (usually juvenile) in the home cage of the experimental subject or in a neutral environment. Social exploration is measured by the time spent around the congener as well as the amount and duration of "social" behaviors (e.g. sniffing, following, grooming, biting, mounting, wrestling...). Social interaction has been described to be rewarding (Krach et al., 2010; Trezza et al., 2011) and is affected in model of mood disorder notably in the social defeat model (Krishnan et al., 2007).



### ***A. Learned helplessness model***

First described by Seligman (1967), the learned helplessness model (LHp), is based on the idea that a repetition of uncontrollable/inescapable negative experience leads to “helplessness” where the individual would not avoid future escapable adverse situations (they give up because they learned that it is useless to avoid). This phenotype has also been reported in human, and it is considered as a marker of depression (Abramson et al., 1978; Maier and Seligman, 1976). The LHp paradigm in rodents (rats and mice) consists of two “training” sessions where subjects are exposed to repetitive uncontrollable and unpredictable stress, such as foot-shocks, followed by a testing day, where the animals are exposed to escapable stressors. About 20% of the rodents become helpless and subsequently fail to escape, as demonstrated by an increasing number of failure and latency to escape in the shuttle box test (see Fig. 3). This phenotype persists for approximately ten days (Chourbaji et al., 2005; Vollmayr and Henn, 2001). Because the percentage of helpless animals is quite low, and the vulnerability to helplessness is highly heritable, breeding of rats presenting helplessness has been done. This congenital learned helplessness (cLHp) rats are more vulnerable and show a deficit in coping strategy without the training phase (Henn and Vollmayr, 2005). Aside the deficit in coping strategy, the learned helpless animals share several characteristics with depressed humans. Indeed, this model presents decreased food consumption and loss of weight (Dess et al., 1988; Weiss, 1968). Different studies also reported an “anhedonia-like” phenotype with a decreased motivation for various kinds of rewards such as sucrose (Enkel et al., 2010; Vollmayr et al., 2004), reduced libido ((Henn and Vollmayr, 2005), reduced social interaction (Christianson et al., 2008; Short and Maier, 1993), or reduced intracranial self-stimulation of brain regions associated with reward such as the NAc or medial forebrain bundle (Zacharko et al., 1983). Furthermore, other aspects of depressive states have also been described such as behavioral despair (Li et al., 2011, 2013), disrupted sleep (Adrien et al., 1991), cognitive impairments, such as spatial learning deficits (Song et al., 2006) as well as biological markers of depression such as altered hypothalamic–pituitary–adrenal (HPA) axis (Greenberg et al., 1989). Depression-like syndrome induced by acute or cLHp can be reduced by pharmacological or non-pharmacological treatment. Indeed, treatment with imipramine has been reported to ameliorate coping strategies in shuttle box and to reduce behavioral despair in the forced swim test (FST) (Chourbaji et al., 2005; Li et al., 2013). Marked reversal of LHp phenotype was also described after ECT (Sherman et al., 1982). Finally, DBS within the LHb, decreases both immobility time in the FST and failure rate in the shuttle box (Li et al., 2011).

Overall, the LHp presents in some measures a good construct and face validity. However one of its weaknesses is that it shows short-lasting depressive phenotype and a fast action to antidepressants which does not reflect the clinical effect of these agents (Pfau and Russo, 2014).

### ***B. The chronic mild stress***

The chronic mild stress (CMS) aims to mimic human everyday life stressors of different nature that have been reported to be a factor of vulnerability for depression. Based on previous work by Katz and colleagues (Katz, 1982), Willner developed the CMS model which consists of exposing rodents (mice or rat) for several hours to different kind of micro-stressors, schedule in relatively unpredictable sequence for several weeks. The mild stressors include short periods of food/ water deprivation, small temperature reductions, change of cage mates, cage tilt, overnight illumination, intermittent white noise among other similar but unpredictable manipulations. One of the core symptoms of this model is the anhedonia, illustrated by the gradual decrease in sucrose preference (or intake) over the stress exposure (Willner, 2017; Willner et al., 1987), but also by the increased threshold current required to support intracranial self-stimulation in VTA (Moreau, 2002). In addition to the decrease in reward responsiveness, the CMS also presents deficits in other motivated behaviors such as social interactions (Erburu et al., 2015), aggressive behavior (Strekalova et al., 2004) or sexual behavior (Grønli et al., 2005) as well as behavioral despair as suggested by the decreased performance in the tail-suspension test (TST) or the FST (Chang and Grace, 2014; Lim et al., 2015; Strekalova et al., 2004; Tye et al., 2013; Venzala et al., 2013). Moreover, studies have also reported other behavioral similarities with depression such as sleep disturbances, with an increase in REM sleep and decreased waking (Grønli et al., 2004), increased anxiety in the elevated plus maze (Erburu et al., 2015; Grønli et al., 2004) and cognitive impairment such as new object recognition or spatial learning deficits (Erburu et al., 2015; Song et al., 2006; Venzala et al., 2013). Concerning its predictive validity, the CMS model responds to chronic, but not acute, administration of a wide range of established antidepressant drugs (Garcia et al., 2009; Willner, 2017; Willner et al., 1987). In addition to this, alternative strategies such as ECT (Moreau, 2002) or DBS (Lim et al., 2015) have also demonstrated its efficiency to ameliorate the depressive like symptoms triggered by CMS. To summarize, the CMS model present excellent face validity and predictive validity since it induces the emergence of a wide range of depressive-like symptoms, which can be reversed by chronic antidepressant treatment or alternative strategies. However, the model has two



significant drawbacks: 1) CMS rodents spend a long part of their lifespan under physical stress somehow not reflecting the true nature of stress exposure in human. 2) CMS experiments are labor intensive and demand space that can be sometimes difficult to carry out and can trigger environmental or experimental bias.

### ***C. Social defeat***

Considering that stress stimuli in humans leading to a psychopathological state are often of social nature, animal models based on social-stress, such as social defeat (SD) present in some measures good construct validity. The SD model consists of introducing an experimental male rodent in the home cage of an aggressive, dominant male usually of bigger size and belonging to a strain with a relatively higher level of aggression. The intruders are rapidly attacked and defeated by the residents, assuming a submissive posture. After this brief physical experience (several minutes), residents and intruders are usually separated by a plastic divider with holes, which allows sensory contacts for the remainder of the 24-h period. Each day, defeated rodents are exposed to a different resident aggressor, and the procedure usually lasts around ten days (Kudryavtseva et al., 1991). Following repeated defeat, subjects exhibit social avoidance behaviors when subsequently exposed to an unfamiliar mouse that persist even 4 weeks after the last exposure (“susceptible” mice) (Berton et al., 2006). Importantly to note, this long-term effect of SD effect are observed only in single housed but not in socially housed animals (Von Frijtag et al., 2000). Around 40% of the defeated mice never developed the behavioral symptoms (“resilient” mice) and which gives the advantages to study the mechanism behind the resilience to chronic stress (Friedman et al., 2014). Moreover, SD induces several other behavioral changes compared to the control, such as increased anxiety in the open field or on the elevated plus-maze (Krishnan et al., 2007; Kudryavtseva et al., 1991; Venzala et al., 2013). This paradigm also triggers a transient decrease in body weight (Krishnan et al., 2007; Venzala et al., 2013) and reduced preference for sucrose solution (Chaudhury et al., 2013; Covington et al., 2010; Friedman et al., 2014; Krishnan et al., 2007). A study from Friedman and co-workers, also reported behavioral despair in susceptible mice assessed in the FST (Friedman et al., 2014), although no such behavior has been observed in other studies (Krishnan et al., 2007; Venzala et al., 2013). Depressive phenotypes are rescued only after chronic, but not acute, administration of antidepressants, and not after non-specific antidepressant treatment such as benzodiazepine providing predictive validity (Berton et al., 2006; Cao et al., 2010; Kudryavtseva et al., 1991). One concern is that only male rodents can be used for model, since female rats or mice do not

fight each other in a resident–intruder confrontation. Yet, epidemiologic studies report a higher incidence of depression in woman (Ferrari et al., 2013).

#### ***D. Maternal separation***

A wide range of studies point out the importance of early-life stress in shaping adult behavior (Kendler et al., 2002; de Kloet et al., 2005). The maternal separation (MS), is one of the most used early-life stressors to model depression and child neglect (Vetulani, 2013). The paradigm consists of separating the pups from both their mother and littermates and temporarily housing them in a new environment during the first two weeks of postnatal life. Two experimental protocols are usually employed: a prolonged 24h of maternal deprivation or periodic briefer periods of maternal separations (3-8h for 1-2 weeks). The separation duration, frequency, and its time windows vary among the studies and can be crucial for the behavioral outcomes. The consequences of MS on the stress axis have been extensively studied, revealing that profound disruption of the natural patterning dam-offspring interaction induced a persistent hyper-responsiveness of the HPA axis. (for review (Heim et al., 2008; Holmes et al., 2005; de Kloet et al., 2005)). Accordingly, studies reported that MS rodents present an increased basal plasma corticosterone levels as well as an increase of CRF mRNA in paraventricular nucleus as well as an excessive increase of adrenocorticotrophic hormone and corticosterone plasma level in responses to an acute stressor (Aisa et al., 2007; Lajud et al., 2012). In parallel to this pathophysiological effect, MS induces anxiety phenotype (Franklin et al., 2010; Lee et al., 2007) and a depressive-like profile including anhedonia (Aisa et al., 2007; Franklin et al., 2010; Gracia-Rubio et al., 2016), helplessness (Lukkes et al., 2017) and behavioral despair (Aisa et al., 2007; Couto et al., 2012; Franklin et al., 2010; Gracia-Rubio et al., 2016; Lajud et al., 2012; Lee et al., 2007; MacQueen et al., 2003) as well as memory impairment (Aisa et al., 2007; Couto et al., 2012; Llorente et al., 2011). Chronic antidepressant treatment can ameliorate the adaptations triggered by MS (Couto et al., 2012; MacQueen et al., 2003) which confirms the predictive validity. Overall, MS is a model with a good face, predictive and strong construct validity, and have the advantage to look at psychosocial stress effect in both male and female individuals. However, such paradigm did not take into account subtle environmental influences, and genetic predispositions and the high variability in the separation protocols used have led to some discrepancies in the behavioral outcomes particularly in the observation of anxiety behaviors (Tractenberg et al., 2016). Despite this, some MS paradigms seem to trigger a robust vulnerability to develop some core symptoms of

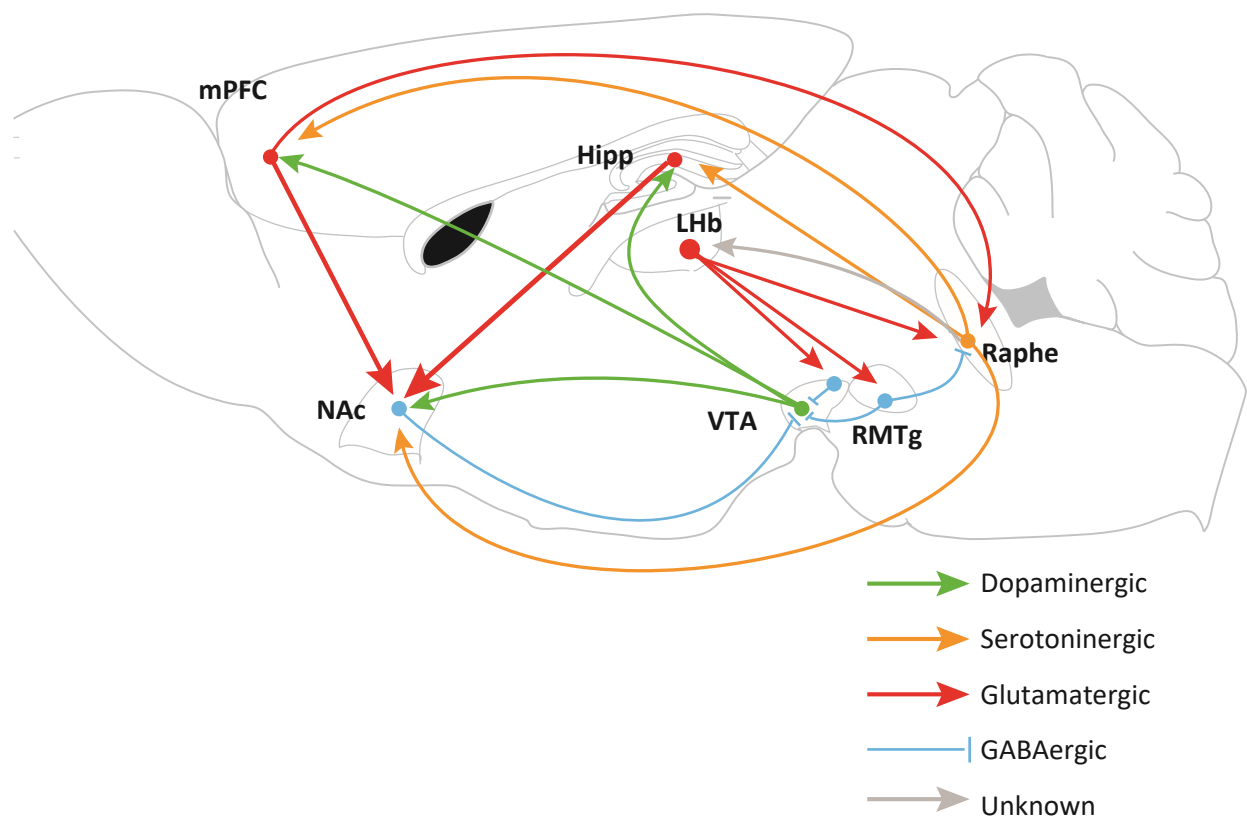
depression, which validated this model to study particular aspects of the pathophysiology of depressive symptoms (Vetulani, 2013).

Taken together, these studies show that different models induce distinct subsets of depressive phenotypes (see Fig.3) that are also heterogeneous in human (Anisman and Matheson, 2005; Monteggia et al., 2014; Nestler and Hyman, 2010). Aside from the inherent limitations in translating human affective disorders into relevant modeling in rodents, the diverse array of useful animal models with their relative strengths can be combined with the recent advances in technologies permitting precise circuit identification and manipulation to expand our understanding of mechanisms underlying depression.

## Neural circuits of depression

The neuronal circuits underlying precise depressive symptoms are complex, and there is not a good association between aberrant function of defined circuits and their behavioral relevance. However, research in the field starts to unravel particular brain structures or circuits that could be implicated in discrete symptoms of depression.

Initial studies firstly focused onto regions that are affected by stress due to its relevance in the etiology of depression (Chattarji et al., 2015; de Kloet et al., 2005). Accordingly, a large body of work centered their attention particularly in hippocampus and PFC. These two regions reported abnormal activity as well as morphological changes in human patients (Chattarji et al., 2015; Fales et al., 2008; Manji et al., 2001; Mayberg et al., 2005) and in animal models (Chattarji et al., 2015; Covington et al., 2010; Kim and Diamond, 2002; Venzala et al., 2013). Moreover, optogenetic manipulation of PFC (Covington et al., 2010; Warden et al., 2012) and hippocampal regions (Ramirez et al., 2015) have been shown to produce an antidepressant effect in rodents. Notably, the hippocampus is mainly recognized for its role in memory formation (Kim and Diamond, 2002) while the PFC is mainly implicated in executive function (Dalley et al., 2004), both aspects being altered in depression (Beck, 2008; Elliott et al., 1996; Marvel and Paradiso, 2004; Wang et al., 2008). However, even if the hippocampus and PFC are likely to be involved in certain aspects of depression such as impaired cognitive function, it is unlikely that these regions account for all symptoms of the disorder (Nestler et al., 2002). As described in previous paragraphs, most depressed patients exhibit a reduced ability to experience pleasure (anhedonia) and a loss of motivation. This led to a growing amount of research (including this thesis work) to investigate the role of reward and motivational circuits in depression.



**Figure 4 Simplified schematic of neural circuits implicated in depression.**

Based on the action of antidepressant and chronic stress effects on the brain, different structures have been implicated in depression such as serotonin nuclei in the raphe, the hippocampus and mPFC and have been the object of considerable amount work (Chattarji et al., 2015; De Deurwaerdère et al., 2017; Duman and Monteggia, 2006; McEwen et al., 2016; Metzger et al., 2017; Owens and Nemeroff, 1994; Turner et al., 2006). However, considering the complexity and the array of symptoms described in this disease it is unlikely that these structures encompassed all aspect of depressive states. Based on the fact that the loss of motivation is a major symptom of depression, researchers get interest to the role of reward/motivational circuits in mood disorders, comprising the VTA and its projection to the NAc (Russo and Nestler, 2013) as well as its direct and indirect input from the LHb and through the RMTg (Aizawa et al., 2013; Lecca et al., 2014; Proulx et al., 2014). Of course, all these various brain areas cannot be considered as distinct, since they are establishing highly overlapping and interacting circuits. (Picture modified from Russo and Nestler, 2013).

DA neurons in the ventral tegmental area (VTA) and its projections to the NAc have a central role in the motivational circuit. Using single unit recording in monkey, Schultz and colleagues, have described that VTA DA neurons respond to unpredicted rewards (Schultz, 2007; Schultz et al., 1997). This leads to DA release in the NAc necessary for the rewarding properties and motivation aspect of natural stimuli such as food and sex (Di Chiara et al., 1999; Schultz, 2007; Wise, 2004). Conversely, aversive and stressful stimuli have been described to inhibit DA neurons phasically (Ungless et al., 2004). Thus, this VTA–NAc circuit is crucial for the recognition of salient stimuli in the environment and for initiating adequate behavioral response that aimed at acquiring rewards and avoiding punishment.

One possible explanation for the information-processing biases characterizing depression (anhedonia or behavior despair) is that hypofunction of this VTA-NAc circuit would lead to the decrease of rewarding experiences and the exaggerated responses to aversive events. Consistent with this idea, human study, documented abnormal functioning of the VTA-NAc in depression, as a reduced activation of the NAc in response to rewarding stimuli (Pizzagalli, 2014). Interestingly, *in vivo* recordings in VTA DA cells in rodents reported altered burst activity (Friedman et al., 2008; Tye et al., 2013) and decreased spontaneously active neurons (Chang and Grace, 2014). Moreover, bidirectional opto-manipulations of DA cells in behaving animal gives further support for the causal link between depressive states and the modulation of mesolimbic DA system. Indeed, inhibition of VTA neurons transiently induced depressive symptoms in naive mice. Conversely, acute phasic bursting stimulation of DA neurons transiently reverse depressive phenotype of CMS mice at the level of the control (Tye et al., 2013). Although, circuit-specific alterations have not been established, local infusion of DA receptors antagonists in the NAc were able to prevent the restorative effect of the stimulation suggesting that VTA neurons projecting to the NAc seem partly involved.

Altogether, these data suggest that alteration of mesolimbic system have a crucial role in depression. Although, the hypodopaminergic hypothesis is nowadays debated (Cao et al., 2010; Chaudhury et al., 2013; Friedman et al., 2014; Krishnan et al., 2007), there is large agreement regarding the fact that alterations in the mesolimbic system represent a specific substrate for discrete depressive symptoms (Cao et al., 2010; Chang and Grace, 2014; Chaudhury et al., 2013; Friedman et al., 2008, 2014; Krishnan et al., 2007; Tye et al., 2013).

Given this fact, the research field started investigating the role of brain structures located upstream the DA system and capable to directly and indirectly influence its activity. In this context, particular attention was focused on the LHb, an epithalamic region that strongly modulates DA neuron activity (Christoph et al., 1986; Lammel et al., 2012, 2014; Proulx et al., 2014; Stamatakis and Stuber, 2012).

## Emerging role of LHb in depression

The habenula is an epithalamic region that is highly phylogenetically conserved (Bianco and Wilson, 2009). It is located close to the midline surrounded by the thalamus and the third ventricle and can be divided in two different main subnuclei, the medial habenula (MHb) and the LHb. These subregions present anatomical and morphological differences and differ in their connectivity (Aizawa et al., 2011; Andres et al., 1999).

Functional and anatomical studies provide evidence that the LHb is mainly composed of long-range projecting glutamatergic neurons (Aizawa et al., 2012; Lammel et al., 2012; Li et al., 2011; Pollak Dorocic et al., 2014; Weiss and Veh, 2011). Although a small population of GABAergic neurons has been also described in the medial part, their functional connectivity is still unspecified (Smith et al., 1987; Zhang et al., 2016b).

The focus of the present thesis in the LHb is primarily due to the growing amount of evidence highlighting its central role in the motivational system and consequently its potential implication in the etiology of mood disorders. Here, I will first provide a brief introduction on how LHb controls midbrain circuits, and its particular role in aversion encoding. Then, I will summarize the current literature supporting the evidence that LHb is hyperactive in depression.

### **I. Lateral habenula as a node to control midbrain regions**

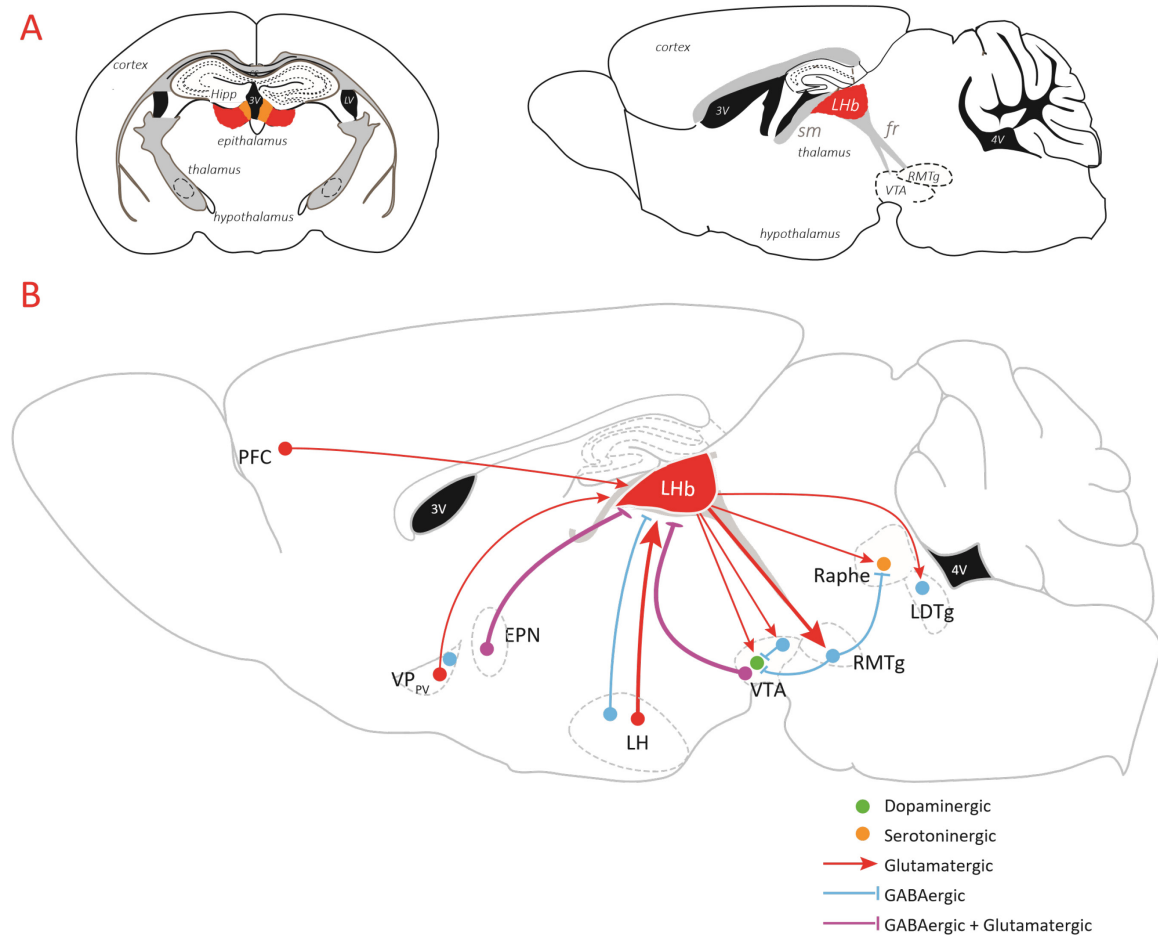
The LHb is a hub connecting forebrain regions and monoaminergic systems in the midbrain. It mainly receives information from the stria medullaris and projects input through the fasciculus retroflexus.

The main functionally identified outputs from the LHb are the rostromedial tegmental nucleus (RMTg), (Stamatakis and Stuber, 2012) the DA neurons of VTA (Lammel et al., 2012) as well as the 5HT nuclei of raphe (Pollak Dorocic et al., 2014) and the Laterodorsal tegmentum (LDT) ; (Yang et al., 2016)).

Using single-unit recording techniques in anesthetized rats, stimulation of the LHb was described to powerfully suppress both the activity of DA neurons in the substantia nigra and VTA (Christoph et al., 1986; Ji and Shepard, 2007). Conversely, pharmacological inhibition of LHb neurons, in behaving animals transiently increased DA release in the NAc, dorsolateral striatum, and to a lower extent in the PFC suggesting that LHb exerts a tonic inhibitory control over the function of DA neurons (Lecourtier et al., 2008). Considering that LHb is mainly glutamatergic, these studies indicate the presence of an inhibitory relay. In line with this hypothesis, tracing experiments reveal the existence of a GABAergic nuclei, caudal to the VTA, the RMTg, which receives a strong input from the LHb (Jhou et al., 2009a; Kaufling et al., 2009). The RMTg projects mainly to the VTA DA cells (Balcita-Pedicino et al., 2011) exerting a strong inhibition onto this neuronal subpopulation (Lecca et al., 2011). Consistently, an optogenetic study suggests opto-stimulation of LHb ChR2-expressing efferent fibers in the midbrain evokes excitatory postsynaptic currents almost exclusively onto GABAergic neurons, rather than DA VTA neurons (Stamatakis and Stuber, 2012).

Nevertheless, direct functional glutamatergic connection between the LHb and a subpopulation of DA VTA neurons that specifically project to the medial prefrontal cortex (mPFC) has also been described (Lammel et al., 2012).

Altogether, these data suggest that LHb exerts a strong inhibitory control of the mesolimbic system implying a fundamental contribution of this structure in encoding motivational states.



**Figure 5: Lateral habenula anatomy: a hub between forebrain structures and neuromodulatory nuclei.**

**A.** Coronal (left) and sagittal (right) section representing the habenula, epithalamic region that can be subdivided into two different nuclei the medial habenula (in orange, MHb) and the lateral habenula (in red, LHb). This complex, located beneath the hippocampus (Hipp), close to the third ventricle (3V) receives input via the stria medullaris (sm) and in turn, sends efferents to the midbrain through the fasciculus retroflexus (fr).

**B.** Optogenetic studies reported that lateral habenula receives glutamatergic input from the prefrontal cortex (PFC), the lateral hypothalamus (LH) and the parvalbumin neurons from the ventral pallidum (VP<sub>PV</sub>) and mixed GABAergic/Glutamatergic input from the entopeduncular nucleus (EPN) and the ventral tegmental area (VTA). Nevertheless, GABAergic current from VP<sub>PV</sub> and the LH have also been described.

In turn, LHb mainly contains long-range projecting glutamatergic neurons. It sends output in the midbrain controlling directly the monoaminergic nuclei (DA of the VTA and 5-HT neurons of the dorsal raphe) and indirectly through the activation of GABAergic relays (RMTg or GABAergic interneurons). Moreover, LHb has also been described to control GABAergic neurons in the LDT.



## II. Lateral habenula function in processing negative information

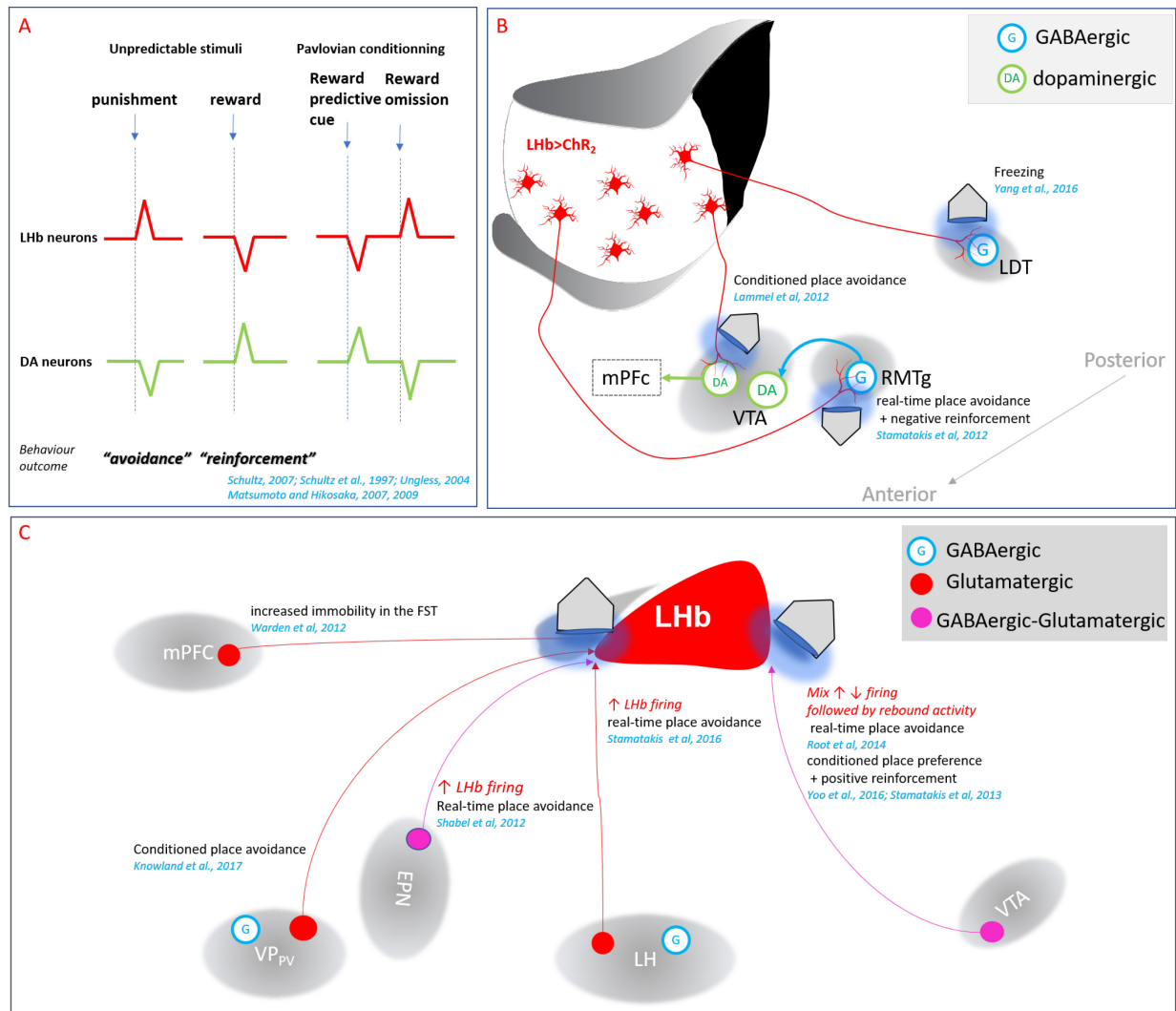
Seminal study of Hikosaka and colleagues, reported that LHB neurons in monkey, are excited by aversive stimuli such as an air puff and inhibited by unpredictable reward. Moreover, after pavlovian conditioning, the absence of reward after a conditioned cue also activates the LHB neurons. Instead during cue-shock associations, LHB is activated both to the cue and to the shock (Matsumoto and Hikosaka, 2009b). Altogether, this suggests a role of LHB in encoding aversive states and negative-reward prediction error. Importantly these responses mirror the responses of the DA neurons and the activation of the LHB precedes the DA inhibition (Matsumoto and Hikosaka, 2007, 2009; Schultz et al., 1997). Altogether these data suggest a role of LHB in conveying negative information signaling to the DA cells of the VTA, potentially via RMTg, which has in turn described to be phasically activated by aversive stimuli and inhibited by reward-related cues (Hong et al., 2011; Zhou et al., 2009b).

Consistently, optogenetic activation of the LHB fibers in the RMTg has been reported to drive real-time aversion in the place preference paradigm as well as decreased motivation for reward (Stamatakis and Stuber, 2012). Although LHB neuron projections to RMTg seem to be an important pathway to drive aversion, alternative pathway rising from LHB neurons are also able to encode negative state. Indeed, direct projections from the LHB to VTA DA neurons that in turn send axons to the mPFC have also been described to drive aversion (Lammel et al., 2012) as well LHB projections to the LDT (Yang et al., 2016).

Optogenetic studies also provided a mean to decipher the respective role of discrete inputs onto the LHB in negative states. Indeed opto-activation of glutamatergic fibers in the LHB from the entopeduncular nucleus (EPN), the lateral hypothalamus, the VTA and the ventral pallidum (VP) drive aversion or avoidance (Knowland et al., 2017; Lammel et al., 2015; Root et al., 2014a; Shabel et al., 2012; Stamatakis et al., 2016). Moreover, optogenetic stimulation of the glutamatergic pyramidal cells mPFC terminals in the LHB increases immobility in the FST (Warden et al., 2012).

Altogether, these studies, mainly taking advantage of optogenetic strategies, provide a strong evidence that LHB is a crucial node processing aversive information consequently highlighting its importance for the expression of negative state. Considering the prevalence of negative states in depression (such as anhedonia, behavioral despair and hopelessness) it is not surprising that the field has started investigating the aberrant functions of the LHB in the context of depressive states.





**Figure 6: Lateral habenula encodes of aversive information and drive motivated behaviors**

**A.** Simplify schematic of response to reward and punishment. Subpopulation of the ventral tegmental area (VTA) dopamine (DA) neurons are excited by unpredictable reward and cue predicted reward and inhibit by reward omission. Inversely, lateral habenula (Lhb) neurons show mirror-inverted phasic responses to DA neurons, excited by unpredicted aversive stimuli, inhibit by reward and potentially providing a source of negative reward prediction error signal.

**B.** Optogenetic studies role of Lhb output in encoding aversive stimuli. Chr2-driven stimulation of Lhb terminals within the RMTg, indirectly inhibits dopaminergic VTA neurons and induces real-time and conditioned place avoidance, negatively reinforces behavior. Moreover, other pathways have also been identified to encode aversive behavior: subpopulation of VTA-projecting Lhb neurons target directly dopamine neurons, this neurons project in turn mainly to the PFC. Opto-stimulation of Lhb neurons projecting to the VTA DA induces conditioned place avoidance. LDT projecting Lhb neurons have also been described to target interneurons and stimulation of this pathway induce freezing behavior.

### III. Lateral habenula modifications in depression

Human studies provide evidences that aberrant volume of the LHb is correlated with the severity of the major depressive disorders (Carceller-Sindreu et al., 2015; Johnston et al., 2015; Ranft et al., 2010; Schmidt et al., 2017). These morphological changes are supported by functional alteration of LHb in depressed patients. Indeed, a positron emission tomography study reported increased metabolic activity of LHb in patients experiencing transient depression upon tryptophan depletion (Morris et al., 1999). Consistently, animal studies also reported an increase of the LHb metabolism in rodent models of depression together with a decreased metabolic activity of the VTA (Caldecott-Hazard et al., 1988; Mirrione et al., 2014; Shumake et al., 2003). Overall, all these studies point out that the LHb is hyperactive in depression. In fact, dampening LHb activity via local DBS was sufficient to ameliorate depressive states both in animal studies and in human depressed patients (Kiening and Sartorius, 2013; Li et al., 2011; Lim et al., 2015; Sartorius et al., 2010).

Electrophysiological studies give further support to an increased activity of LHb neurons in rodent models of depression allowing a better understanding of the underlying mechanisms. Indeed, *in vitro* studies reported increased spontaneous firing activity and altered burst (Li et al., 2011; Seo et al., 2017). Neuronal activity is controlled by both excitatory/inhibitory balance as well as intrinsic neuronal properties. Several mechanisms underlying this neuronal hyperactivity have been proposed, all converging toward an increased excitatory drive and a decreased inhibitory control of a subset of LHb neurons (Namboodiri et al., 2016; Proulx et al., 2014).

Indeed, a specific LHb population projecting to the VTA was described to have a presynaptic potentiation of glutamatergic transmission in the LHp rats model of depression (Li et al., 2011). Using the same model, proteomic analysis of the LHb neurons reported an increased level of the  $\beta$ - calcium calmoduline-dependent protein kinase type II ( $\beta$ CaMKII) that resulted to be instrumental both for the increased glutamatergic transmission and the expression of depressive-like states (Li et al., 2013). Instead, LHb neurons in LHp rats showed decreased GABA/AMPA ratio from the EPN due to a reduced GABAergic drive, restored by antidepressant treatment (Shabel et al., 2014).

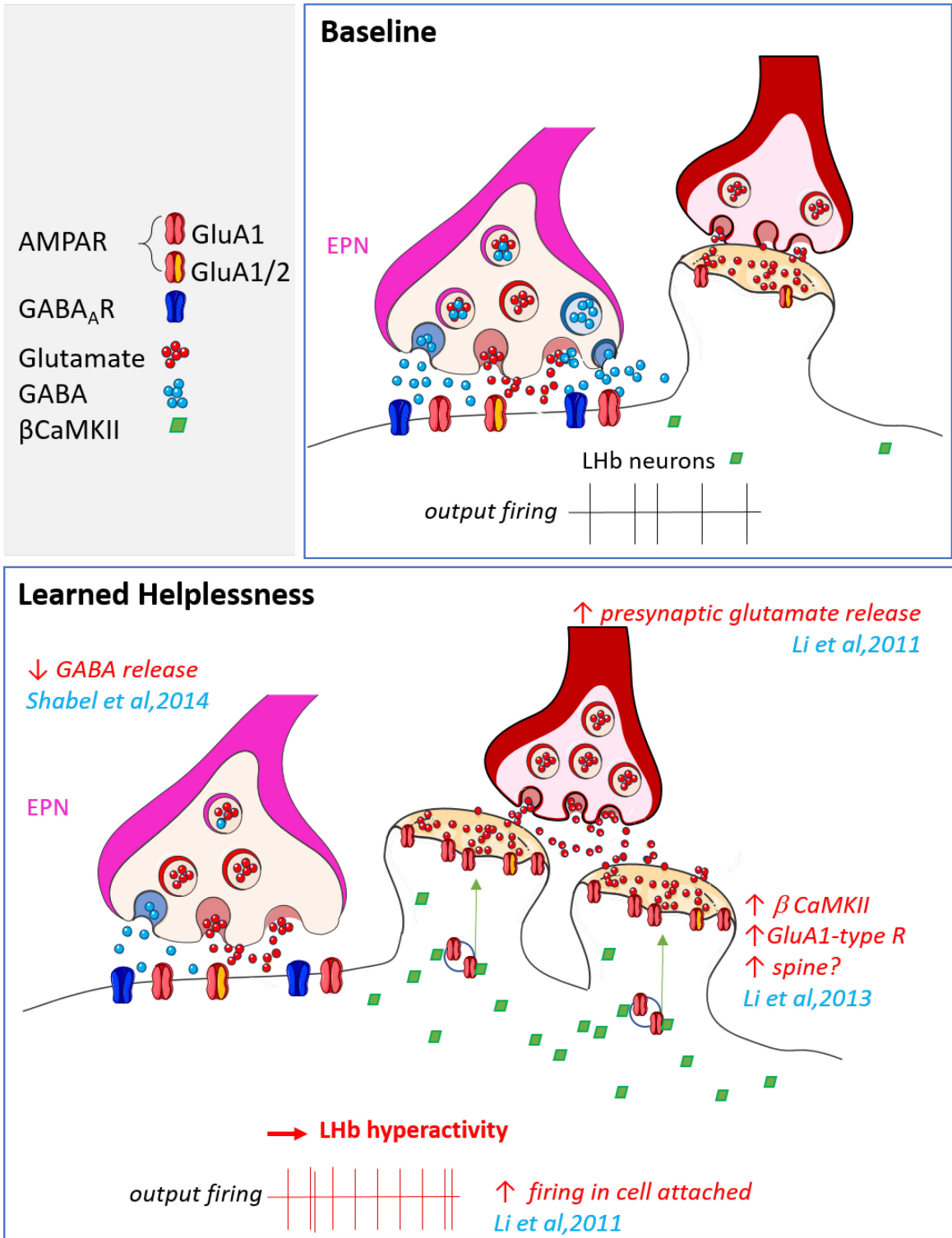


Figure 7: Cellular and molecular adaptations within the habenula in a rodent model of depressive-like states.

Increased level of the  $\beta$ -CaMKII in Lhb neurons has been described in the learned helplessness model potentially increasing the number of spines and driving the GluA1-type receptors in the synapse, resulting in a strengthening of the AMPAR-transmission. Moreover, parallel mechanisms have also been described in particular Lhb neurons sub-populations. Indeed, studies reported an increased presynaptic excitatory drive in Lhb neurons projecting to the ventral tegmental area (VTA) and a decrease of GABA release from the EPN terminal onto Lhb neurons. All these mechanisms induce an imbalance in excitatory/inhibitory fast transmission triggering Lhb neurons hyperactivity and underlying the depressive like symptoms. (Adapted from Lecca et al., 2014).

To conclude, several lines of evidence point out toward an increased excitability of LHb as a base for the expression of specific depressive like symptoms. However, several points remain elusive. For instance, given that previous studies mainly focused on a single animal model of depression (mostly LHp), whether LHb hyperactivity is a common feature of depression independently of its etiology has still to be proven. Moreover, the early changes following a traumatic event able to induce long-term cellular and behavioral adaptations within the LHb remain poorly investigated.

The sets of data presented in this thesis touch upon these exact distinct aspects. Differently from the findings I have described above, during my thesis I have highlighted the GABA<sub>B</sub>-R and its effector the G-protein inwardly-rectifying potassium (GIRK) channel as important players for the control of the LHb neuronal activity in both physiological and pathological conditions. In the next paragraph, I will present the structure, the different signaling pathways and their functions, as well as the trafficking and plasticity of the GABA<sub>B</sub>-Rs.

## GABA<sub>B</sub> receptors: master of the neuronal activity

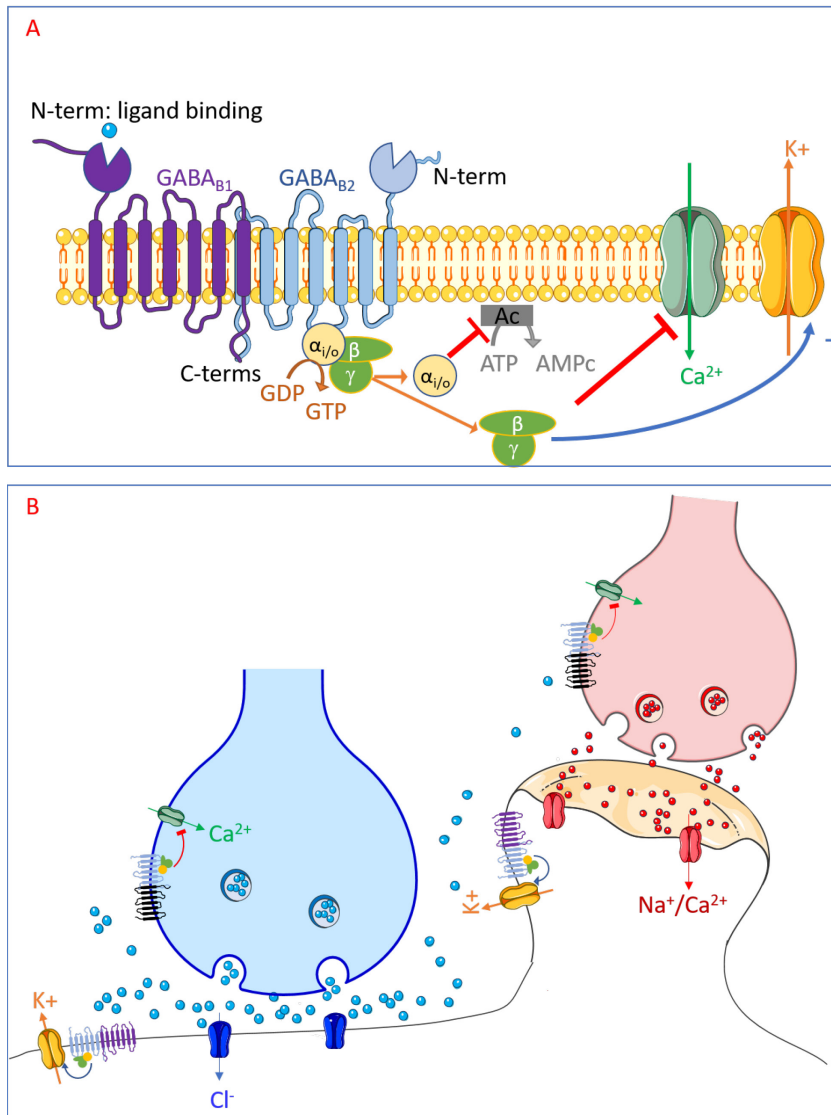
### I. GABA<sub>B</sub> receptor structure and function

GABA is the major inhibitory neurotransmitter in the central nervous system (CNS) playing a key role in modulating neuronal activity. GABA mediates its action via distinct receptors, the ionotropic gamma aminobutyric acid type A receptor (GABA<sub>A</sub>) and the metabotropic gamma aminobutyric acid type B receptor (GABA<sub>B</sub>R), the latter mediating the so-called slow inhibition. The GABA<sub>B</sub>R was originally defined based on pharmacological responses to GABA and specific agonists, including baclofen (Bowery et al., 1981; Hill and Bowery, 1981). It mediates slow inhibitory neurotransmission in the central nervous system. In general, electrophysiological activation of GABA<sub>B</sub>Rs requires strong stimulus intensities capable to trigger GABA spillover consistent with an extrasynaptic location of GABA<sub>B</sub>Rs (Scanziani, 2000).

The GABA<sub>B</sub>R is a 7-transmembrane domain protein that couples the Gi protein (Kaupmann et al., 1997). When GABA binds to GABA<sub>B</sub>R, it activates the *ai/o*-type G proteins, which inhibit adenylyl cyclase via G $\alpha$ i/o reducing the protein kinase A (PKA) activity, and inhibits gate ion channels via G $\beta$  $\gamma$  subunits activation (Bettler et al., 2004; Chalifoux and Carter, 2011; Couve et al., 2000). GABA<sub>B</sub>Rs are formed by the association of two different subunits: GABA<sub>B1</sub> and GABA<sub>B2</sub> both required for the formation of a functional receptor (Jones et al., 1998; Kaupmann et al., 1997; Kuner et al., 1999; White et al., 1998). Indeed, GABA<sub>B1</sub>

contains the agonist binding site (Galvez et al., 1999; Malitschek et al., 1999) while GABA<sub>B2</sub> provides the domain that links the G-coupled protein and is needed for signaling (Robbins et al., 2001). Moreover, the GABA<sub>B1</sub> subunit shows two possible splice variants: the GABA<sub>B1a</sub> and the GABA<sub>B1b</sub> (Kaupmann et al., 1997). The GABA<sub>B1a</sub> is mainly identified in presynaptic sites, while the GABA<sub>B1b</sub> shows a postsynaptic expression (Biermann et al., 2010; Billinton et al., 1999; Pinard et al., 2010). Nevertheless, GABA<sub>B(1b,2)</sub> is also described as autoreceptor in GABAergic terminal (Ulrich et al., 2007; Vigot et al., 2006). Importantly, the localization of the receptor is also indicative of the transduction signaling. In fact, the presynaptic GABA<sub>B</sub>Rs usually inhibit the voltage-gated calcium channels (VGCC), decreasing the synaptic release of neurotransmitter (notably glutamate and GABA release) (Guettg et al., 2009; Shaban et al., 2006; Ulrich et al., 2007; Vigot et al., 2006). Instead, the postsynaptically located GABA<sub>B</sub>Rs via the  $\beta\gamma$  subunit activation mainly trigger the opening of the inward rectifying potassium channels (GIRKs), hyperpolarizing the neuron (Vigot et al., 2006) and thereby tuning neuronal excitability in several brain regions (Cruz et al., 2004; Edwards et al., 2017; Gao et al., 2017; Padgett et al., 2012; Scanziani, 2000; Wang et al., 2015).

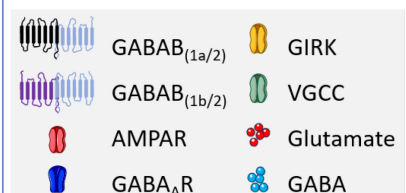
Other evidence also suggests that GABA<sub>B</sub>Rs inhibit VGCC subtypes at postsynaptic sites (Harayama et al., 1998; Pérez-Garci et al., 2006). On top of this, other transduction pathways responsible for the GABA<sub>B</sub>R-dependent signaling were described (Zhang et al., 2016a and see review Bettler et al., 2004; Xu et al., 2014) although not thoroughly investigated. Interestingly, the presence of GABA<sub>B2</sub> and both variants of GABA<sub>B1</sub> were identified in the LHb suggesting a pre- and postsynaptic expression of functional GABA<sub>B</sub>Rs (Charles et al., 2001; Geisler et al., 2003). Several distinct and highly regulated processes affect the presence of a functional receptor at the surface including its stabilization, receptor recycling, and eventually degradation. After a brief overview of the GABA<sub>B</sub>R trafficking, I will give some examples of how the surface expression of the receptor could be regulated.



**Figure 8: GABA<sub>B</sub>R subunits and functions**

**A.** Ligand binding to the GABA<sub>B</sub> receptor triggers GDP/GTP exchange at the  $\alpha_i$  subunit of the heterotrimeric ( $\alpha$ ,  $\beta$ , and  $\gamma$ ) G-proteins, resulting in dissociation of the  $\alpha_i$ -GTP from the  $\beta\gamma$  dimer. In turn, these G-proteins trigger activation of downstream effectors, including ion channels and enzymes.

**B.** Subunit composition and localization of GABA<sub>B</sub>Rs at synapses. Autoreceptors composed of GABA<sub>B1a</sub> or GABA<sub>B1b</sub> and GABA<sub>B2</sub> mediate presynaptic inhibition at GABA terminals by decreasing  $\text{Ca}^{2+}$  entry through inactivation of the voltage-gated channel (VGCCs), whereas heteroreceptors containing mostly GABA<sub>B1a</sub> mediate reduction of glutamate release. On the postsynaptic side, spillover of GABA activates the perisynaptic and extrasynaptic receptors (mostly GABA<sub>B1b/2</sub> heterodimers) that hyperpolarize the neuron by activating GIRK channels.



## II. GABA B receptors trafficking

Newly synthesized cell-surface receptors are processed and passed through distinct membrane compartments before reaching the plasma membrane, including the endoplasmic reticulum (ER), cis-Golgi network, and trans-Golgi network. Different check points regulate GABA<sub>B</sub>R transport to the surface membrane. Notably an Arginine-rich endoplasmic reticulum retention signal is present within the C-terminal tail of the GABA<sub>B1</sub> subunit (Calver et al., 2001; Margeta-Mitrovic et al., 2000; Pagano et al., 2001) as well as an di-lysine motif that inhibits its transport from trans-Golgi to the cell surface (Restituito et al., 2005). Heterodimerization with GABA<sub>B2</sub> seems to induce a conformational change that masks retention signals promoting its exit from the endoplasmic reticulum and the GABA<sub>B1</sub> transport to the cell surface (Gassmann et al., 2005; Pagano et al., 2001). Once at the plasma membrane GABA<sub>B</sub>Rs undergo constitutive clathrin and dynamin-dependent endocytosis

(Grampp et al., 2007, 2008; Pooler et al., 2009; Vargas et al., 2008; Wilkins et al., 2008). After internalization, GABA<sub>B</sub>Rs are transferred to fast and slow recycling endosomes, as well as lysosomes. The non-degraded receptors can then recycle back to the membrane (Grampp et al., 2008). Blocking vesicle fusion to the plasma membrane by monensin induced degradation of 50% of the receptors by redirecting them to lysosomes, suggesting a stable equilibrium between internalization and recycling (for review see Benke, 2010). In the following paragraph, I will give several examples of how this process could be regulated determining the surface expression of GABA<sub>B</sub>Rs.

### III. GABA<sub>B</sub> receptor regulation

Desensitization following prolonged exposure to the agonist is a common feature of G-protein coupled receptors (GPCRs) down-regulation, reducing protein levels at the surface to prevent overstimulation. Usually, desensitization involves phosphorylation by the G protein-coupled receptor kinases (GRK) recruiting arrestin, dynamin, and clathrin, leading to internalization of the receptor downregulating signaling at the membrane (Gainetdinov et al., 2004). However, GABA<sub>B</sub>Rs do not seem to follow this common regulatory pathway. Instead, prolonged exposure to GABA<sub>B</sub>R agonist, baclofen leads to decreased phosphorylation level (at the serine residue (S)892 of the GABA<sub>B2</sub>) promoting degradation of the receptor; an effect that is attenuated by increasing PKA activity (Fairfax et al., 2004). Consistently, PKA phosphorylation of GABA<sub>B2</sub> S892 has been shown to decrease the desensitization rate through potential stabilization of the receptor at the membrane and promotes GABA<sub>B</sub>R signaling (Couve et al., 2002). Instead, protein kinase C (PKC)-dependent desensitization decreased coupling of the receptor to the G protein following prolonged receptor activation. This mechanism involved phosphorylation of GABA<sub>B1</sub> subunit by PKC and subsequent N-ethylmaleimide-sensitive fusion (NSF) protein dissociation from GABA<sub>B</sub>Rs both necessary to reduce G protein activation (Pontier et al., 2006)

Apart from the agonist-dependent desensitization, sustained application of glutamate or N-methyl-D-aspartic acid (NMDA) has also been described to regulate GABA<sub>B</sub>R function. This regulatory pathway increases GABA<sub>B</sub>R targeting to lysosomes and its subsequent degradation, resulting in a decrease in receptor expression at the cell surface (Guettg et al., 2010; Kantamneni et al., 2014; Maier et al., 2010; Terunuma et al., 2010a; Vargas et al., 2008). Mechanistically, prolonged NMDARs activation triggers phosphorylation of GABA<sub>B1</sub> at S867 by the CaMKII promoting the degradation of the receptor (Guettg et al., 2010). Moreover, in cortical and hippocampal cultured neurons, the balance between GABA<sub>B2</sub>-S783



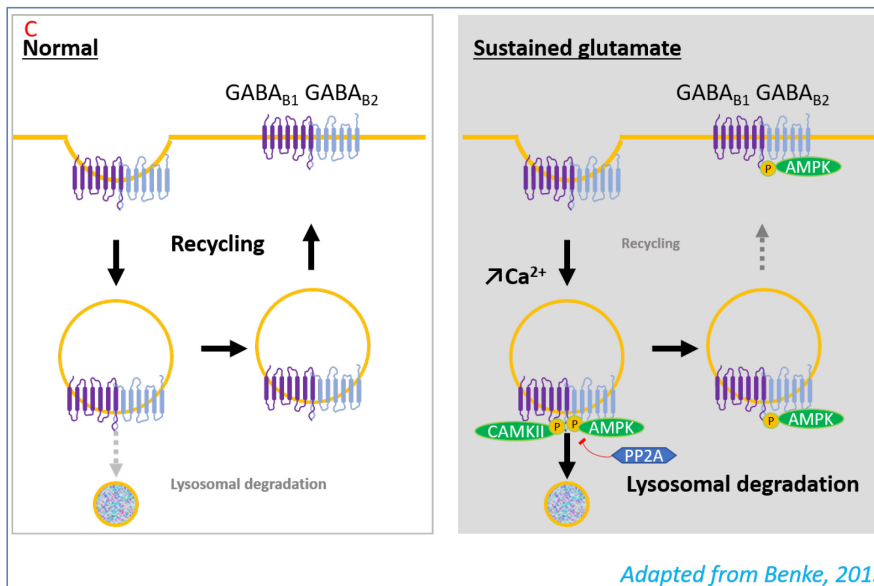
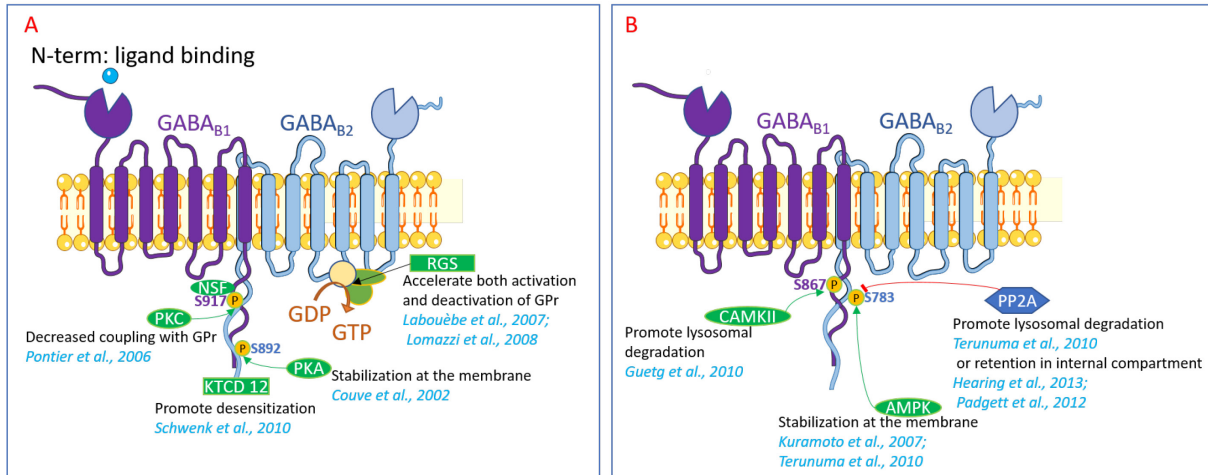
phosphorylation and dephosphorylation by the AMP-activated protein kinase (AMPK) and the protein phosphatase type 2 (PP2A) respectively, governs post-endocytic sorting of GABA<sub>B</sub>Rs. Indeed, phosphorylation of S783 on GABA<sub>B2</sub> subunit by the AMP-activated protein kinase (AMPK) stabilizes the complex at the membrane and decreases desensitization (Kuramoto et al., 2007; Terunuma et al., 2010a) whereas dephosphorylation of S783 by PP2A following prolonged NMDA exposure targets the receptors for lysosomal degradation (Terunuma et al., 2010a). Interestingly, electrophysiological studies in brain slice also reported PP2A-dependent down-regulation of GABA<sub>B</sub>Rs involving a retention within the internal compartments in a pathophysiological context (Hearing et al., 2013; Padgett et al., 2012).

Importantly, GABA<sub>B</sub>R signaling depends on several other proteins interacting with the receptor or their effectors (GIRK/VGCC), such as the members of the potassium channel tetramerization Domain containing proteins (KCTD), the regulator of G protein signaling (RGS), the transcription factor CCAAT/enhancer-binding protein homologous protein (CHOP), the Sorting nexin 27 (SNX27), among many others (Labouèbe et al., 2007; Munoz and Slesinger, 2014a; Sauter et al., 2005; Schwenk et al., 2010). Indeed interacting proteins not only regulate their targeting to specific compartments but are also needed for synthesis modulation; their intracellular signaling, for their cross-linkage to neuronal cytoskeleton, membrane assembly as well as for their allosteric activation/inactivation (for review see see (Benke, 2013; Bettler and Fakler, 2017; Couve et al., 2004; Lujan and Ciruela, 2012; Luján et al., 2014; Lüscher and Slesinger, 2010; Padgett and Slesinger, 2010; Pinard et al., 2010; Terunuma et al., 2010b). As example, RGS proteins enhance the GTPase activity of G $\alpha$  subunits, accelerating the deactivation of G protein signaling (Doupnik, 2015; Sjögren, 2011). Consistently, genetically silencing RGS2 has been reported to lead to a higher GABA<sub>B</sub>R-GIRK coupling efficiency in the VTA (Labouèbe et al., 2007). One other example is the four K<sup>+</sup> channel tetramerization domain-containing (KCTD) proteins. KCTDs have been identified as auxiliary subunits of the GABA<sub>B</sub>Rs. By forming tetramers and binding to the C-terminal tail of GABA<sub>B2</sub>, KCTDs stabilize GABA<sub>B</sub>R at the cell surface (Ivankova et al., 2013), increase agonist potency, accelerate onset and promote desensitization of the GABA<sub>B</sub>Rs (Fritzius et al., 2017; Schwenk et al., 2010).

Additionally, the modulation of GABA<sub>B</sub>R function also rely on regulation of its effectors such as GIRK channels. For example, a proteomic study reveals that GirK3 subunit interacts with the SNX27, a protein implicated in the trafficking of an array of neuronal signaling proteins between the endosome and the plasma membrane (Balana et al., 2011; Lauffer et al., 2010;



Lunn et al., 2007; Temkin et al., 2011). Functionally, genetical ablation of the SNX27 in the VTA DA neurons has been described to reduce the GABA<sub>B</sub>R -GIRK signaling (Munoz and Slesinger, 2014b).



**Figure 9: GABA<sub>B</sub>Rs regulations**

**A.** Mechanisms of GABA<sub>B</sub>Rs desensitization.

**B-C.** Regulation of GABA<sub>B</sub>Rs by trafficking. Under normal conditions GABA<sub>B</sub>Rs are constitutively internalized and recycled back to the plasma membrane. Sustained activation of glutamate receptors induces phosphorylation of GABA<sub>B1</sub> by CaMKII and dephosphorylation by PP2A. These events shift the recycling/degradation balance towards increase degradation by the lysosomes, resulting in a rapid down-regulation of GABA<sub>B</sub>Rs.

Overall, these studies suggest an important role of GABA<sub>B</sub>Rs in dampening neuronal activity, presynaptically modulating neurotransmitter release via inactivation of VGCCs but also through modulation of postsynaptic GIRK channels that control neuronal excitability.

LHb hyperactivity has been related to the expression of depressive like symptoms (Li et al., 2011, 2013; Seo et al., 2017). Previous studies mainly focused on the role of fast glutamatergic and GABAergic transmission onto LHb in a rodent model of depression (Li et al., 2011, 2013; Shabel et al., 2014). However, considering the critical role of GABA<sub>B</sub>Rs in controlling neuronal activity, whether GABA<sub>B</sub>Rs dysregulation within LHb could contribute to the establishment of a depressive phenotype has still to be investigated. Importantly,

GABA<sub>B</sub>Rs signaling have been described in pathological states including addiction, anxiety and mood disorder (for review Bowery, 2006; Cryan and Slattery, 2010; Lüscher and Slesinger, 2010). Regarding depression, the role of the GABA<sub>B</sub>Rs is still under debate (Cryan and Slattery, 2010; Lujan and Ciruela, 2012). Indeed, an unidirectional relationship between GABA<sub>B</sub>R signaling and a precise depressive like behavioral outcome has not been provided. One possible explanation is that the different results so far obtained are not taking into account the topographical localization (pre and post-synaptic) or region specificity of the receptors. In this thesis, I will present two sets of data investigating the plasticity of GABA<sub>B</sub>Rs in the LHb as an early cellular process following exposure to stress that is not only crucial for neuronal output but also for behavioral traits of mood disorders.

## Methodological section

---

### Experimental subjects and stress paradigms

For the first study, 4- to 7-week-old wild-type male C57Bl/6J mice (Janvier laboratories, France) were used in accordance with the guidelines of the French Agriculture and Forestry Ministry for handling animals and of the ethics committee Charles Darwin #5 of the University Pierre et Marie Curie. Mice were housed in groups of 4–6 per cage with water and food ad libitum. Mice were randomly allocated to experimental groups.

In the second study, 4-9 weeks wild-type male and female C57Bl/6J were used. All procedures were used in accordance with the guidelines of the French Agriculture and Forestry Ministry for handling animals (Committee Charles Darwin #5, University Pierre et Marie Curie, Paris). Part of the current study was carried out in the Department of Fundamental Neuroscience (Lausanne, Switzerland). Pregnant dams C57Bl/6J were received at the gestational stage E13-18 (Janvier laboratories, France). Mothers were housed two per cages with access of food and water at libitum. After birth, pups of either sex remained untouched until postnatal day (P) 7. At P7, litters were randomly divided in 2 groups. Control group were weaned at P22/23 and housed in groups of 3-5 mice per cage with water and food ad libitum. Maternally separated (MS) mice were weaned at P17 and housed in groups of 3-5 mice per cage. Control and MS mice were housed separately.

### *Foot shock paradigm (FS)*

The inescapable-shock procedure was previously described (Stamatakis and Stuber, 2012). Briefly, we placed mice into standard mouse behavioral chambers (Imetronics) equipped with a metal grid floor. We let them habituate to the new environment for 5 min. In a 20-min session animals received either 19 or 0 unpredictable foot shocks (1 mA, 500 ms) with an intershock interval of 30, 60 or 90 s. We anesthetized mice for patch-clamp electrophysiology 1 h, 24 h, 7 d, 14 d or 30 d after the session ended.

### *Learned-helplessness model (LHp)*

The procedure consisted of two sessions of inescapable foot shocks (one session per day; 360 foot shocks per session; 0.3 mA; shock duration between 1 and 3 s; and random intershock intervals) followed 24 h after the last session by a test session to assess the LHp. The testing was performed in a shuttle box (13 × 18 × 30 cm) equipped with a grid floor and a door separating the two compartments. The test consisted of 30 trials of escapable foot shocks. Each trial started with a 5-s-long light stimulus followed by a 10 s shock (0.1–0.3 mA). The

intertrial interval was 30 s. When the mouse shuttled in the other compartments during the light cue, the avoidance was scored. When it shuttled during the shock, the escape latency was measured. When the mouse was unable to escape, the failure was scored. The shock terminated any time that the animal shuttled in the other compartment. Out of the 30 trials, more than 15 failures were defined as an LH. Only LHp mice were behaviorally and electrophysiologically tested.

### *Maternal separation paradigm*

The maternal separation group consisted of pups removed from their litter and isolated in small compartments for 6 hours per day (light phase 8:19h) repeated from P7 to P15 and followed by an early weaning at P17. During the separation, animals were maintained in heating plate and water was provided, maintaining constant temperature and humidity. The control group consisted of mice from independent litters, which were not manipulated until the regular weaning at P21 except during cage changing. During cage changing some old bedding and nest were transferred into the new cage in order to limit novelty stress. Behavior testing and recording were performed 2 to 5 weeks after the stress protocol.

### *Behavioral tests*

All behavioral tests were conducted during the light phase (8:00–19:00), 1 or 7 d after the shock procedure. Animals were tested only for a single behavioral paradigm, and operators were blinded to the experimental group during the scoring.

*Locomotor activity.* To assess the locomotor activity we tested mice in an open-field arena. Mice were placed in the center of a plastic box (50 cm × 50 cm × 45 cm) in a room with dim light. We let them to explore the arena for 5 min and then we acquired the video tracks. During the 15-min session, animal behavior was videotaped and subsequently analyzed (Anymaze, Ireland).

*Forced-swim test.* The forced-swim test was conducted in normal light conditions. Mice were placed in a cylinder of water (temperature of 23–25 °C; 14 cm in diameter, 27 cm in height for mice) for 6 min. The depth of water was set to prevent animals from touching the bottom with their hind limbs. Animal behavior was video-tracked from the top (Viewpoint, France). The latency to the first immobility event and the immobility time of each animal spent during the test were counted online by two independent observers in a blinded manner. Immobility was defined as floating or remaining motionless, which means absence of all movement except for the motions required to maintain the head above water.

**The tail suspension test** The tail suspension test was performed with mice being suspended by their tails with adhesive tape for a single session of 6 min. Immobility time of each animal was scored online by the experimenter. Mice were considered immobile only when they suspended passively and motionless

**Sucrose preference test.** For the sucrose preference test, mice were single-housed and habituated with two bottles of 1% sucrose for 2 d. At day 3 (test day) mice were exposed to two bottles filled with either 1% sucrose or water for 24 h. The sucrose preference was defined as the ratio of the consumption of sucrose solution versus total intake (sucrose + water) during the test day and expressed as a percentage.

**The shuttle box test** The shuttle box (13 × 18 × 30 cm) was equipped with an electrified grid floor and a door separating the two compartments. The test session consisted of 30 trials of escapable foot-shocks (10 sec at 0.1–0.3 mA) separated by an interval of 30s. The shock terminated any time that the animal shuttled in the other compartment. Failure is defined as the absence of shuttling to the other compartment within the 10 sec shock delivery.

#### Drug/intervention

**LB-100 treatment:** Mice were injected with LB-100 (1.5 mg/kg; i.p.; Lixte Inc.) or saline 6–8 h after the FS (2 h was used for biochemical assays). LHp animals received LB-100 24 h after the test day. A set of mice (aged 5 weeks), were single-housed for 3 d and were then treated with LB-100 i.p. (1.5 mg/kg/d) for 7 d. Body weight and food pellet and water intake were monitored every 2 d. Three days after the last injections, the mice were tested for their locomotor activity

**Dreadd(Gi) experiment :** Behavioral experiments in DREADD-injected animals were performed three weeks after viral infusion. For the shuttle Box, the tail suspension test, and the locomotor activity all the groups (YFP or DREADDi injected animals) were injected 15 minutes with CNO i.p. (1mg kg<sup>-1</sup>). For sucrose preference experiments, all groups were injected with CNO i.p. (1mg kg<sup>-1</sup>) every 3h for the extent of the preference session (24h) to maintain a constant DREADD-mediated inhibition.

**Deep brain stimulation** MS mice for DBS experiments were first preselected on the basis of their failure rate in the Shuttle box test (A cutoff of 12 failures was used for the preselection). 50 mice were tested, and 17 of these animals met the criteria. Standard surgical procedures were used to implant bipolar concentric electrodes unilaterally into the LHb (coordinates –1.45 mm AP, ± 0.45 mm ML and –3.1 mm DV). After 5 days recovery from surgery, DBS or

no (Sham) stimulation was applied for 1h (seven stimulus trains of 130 Hz, separated by 40 ms intervals; 150  $\mu$ A intensity) prior testing each mouse in the shuttle box test.

### Surgery

Animals were anesthetized with ketamine (150 mg/kg) and xylazine (10 mg/kg; i.p.) (Sigma-Aldrich, France).

The following coordinates were used for LHb: (from bregma, in mm): A-P:  $-1.45$ ; M-L:  $\pm 0.45$ ; D-V:  $-3.1$ ; the EPN (from bregma, in mm: A-P:  $-1.25$ ; M-L:  $\pm 1.8$ ; D-V:  $-4.65$ ) RMTg: from bregma, in mm: A-P:  $-2.9$ ; M-L:  $\pm 0.5$ ; D-V:  $-4.3$  and VTA: from bregma, in mm: A-P:  $-2.4$ ; M-L:  $\pm 0.65$ ; D-V:  $-4.9$ ).

**DREADDi expression** MS and control animals, aged at least 24 days were anesthetized with Ketamine (150 mg  $\text{kg}^{-1}$ )/Xylazine (100 mg  $\text{kg}^{-1}$  i.p.) before bilateral injection of rAAV8-Hsyn-Gi-DREADD-mCherry (University of Pennsylvania, US) in. After three weeks, mice were subjected to CNO i.p injection (1mg/kg) for the DREADD activation.

**CochR expression** For optogenetic experiments rAAV2.1-hSyn-CoChr-eGFP (University of North Carolina, US) was infused in the entopeduncular nucleus. Recordings were performed 3 weeks after surgery. The injection sites were carefully examined and only animals with correct injections were kept for behavioral and electrophysiological analysis.

**DBS electrodes implantation** Electrodes (Bilaney, UK) were unilaterally implanted using similar procedures and coordinates in the LHb. DBS electrodes were chronically implanted using a Superbond resin cements (Sun medical, Japan).

**Retrolabelling of VTA and RMTg projecting neurons** For the experiment analyzing the output specificity of I-Baclofen, mice were bilaterally injected with a mixture of herpes simplex virus (McGovern Institute, US) expressing enhanced GFP and red retrobeads (Lumafuor, US) into the RMTg or the VTA. Recordings from fluorescent LHb neurons were performed  $\pm 12$  days following the surgery, and injection site were verified using the retrobeads labelling.

### Electrophysiology

Animals were anesthetized with ketamine and xylazine (50 mg/kg and 10 mg/kg, respectively; i.p.; Sigma-Aldrich, France). Analysis was performed in a non-blinded fashion.

**Preparation** LHb-containing brain slices was done in bubbled ice-cold 95%  $\text{O}_2$ /5%  $\text{CO}_2$ -equilibrated solution containing: 110 mM choline chloride; 25 mM glucose; 25 mM  $\text{NaHCO}_3$ ; 7 mM  $\text{MgCl}_2$ ; 11.6 mM ascorbic acid; 3.1 mM sodium pyruvate; 2,5 mM KCl; 1.25 mM  $\text{NaH}_2\text{PO}_4$ ; 0.5 mM  $\text{CaCl}_2$ . 250  $\mu\text{m}$  thick sagittal slices (or coronal 2nd study), were stored at

room temperature in 95% O<sub>2</sub>/5% CO<sub>2</sub>-equilibrated artificial cerebrospinal fluid (ACSF) containing: 124 mM NaCl; 26.2 mM NaHCO<sub>3</sub>; 11 mM glucose; 2.5 mM KCl; 2.5 mM CaCl<sub>2</sub>; 1.3 mM MgCl<sub>2</sub>; 1 mM NaH<sub>2</sub>PO<sub>4</sub>. Recordings (flow rate of 2.5 ml/min) were made under an Olympus-BX51 microscope (Olympus, France) at 31 °C. Currents were amplified, filtered at 5 kHz and digitized at 20 kHz. Access resistance was monitored by a step of -4 mV (0.1 Hz). Experiments were discarded if the access resistance increased more than 20%. Animals were anesthetized with ketamine and xylazine (50 mg/kg and 10 mg/kg, respectively; i.p.; Sigma-Aldrich, France). Analysis was performed in a non-blinded fashion.

**Internal solution** The internal solution used to examine GABAB and/or GIRK currents and neuronal excitability contained: 140 mM potassium gluconate, 4 mM NaCl, 2 mM MgCl<sub>2</sub>, 1.1 mM EGTA, 5 mM HEPES, 2 mM Na<sub>2</sub>ATP, 5 mM sodium creatine phosphate, and 0.6 mM Na<sub>3</sub>GTP (pH 7.3 with KOH). The liquid junction potential was ~12 mV. When we measured the synaptic inhibitory or excitatory release, the internal solution contained: 130 mM CsCl; 4 mM NaCl; 2 mM MgCl<sub>2</sub>; 1.1 mM EGTA; 5 mM HEPES; 2 mM Na<sub>2</sub>ATP; 5 mM sodium creatine phosphate; 0.6 mM Na<sub>3</sub>GTP; and 0.1 mM spermine. The liquid junction potential was -3 mV.

Whole-cell voltage clamp recordings were achieved to measure GABAB-GIRK currents in presence of bicuculline (10 μM), NBQX (20 μM) and AP5 (50 μM). For agonist-induced currents, changes in holding currents in response to bath application of baclofen were measured (at -50 mV every 5-10 s). The plotted values correspond to the difference between the baseline and the plateau (for the baclofen and ML297 experiments) or the difference between the plateau and the value of holding current after barium (for the I-GTP-γS). GABAB-GIRK currents were confirmed by antagonism with 10 μM of CGP54626. When stated, 100 μM of GTP-γS was added to the internal solution in place of Na<sub>3</sub>GTP. Plateau currents were then reversed by 1 mM Barium application, a selective inhibitor of K<sup>+</sup> channels. Changes in holding currents in response to GIRK agonist were measured (at -50 mV every 5-10 s) by bath application of ML-297 (50 μM), a Selective GIRK1/2 channel activator then reversed by 1 mM Barium application. Synaptic GABAB slow IPSCs were optically evoked by trains of 10 pulses delivered at 20 Hz through a 470 nm LED. The fast GABA amplitude correspond to the amplitude of the first pic of the train, the slow GABA current instead were measured after picrotoxin bath application, and correspond to the I-max. Miniature excitatory postsynaptic currents (mEPSCs) were recorded in voltage-clamp mode at -60 mV in presence of bicuculline (10 μM), AP5 (50 μM) and tetrodotoxin (TTX, 1 μM). Miniature inhibitory postsynaptic currents (mIPSCs) were recorded (-60 mV) in presence of



NBQX (20  $\mu$ M) AP5 (50  $\mu$ M) and TTX (1  $\mu$ M). EPSCs were evoked through an ACSF-filled monopolar glass electrode placed in the LHb. For the experiments in which high-frequency stimulation trains were used to determine presynaptic release probability (5 pulses at 20 Hz), QX314 (5 mM) was included in the internal solution to prevent the generation of sodium spikes.

Current-clamp experiments were performed using a series of current steps (from  $-80$  pA to  $100$  pA or when the cell reached a depolarization block) injected to induce action potentials (10-pA injection current per step, duration of 500 ms). Cells were maintained at  $-55$ mV throughout the experiment. When testing changes in tonic firing, cells were depolarized to obtain stable firing activity in current clamp mode.

### Analysis and drugs.

All drugs were obtained from Abcam (Cambridge, UK) and Hello Bio, and Tocris (Bristol, UK) and dissolved in water, except for TTX (citric acid 1%), ML297 and CNO (DMSO). Online/offline analysis were performed using IGOR-6 (Wavemetrics, US) and Prism (Graphpad, US). Data analysis for in vivo electrophysiology was performed off-line using Spike2 (CED, UK) software. Sample size required for the experiment was empirically tested by running pilots experiments in the laboratory. While behavioral experiments were run in a single-to-triple trial, electrophysiological experiments were replicated at least 5 times. Experiments were replicated in the laboratory at least twice. Animals were randomly assigned to experimental groups. Data distribution was assumed to be normal, and single data points are always plotted. Compiled data are expressed as mean  $\pm$  s.e.m. All groups were tested with Grubbs exclusion test (limit set at 0.05) to determine outliers. Significance was set at  $p < 0.05$  using Student's t-test two-sided, Kolmogorov-smirnov test, one-way, two-way or three-way Anova with multiple comparison when applicable.



## Context and objectives of the study I: GABA<sub>B</sub> receptors trigger LHb hyperactivity, an early marker of depressive like symptoms

Major depressive disorder is one of the leading causes of disability worldwide, that afflict nowadays more than 300 million of people. Yet, more than 30% of the patients do not respond adequately to the currently available treatment. One explanation remains the poor understanding of the etiology of the disease. Depression is characterized by alteration of motivational behavior such as anhedonia and deficit in coping with aversive stimuli. In this context, LHb have gained a particular attention. Indeed the literature presented so far, highlight a pivotal role of the LHb in regulating monoaminergic activity and motivated behavior. Particularly, LHb neurons encode aversive stimuli by phasically increasing their firing rate and activation of LHb terminals onto midbrain neurons induces avoidance behavior in mice. Moreover, previous studies provide evidence that LHb hyperactivity could underlie certain symptoms of depression. However, insights in the cellular and molecular mechanism underlying this hyperexcitability and their causal link with the emergence of depressive like symptoms remain poor. In this study, we aimed to understand early cellular modifications occurring in the LHb after a stressful experience, one of the main triggers to engage depressive behaviors in animals and humans. Neuronal activity is tightly control by the balance of excitatory and inhibitory transmission. We focused in the GABA<sub>B</sub>R signaling which (1) play an important role in the dampening of the neuronal activity in other brain areas and (2) present modification of expression in neuropsychiatric disorder such as addiction and depression both in humans and animal model of depression rodents. Yet, there is no functional evidence of a role of GABA<sub>B</sub>Rs in controlling LHb neurons functions and its involvement in encoding negative state. Here we reported that, aversive experience, such as foot-shock exposure, induces LHb neuronal hyperactivity and depressive-like symptoms. This occurs along with an increase in PP2A activity together with a GABA<sub>B</sub>R-GIRK internalization leading to rapid and persistent weakening of GABA<sub>B</sub>R-GIRK currents. The inhibition of protein phosphatase-2A (PP2A), a regulator of GABA<sub>B</sub>R-GIRK surface expression, restores stress-induced GABA<sub>B</sub>R-GIRK reduction and neuronal hyperexcitability. Furthermore, PP2A inhibition ameliorates depressive symptoms after FS and in a LHb of depression. These data establish causality between GABA<sub>B</sub>R-GIRK plasticity LHb hyperexcitability and the emergence of depressive like symptoms opening a new window toward new target in the treatment of mood disorder.

## Rescue of GABA<sub>B</sub>-GIRK function in the lateral habenula by protein phosphatase 2A inhibition ameliorates symptoms of depression in mice

Salvatore Lecca<sup>1,2,3</sup>, Assunta Pelosi<sup>1,2,3</sup>, Anna Tchenio<sup>1,2,3</sup>, Imane Moutkine<sup>1,2,3</sup>, Rafael Lujan<sup>4,5</sup>, Denis Herve<sup>1,2,3</sup> and Manuel Mameli<sup>1,2,3</sup>

<sup>1</sup> Institut du Fer à Moulin, Paris, France.

<sup>2</sup> Institut national de la santé et de la recherche médicale, UMR-S 839, Paris, France.

<sup>3</sup> Université Pierre et Marie Curie Paris, France.

<sup>4</sup> Instituto de Investigación en Discapacidades Neurológicas, Albacete, Spain

<sup>5</sup> Universidad Castilla-La Mancha, Facultad de Medicina, Dept. Ciencias Médicas, Campus Biosanitario, Albacete, Spain.

Number of pages: 35

Number of figures: 6

Word Count; Introduction, results, discussion 3447; Abstract: 163

To whom correspondence should be addressed:

Manuel Mameli, PhD

Email [manuel.mameli@inserm.fr](mailto:manuel.mameli@inserm.fr)

### Abstract

*The lateral habenula (LHb) encodes aversive signals and its aberrant activity contributes to depressive-like symptoms. However, a limited understanding of the cellular mechanisms underlying LHb hyperactivity has precluded the development of pharmacological strategies to ameliorate depressive phenotypes. Here, we report that aversive experience in mice, such as foot-shock exposure (FsE), induces LHb neuronal hyperactivity and depressive-like symptoms. This occurs along with increased protein-phosphatase-2A (PP2A) activity, a known regulator of GABA<sub>B</sub> receptor (GABA<sub>B</sub>R) and G-protein-gated inwardly rectifying potassium (GIRK) channel surface expression. Accordingly, FsE triggers GABA<sub>B1</sub> and GIRK2 internalization leading to rapid and persistent weakening of GABA<sub>B</sub>-activated GIRK-mediated (GABA<sub>B</sub>-GIRK) currents. Pharmacological inhibition of PP2A restores both GABA<sub>B</sub>-GIRK function and neuronal excitability. As a consequence, PP2A inhibition ameliorates depressive-like symptoms after FsE and in a learned helplessness model of depression. Thus, GABA<sub>B</sub>-GIRK plasticity in the LHb represents a cellular substrate for aversive experience. Furthermore, its reversal by PP2A inhibition may provide a novel therapeutic approach to alleviate depressive symptoms in disorders characterized by LHb hyperactivity.*

## Introduction

Unpredictable aversive stimuli trigger rapid avoidance responses and, if persistent, contribute to the emergence of depressive-like symptoms in both animals and humans<sup>1</sup>. The lateral habenula (LHb) bridges forebrain and midbrain nuclei and encodes aversive stimuli<sup>2</sup>. Analysis of fMRI data in depressed humans<sup>3</sup> and metabolic activity in rodent models of depression<sup>4</sup> (e.g. learned helplessness<sup>5</sup>) suggests that LHb hyperactivity may contribute to depressive-like symptoms<sup>6,7-9</sup>. However, the early cellular adaptations and precise molecular targets responsible for LHb hyperexcitability remain elusive.

Modifications in GABA<sub>B</sub> receptor (GABA<sub>B</sub>-R) expression and polymorphisms of the *GIRK* genes contribute to depressive symptoms in humans and rodents. This provides substantial evidence for the involvement of the GABA<sub>B</sub>-mediated G-protein-gated inwardly rectifying potassium channels (GABA<sub>B</sub>-GIRK) signaling in the etiology of mood disorders<sup>10,11</sup>.

Furthermore, pharmacological and genetic-based observations support the idea that adaptations in GABA<sub>B</sub>-GIRK signaling may represent a viable target to ameliorate depressive-like symptoms<sup>12,13,14</sup>. Although these findings suggest that GABA<sub>B</sub>-GIRK function plays a role in mood disorders, they fail to provide a precise anatomical substrate in which modifications of GABA<sub>B</sub>-GIRK occur, and how they may ultimately contribute to depressive symptoms.

Here, we provide evidence that GABA<sub>B</sub>-GIRK signaling in the LHb is involved in the expression of depressive-like symptoms in mice. Unpredictable foot-shock exposure (FsE) triggered a reduction in GABA<sub>B</sub>-GIRK signaling, increased PP2A activity (a known regulator of membrane GABA<sub>B</sub>-GIRK complexes<sup>15</sup>) and neuronal hyperexcitability in the LHb, promoting depressive-like behaviors. We found that local GIRK overexpression or pharmacological inhibition of PP2A rescue these FsE-driven cellular modifications. As a consequence, these interventions ameliorated behavioral phenotypes including despair, anhedonia and learned helplessness, which model distinct aspects of depression<sup>5,16,17</sup>. These data establish causality between GABA<sub>B</sub>-GIRK plasticity and LHb hyperexcitability, offering a viable rescue strategy to reverse cellular adaptations and behavioral traits of depression.

## Results

### Depressive-like symptoms and cellular modifications in the LHb

Although LHb neuronal firing contributes to depressive-like states<sup>18</sup>, whether cellular modifications occur in the LHb after an aversive experience that ultimately contributes to depressive symptoms remains unknown. In humans uncontrollable and unpredicted stressful events lead to negative emotional feelings and behaviour similar to those found in depression<sup>19</sup>. The inescapable shock represents a paradigm that recapitulates symptoms of depression in a variety of animals<sup>20</sup>. Here, we examined the behavioral consequences of aversive experience by exposing C57/BL6J mice to inescapable and unpredictable foot-shocks<sup>21</sup>. Control mice were exposed to the same behavioral chamber in the absence of any foot-shocks. Re-exposure of mice to the shock-associated context 24 hours after the protocol led to a high level of freezing behavior (**Fig. 1a**), typical of fear memory<sup>22</sup>, without modifying the animals' locomotor activity (**Supplementary Fig. 1a**). Seven days after FsE, animal behavior analyzed in the forced swim test paradigm (FST)<sup>23</sup> revealed a reduced latency to first immobility and increased total immobility, indicative of a depressive-like state (**Fig. 1b**). As hyperexcitability in the LHb contributes to depressive-like phenotypes in rodents<sup>7,24,25</sup>, we hypothesized that the establishment of FsE-driven depressive-like traits relies, at least in part, on modifications in LHb function. In acute brain slices prepared 1 hour after FsE, we found that the spontaneous firing of LHb neurons recorded in cell-attached configuration was higher in slices from FsE mice compared to control (**Supplementary Fig. 1b**). Furthermore, in whole-cell mode, LHb neurons in the FsE group exhibited a higher number of action potentials evoked by current injections compared to control (**Figs. 1c and d**). Together, these data suggest that FsE produces behavioral responses reminiscent of depressive-like states as well as LHb neuronal hyperexcitability.

### GABA<sub>B</sub>-GIRK signaling in the LHb

GABA<sub>B</sub>-Rs exert control over neuronal excitability via the activation of hyperpolarizing actions of GIRK channels<sup>26</sup>. To address whether GABA<sub>B</sub>-Rs and/or GIRKs represent a cellular substrate in the LHb underlying neuronal hyperexcitability and the emergence of depressive-like behaviors, we first assessed GABA<sub>B</sub>-GIRK signaling in the LHb of naïve mice. A saturating dose of the GABA<sub>B</sub>-R agonist baclofen (100 μM) evoked an outward current (I-Baclofen) reversed by the GABA<sub>B</sub>-R antagonist CGP54626 (10 μM; **Supplementary Figs. 2a and b**). I-Baclofen was dose-dependent, occurred along with a decrease in input resistance, and was reduced in presence of barium (Ba<sup>2+</sup>, 1 mM, **Supplementary Figs. 2a-e**), consistent with the activation of GIRK channels. In support of this conclusion, reverse-transcription PCR in LHb revealed the expression of GIRK1-2-3-4 subunits (**Supplementary Fig. 2f**)<sup>26</sup>. Furthermore, GABA<sub>B</sub>-GIRK signaling controls baseline LHb neuronal activity as bath application of the antagonist CGP54626 led to inward currents and increased firing

(**Supplementary Figs. 2g and h**). These results indicate that GABA<sub>B</sub>-GIRK signaling provide a relevant inhibitory control over LHB neuronal activity.

### **FsE-driven plasticity of GABA<sub>B</sub>-GIRK in the LHB**

To test the role of GABA<sub>B</sub>-GIRK signaling in FsE-induced LHB hyperexcitability, we assessed I-Baclofen 1 hour after FsE. I-Baclofen in slices from FsE mice was reduced compared to controls throughout the LHB (**Fig. 1e**; **Supplementary Fig. 3a**). The FsE-evoked reduction in I-Baclofen persisted up to 14 days and returned to control values by 30 days after the FsE (**Fig. 1e**). I-Baclofen in the presence of Ba<sup>2+</sup> was comparable between groups (**Supplementary Fig. 3b**), indicating that solely the GABA<sub>B</sub>-GIRK component is diminished after aversive experience. To also probe GIRK channel function we constitutively activated GIRKs via G $\beta$ / $\gamma$ -dependent mechanisms through the infusion of GTP- $\gamma$ S<sup>27</sup>. Intracellular dialysis of GTP- $\gamma$ S (100  $\mu$ M) led to an outward current sensitive to extracellular Ba<sup>2+</sup>, indicative of GIRK channel activation (**Fig. 1f**). LHB neurons from slices of FsE mice showed reduced GTP- $\gamma$ S-induced currents (**Fig. 1f**), suggesting that FsE weakens GABA<sub>B</sub>-GIRK signaling in the LHB.

FsE pairs a painful stimulus with a negative experience. We therefore tested whether aversive conditions independent of painful stimuli also modify GABA<sub>B</sub>-GIRK signaling in LHB<sup>28,29</sup>. The predator odor stress paradigm involves an aversive natural stimulus, as opposed to foot-shock. Similarly to FsE mice, I-Baclofen was depressed in animals exposed to the predator odor (**Supplementary Fig. 3c**). Furthermore, 1 hour of restraint stress, classically employed to cause depressive-like states in rodents, also reduced I-Baclofen in LHB neurons (**Supplementary Fig. 3d**)<sup>28,29</sup>.

To test whether FsE also modifies fast synaptic neurotransmission, we recorded miniature excitatory-inhibitory postsynaptic currents (mEPSCs-mIPSCs) after the FsE (**Supplementary Figs. 4a and b**). Quantal excitatory and inhibitory synaptic transmission remained unaffected in frequency and amplitude (**Supplementary Figs. 4a and b**). No modifications were found of excitatory synaptic strength or AMPA-R subunit composition, as AMPA-NMDA ratios and rectification indices remained unaffected (**Supplementary Fig. 4c**). We next evoked EPSCs and IPSCs by high-frequency extracellular stimulation<sup>30</sup>, which yields responses comparable between control and FsE mice (**Supplementary Fig. 4d**). This indicates that fast synaptic transmission onto LHB neurons, recorded 1 hour after FsE remained unaffected.

Together these findings indicate that FsE, and alternative aversive experience, rapidly and persistently modify GABA<sub>B</sub>-GIRK signaling throughout the LHB, thereby representing a common cellular substrate for encoding aversive experience of different nature.

### **FsE-induced subcellular redistribution of GABA<sub>B</sub>-GIRK within the LHB**

The reduction of GABA<sub>B</sub>-GIRK function upon aversive experience may rely on receptor-effector complex internalization<sup>31,32</sup>. To test this, we employed quantitative immunoelectron microscopy to compare the LHB subcellular distribution of GABA<sub>B1</sub> and GIRK2 in control and FsE mice (**Fig. 2a**). FsE led to a reduction in GABA<sub>B1</sub> and GIRK2 membrane immunolabeling, with a corresponding increase in their intracellular labeling. However, total GABA<sub>B1</sub> and GIRK2 immunolabeling remained unchanged (**Figs. 2a-c**). These subcellular modifications support a scenario in which macrocomplexes of GABA<sub>B</sub>Rs and GIRKs are internalized after FsE.

### **PP2A inhibition in LHB rescues GABA<sub>B</sub>-GIRK signaling after FsE**

The phosphorylation-de-phosphorylation of specific serine residues on the GABA<sub>B1</sub> and B2 subunits controls GABA<sub>B</sub>Rs surface expression, trafficking and function<sup>15,33</sup>. The protein phosphatase-2A (PP2A)-mediated de-phosphorylation of serine 783 (S783) in the GABA<sub>B2</sub> subunit represents a rate limiting factor for GABA<sub>B</sub>-Rs surface expression<sup>15,31,32</sup>. Stressful events modify PP2A activity in the central nervous system<sup>34,35</sup>. PP2A activity analyzed from LHB-containing microdissected epithalamus was higher than control mice when measured 24 hours after FsE (**Supplementary Fig. 5a**). We therefore predicted that inhibition of PP2A in the LHB could rescue FsE-evoked GABA<sub>B</sub>-GIRK plasticity. To test this, we examined the effect of intracellular dialysis of okadaic acid, an inhibitor of PP1/PP2A phosphatases (OA; 100 nM). In control mice, OA did not modify I-Baclofen indicating that PP1/PP2A activity does not provide substantial control of GABA<sub>B</sub>-GIRKs signaling at baseline (**Fig. 3a**; t-test,  $t_{21}=1.1$ ;  $p>0.05$ ). In FsE mice, OA led to I-Baclofen amplitudes comparable to control animals (**Fig. 3a**), promptly restoring GABA<sub>B</sub>-GIRK signaling. The use of OA to inhibit PP2A activity is however limited to its intracellular application, as it lacks membrane permeability. Recent advances in drug development targeted PP2A for pharmacotherapy, allowing for the generation of a membrane permeable inhibitor, LB-100<sup>36</sup>. In the presence of LB-100 (0.1  $\mu$ M), I-Baclofen was comparable between control and FsE conditions (**Fig. 3b**). To address whether inhibition of PP2A rescues solely GABA<sub>B</sub>-Rs, or also GIRKs function, we employed the intracellular dialysis of GTP- $\gamma$ S to activate GIRKs independently of GABA<sub>B</sub>Rs. We found that GTP- $\gamma$ S-mediated outward currents in LHB neurons from FsE and control mice were comparable in presence of LB-100 (**Fig. 3c**), indicating that both GABA<sub>B</sub> and GIRK signaling are restored when inhibiting PP2A.

The CaMKII-mediated phosphorylation at S867 of GABA<sub>B1</sub> represents an alternative pathway controlling GABA<sub>B</sub>Rs surface expression<sup>33</sup>. As opposed to OA and LB-100, application of the CaMKII inhibitor KN93 (10  $\mu$ M<sup>37,38</sup>) failed to recover I-Baclofen in slices from FsE mice (**Fig. 3d**). These findings suggest that FsE triggers an internalization of GABA<sub>B</sub>-GIRK complexes and subsequent reduction of GABA<sub>B</sub>-GIRK signaling, that can be promptly restored by inhibition of PP2A *in vitro*.

### **FsE-driven GABA<sub>B</sub>-GIRK plasticity and LHb hyperexcitability**

Our data suggest that FsE triggers a reduction in GABA<sub>B</sub>-GIRK signaling and increases LHb neuronal activity (**Figs. 1d–f; Supplementary Fig. 1b**). To determine if these two functional modifications are linked, we examined baclofen-evoked inhibition of LHb neuronal output firing (**Figs. 4a and b; Supplementary Fig. 6**). We predicted that a reduction in GABA<sub>B</sub>-GIRK function would not only increase baseline firing of LHb neurons, but also weaken GABA<sub>B</sub>-GIRK-induced firing suppression and reduce the modulation of activity by GABA<sub>B</sub>-Rs blockade. Baclofen application in slices from control animals produced an almost-complete reduction of LHb neuronal firing, while GABA<sub>B</sub>-R blockade by CGP54626 increased the firing frequency (**Figs. 4a and b; Supplementary Figs. 6a–c**). In slices from FsE mice, LHb neurons exhibited increased excitability, but firing was modified to a smaller extent by baclofen and CGP54626 (**Figs. 4a and b; Supplementary Figs. 6b and c**).

Taken together, these findings suggest that FsE-induced GABA<sub>B</sub>-GIRK reduction diminishes the GABA<sub>B</sub>-R driven inhibition of LHb neuronal activity. In order to establish whether rescuing GABA<sub>B</sub>-GIRK signaling causally recovers FsE-evoked hyperexcitability, we examined the effect of PP2A inhibition on cell excitability in slices from control and FsE mice. FsE shifted the input-output (I-O) relationship of LHb neurons, indicative of neuronal hyperexcitability (**Fig. 4c**). In contrast, inhibition of PP2A by bath application of LB-100 in slices from FsE mice, led to I-O curves comparable to control conditions (**Fig. 4d**).

Together these results demonstrate that PP2A inhibition is sufficient to rescue the loss of GABA<sub>B</sub>-GIRK function in LHb neurons and FsE-evoked hyperexcitability.

### **Inhibiting PP2A *in vivo* rescues FsE-driven cellular adaptations in the LHb**

In light of our results *in vitro*, we predicted that inhibition of PP2A *in vivo* would also normalize FsE-induced GABA<sub>B</sub>-GIRK reduction and hyperexcitability. To test this, we treated mice systemically with vehicle or LB-100 (1.5 mg/kg i.p.) 6-8 hours after FsE, a time point at which I-Baclofen is reduced (**Fig. 1e**). In line with previous results<sup>39</sup>, LB-100 treatment did not modify physiological parameters including body weight, locomotor activity, or food and water consumption (**Supplementary Figs. 7a and d**). LB-100 efficiently inhibits PP2A in the brain for ~12 hours, with a peak of its activity at ~8 hours<sup>36</sup>. Accordingly, we found that a single administration of LB-100 restored PP2A activity in the LHb to control levels when measured 24 hours after FsE (**Supplementary Fig. 5a**).

LHb-containing slices were prepared 1 or 7 days after FsE. We observed that, 1 day after FsE, vehicle-treated mice had reduced I-Baclofen (**Fig. 5a**). In contrast, I-Baclofen was comparable between the control and FsE group after systemic injections of LB-100 (**Fig. 5a**). This indicates that *in vivo* inhibition of PP2A rescues the FsE-evoked plasticity of GABA<sub>B</sub>-GIRK signaling in LHb. We next explored whether the rescue of GABA<sub>B</sub>-GIRK currents by PP2A inhibition occurs along with a functional recovery of LHb neuronal excitability. Vehicle-treated FsE animals, exhibited a shift in the I-O curve that was absent in slices from animals treated with LB-100 (**Fig. 5b**). Consistently, LB-100 treatment normalized I-Baclofen and LHb neuronal excitability in FsE mice to control levels when assayed 7 days after FsE, (**Figs. 5c and d**). Thus, *in vivo* PP2A-inhibition is sufficient to rescue the FsE-evoked cellular modifications in the LHb.

### **GABA<sub>B</sub>-GIRK plasticity in the LHb for depressive-like symptoms**

If PP2A inhibition rescues GABA<sub>B</sub>-GIRK function and hyperexcitability upon FsE, it may also represent an effective and therapeutically viable intervention to ameliorate the FsE-mediated depressive-like phenotype. We found that systemic LB-100 treatment did not affect FsE-driven increase in freezing behavior (**Fig. 6a**), indicating that the cellular modifications and neural circuits underlying this phenomenon are independent of PP2A-driven GABA<sub>B</sub>-GIRK plasticity within the LHb<sup>22</sup>. Seven days after FsE, vehicle-treated mice exhibited reduced latency to the first immobility along with an increased total immobility in the FST (**Fig. 6b**). In contrast, LB-100 treatment led to a normalization of this depressive-like phenotype (**Fig. 6b**). Similarly, LB-100 treatment prior the shock prevented FsE-driven cellular and behavioral modifications (**Supplementary Figs. 8a and b**). Consistent with the increased PP2A activity, this finding points to a necessary role of PP2A to induce GABA<sub>B</sub>-GIRK plasticity in the LHb and consequent depressive-like phenotype.

To define the anatomical substrate for PP2A actions, we infused vehicle solution or LB-100 locally in the LHb of control and FsE mice (**Fig. 6c**). At day 7, we tested mice in the FST paradigm to assess their depressive-like phenotype. Consistent with the systemic injection, we found that LB-100 infusion in the LHb led to a normalization of the FsE-driven depressive-like phenotype (**Fig. 6c**). Similarly, doxycycline-driven GIRK2a

overexpression within the LHb after FsE (AAV-TRE-GIRK2-eGFP-tTA; **Supplementary Figs. 8c–e**) also rescued FsE-evoked GABA<sub>B</sub>-GIRK plasticity and depressive-like behaviors (**Supplementary Figs. 8f and g**). Hence, increased PP2A activity and the consequent reduction of GABA<sub>B</sub>-GIRK signaling in the LHb mediate FsE-driven depressive-like phenotype.

Therefore, PP2A inhibition-driven rescue of FsE-induced GABA<sub>B</sub>-GIRK plasticity and hyperexcitability in the LHb may represent a valid therapeutic strategy to ameliorate depressive symptoms in mice.

To extend these findings, we employed a learned helplessness model in mice, a depression-like phenotype whereby animals present a diminished escape rate after a stressor<sup>20</sup>. We used control mice exposed to the context and mice subjected to two sessions of inescapable and unpredictable foot-shock. 59 out of 119 mice displayed learned helplessness (LH mice), measured as a reduced escape after foot-shocks in a shuttle box paradigm. The failure rate to escape classically reflects depressive symptoms in rodents<sup>5,17,40</sup> (**Supplementary Fig. 9a**). To establish proof of principle for PP2A inhibition as a viable antidepressant strategy, we compared control mice exposed only to the context to mice showing the highest failure rate, as readout of severe depressive symptoms. Half of LH mice were injected with vehicle and the other half systemically with LB-100, 24 hours after the shuttle box paradigm (**Fig. 6d**). Different batches of mice were then tested in the FST, for their sucrose preference, or in the shuttle box one week after the paradigm to assess depressive-like phenotypes. Vehicle-treated LH mice displayed decreased latency to the first immobility and increased total immobility in the FST, decreased sucrose preference, and high failure rates in escape behavior (**Figs. 6e–g**), indicating depressive-like symptoms. In contrast these parameters improved when treating LH animals with LB-100. We found that LH vehicle-treated mice presented a smaller I-Baclofen and increased excitability of LHb neurons compared to LH LB-100-treated mice (**Supplementary Fig. 9b**). These data suggest that inhibition of PP2A reverses GABA<sub>B</sub>-GIRK plasticity and hyperexcitability in the LHb in a more established model of depression.

## Discussion

Depressive-like symptoms in neuropsychiatric disorders occur along with hyperactivity of LHb neurons in rodents and humans<sup>7,8,24</sup>. This heightens the necessity to understand the underlying mechanisms of LHb hyperactivity and design viable tools to reverse these cellular adaptations and ultimately ameliorate depressive symptoms. Here we report that aversive experience weakens GABA<sub>B</sub>-GIRK signaling and increases LHb neuronal activity. FsE-induced reduction of I-Baclofen within the LHb occurs along with local increased PP2A activity and internalization of GABA<sub>B</sub>-Rs and GIRK channels leading to LHb neuronal hyperexcitability. PP2A inhibition rescues GABA<sub>B</sub>-GIRK signaling, LHb neuronal excitability and alleviates FsE-driven depressive-like phenotype. The therapeutic relevance of our findings is emphasized by the amelioration of depressive symptoms in a learned helplessness (LH) rodent model of depression by PP2A inhibition.

The LH model has the advantage to mimic, at least in part, etiology and symptomatology of human depression<sup>5,17,41</sup>. Nevertheless, to extend the validity of PP2A as a therapeutically relevant target for depressive symptoms, future studies will need to test its efficacy in additional alternative models such as social defeat or chronic mild stress<sup>42</sup>.

We describe that exposure to aversive events selectively depresses the dominant GIRK-dependent component of I-Baclofen via the internalization of both receptor and effector<sup>15,31–33</sup>. GABA<sub>B</sub>-R endocytosis requires the balance of AMP-activated protein kinase-dependent phosphorylation and consecutive PP2A-dependent de-phosphorylation of the S783 on the GABA<sub>B2</sub> subunit<sup>15,32,43</sup>. Indeed, we report a local increased PP2A activity after FsE in line with a scenario in which PP2A levels change upon stressful events<sup>34,35</sup>. Glutamate receptors and dopamine type 2 receptors can promote PP2A activity using *in vitro* preparation, suggesting potential, although yet to be proven, mechanisms of induction for the FsE-driven processes within the LHb<sup>44,45</sup>. We report that PP2A inhibition after aversive experience, not only restores its activity, but also rescues GABA<sub>B</sub>-GIRK function presumably redistributing GABA<sub>B</sub>-Rs from intracellular to membrane compartments.

While the above-described mechanisms regulate trafficking of GABA<sub>B</sub>-Rs, we find that endocytosis of GIRK channels occurs along with GABA<sub>B</sub>-Rs internalization after aversive experience. As predicted, GIRK2 overexpression within the LHb increases I-Baclofen in baseline conditions, and importantly it rescues FsE-driven GABA<sub>B</sub>-GIRK plasticity and depressive-like phenotype. This supports a scenario in which GABA<sub>B</sub>Rs and GIRK channels may internalize in a macromolecular signaling complex<sup>31,32,38,46–49</sup>. PP2A may therefore control GABA<sub>B</sub>-GIRK membrane dynamics either by solely targeting the GABA<sub>B</sub>Rs, or de-phosphorylating an intermediate accessory protein bridging GABA<sub>B</sub>Rs with GIRKs<sup>50</sup>.

How does the reduction of GABA<sub>B</sub>-GIRK signaling in the LHb contribute to the depressive symptoms? We show that, in the LHb, pharmacological GABA<sub>B</sub>R activation readily suppresses LHb neuronal firing, while in contrast GABA<sub>B</sub>R blockade produces increased activity. This indicates that LHb neuronal excitability is, at least in part, under a tonic GABA<sub>B</sub>-mediated control. Notably, increased excitatory drive onto LHb neurons and  $\beta$ CaMKII overexpression are sufficient to promote neuronal hyperexcitability and depressive symptoms<sup>7,8</sup>. Therefore, the FsE-evoked rapid GABA<sub>B</sub>-GIRK reduction in the LHb may represent either a permissive initial

cellular trigger for consequent adaptations such as  $\beta$ CaMKII-mediated synaptic modifications, or a parallel cellular process that contributes to LHB hyperactivity.

In light of the downstream projections of LHB neurons to midbrain targets, the FsE-induced depression of GABA<sub>B</sub>-GIRK signaling and LHB neuronal hyperactivity may have profound repercussions at the circuit level<sup>7,24</sup>. Our data indicate that FsE-evoked GABA<sub>B</sub>-GIRK plasticity occurs throughout the LHB, with no apparent territorial specificity. This suggests that FsE may alter neuronal populations within the LHB having diverse downstream targets<sup>51</sup>. Functional retrograde mapping of FsE-driven cellular modifications could further provide indications on whether modifications occur in LHB neurons sending axons to midbrain dopamine or GABA neurons or alternatively raphe serotonin neurons<sup>18</sup>. Together, these findings reveal an intracellular cascade within the LHB that may in turn remodel midbrain as well as other targets activity contributing to the establishment of depressive-like phenotypes<sup>26,52,53</sup>.

The rescue of an FsE-induced depressive symptom by local GIRK2a overexpression and inhibition of PP2A suggests the necessity of reduced GABA<sub>B</sub>-GIRK function within the LHB. This is consistent with the idea that a local intervention at the level of LHB, in rodents and humans, ameliorates depressive phenotypes<sup>7</sup>.

The pharmacotherapy for mood disorders makes use of serotonin-norepinephrine reuptake inhibitors, or tricyclic antidepressants<sup>54,55</sup>. However, the mechanistic-level understanding for their actions remains limited, and chronic treatments are necessary to achieve delayed beneficial effects<sup>55,5,25</sup>. Our results highlight PP2A inhibition as an efficient and rapid antidepressant strategy. LHB hyperactivity drives depressive symptoms also after exposure to addictive substances<sup>24,56</sup> potentially extending the use of this pharmacological strategy to disorders of a different etiology.

Although these observations provide a strong basis to explore the use of PP2A inhibitors to ameliorate depressive-like symptoms, further investigations need to assess its validity in the context of neuropsychiatry.

In conclusion, our findings indicate that experience with a strong aversive component reduces LHB GABA<sub>B</sub>-GIRK signaling removing a cellular “brake” on neuronal activity ultimately contributing to the emergence of depressive symptoms. Furthermore, the rescue of GABA<sub>B</sub>-GIRK signaling by targeting PP2A might open therapeutically-relevant strategies for disorders characterized by LHB hyperactivity.

### **Acknowledgements**

**We thank C. Bellone, M. Carta, E. Schwartz, C. Lüscher, F.J. Meye and the entire Mameli laboratory for discussions and comments on the manuscript. This work was supported by funds from the INSERM Atip-Avenir, ERC StG SalienSy 335333 and the Paris School of Neuroscience Network (ENP) to M.M. and from Junta de Comunidades de Castilla-La Mancha (PIII-2014-005-P) to R.L. The Mameli Laboratory is part of the network Initiative of Excellence Labex BioPsy. We thank J. Kovach and Lixte Biotechnology Holdings, Inc. for the gift of LB-100. The monoclonal antibody GABA<sub>B1</sub> (Clone N93A/49) was developed by the UC Davis/NIH NeuroMab Facility (Department of Neurobiology, Physiology and Behaviour, College of Biological Sciences, University of California, Davis, CA).**

### **Author Contributions**

**S.L. and M.M. performed and analyzed all of the in vitro electrophysiological recordings and behavioral experiments with the help of A.T., A.P. and D.H. designed and performed biochemical assays. I.M. performed immunohistochemistry and viral vector design. R.L. performed and analyzed the electron microscopy. S.L. and M.M. wrote the manuscript.**

### **Conflict of interests statement.**

**The authors declare no conflict of interests.**

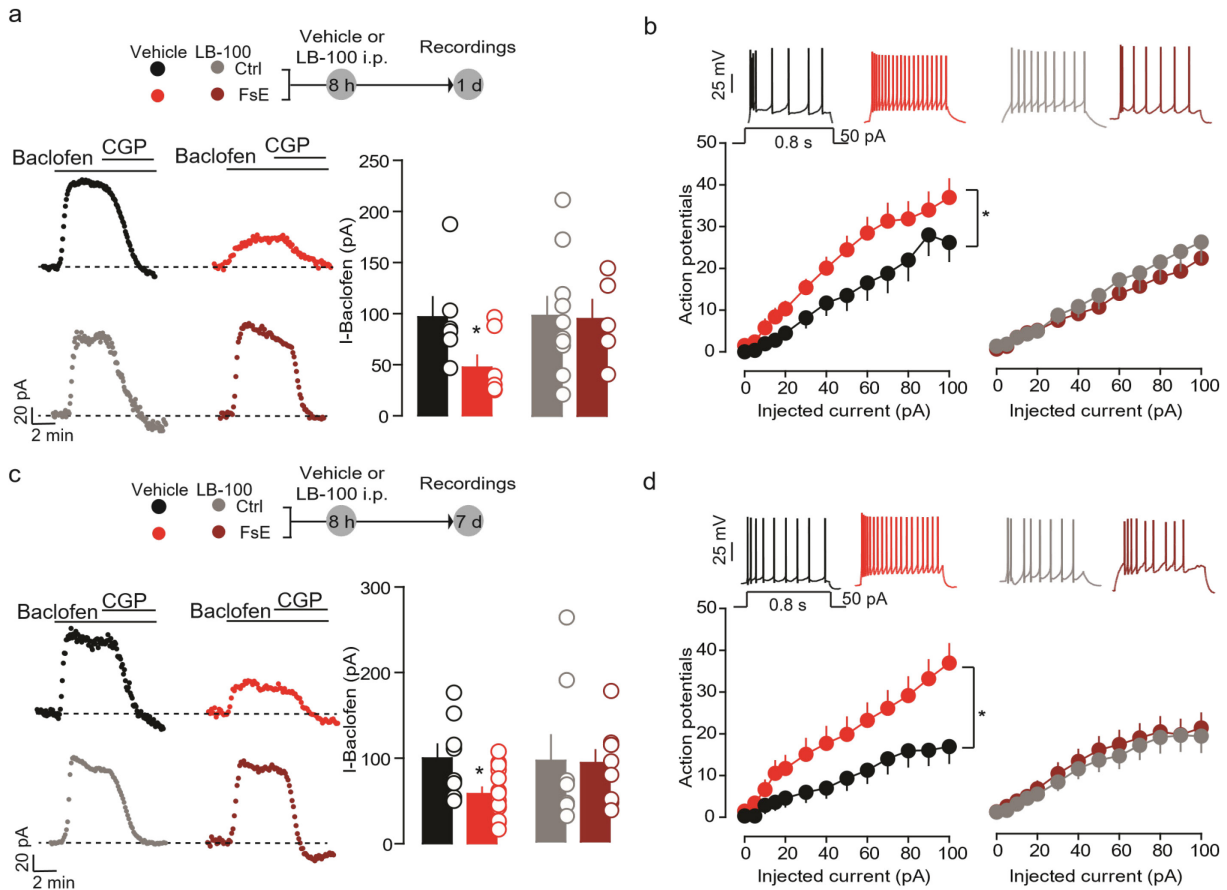
## References

1. Knoll, A. T. & Carlezon, W. A. J. Dynorphin, stress, and depression. *Brain Res* **1314**, 56-73 (2010).
2. Matsumoto, M. & Hikosaka, O. Lateral habenula as a source of negative reward signals in dopamine neurons. *Nature* **447**, 1111-1115 (2007).
3. Morris, J. S., Smith, K. A., Cowen, P. J., Friston, K. J. & Dolan, R. J. Covariation of activity in habenula and dorsal raphe nuclei following tryptophan depletion. *Neuroimage* **10**, 163-172 (1999).
4. Shumake, J., Edwards, E. & Gonzalez-Lima, F. Opposite metabolic changes in the habenula and ventral tegmental area of a genetic model of helpless behavior. *Brain Res* **963**, 274-281 (2003).
5. Chourbaji, S. et al. Learned helplessness: validity and reliability of depressive-like states in mice. *Brain Res Brain Res Protoc* **16**, 70-78 (2005).
6. Proulx, C. D., Hikosaka, O. & Malinow, R. Reward processing by the lateral habenula in normal and depressive behaviors. *Nat Neurosci* **17**, 1146-1152 (2014).
7. Li, B. et al. Synaptic potentiation onto habenula neurons in the learned helplessness model of depression. *Nature* **470**, 535-539 (2011).
8. Li, K. et al. betaCaMKII in lateral habenula mediates core symptoms of depression. *Science* **341**, 1016-1020 (2013).
9. Brown, P. L. & Shepard, P. D. Lesions of the fasciculus retroflexus alter footshock-induced cFos expression in the mesopontine rostromedial tegmental area of rats. *PLoS One* **8**, e60678 (2013).
10. Bagdy, G., Juhasz, G. & Gonda, X. A new clinical evidence-based gene-environment interaction model of depression. *Neuropsychopharmacol Hung* **14**, 213-220 (2012).
11. Fatemi, S. H., Folsom, T. D. & Thuras, P. D. Deficits in GABA(B) receptor system in schizophrenia and mood disorders: a postmortem study. *Schizophr Res* **128**, 37-43 (2011).
12. Cryan, J. F. & Slattery, D. A. GABAB receptors and depression. Current status. *Adv Pharmacol* **58**, 427-451 (2010).
13. Kawaura, K., Honda, S., Soeda, F., Shirasaki, T. & Takahama, K. [Novel antidepressant-like action of drugs possessing GIRK channel blocking action in rats]. *Yakugaku Zasshi* **130**, 699-705 (2010).
14. Llamosas, N., Bruzos-Cidon, C., Rodriguez, J. J., Ugedo, L. & Torrecilla, M. Deletion of GIRK2 Subunit of GIRK Channels Alters the 5-HT1A Receptor-Mediated Signaling and Results in a Depression-Resistant Behavior. *Int J Neuropsychopharmacol* **18**, (2015).
15. Terunuma, M., Pangalos, M. N. & Moss, S. J. Functional modulation of GABAB receptors by protein kinases and receptor trafficking. *Adv Pharmacol* **58**, 113-122 (2010).
16. Overmier, J. B. & Seligman, M. E. Effects of inescapable shock upon subsequent escape and avoidance responding. *J Comp Physiol Psychol* **63**, 28-33 (1967).
17. Vollmayr, B. & Henn, F. A. Learned helplessness in the rat: improvements in validity and reliability. *Brain Res Brain Res Protoc* **8**, 1-7 (2001).
18. Lecca, S., Meye, F. J. & Mameli, M. The lateral habenula in addiction and depression: an anatomical, synaptic and behavioral overview. *Eur J Neurosci* **39**, 1170-1178 (2014).
19. Breier, A. et al. Controllable and uncontrollable stress in humans: alterations in mood and neuroendocrine and psychophysiological function. *Am J Psychiatry* **144**, 1419-1425 (1987).
20. Maier, S. F. Learned helplessness and animal models of depression. *Prog Neuropsychopharmacol Biol Psychiatry* **8**, 435-446 (1984).
21. Stamatakis, A. M. & Stuber, G. D. Activation of lateral habenula inputs to the ventral midbrain promotes behavioral avoidance. *Nat Neurosci* **15**, 1105-1107 (2012).
22. Luthi, A. & Luscher, C. Pathological circuit function underlying addiction and anxiety disorders. *Nat Neurosci* **17**(12), 1635-1643 (2014).
23. Porsolt, R. D., Bertin, A. & Jalfre, M. Behavioral despair in mice: a primary screening test for antidepressants. *Arch Int Pharmacodyn Ther* **229**, 327-336 (1977).
24. Meye, F. J. et al. Cocaine-evoked negative symptoms require AMPA receptor trafficking in the lateral habenula. *Nat Neurosci* **18**, 376-378 (2015).
25. Shabel, S. J., Proulx, C. D., Piriz, J. & Malinow, R. Mood regulation. GABA/glutamate co-release controls habenula output and is modified by antidepressant treatment. *Science* **345**, 1494-1498 (2014).
26. Luscher, C. & Slesinger, P. A. Emerging roles for G protein-gated inwardly rectifying potassium (GIRK) channels in health and disease. *Nat Rev Neurosci* **11**, 301-315 (2010).
27. Logothetis, D. E., Kurachi, Y., Galper, J., Neer, E. J. & Clapham, D. E. The beta gamma subunits of GTP-binding proteins activate the muscarinic K<sup>+</sup> channel in heart. *Nature* **325**, 321-326 (1987).
28. Buynitsky, T. & Mostofsky, D. I. Restraint stress in biobehavioral research: Recent developments. *Neurosci Biobehav Rev* **33**, 1089-1098 (2009).
29. Takahashi, L. K., Nakashima, B. R., Hong, H. & Watanabe, K. The smell of danger: a behavioral and neural



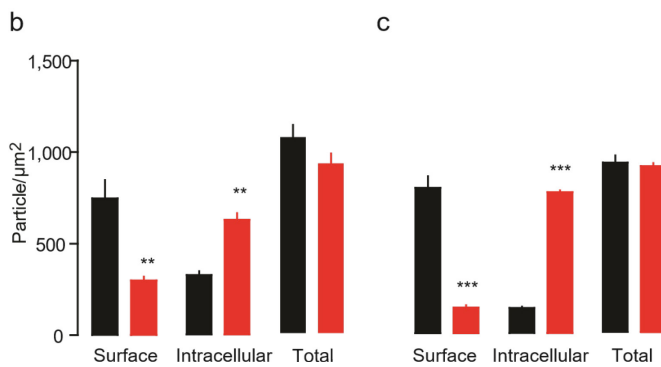
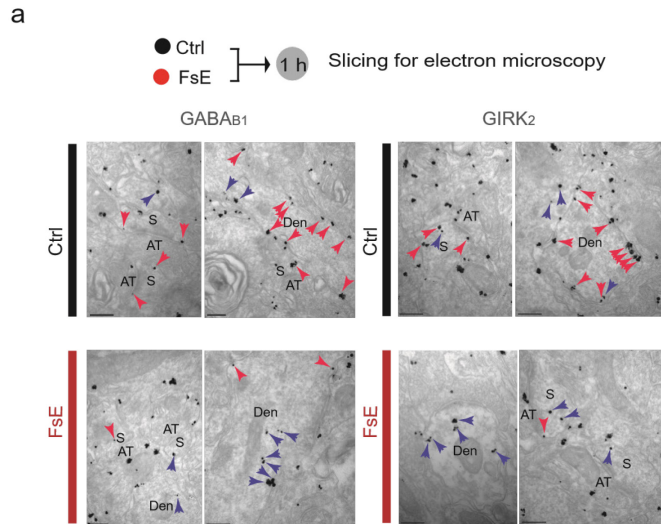
- analysis of predator odor-induced fear. *Neurosci Biobehav Rev* **29**, 1157-1167 (2005).
30. Zucker, R. S. & Regehr, W. G. Short-term synaptic plasticity. *Annu Rev Physiol* **64**, 355-405 (2002).
  31. Hearing, M. et al. Repeated cocaine weakens GABA(B)-GIRK signaling in layer 5/6 pyramidal neurons in the prelimbic cortex. *Neuron* **80**, 159-170 (2013).
  32. Padgett, C. L. et al. Methamphetamine-evoked depression of GABA(B) receptor signaling in GABA neurons of the VTA. *Neuron* **73**, 978-989 (2012).
  33. Guetg, N. et al. NMDA receptor-dependent GABAB receptor internalization via CaMKII phosphorylation of serine 867 in GABAB1. *Proc Natl Acad Sci U S A* **107**, 13924-13929 (2010).
  34. Morinobu, S. et al. Influence of immobilization stress on the expression and phosphatase activity of protein phosphatase 2A in the rat brain. *Biol Psychiatry* **54**, 1060-1066 (2003).
  35. Mucic, G., Sase, S., Stork, O., Lubec, G. & Li, L. Networks of protein kinases and phosphatases in the individual phases of contextual fear conditioning in the C57BL/6J mouse. *Behav Brain Res* **280**, 45-50 (2015).
  36. Lu, J. et al. Inhibition of serine/threonine phosphatase PP2A enhances cancer chemotherapy by blocking DNA damage induced defense mechanisms. *Proc Natl Acad Sci U S A* **106**, 11697-11702 (2009).
  37. Jourdain, P., Fukunaga, K. & Muller, D. Calcium/calmodulin-dependent protein kinase II contributes to activity-dependent filopodia growth and spine formation. *J Neurosci* **23**, 10645-10649 (2003).
  38. Lalive, A. L. et al. Firing modes of dopamine neurons drive bidirectional GIRK channel plasticity. *J Neurosci* **34**, 5107-5114 (2014).
  39. Wei, D. et al. Inhibition of protein phosphatase 2A radiosensitizes pancreatic cancers by modulating CDC25C/CDK1 and homologous recombination repair. *Clin Cancer Res* **19**, 4422-4432 (2013).
  40. Wang, M., Perova, Z., Arenkiel, B. R. & Li, B. Synaptic modifications in the medial prefrontal cortex in susceptibility and resilience to stress. *J Neurosci* **34**, 7485-7492 (2014).
  41. Strekalova, T., Spanagel, R., Bartsch, D., Henn, F. A. & Gass, P. Stress-induced anhedonia in mice is associated with deficits in forced swimming and exploration. *Neuropsychopharmacology* **29**, 2007-2017 (2004).
  42. Menard, C., Hodes, G. E. & Russo, S. J. Pathogenesis of depression: Insights from human and rodent studies. *Neuroscience* (2015).
  43. Gonzalez-Maeso, J., Wise, A., Green, A. & Koenig, J. A. Agonist-induced desensitization and endocytosis of heterodimeric GABAB receptors in CHO-K1 cells. *Eur J Pharmacol* **481**, 15-23 (2003).
  44. Beaulieu, J. M. et al. An Akt/beta-arrestin 2/PP2A signaling complex mediates dopaminergic neurotransmission and behavior. *Cell* **122**, 261-273 (2005).
  45. Chan, S. F. & Sucher, N. J. An NMDA receptor signaling complex with protein phosphatase 2A. *J Neurosci* **21**, 7985-7992 (2001).
  46. Lavine, N. et al. G protein-coupled receptors form stable complexes with inwardly rectifying potassium channels and adenylyl cyclase. *J Biol Chem* **277**, 46010-46019 (2002).
  47. Nobles, M., Benians, A. & Tinker, A. Heterotrimeric G proteins precouple with G protein-coupled receptors in living cells. *Proc Natl Acad Sci U S A* **102**, 18706-18711 (2005).
  48. Riven, I., Iwanir, S. & Reuveny, E. GIRK channel activation involves a local rearrangement of a preformed G protein channel complex. *Neuron* **51**, 561-573 (2006).
  49. Clancy, S. M., Boyer, S. B. & Slesinger, P. A. Coregulation of natively expressed pertussis toxin-sensitive muscarinic receptors with G-protein-activated potassium channels. *J Neurosci* **27**, 6388-6399 (2007).
  50. Lujan, R., Marron Fernandez de Velasco, E., Aguado, C. & Wickman, K. New insights into the therapeutic potential of GIRK channels. *Trends Neurosci* **37**, 20-29 (2014).
  51. Lammel, S. et al. Input-specific control of reward and aversion in the ventral tegmental area. *Nature* **491**, 212-217 (2012).
  52. Jhou, T. C., Fields, H. L., Baxter, M. G., Saper, C. B. & Holland, P. C. The rostromedial tegmental nucleus (RMTg), a GABAergic afferent to midbrain dopamine neurons, encodes aversive stimuli and inhibits motor responses. *Neuron* **61**, 786-800 (2009).
  53. Tye, K. M. et al. Dopamine neurons modulate neural encoding and expression of depression-related behaviour. *Nature* **493**, 537-541 (2013).
  54. Nemeroff, C. B. The neurobiology of depression. *Sci Am* **278**, 42-49 (1998).
  55. Henn, F. A. Pharmacogenetic studies of depression. *Biol Psychiatry* **63**, 1101-1102 (2008).
  56. Jhou, T. C. et al. Cocaine drives aversive conditioning via delayed activation of dopamine-responsive habenular and midbrain pathways. *J Neurosci* **33**, 7501-7512 (2013).

## Figures



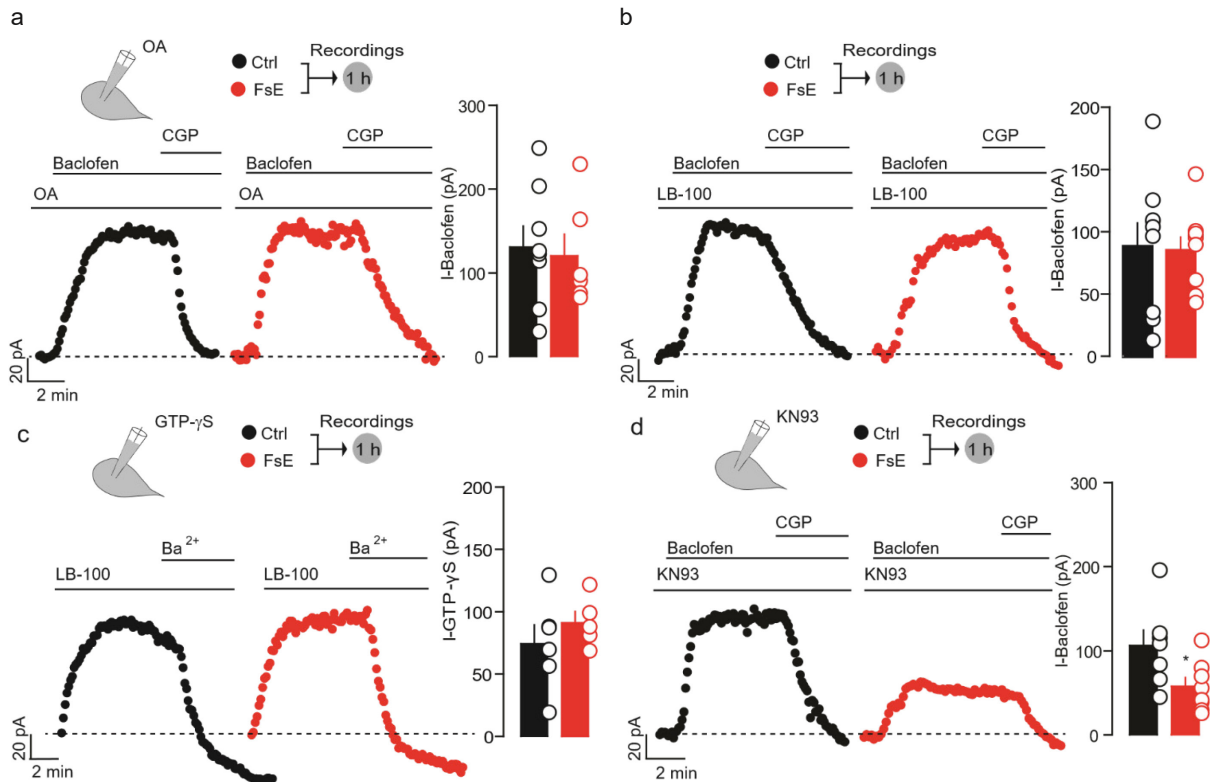
**Figure 1** FsE induces cellular adaptations in the LHb and a depressive-like phenotype.

**(a)** Context re-exposure (ReC) 1 day after the procedure (Ctrl vs FsE  $n_{mice} = 8$ ;  $1.2 \pm 0.8$  vs  $55.6 \pm 8.3\%$ ,  $t$ -test:  $t_{14} = 6.5$ ;  $***P < 0.001$ ). **(b)** Forced swim test (FST) in all experimental groups. Latency to first immobility (left, Ctrl  $n_{mice} = 10$  vs FsE  $n_{mice} = 11$ ;  $61.1 \pm 6.3$  vs  $45.2 \pm 4.3$  s;  $t$ -test,  $t_{19} = 2.12$ ;  $*P < 0.05$ ) and total immobility (right, Ctrl vs FsE;  $131.1 \pm 16.1$  vs  $199.7 \pm 9.0$  s;  $t$ -test,  $t_{19} = 3.82$ ,  $**P < 0.01$ ). **(c)** Site of recordings (scale bar, 1 mm). **(d)** Timeline and sample traces. Right, action potentials vs injected current in all experimental groups (Ctrl vs FsE;  $n_{mice} = 3$ ;  $n_{cells} = 12-14$ ; two way ANOVA repeated measure (RM)  $F_{1,288} = 4.78$ ,  $*P < 0.05$ ). **(e)** Baclofen-activated currents (I-Baclofen) in Ctrl and FsE conditions. Right, I-Baclofen at different time points (Ctrl  $n_{mice} = 4$  vs FsE 1 hour  $n_{mice} = 5$ , 1 day  $n_{mice} = 4$ , 7 days  $n_{mice} = 3$ , 14 days  $n_{mice} = 2$ , 30 days  $n_{mice} = 2$ ;  $n_{cells} = 7-15$ ;  $104.5 \pm 11.3$  vs  $55.4 \pm 7.2$ ,  $59.8 \pm 9.6$ ,  $40.1 \pm 9.0$ ,  $39.6 \pm 6.6$ ,  $133.0 \pm 26.1$  pA; one way ANOVA and Dunnett's test,  $F_{5,64} = 9.1$ ,  $***P < 0.0001$ ,  $**P < 0.001$ ,  $*P < 0.05$ ). **(f)** GTP- $\gamma$ S-evoked currents, bar graphs and scatter plot (Ctrl vs FsE;  $n_{mice} = 3$ ;  $n_{cells} = 6$ ;  $92.5 \pm 21.8$  vs  $38.0 \pm 5.3$  pA;  $t$ -test,  $t_{10} = 2.43$ ,  $*P < 0.05$ ). Data are represented as mean  $\pm$  s.e.m..



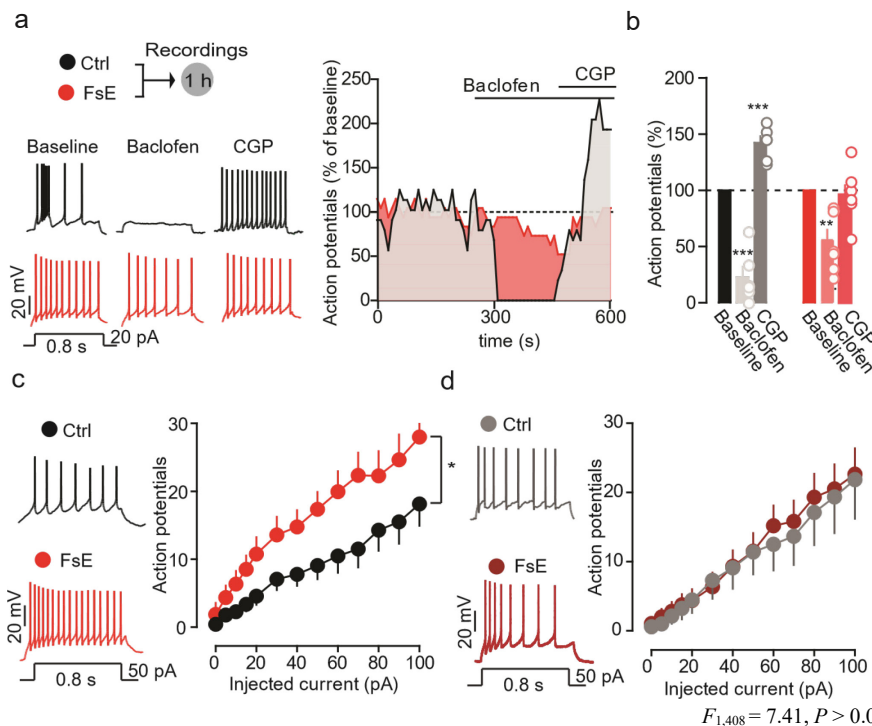
## Figure 2 Subcellular plasticity of GABA<sub>B</sub>Rs and GIRKs in the Lhb

**(a)** Timeline of experiment and examples of pre-embedding immunoreactivity for GABA<sub>B1</sub> and GIRK2. Immunoparticles for GABA<sub>B1</sub> and GIRK2 found along the plasma membrane (red arrows) and intracellularly (blue arrows) as well as at dendritic spines (S), dendritic shafts (Den) and axon terminals (AT). Scale bars, 0.2 μm. **(b)** Bar graph representing the surface, intracellular and total particle of GABA<sub>B1</sub> in slices from Ctrl and FsE mice. (Ctrl vs FsE,  $n_{mice} = 3$ ; Surface,  $747.0 \pm 58.0$  vs  $298.7 \pm 22.2$  particle/μm<sup>2</sup>  $t$ -test,  $t_4 = 7.21$ ,  $**P < 0.01$ ; Intracellular,  $328.7 \pm 16.8$  vs  $633.0 \pm 36.3$  particle/μm<sup>2</sup>  $t$ -test,  $t_4 = 7.92$ ,  $**P < 0.01$ ; Total,  $1,076.0 \pm 69.1$  vs  $931.7 \pm 55.9$  particle/μm<sup>2</sup>  $t$ -test,  $t_4 = 1.62$ ,  $P > 0.05$ ). **(c)** Same as **(b)** but for immunoparticles of GIRK2 (Surface,  $796.7 \pm 36.7$  vs  $142.7 \pm 12.1$  particle/μm<sup>2</sup>,  $t$ -test,  $t_4 = 16.93$ ,  $***P < 0.0001$ ; Intracellular,  $139.7 \pm 6.7$  vs  $773.7 \pm 10.3$  particle/μm<sup>2</sup>  $t$ -test,  $t_4 = 51.50$ ,  $***P < 0.0001$ ; Total,  $936.3 \pm 40.4$  vs  $916.3 \pm 17.8$  particle/μm<sup>2</sup>  $t$ -test,  $t_4 = 0.45$ ,  $P > 0.05$ ). Data are represented as mean ± s.e.m..



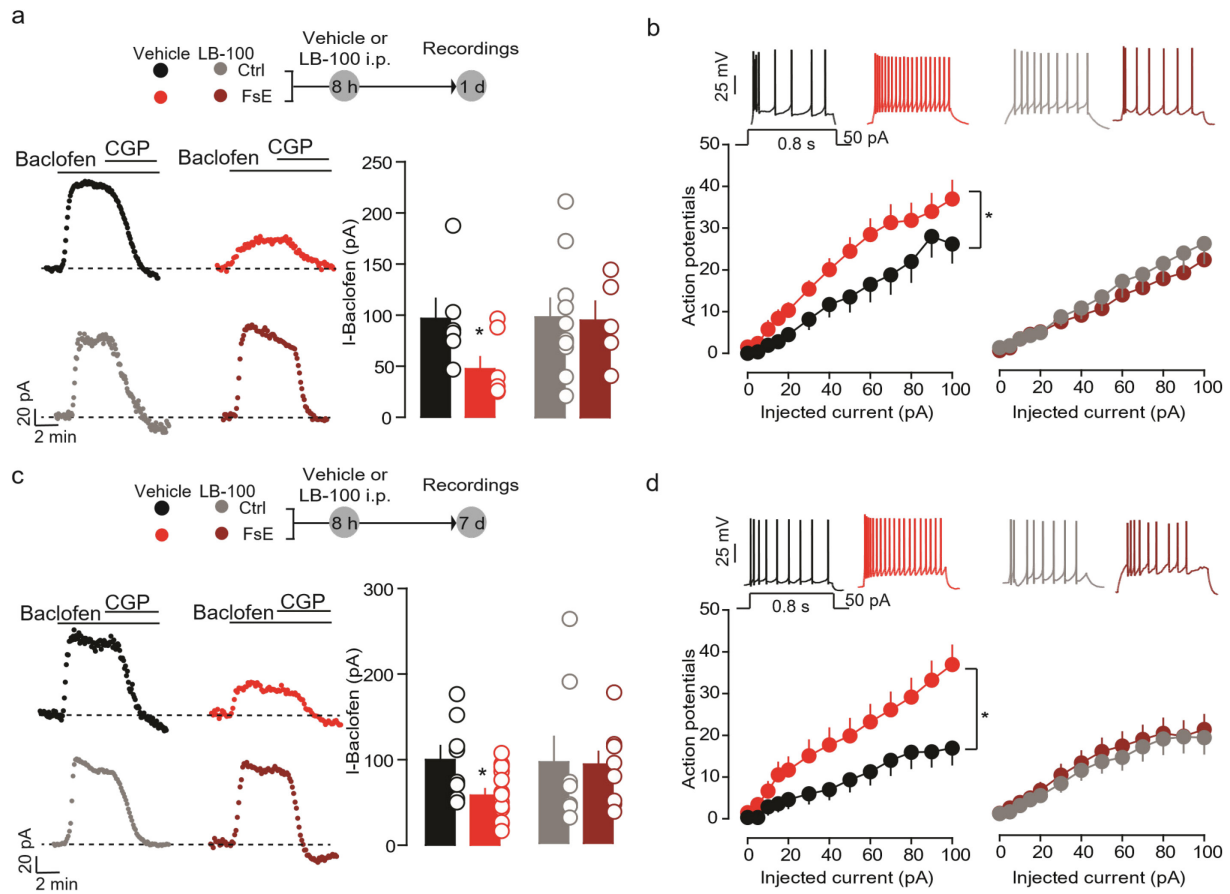
**Figure 3 PP2A inhibition rescues GABA<sub>B</sub>-GIRK function in the Lhb after FsE**

(a) Timeline, protocols of the experiments and sample traces obtained in presence of PP2A-PP1 inhibitor okadaic acid (OA, 100 nM) in the internal solution. Bar graph and scatter plot of I-Baclofen in the presence of OA (Ctrl  $n_{mice} = 2$  vs FsE  $n_{mice} = 3$ ;  $n_{cells} = 6-8$ ;  $130.7 \pm 25.2$  pA vs  $120.4 \pm 25.6$  pA;  $t$ -test,  $t_{12} = 0.28$ ,  $P > 0.05$ ). (b) Sample traces and graph showing the effect of LB-100 (0.1  $\mu$ M) bath application on I-Baclofen (Ctrl vs FsE;  $n_{mice} = 3$ ;  $n_{cells} = 9$ ;  $88.4 \pm 18.6$  vs  $85.1 \pm 10.7$  pA;  $t$ -test,  $t_{16} = 0.15$ ,  $P > 0.05$ ). (c) LB-100 restored also the Ba<sup>2+</sup>-sensitive I-GTP- $\gamma$ S in FsE animals (Ctrl vs FsE;  $n_{mice} = 3$ ;  $n_{cells} = 6$ ;  $94.3 \pm 13.3$  vs  $110.6 \pm 20.8$  pA;  $t$ -test,  $t_{10} = 0.66$ ,  $P > 0.05$ ). (d) Sample traces and graph showing the effect of CaMKII inhibitor KN93 dialysis (10  $\mu$ M) on I-Baclofen (Ctrl  $n_{mice} = 2$  vs FsE  $n_{mice} = 3$ ;  $n_{cells} = 7-8$ ,  $106.3 \pm 18.4$  vs  $57.8 \pm 10.4$  pA;  $t$ -test,  $t_{13} = 2.37$ ,  $*P < 0.05$ ). Data are represented as mean  $\pm$  s.e.m..



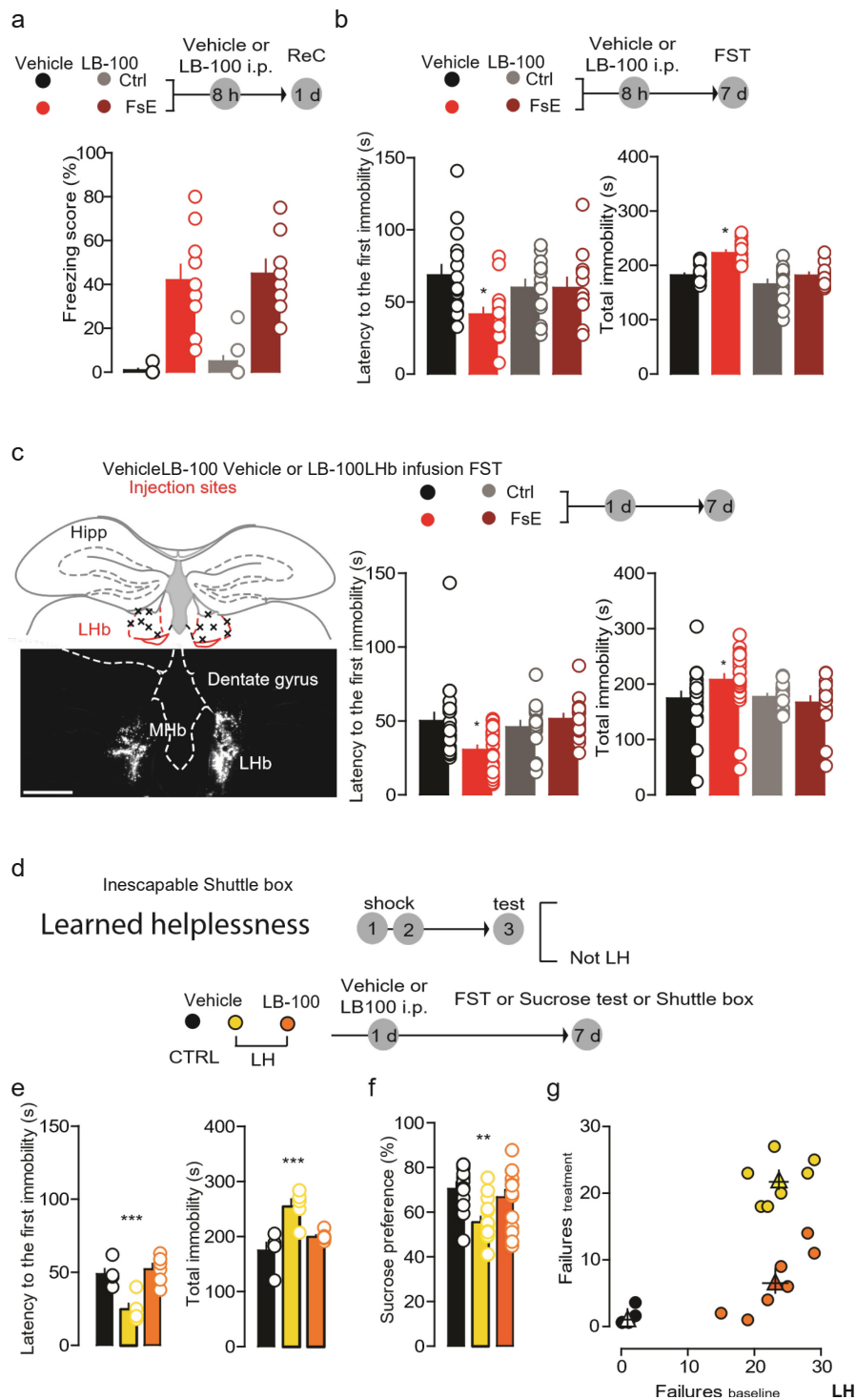
**Figure 4 GABA<sub>B</sub>-R-dependent control of activity in the Lhb after FsE**

(a) Protocol, sample traces (20 pA) and time vs firing plot representing GABA<sub>B</sub>-dependent modulation of action potential frequency in Ctrl and FsE. (b) Bar graph and scatter plot for the baclofen and CGP-dependent modulation of Lhb neurons activity in Ctrl and FsE mice (Ctrl vs FsE,  $n_{mice} = 3$ ;  $n_{cells} = 6-7$ ; two way ANOVA RM, interaction,  $F_{2,22} = 14.5$ ;  $***P < 0.0001$ ). Baclofen-dependent inhibition in Ctrl is larger than in FsE group (two way ANOVA multiple comparison,  $t_{33} = 3.2$ ;  $**P < 0.01$ ), while CGP application fails to increase activity (FsE, baseline vs CGP, Dunnett's post hoc test,  $P > 0.05$ ). (c) Sample traces (50 pA injected) and action potentials obtained from Ctrl and FsE (Ctrl  $n_{mice} = 4$  vs FsE  $n_{mice} = 5$ ;  $n_{cells} = 14-17$ ; two way ANOVA RM,  $F_{1,348} = 7.41$ ,  $*P < 0.05$ ). (d) Same as (c) but in the presence of LB-100 (Ctrl  $n_{mice} = 4$  vs FsE  $n_{mice} = 5$ ;  $n_{cells} = 16-20$ ; two way ANOVA RM,  $F_{1,408} = 7.41$ ,  $P > 0.05$ ). Data are represented as mean  $\pm$  s.e.m..



**Figure 5 PP2A inhibition *in vivo* rescues GABA<sub>B</sub>-GIRK function and hyperexcitability in the LHb**

**(a)** *In vivo* experimental protocol and timeline of experiments. I-Baclofen current, graph and scatter plot in all experimental groups (1.5 mg/kg i.p.) (vehicle: Ctrl vs FsE;  $n_{mice} = 3$ ;  $n_{cells} = 6-7$ ;  $96.7 \pm 19.6$  vs  $47.4 \pm 11.8$  pA; *t*-test,  $t_{11} = 2.23$ ,  $*P < 0.05$ ; LB-100; Ctrl  $n_{mice} = 2$  vs FsE  $n_{mice} = 3$ ;  $n_{cells} = 5-10$ ;  $93.9 \pm 18.4$  vs  $97.0 \pm 18.0$  pA; *t*-test,  $t_{13} = 0.11$ ,  $P > 0.05$ ). **(b)** Sample traces and input-output curve after LB-100 (vehicle; Ctrl  $n_{mice} = 4$  vs FsE  $n_{mice} = 3$ ;  $n_{cells} = 13-14$ ; two way ANOVA RM,  $F_{1,300} = 4.71$ ,  $*P < 0.05$ ; LB-100; Ctrl  $n_{mice} = 3$  vs FsE  $n_{mice} = 4$ ;  $n_{cells} = 12-15$ ; two way ANOVA RM,  $F_{1,300} = 0.43$ ,  $P > 0.05$ ). **(c)** Same as **(a)** but at 7 days (vehicle; Ctrl  $n_{mice} = 3$  vs FsE  $n_{mice} = 4$ ;  $n_{cells} = 8-14$ ;  $99.8 \pm 16.4$  vs  $58.3 \pm 7.6$  pA; *t*-test,  $t_{20} = 2.62$ ,  $*P < 0.05$ ; LB-100; Ctrl vs FsE;  $n_{mice} = 3$ ;  $n_{cells} = 8-9$ ;  $95.5 \pm 30.0$  vs  $93.0 \pm 14.8$  pA; *t*-test,  $t_{15} = 0.079$ ,  $P > 0.05$ ). **(d)** Same as **(b)** but at 7 days (vehicle; Ctrl  $n_{mice} = 3$  vs FsE  $n_{mice} = 5$ ;  $n_{cells} = 15-24$ ; two way ANOVA RM,  $F_{1,444} = 5.19$ ,  $*P < 0.05$ ; LB-100; Ctrl  $n_{mice} = 3$  vs FsE  $n_{mice} = 4$ ;  $n_{cells} = 16-19$ ; two way ANOVA RM,  $F_{1,396} = 0.20$ ,  $P > 0.05$ ). Data are represented as mean  $\pm$  s.e.m..

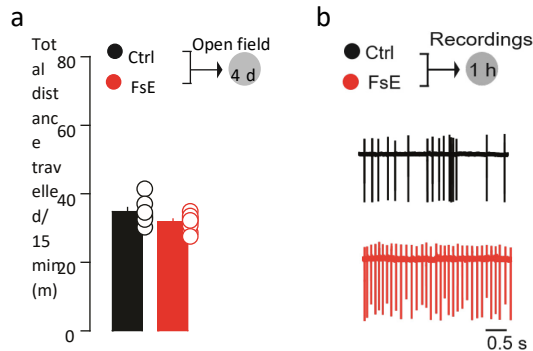


**Figure 6 PP2A inhibition ameliorates core symptoms of depression**

(a) Systemic LB-100 and freezing behavior (Ctrl<sub>vehicle</sub>, FsE<sub>vehicle</sub>, Ctrl<sub>LB-100</sub>, FsE<sub>LB-100</sub>;  $n_{mice} = 10, 10, 11, 8$  respectively; two way ANOVA, interaction,  $F_{1,35} = 0.01$ ,  $P > 0.05$ ). (b) FST analysis (Ctrl<sub>vehicle</sub>, FsE<sub>vehicle</sub>, Ctrl<sub>LB-100</sub>, FsE<sub>LB-100</sub>;  $n_{mice} = 16, 16, 14, 12$  respectively; latency to the first immobility: two way ANOVA, interaction,  $F_{1,54} = 4.90$ ,  $*P < 0.05$ ; total immobility: two way ANOVA, interaction,  $F_{1,54} = 4.44$ ,  $*P < 0.05$ ). (c) Left, schematic and sample image for local LB-100 infusion. Scale bar, 400  $\mu$ m. Right, FST analysis for LB-100 local infusion (Ctrl<sub>vehicle</sub>, FsE<sub>vehicle</sub>, Ctrl<sub>LB-100</sub>, FsE<sub>LB-100</sub>;  $n_{mice} = 21, 26, 16, 16$  respectively; latency to the first immobility: two way ANOVA, interaction,  $F_{1,75} = 9.06$ ,  $**P < 0.01$ ; total immobility: two way ANOVA, interaction,  $F_{1,75} = 3.96$ ,  $*P = 0.05$ ). (d) Learned helplessness protocol and LB-100 treatment. (e) Bar graph and scatter plot for FST analysis (Ctrl<sub>vehicle</sub>, LH<sub>vehicle</sub>, LH<sub>LB-100</sub>;  $n_{mice} = 5, 5, 6$  respectively; latency to the first immobility: one way ANOVA,  $F_{2,15} = 15.1$ ,  $***P < 0.001$ ; total immobility: one way ANOVA,  $F_{2,15} = 13.5$ ;  $***P < 0.001$ ). (f) Sucrose preference across all experimental groups (Ctrl<sub>vehicle</sub>, LH<sub>vehicle</sub>, LH<sub>LB-100</sub>;  $n_{mice} = 12, 15, 14$  respectively; one way ANOVA,  $F_{2,41} = 6.89$ ,  $**P < 0.002$ ). (g) Scatter plot indicating failure rates in escaping behavior in all experimental groups (Ctrl<sub>vehicle</sub>, LH<sub>vehicle</sub>, LH<sub>LB-100</sub>;  $n_{mice} = 7$ ; two way ANOVA RM, interaction,  $F_{2,18} = 77.06$ ,  $***P < 0.0001$ ). Data are represented as mean  $\pm$  s.e.m..



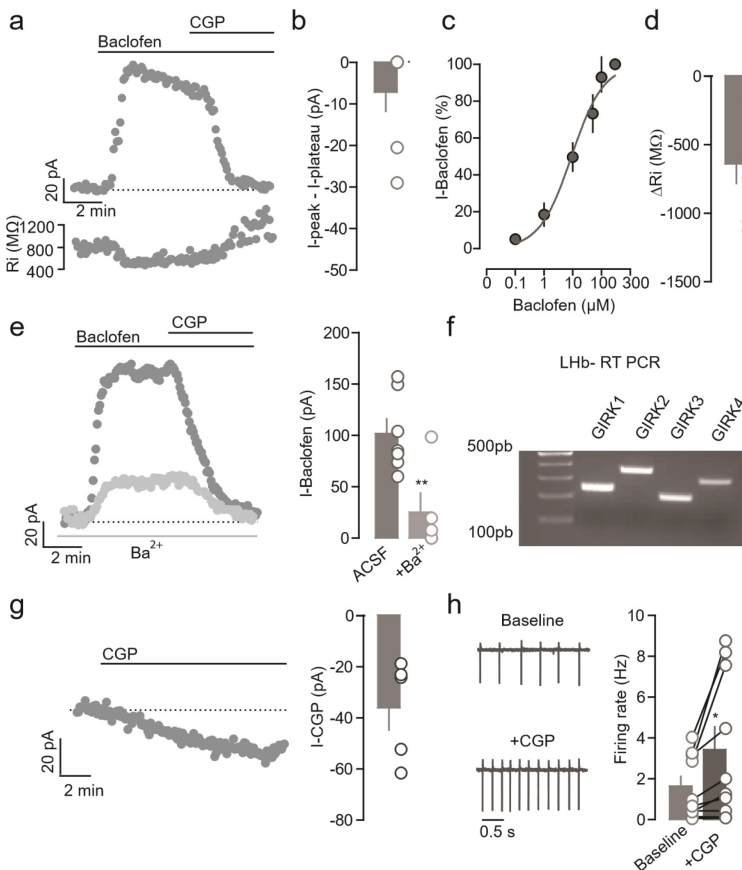
## Supplemental information



### Supplementary Figure 1 **FsE does not affect locomotor activity and increases Lhb neuronal firing rate**

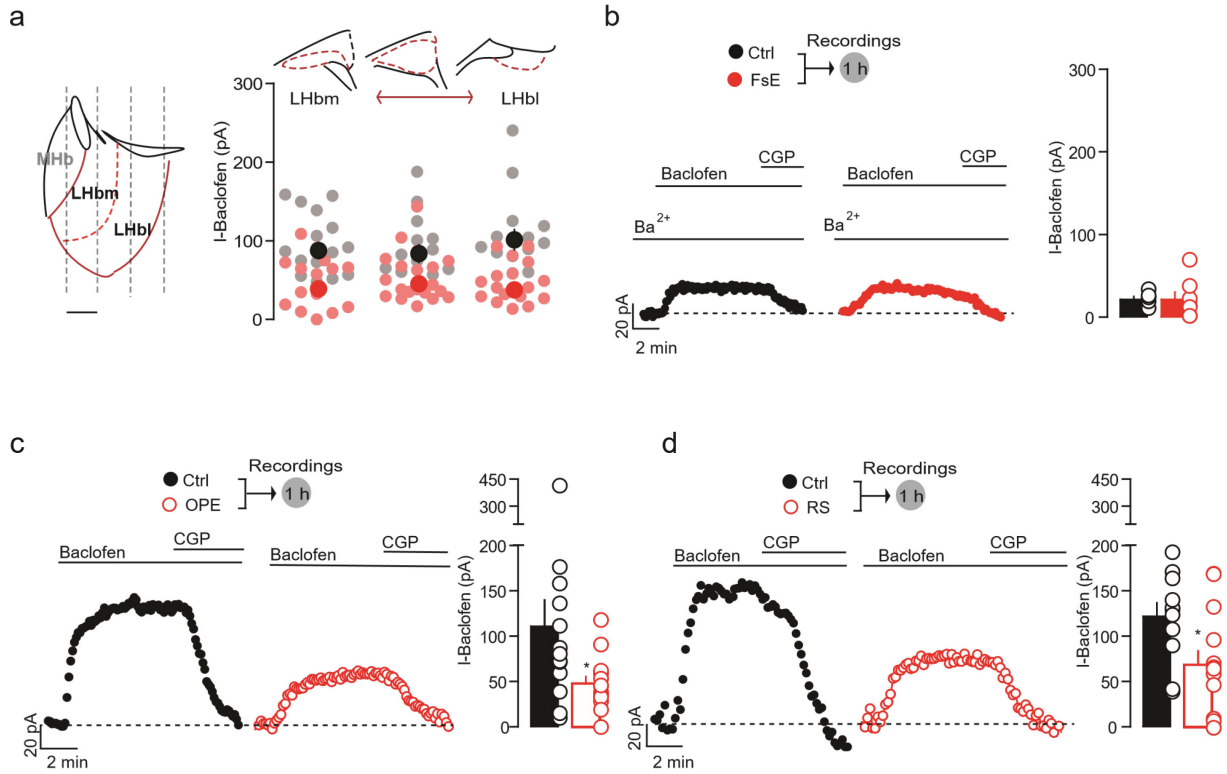
**(a)** Bar graph and scatter plot reporting locomotion in the open field (Ctrl vs FsE;  $n_{mice} = 8$ ;  $34.4 \pm 1.2$  vs  $31.8 \pm 0.8$  m;  $t$ -test,  $t_{14} = 2.03$ ;  $P > 0.05$ ). **(b)** Representative traces from two cells recorded in a Ctrl (black) and FsE (red) mouse. Right, bar graph and scatter plot for basal action potential firing recorded in cell-attached mode in the Ctrl and FsE groups (Ctrl vs FsE;  $n_{mice} = 8$ ;  $n_{cells} = 42-43$ ;  $3.1 \pm 0.9$  vs  $5.8 \pm 1.3$  Hz;

Mann Whitney test;  $**P < 0.01$ ). Data are represented as mean  $\pm$  s.e.m..



### Supplementary Figure 2 **Properties of GABA<sub>B</sub>-GIRK signaling in the Lhb**

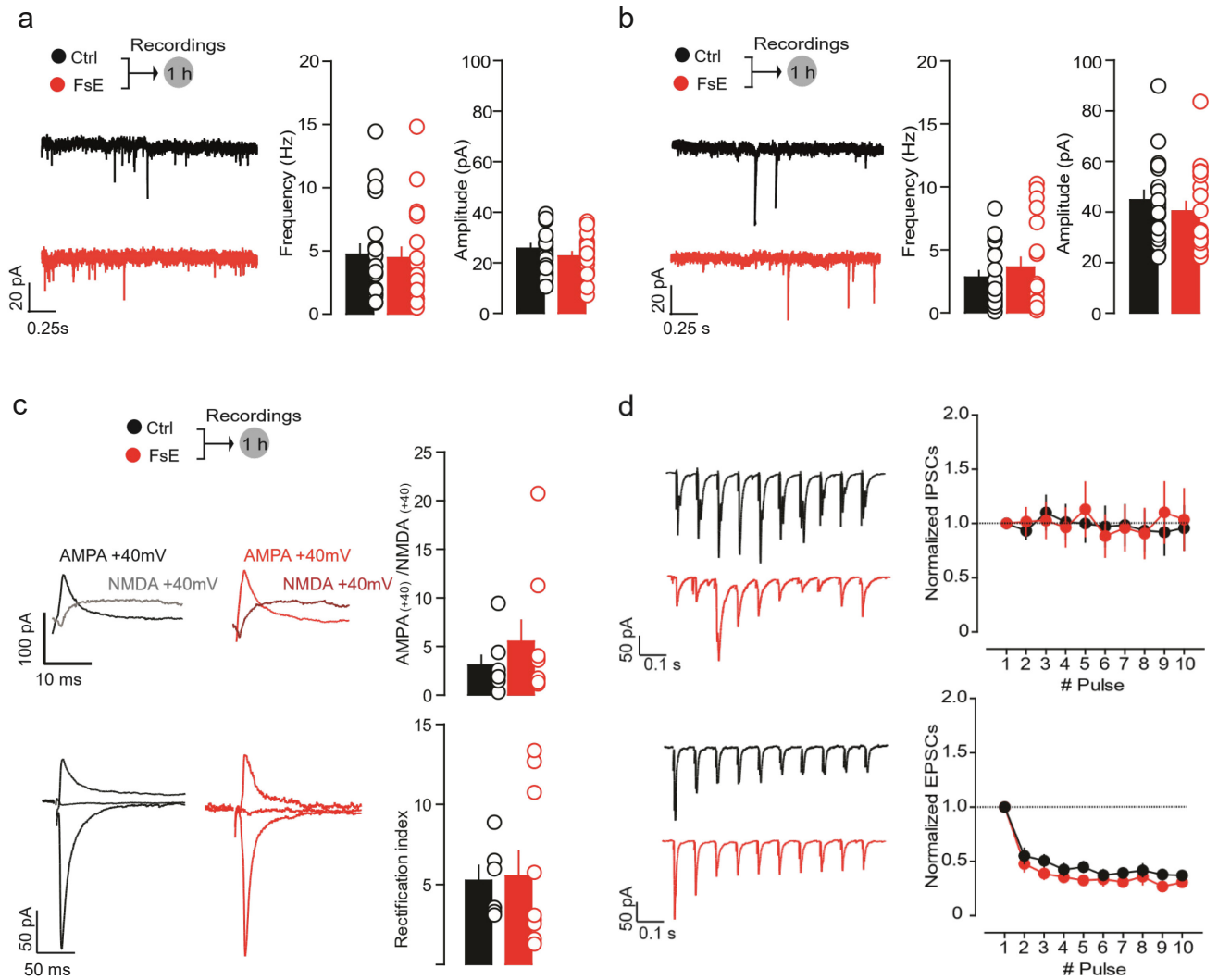
**(a)** I-Baclofen sample (100  $\mu$ M) and simultaneous reduction in input resistance in Lhb neuron. **(b)** Lhb neurons show minimal current desensitization after the GABA<sub>B</sub> activation ( $n_{mice} = 3$ ;  $n_{cells} = 7$ ,  $I_{peak} - I_{plateau} = -7.1 \pm 4.6$  pA) **(c)** Dose-response curve ( $n_{mice} = 3$ ;  $n_{cells} = 5$ ,  $EC_{50} = 9.0 \pm 1.0$   $\mu$ M; Hill-slope =  $0.8 \pm 0.1$ ) **(d)** Bar graph representing Baclofen-mediated changes in input resistance ( $n_{mice} = 3$ ;  $n_{cells} = 7$ ,  $\Delta Ri = -639.2 \pm 142.9$  M $\Omega$ ) **(e)** Traces and bar graph depicting the I-Baclofen without (darker trace) and with (brighter trace) barium in the bath ( $Ba^{2+}$ , 1 mM) (without vs in presence of  $Ba^{2+}$ ;  $n_{mice} = 2$ ;  $n_{cells} = 5-7$ ;  $101.7 \pm 14.2$  vs  $25.2 \pm 18.7$  pA,  $t$ -test,  $t_{10} = 3.3$ ,  $**P < 0.01$ ) **(f)** RT-PCR qualitative expression of GIRK subunits **(g)** Sample trace and bar graph unmasking GABA<sub>B</sub>Rs function at baseline after bath application of CGP54626 ( $n_{mice} = 2$ ;  $n_{cells} = 5$ ,  $I-CGP = -36.0 \pm 8.7$  pA) **(h)** Example traces reporting the firing activity of a Lhb neuron record in cell-attached mode before and after CGP54626 (10  $\mu$ M) bath application ( $n_{mice} = 3$ ;  $n_{cells} = 10$ , paired  $t$ -test,  $t_9 = 2.7$ ,  $*P < 0.05$ ). Data are represented as mean  $\pm$  s.e.m..



**Supplementary Figure 3 FsE and painless aversive experience weakens GABA<sub>B</sub>-GIRK signaling throughout the LHB**

(a) LHB-containing coronal section illustrating the medial habenula (MHb) and the LHB in its medial (LHbm) and lateral division (LHbl). Dotted gray lines represent sagittal sections. Bar scale: 250  $\mu$ m. Right, schematics and graph reporting the medio-lateral distribution of the recordings (x axis) and the I-Baclofen (y-axis) in Ctrl and FsE mice (brighter scatter plot represent single recordings; darker symbols report the mean  $\pm$  s.e.m.). (b) Sample I-Baclofen, bar graphs and scatter plots in presence of Ba<sup>2+</sup> (1 mM). (Ctrl  $n_{mice}$  = 2 vs FsE  $n_{mice}$  = 3,  $n_{cells}$  = 5–7;  $21.3 \pm 3.7$  vs  $21.3 \pm 9.1$  pA;  $t$ -test,  $t_{10}$  = 0.002,  $P > 0.05$ ). (c) Sample traces, bar graphs and scatter plot representing I-Baclofen recorded from LHB neurons in Ctrl mice and 1h after the odor predator exposure (OPE, fox urine) (Ctrl vs OPE,  $n_{mice}$  = 4,  $n_{cells}$  = 13–14;  $110.5 \pm 29.1$  vs  $47.4 \pm 7.9$  pA;  $t$ -test,  $t_{25}$  = 2.16,  $*P < 0.05$ ). (d) Same as (c) but for Ctrl mice and animals subjected to restraint stress (RS, 1 hour) (Ctrl  $n_{mice}$  = 3 vs RS  $n_{mice}$  = 4,  $n_{cells}$  = 11–14;  $121.7 \pm 14.8$  vs  $68.3 \pm 15.3$  pA;  $t$ -test,  $t_{23}$  = 2.46,  $*P < 0.05$ ). Data are represented as mean  $\pm$  s.e.m..

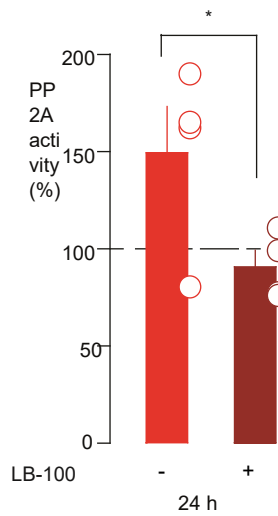




### Supplementary Figure 4 FsE does not affect the fast glutamatergic and GABAergic transmission

(a) Sample traces, bar graphs and scatter plot showing mEPSCs frequency and amplitude recorded from Lhb neurons in Ctrl and FsE mice (Ctrl vs FsE;  $n_{\text{mice}} = 5$ ,  $n_{\text{cells}} = 20-21$ ; Frequency,  $4.7 \pm 0.8$  vs  $4.5 \pm 0.8$  Hz, Mann Whitney test,  $P > 0.05$ ; Amplitude,  $25.7 \pm 1.8$  vs  $22.7 \pm 1.7$  pA,  $t$ -test,  $t_{39} = 1.21$ ,  $P > 0.05$ ). (b) Same as (a) but for mIPSCs (Ctrl vs FsE;  $n_{\text{mice}} = 5$ ;  $n_{\text{cells}} = 20$ ; Frequency,  $2.8 \pm 0.5$  vs  $3.6 \pm 0.7$  Hz;  $t$ -test,  $t_{38} = 0.86$ ,  $P > 0.05$ ; Amplitude,  $44.8 \pm 3.7$  vs  $40.4 \pm 3.7$  pA;  $t$ -test,  $t_{38} = 0.82$ ,  $P > 0.05$ ). (c) Timeline of experiments, representative traces and bar graph for the AMPA/NMDA ratio (top, Ctrl vs FsE,  $n_{\text{mice}} = 3$ ,  $n_{\text{cells}} = 8-9$ ;  $3.1 \pm 0.9$  vs  $5.5 \pm 2.2$ ; Mann Whitney test,  $P > 0.05$ ) and the rectification index (bottom, Ctrl vs FsE,  $n_{\text{mice}} = 3$ ,  $n_{\text{cells}} = 6-10$ ;  $5.2 \pm 0.9$  vs  $5.5 \pm 1.5$ ;  $t$ -test,  $t_{14} = 0.14$ ,  $P > 0.05$ ). (d) Example traces and graph of evoked inhibitory post synaptic currents (eIPSCs, 20 Hz train, top panel) (Ctrl  $n_{\text{mice}} = 4$  vs FsE  $n_{\text{mice}} = 5$ ;  $n_{\text{cells}} = 18-22$ ; two way ANOVA repeated measures (RM),  $F_{1,342} = 0.01$ ,  $P > 0.05$ ). The bottom panel shows traces and graph of a 20 Hz train of evoked excitatory post-synaptic currents (eEPSCs; Ctrl vs FsE;  $n_{\text{mice}} = 3$ ,  $n_{\text{cells}} = 8-7$ ; two way ANOVA RM,  $F_{1,117} = 1.72$ ,  $P > 0.05$ ). Data are represented as mean  $\pm$  s.e.m..

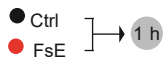
a



**Supplementary Figure 5 FsE-driven enhancement of PP2A activity within the LHb is reversed by *in vivo* treatment with LB-100.**

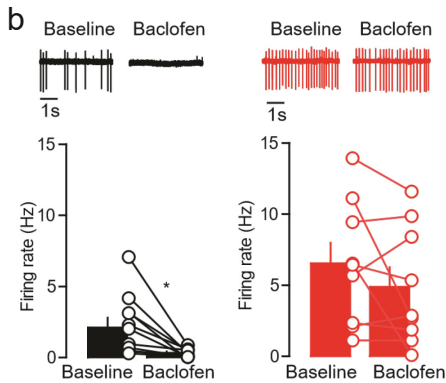
(a) Bar graph and scatter plot showing the PP2A activity within the habenula 24 hours after FsE, with or without LB-100 treatment. Bar graphs report normalized values versus control conditions (%) (FsE<sub>vehicle</sub> vs FsE<sub>LB-100</sub> % of control;  $n_{mice} = 40$ ;  $n_{replicates} = 10-10$ ;  $150.9 \pm 22.4$  vs  $90.8 \pm 8.5$  %;  $t$ -test,  $t_6 = 2.51$ ,  $*P < 0.05$ ). LB-100 treatment did not alter baseline PP2A activity (Raw values. Ctrl<sub>vehicle</sub> vs Ctrl<sub>LB-100</sub>;  $n_{mice} = 24$ ;  $n_{replicates} = 6-6$ ;  $556 \pm 39.7$  vs  $428.7 \pm 84.22$  pmoles;  $t$ -test,  $t_{10} = 1.36$ ,  $P > 0.05$ ). Data are represented as mean  $\pm$  s.e.m..

a



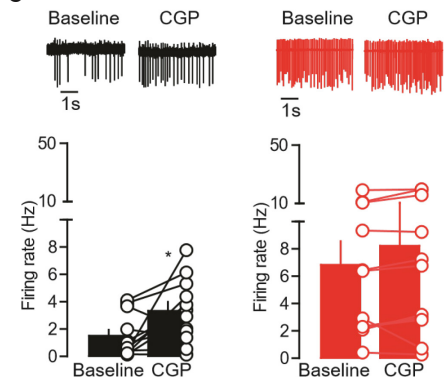
**Supplementary Figure 6 Loss of GABA<sub>B</sub>-mediated modulation of firing in LHb after FsE**

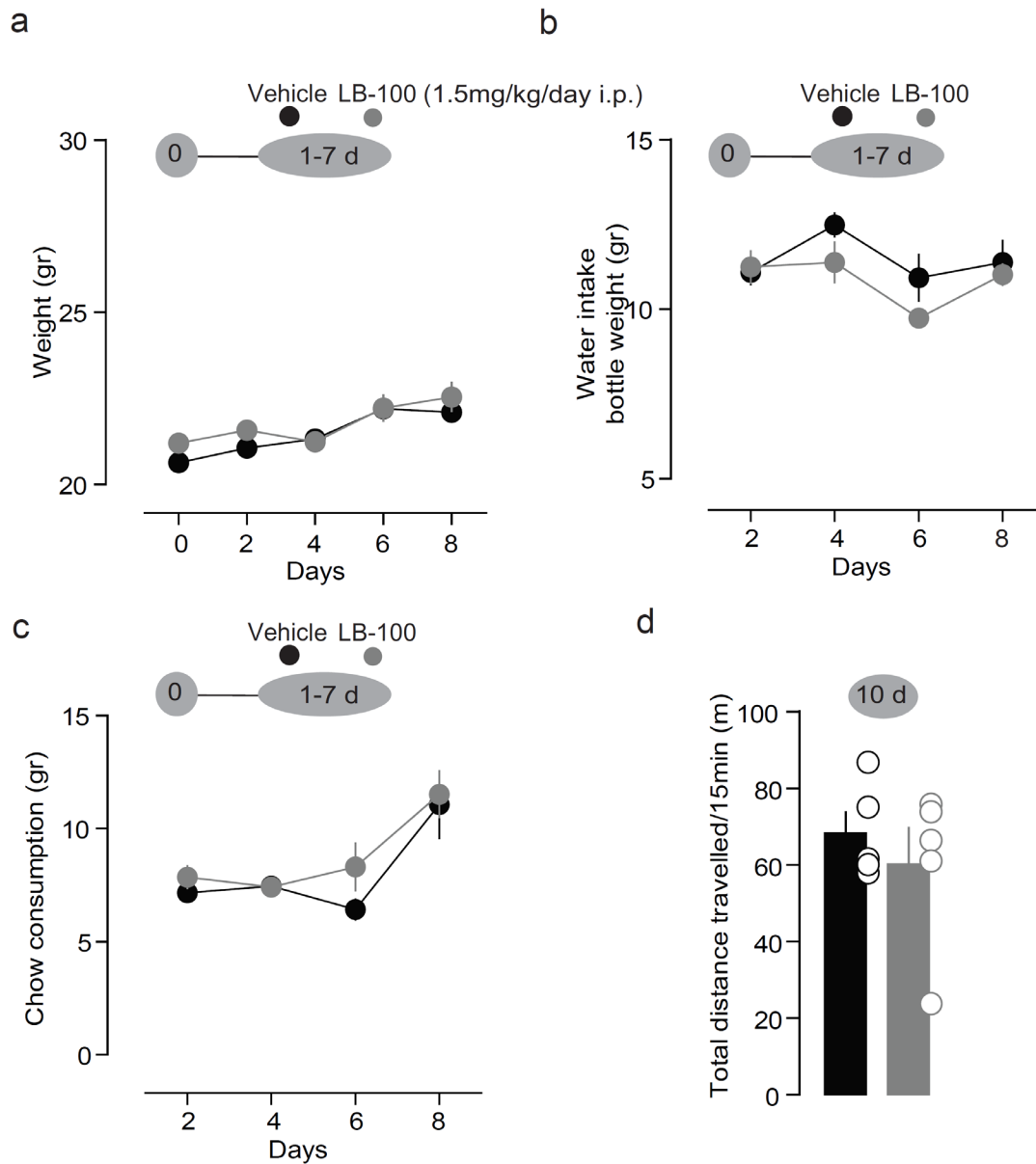
b



(a) Timeline of cell attached recordings. (b) Baclofen (100  $\mu$ M) differentially affects the firing activity of LHb neurons in Ctrl (left) and FsE (right) (Ctrl,  $n_{mice} = 4$ ;  $n_{cells} = 10$ ; Baseline vs Baclofen,  $2.1 \pm 0.7$  vs  $0.3 \pm 0.1$  Hz; paired  $t$ -test,  $t_9 = 2.98$ ,  $*P < 0.05$ ) (FsE,  $n_{mice} = 4$ ;  $n_{cells} = 9$ , Baseline vs Baclofen,  $6.5 \pm 1.4$  vs  $4.9 \pm 1.4$  Hz; paired  $t$ -test,  $t_8 = 1.38$ ,  $P > 0.05$ ). (c) CGP54626 (10  $\mu$ M) increases the firing rate in Ctrl (left) but not in FsE (right) (Ctrl,  $n_{mice} = 4$ ,  $n_{cells} = 10$ ; Baseline vs CGP,  $1.7 \pm 0.5$  vs  $3.8 \pm 0.7$  Hz; paired  $t$ -test,  $t_9 = 2.53$ ,  $*P < 0.05$ ) (FsE,  $n_{mice} = 4$ ;  $n_{cells} = 11$ , Baseline vs Baclofen,  $6.8 \pm 1.7$  vs  $8.2 \pm 2.2$  Hz; paired  $t$ -test,  $t_{10} = 1.56$ ,  $P > 0.05$ ). Data are represented as mean  $\pm$  s.e.m.

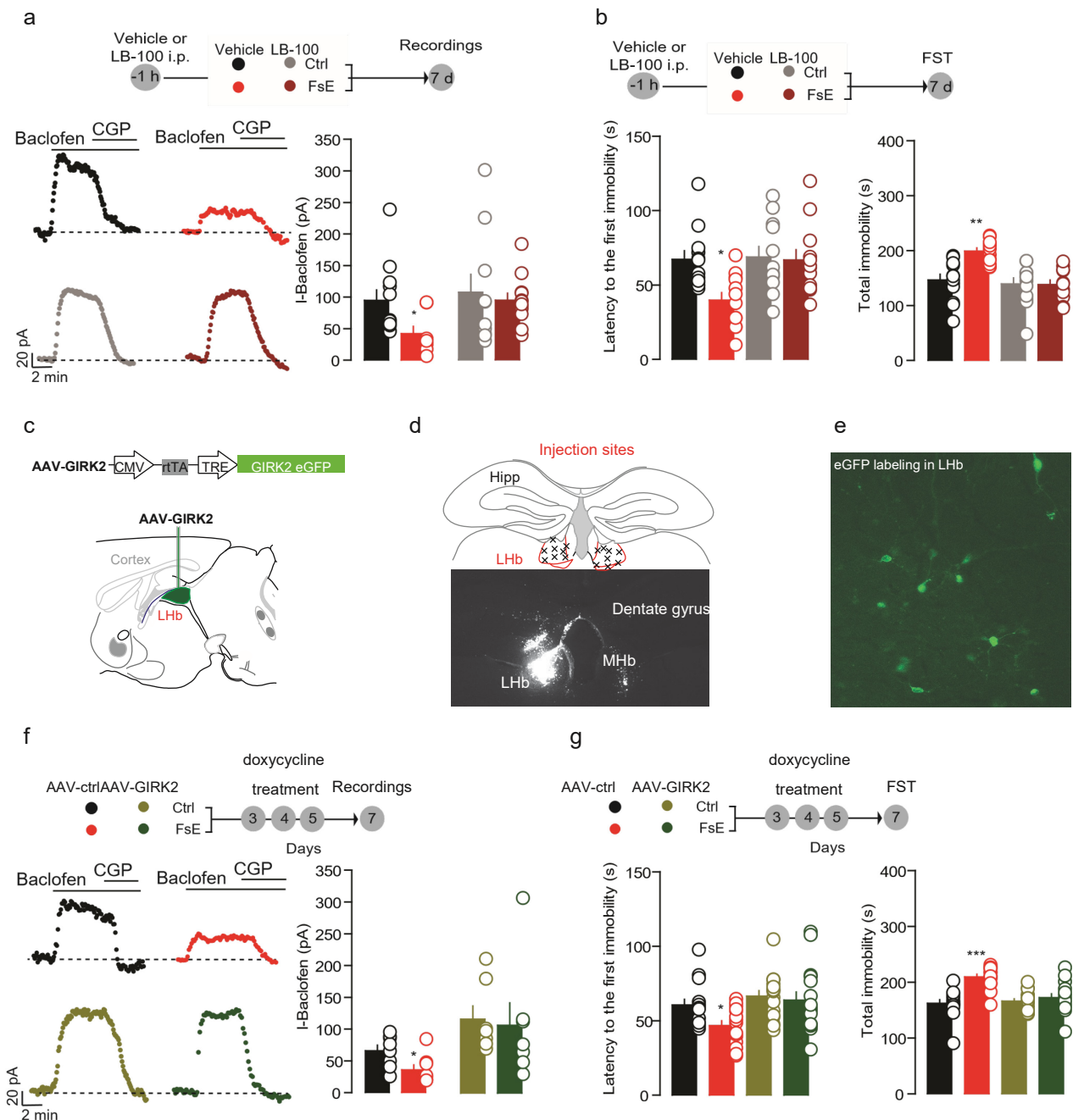
c





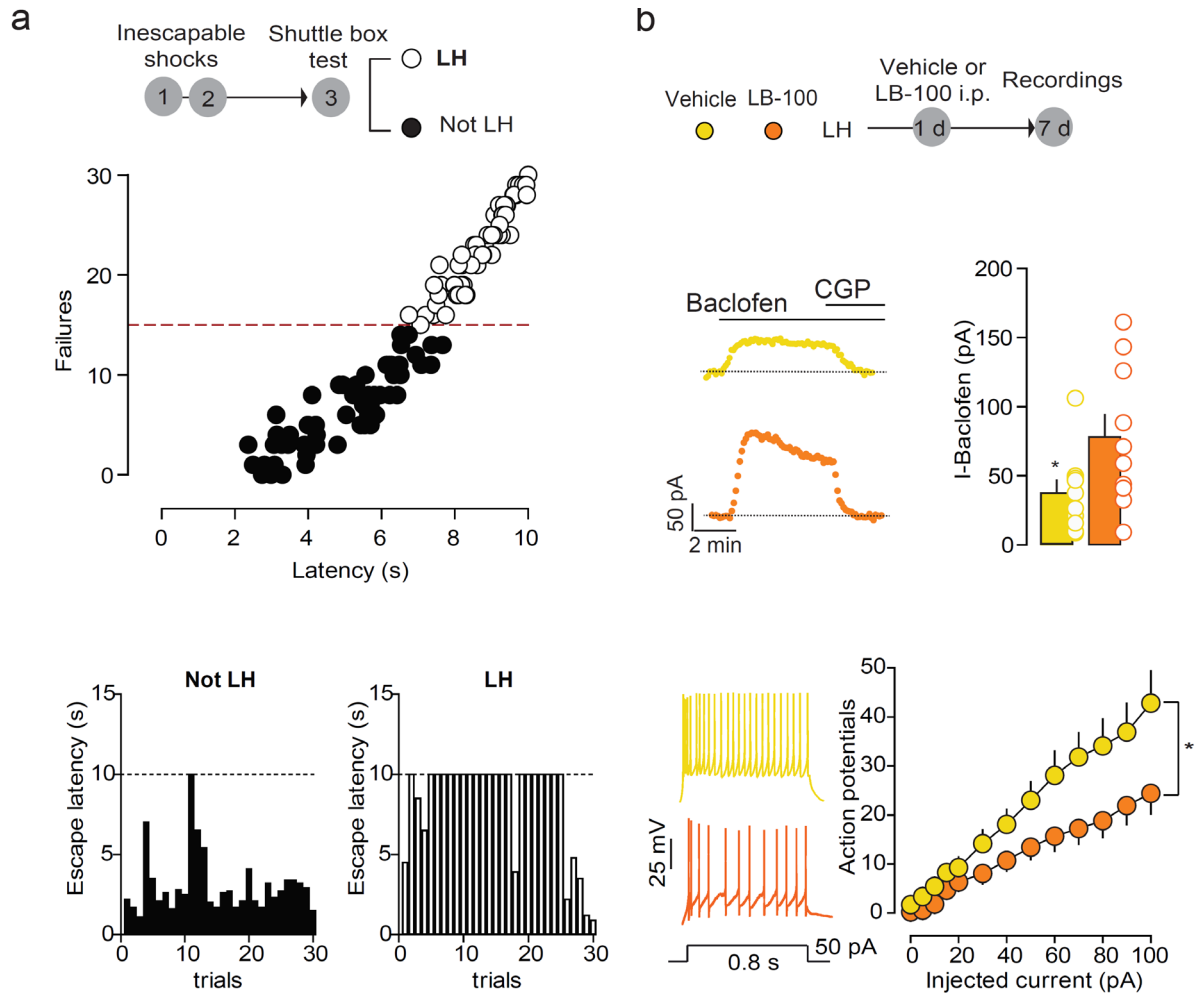
**Supplementary Figure 7 Safe profile of LB-100 treatment *in vivo***

**(a)** Experimental protocol. Time course representing the weight gain during the treatment (vehicle vs LB-100;  $n_{\text{mice}} = 5$ ; two way ANOVA RM;  $F_{1,32} = 0.86$ ;  $P > 0.05$ ). **(b)** Time course of water consumption during the treatment (vehicle vs LB-100;  $n_{\text{mice}} = 5$ ; two way ANOVA RM;  $F_{1,24} = 1.72$ ;  $P > 0.05$ ). **(c)** Chow consumption (vehicle vs LB-100;  $n_{\text{mice}} = 5$ ; two way ANOVA RM;  $F_{1,24} = 0.81$ ;  $P > 0.05$ ). **(d)** Bar graph and scatter plot showing locomotor activity (vehicle vs LB-100;  $n_{\text{mice}} = 5$ ;  $68.26 \pm 5.5$  vs  $60.17 \pm 9.5$  m;  $t$ -test;  $t_8 = 0.93$ ;  $P > 0.05$ ). Data are represented as mean  $\pm$  s.e.m..



**Supplementary Figure 8 LB-100 pre-treatment and Lhb-GIRK2 overexpression prevent and rescue GABA<sub>B</sub>-GIRK plasticity and depressive-like states**

(a) Schematic of the protocol, representative traces and bar graphs showing the effect of LB-100 pre-treatment on GABA<sub>B</sub>-GIRK plasticity in the Lhb (vehicle: Ctrl vs FsE;  $n_{\text{mice}} = 3$ ,  $n_{\text{cells}} = 12-8$ ;  $94.9 \pm 16.5$  vs  $42.4 \pm 11.5$  pA;  $t$ -test,  $t_{18} = 2.36$ ,  $*P < 0.05$ ; LB-100; Ctrl vs FsE;  $n_{\text{mice}} = 3$ ,  $n_{\text{cells}} = 10-12$ ;  $106.9 \pm 28.6$  vs  $94.6 \pm 11.0$  pA;  $t$ -test,  $t_{20} = 0.42$ ,  $P > 0.05$ ). (b) Schematic of the protocol and bar graphs reporting the FST analysis (Ctrl vs FsE and vehicle vs LB-100;  $n_{\text{mice}} = 12$ ; latency to the first immobility: two way ANOVA, interaction,  $F_{1,44} = 4.11$ ,  $*P < 0.05$ ; total immobility: two way ANOVA, interaction,  $F_{1,44} = 8.59$ ,  $*P < 0.05$ ). (c) AAV-based construct designed for the doxycycline-inducible overexpression of GIRK2a and schematic of experimental protocol. (d) Representative brain coronal section including the site of injections for the behavioral experiments. Scale bar: 400  $\mu\text{m}$ . (e) Lhb immunostaining for the GIRK2a-eGFP upon doxycycline treatment. Scale bar, 20  $\mu\text{m}$ . (f) Schematic of the protocol, representative traces and bar graphs showing the effect of GIRK2a overexpression on FsE-induced I-Baclofen reduction (AAV-ctrl: Ctrl vs FsE;  $n_{\text{mice}} = 3$ ,  $n_{\text{cells}} = 8$ ;  $65.7 \pm 8.9$  vs  $35.8 \pm 7.9$  pA;  $t$ -test,  $t_{14} = 2.51$ ,  $*P < 0.05$ ; AAV-GIRK2: Ctrl vs FsE;  $n_{\text{mice}} = 3$ ,  $n_{\text{cells}} = 7$ ;  $116.6 \pm 20.8$  vs  $107.0 \pm 35.2$  pA;  $t$ -test,  $t_{12} = 0.23$ ,  $P > 0.05$ ; AAV-ctrl Ctrl vs AAV-GIRK2 Ctrl;  $t$ -test,  $t_{13} = 2.35$ ,  $*P < 0.05$ ). (g) Schematic of the protocol and bar graphs for FST (Ctrl<sub>AAV-ctrl</sub>, FsE<sub>AAV-ctrl</sub>, Ctrl<sub>AAV-GIRK2</sub>, FsE<sub>AAV-GIRK2</sub>  $n_{\text{mice}} = 15, 15, 17, 16$  respectively; latency to the first immobility: two way ANOVA, treatment,  $F_{1,59} = 7.47$ ,  $**P < 0.01$ ; total immobility: two way ANOVA, interaction,  $F_{1,59} = 13.4$ ,  $***P < 0.001$ ). Data are represented as mean  $\pm$  s.e.m..



**Supplementary Figure 9 Learned helplessness in mice and cellular plasticity in LHB**

(a) On the top, the graph shows the behavioral measurements (escape latency and failures) to assess the learned helplessness. Single dot plot represents individual mouse performance (LH= 59 mice; not LH= 60 mice). On the bottom, the graphs illustrate the behavioral measurement for two representative mice. Each graph reports the escape latency (y-axis) during the trials (x-axis). (b) Schematic of the experiments, sample traces and bar graph showing that LB-100 treatment (1.5 mg/kg i.p.) improves I-baclofen in the LH model (top panel, LH<sub>vehicle</sub> vs LH<sub>LB-100</sub>;  $n_{mice} = 2$ ,  $n_{cells} = 10$ ;  $37.5 \pm 9.1$  vs  $78.0 \pm 16.1$  pA;  $t$ -test,  $t_{18} = 2.18$ ,  $*P < 0.05$ ). On the bottom the representative traces and the graph illustrate the reduced excitability in the LH mice treated with LB-100 (LH<sub>vehicle</sub> vs LH<sub>LB-100</sub>;  $n_{mice} = 2$ ,  $n_{cells} = 11-12$ ; two way ANOVA RM,  $F_{1,252} = 5.39$ ,  $*P < 0.05$ ). Data are represented as mean  $\pm$  s.e.m..

## Online methods

### *Experimental subjects and inescapable shock procedure*

C57Bl/6J mice wild-type males of 4–7 weeks were used in accordance with the guidelines of the French Agriculture and Forestry Ministry for handling animal, and the ethic committee Charles Darwin #5 of the University Pierre et Marie Curie. They were housed at groups of 4-6 per cage with water and food *ad libitum* available. Mice were randomly allocated to experimental groups.

The inescapable shock procedure was previously described in<sup>21</sup>. Briefly, we placed mice into standard mouse behavioral chambers (Imetronics) equipped with a metal grid floor. We let them to habituate at the new environment for 5 m. In a 20-minutes session animals received either 19 or 0 unpredictable foot-shocks (1 mA, 500 ms) with an intershock interval of 30, 60 or 90 sec. We anesthetized mice for patch-clamp electrophysiology 1 h, 24 h, 7 d, 14 d or 30 d after the session ended.

### *Electrophysiology*

Animals were anesthetized with Ketamine/Xylazine (50mg/10mg Kg<sup>-1</sup> i.p.; Sigma-Aldrich, France). Analysis was performed in a non-blinded fashion.

The preparation of Lhb-containing brain slices was done in bubbled ice-cold 95% O<sub>2</sub>/5% CO<sub>2</sub>-equilibrated solution containing (in mM): cholineCl 110; glucose 25; NaHCO<sub>3</sub> 25; MgCl<sub>2</sub> 7; ascorbic acid 11.6; Na<sup>+</sup>-pyruvate 3.1; KCl 2.5; NaH<sub>2</sub>PO<sub>4</sub> 1.25; CaCl<sub>2</sub> 0.5. Sagittal slices (250 μm) were stored at room temperature in 95% O<sub>2</sub>/5% CO<sub>2</sub>-equilibrated artificial cerebrospinal fluid (ACSF) containing (in mM): NaCl 124; NaHCO<sub>3</sub> 26.2; glucose 11; KCl 2.5; CaCl<sub>2</sub> 2.5; MgCl<sub>2</sub> 1.3; NaH<sub>2</sub>PO<sub>4</sub> 1. Recordings (flow rate of 2.5 ml/min) were made under an Olympus-BX51 microscope (Olympus, France) at 32 °C. Currents were amplified, filtered at 5 kHz and digitized at 20 kHz. Access resistance was monitored by a step of -4 mV (0.1 Hz). Experiments were discarded if the access resistance increased more than 20%.

The internal solution to measure GABA<sub>B</sub>-GIRK currents and neuronal excitability contained (in mM): potassium gluconate 140, NaCl 4, MgCl<sub>2</sub> 2, EGTA 1.1, HEPES 5, Na<sub>2</sub>ATP 2, sodium creatine phosphate 5, and Na<sub>3</sub>GTP 0.6 (pH 7.3 with KOH). The liquid junction potential was ~12 mV. When we measured the synaptic inhibitory or excitatory release the internal solution contained (in mM): CsCl 130; NaCl 4; MgCl<sub>2</sub> 2; EGTA 1.1; HEPES 5; Na<sub>2</sub>ATP 2; Na<sup>+</sup>-creatine-phosphate 5; Na<sub>3</sub>GTP 0.6, and spermine 0.1. The liquid junction potential was -3 mV. For cell-attached recordings the internal solution consisted of ACSF.

Cell-attached recordings were performed in GΩ seal and in presence of synaptic blockers for AMPA- (NBQX, 20μM) and GABA-dependent (Bicuculline, 10μM) transmission. Pipettes were filled with ACSF. Action potential activity was recorded in voltage-clamp mode, maintaining an average 0 pA holding current.

Whole-cell voltage clamp recordings were achieved to measure GABA<sub>B</sub>-GIRK currents in presence of Bicuculline (10μM), NBQX (20μM) and AP5 (50μM). For agonist-induced currents, changes in holding currents in response to bath application of baclofen were measured (at -50 mV every 5 s). GABA<sub>B</sub>-GIRK currents were confirmed by antagonism with either 10 μM of CGP54626, a specific GABA<sub>B</sub>-Rs antagonist or 1 mM Ba<sup>2+</sup>, a selective inhibitor of inward rectifiers K<sup>+</sup> channels. For the GTP-γS experiment, 100μM of GTP-γS was added to the internal solution in place of Na<sub>3</sub>GTP. For the Okadaic acid (OA) and the CaMKII inhibitor KN93 experiments, respectively 100nM of OA or 10μM of KN93 were added in the internal solution. The PP2A inhibitor LB-100 (0.1μM) was bath applied.

Miniature excitatory postsynaptic currents (mEPSCs) were recorded in voltage-clamp mode at -60 mV in presence of bicuculline (10 μM) and TTX (1 μM). Miniature inhibitory postsynaptic currents (mIPSCs) were recorded (-60 mV) in presence of NBQX (20 μM) and TTX (1 μM). EPSCs and IPSCs were evoked through an ACSF-filled monopolar glass electrode placed ~200 μm from the recording site in the stria medullaris. AMPA: NMDA ratios of evoked-EPSC were obtained by AMPA-EPSC +40 mV/NMDA-EPSCs at +40 mV. Rectification Index (RI) was computed by AMPA-EPSC-60/AMPA-EPSC+40. For the experiments in which high-frequency stimulation trains were used to determine presynaptic release probability, QX314 (5 mM) was included in the internal solution to prevent the generation of sodium spikes.

Current-clamp experiments were performed using a series of current steps (from -80 pA to 100 pA or when the cell reached a depolarization block) injected to induce action potentials (5-10 pA injection current per step, duration of 800 ms). ACSF was complemented with synaptic blockers for AMPA- (NBQX, 20μM) and GABA-dependent (Bicuculline, 10μM) transmission. Cells were maintained to their original resting membrane potential (after breakthrough) throughout the experiment.

### *Surgery, viral strategy and local infusion*

Animals were anesthetized with Ketamine (150 mg/kg)/Xylazine (10 mg/kg i.p.) (Sigma-Aldrich, France). For LB-100 local infusion bilateral injections of LB-100 (1 μM; ~300 nl) in the Lhb were performed: A-P: -1.7; M-L: ±0.45; D-V: -3.1. Control animals were infused with PBS. For GIRK2a overexpression, a recombinant adeno-associated virus (AAV) coding for the mouse GIRK2a sequence was used (NM\_010606.2) (AAV-GIRK2a particles were custom made at UNC North Carolina, USA). The GIRK2a sequence is fused to EGFP

and inserted under the control of a TET-ON system. AAV-GIRK2a-EGFP and AAV-Venus as a control were injected bilaterally in the LHb at a final volume of 300-500 nl. After three weeks, mice were subjected first to the FsE procedure and then to the doxycycline treatment that consisted of intragastric administrations of 5 mg/100µl twice per day for three consecutive days (from day 2 to day 5 after FsE). Retrobeads (Lumafloor, Nashville, US) were added in all cases to the infused solution for post histological identification of the injection site. Brain slices from injected mice were directly examined under fluorescent microscope for the identification of the injection site. Only animals with correct injections site were included in the analysis.

#### Reverse transcription-PCR

Total RNA of lateral habenula was extracted using Trizol (Invitrogen) and transcribed into cDNA using SuperScript II Reverse Transcriptase (Invitrogen). PCR were conducted with Taq DNA polymerase (Invitrogen) according to manufacturer's protocol using the following primers: GIRK1: forward primer 5'-GTGAGTTCCTTCCCCTTGACCA-3', reverse primer 5'-TCGTCCTCTGTGTATGATGTTTCG-3', GIRK2: forward primer 5'-GACGACCTGCCGAGACACAT-3', reverse primer 5'-CGATGGTGGTTTCTGTCTCTATGG-3', GIRK3: forward primer 5'-GGGACGACCGCCTCTTTCTC-3', reverse primer 5'-GCCCCACAACACTTCATCCA-3', GIRK4: forward primer 5'-GAAGGAATGGTAGAAGCAACAGG-3', reverse primer 5'-GAAGGAATGGTAGAAGCAACAGG-3'

#### Immunostaining

Mice were anesthetized with pentobarbital (30 mg/kg, i.p.; Sanofi-Aventis) and perfused transcardially with 4% (w/v) paraformaldehyde in 0.1 M sodium phosphate buffer, pH 7.5. Brains were post-fixed overnight in the same solution and stored at 4°C. Fifty-micrometer-thick sections were cut with a VT1000S (Leica). Sections were incubated 48 hours with rabbit anti-GFP primary antibody (1:2000, Molecular Probe) in PBS, 10% horse serum, 0,1% Triton at 4°C. Sections were then washed in PBS solution and incubated two hours with secondary antibody (Donkey anti-rabbit Alexa 488-conjugated antibody, 1:400, Jackson Immunoresearch). Finally, sections were cover-slipped in anti-fading mounting medium (moviol-DABCO 25 mg/ml). Images were taken using an Olympus microscope and a DM-6000 Leica microscope.

#### Electron microscopy

Immunohistochemical reactions at the electron microscopic level were carried out using the pre-embedding immunogold method. Free-floating sections containing the lateral habenula were incubated in 10% NGS diluted in TBS. Sections were then incubated in either anti-GIRK2 antibodies or anti-GABA<sub>B1</sub> (1-2 µg/ml diluted in TBS containing 1% NGS), followed by incubation in goat anti-rabbit IgG coupled to 1.4 nm gold or goat anti-mouse IgG coupled to 1.4 nm gold (Nanoprobes Inc., Stony Brook, NY, USA), respectively. Sections were post-fixed in 1% glutaraldehyde and washed in double distilled water, followed by silver enhancement of the gold particles with a HQ Silver kit (Nanoprobes Inc.). Sections were then treated with osmium tetroxide (1% in 0.1 M PB), block-stained with uranyl acetate, dehydrated in graded series of ethanol and flat-embedded on glass slides in Durcupan (Fluka) resin. Regions of interest were cut at 70-90 nm on an ultramicrotome (Reichert Ultracut E, Leica, Austria) and collected on pioloform-coated single slot copper grids. Staining was performed on drops of 1% aqueous uranyl acetate followed by Reynolds's lead citrate. Ultrastructural analyses were performed in a Jeol-1010 electron microscope. Electron photomicrographs were captured with ORIUS SC600B CCD camera (Gatan, Munich, Germany). Digitized images were then modified for brightness and contrast using Adobe PhotoShop CS5 (Mountain View, CA, USA) to optimize them for printing.

Next, we performed quantitative analyses to establish the relative frequency of GIRK2 and GABA<sub>B1</sub> immunoreactivity in the LHb in control and FsE condition.

We used 60-µm coronal slices processed for pre-embedding immunogold immunohistochemistry. The procedures were similar to those used previously<sup>57</sup>. Briefly, for each of three animals from the experimental groups, three samples of tissue were obtained for the preparation of embedding blocks, totaling n = nine blocks per group. To minimize false negatives, electron microscopic serial ultrathin sections were cut close to the surface of each block, as immunoreactivity decreased with depth. We estimated the quality of immunolabeling by always selecting areas with optimal gold labeling at approximately the same distance from the cutting surface, which was defined within 5 to 10 µm from the surface. Randomly selected areas were then photographed from the selected ultrathin sections and printed with a final magnification of 45,000X. Quantification of immunogold labeling was carried out in reference areas totaling ~2,000 µm<sup>2</sup> for each age. Immunoparticles identified in each reference area and present along the plasma membrane and intracellular sites in dendrites, spines and axon terminals were counted.

#### PP2A phosphatase activity assay.

Wild-type C57Bl6 mice were used to test PP2A phosphatase activity after FsE in three different conditions: Controls, 24 h after the FsE, 24 h after the FsE with an intraperitoneal injection of LB-100 (1.5 mg/kg) 2h before the sacrifice. Habenula was dissected on ice and placed in cold extraction buffer (20 mmol/L imidazole-HCl, 2 mmol/L EDTA, 2 mmol/L EGTA, pH7.0) supplemented with protease inhibitors (Roche, France). Tissues from

two animals were pooled and homogenized using a pestle and sonicated for 10 sec, and lysates were centrifuged at  $2,000 \times g$  for 5 min. Lysates were quantified using a bicinchoninic acid assay kit (Pierce Europe) and an equal amount of proteins (130  $\mu$ g), for each pool, were assayed with the PP2A Immunoprecipitation Phosphatase Assay Kit (Millipore, France) according to the manufacture's protocol.

### *Behavioral paradigms*

All behavioral tests were conducted during the light phase (8:00–19:00), 1 or 7 days after the shock procedure. Animals were tested only for a single behavioral paradigm, and operators were blind to the experimental group during the scoring.

#### *Predator odor test*

Mice were exposed to a predator odor by presenting for 5 min a cotton ball soaked with red fox urine (5 ml Red fox P; Timk's, Safariland Hunting Corp., Trappe, MA) placed in a plastic container (holes equipped) in a corner of a transport cage. For the control group, instead of fox urine we added 5ml of water. One hour after the procedure, the mice were anesthetized for the vitro recordings.

#### *Restraint stress*

A ventilated 50 ml falcon tube placed at the center of a transport cage was employed to constrain the mice for 1h (from 9.00 to 10.00 am). Control animals were left undisturbed in a transport cage for the same amount of time. The mice were anesthetized for the vitro recordings, one hour after the procedure.

#### *Re-exposure to the context*

For this experiment mice were re-exposed 24 h after to the chamber where they received (or not) shocks for a total duration of 5 m. Online analysis of the freezing was performed by scoring videos in a room separate from the mice during the test period. Offline analysis was performed by a second observer. Freezing was defined as the absence of visible movement except that required for respiration (fluctuation in the volume of the thorax) (score: 1). Scanning was scored when the animal showed a sole movement of the head to scan the environment in a defensive position (score: 0.5). The behavior was scored according to a 5-sec time-sampling procedure every 25 sec. The observer scored the animal as freezing, scanning or active during the 5 sec time frame and then proceeded to the next chamber. A single episode of freezing or scanning during the 5 sec observation was taken as an episode. Each animal was observed 10 times for total 5 minutes session. The cumulative score were converted into percent time freezing by dividing the number of freezing-scanning observations by the total number of observations for each mouse<sup>58</sup>.

#### *Locomotor activity*

To assess the locomotor activity we tested mice in an open field arena. Mice were placed in the center of a plastic box (50 cm x 50 cm x 45 cm) in a room with dim light. We let them to explore for 5m and then we acquired the videotracks. During the 15m session, animal behavior was videotaped and subsequently analyzed (Viewpoint, France).

#### *Forced swim test*

Forced swim test was conducted under normal light condition as previously described<sup>24,59</sup>. Mice were placed in a cylinder of water (temperature 23-25°C; 14 cm in diameter, 27 cm in height for mice) for 6 min. The depth of water was set to prevent animals from touching the bottom with their hind limbs. Animal behavior was video-tracked from the top (Viewpoint, France). The latency to the first immobility event and the immobility time of each animal spent during the test was counted online by two independent blind observers. Immobility was defined as floating or remaining motionless, which means absence of all movement except motions required to maintain the head above the water.

#### *Sucrose preference test*

For the sucrose preference test, mice were single housed and habituated with two bottles of 1% sucrose for 2 days. At day 3 (test day) mice were exposed to two bottles filled with either 1% sucrose or water for 24h. The sucrose preference was defined as the ratio of the consumption of sucrose solution versus total intake (Sucrose + water) during the test day expressed as percentage.

#### *Learned helplessness model*

The procedure consisted in 2 session of inescapable foot-shock (1 session per day, 360 foot-shock per session, 0.3 mA, shock duration between 1 and 3 s and random intershock intervals) followed 24h after the last session by a test session to assess the LH<sup>5</sup>. The testing was performed in a shuttle box (13 x 18 x 30 cm) equipped with a grid floor and a door separating the two compartments. The test consisted of 30 trials of escapable foot-shock. Each trial started with a 5 s duration light stimulus followed by a 10 s shock (0.1 - 0.3mA). The intertrial interval was 30s. When the mouse shuttled in the other compartments during the light cue the avoidance was scored. When it shuttled during the shock the escape latency was measured. When the mouse was unable to escape the failures were scored. The shock terminated any time that the animal shuttled in the other compartment. Out of



the 30 trials, more than 15 failures were defined as LH. Only LH mice were behaviorally and electrophysiologically tested.

*Analysis and drugs.*

All drugs were obtained from Abcam (Cambridge, UK), Tocris (Bristol, UK) and Sigma-Aldrich (France) and dissolved in water, except for TTX (citric acid 1%).

Mice were injected with LB-100 (1.5 mg/Kg i.p.; Lixte Inc.) or saline 6-8 hours after the FsE (2 hours were instead used for biochemical assays). LH animals received LB-100 24 hours after the test day. A set of mice (5 weeks), were single housed for 3 days and then underwent LB-100 i.p. (1.5 mg/kg/day) treatment for 7 days to assess the health profile of the molecule. Body weight, pellet and water intake were monitored every 2 days. Three days after the last injections mice were tested for their locomotor activity.

Online/offline analyses were performed using IGOR-6 (Wavemetrics, US) and Prism (Graphpad, US). Data distribution was previously tested with the Kolmogorov Smirnov and D'Agostino Pearson test. Depending on the distribution, parametric or not parametric test were used. Single data points are always plotted. Electrophysiological and behavioral experiments were replicated within the laboratory. Sample size was pre-estimated from previously published research and from pilot experiments performed in the laboratory. Compiled data are expressed as mean  $\pm$  s.e.m. Significance was set at  $p < 0.05$  using unpaired t-test, one or two-way ANOVA with multiple comparison when applicable. The use of the paired t-test and two way ANOVA for repeated measured were stated in the legend figure text. The Mann Whitney test was used when required.

References

57. Mamei, M., Balland, B., Lujan, R. & Luscher, C. Rapid synthesis and synaptic insertion of GluR2 for mGluR-LTD in the ventral tegmental area. *Science* 317, 530-533 (2007).
58. Fanselow, M. S. & Bolles, R. C. Naloxone and shock-elicited freezing in the rat. *J Comp Physiol Psychol* 93, 736-744 (1979).
59. Can, A. et al. The mouse forced swim test. *J Vis Exp* e3638 (2012).

## Context and objectives of the study II: LHb hyperactivity as a long term adaptation underlying MS-driven depressive like symptoms

In the previously presented work I contributed to establish that GABA<sub>B</sub>R-GIRK plasticity represents an early event occurring following an aversive experience, leading to increasing LHb excitability and triggering depressive like symptoms. However, how persistent are these adaptations remains unknown. Our previous study, together with other findings, strength the idea that LHb hyperactivity could be an important substrate underlying depressive like symptoms. However, the data are limited to animal models that rely on the repeated exposure to painful stimuli. If LHb dysfunctions could represent long-term adaptation underlying depressive symptoms independently of the kind of stressors that trigger it, remains to be determined.

Beyond the physical stress, chronic psychosocial stress and early life adversity, such as child neglect play a major role in the etiology of depression. The prolonged separation of newborn rodents from their mother represents an animal model of early-life stress that recapitulates aspects of child neglect including the emergence of depressive-like symptoms in adulthood. As for the foot-shock model, mice that undergo MS present deficits in coping with stressful events. This raises the hypothesis that MS-driven behavioral adaptations may also emerge from the dysfunction of neural circuits devoted to aversion processing thereby implicating LHb dysfunction. In this study, we aimed to understand if LHb hyperexcitability may underlie early-life stress-induced depressive-like phenotype. We find that maternal separation triggers depressive-like phenotype together with GABA<sub>B</sub>R-GIRK dependent LHb hyperexcitability. Moreover, reversal strategy such as chemogenetic and DBS intervention diminished LHb activity and ameliorated depressive phenotype providing a causal relationship between cellular adaptations in the LHb and the MS-driven depressive-like symptoms. This provides mechanistic insights in LHb dysfunction contributing to early life stress-induced depressive symptoms, giving further support to targeting LHb hyperexcitability to ameliorate depressive symptoms.

## Limiting habenular hyperactivity ameliorates maternal separation-driven depressive-like symptoms

Anna Tchenio<sup>1,2,3,4</sup>, Salvatore Lecca<sup>1,2,3,4</sup>, Kristina Valentinova<sup>1,2,3,4</sup> and Manuel Mameli<sup>1,2,3,4</sup>

<sup>1</sup> Institut du Fer à Moulin, 75005 Paris, France.

<sup>2</sup> Inserm, UMR-S 839, 75005 Paris, France.

<sup>3</sup> Université Pierre et Marie Curie 75005 Paris, France.

<sup>4</sup> The University of Lausanne, Department of Fundamental Neuroscience, 1005 Lausanne, Switzerland.

To whom correspondence should be addressed:

Manuel Mameli, PhD

The University of Lausanne, Department of Fundamental Neuroscience

Rue du Bugnon 9 1005, Lausanne, Switzerland.

Email [manuel.mameli@unil.ch](mailto:manuel.mameli@unil.ch)

### Abstract

*Early-life stress, including maternal separation (MS), increases the vulnerability to develop mood disorders later in life, but the underlying mechanisms remain elusive. We report that MS promotes depressive-like symptoms in mice at a mature stage of life. Along with this behavioral phenotype, MS drives reduction of GABAB-GIRK signaling and the subsequent lateral habenula (LHb) hyperexcitability – an anatomical substrate devoted to aversive encoding. Attenuating LHb hyperactivity using chemogenetic tools and deep-brain stimulation ameliorates MS depressive-like symptoms. This provides insights on mechanisms and strategies to alleviate stress-dependent affective behaviors.*

## Introduction

Childhood neglect (i.e. maternal separation, MS) is aversive, has negative long-term repercussions on child development and primes depression in adulthood<sup>1,2</sup>. The prolonged separation of newborn rodents from their mother represents an animal model of severe early-life stress that recapitulates aspects of child neglect. Animals undergoing MS present deficits in coping with stressful events. Moreover, such paradigm promotes anxiety, addictive and depressive-like behavioral phenotypes<sup>3-5</sup>. This raises the hypothesis that MS-driven behavioral adaptations may, at least partly, emerge from the dysfunction of neural circuits devoted to aversion processing.

The lateral habenula (LHb) contributes to encode aversion and negative reward prediction error as neurons in this structure are excited by external aversive stimuli<sup>6</sup>. The LHb provides such aversive-related information to monoaminergic centers suggesting a relevant role in motivated behaviors<sup>7-9</sup>. Stressors of different nature increase the activity of LHb neurons, and lesioning experiments indicate that the LHb regulates coping behaviors when facing aversive stimuli<sup>10-12</sup>. Furthermore, when such stressful events (i.e. foot-shocks) become inescapable and persistent, this produces aberrant LHb hyperactivity, which is instrumental for the emergence of depressive-like symptoms<sup>10,11,13,14</sup>.

However, whether chronic, painless stressful events, such as MS, promote depressive-like phenotypes through LHb adaptations remains elusive. If this holds true, we propose that reversal strategies restoring LHb function can ameliorate MS-dependent depressive-like symptoms.

Here, we demonstrate that, at a mature stage of life, mice undergoing MS present depressive-like behaviors along with increased LHb neuronal excitability. In addition, we show that MS-mediated reduction in GABA<sub>B</sub>-GIRKs signaling is causal for such LHb hyperexcitability, and that limiting LHb neuronal activity through chemogenetics or deep brain stimulation ameliorates MS-driven behavioral phenotypes. These findings support the notion that aberrant habenular neuronal hyperactivity represents a neurobiological substrate underlying discrete stress-driven (i.e. acute and chronic) depressive-like symptoms.

## Results

### MS drives depressive-like states and habenular hyperexcitability in mice

We examined the early-life stress-dependent behavioral ramifications exposing mice to maternal separation (MS)<sup>15</sup> (Methods, Fig. 1a). Briefly, pups aged seven days were, or not (Control), removed from their litter, separated from their mother, and kept in isolation for six hours daily for a week. When tested three weeks later, Control and MS mice had comparable weight, locomotion and performance in the open field (Supplementary Fig. 1a-c). In contrast, MS mice presented higher failure rates when challenged with escapable foot-shocks (shuttle box), behavioral despair (higher immobility in tail suspension test; TST), and diminished sucrose preference (Fig. 1b-d). Furthermore, *ex-vivo* recordings in acute LHb-containing brain slices revealed that LHb neurons from MS mice exhibit hyperexcitability, with no alterations of the resting membrane potential (Fig. 1e; Supplementary Fig. 1d). Altogether, these findings suggest that MS promotes depressive-like symptoms and LHb hyperactivity later in life.

### Cellular mechanisms underlying MS-driven plasticity

Tonic GABA<sub>B</sub>-GIRK signaling controls LHb neuronal firing and its reduction promotes cell hyperexcitability<sup>10</sup>. Patch-clamp recordings from LHb neurons revealed that bath application of the GABA<sub>B</sub>-R agonist baclofen evoke an outward current (I-Baclofen) readily reversed by the specific antagonist CGP-54626 (Fig. 2a). I-Baclofen was significantly reduced throughout the LHb of MS mice (Fig. 2b, Supplementary Fig. 2a, b). The reduction of I-Baclofen with no evident territorial specificity suggests that MS reduces GABA<sub>B</sub>-GIRKs independently of the structures to which LHb neurons send their axons. To test this prediction, we used fluorescent tract tracing to retrogradely label LHb neurons projecting either to the ventral tegmental area (LHb<sup>VTA</sup>) or the rostromedial tegmental nucleus (LHb<sup>RMTg</sup>). These are prominent habenular-midbrain projections that, if disrupted, contribute to the establishment of depressive-like symptoms<sup>7,11</sup>. MS significantly reduced I-Baclofen in both LHb<sup>VTA</sup> and LHb<sup>RMTg</sup> neurons supporting a scenario in which GABA<sub>B</sub>-GIRK signaling reduction occurs throughout the LHb, likely affecting multiple downstream targets (Fig. 2c, d).

GABA<sub>B</sub>-R activation within the LHb leads to cell hyperpolarization through GIRK channels opening<sup>10</sup>. Along with the reduced I-Baclofen, MS also diminished GIRK currents. Indeed, responses generated by the intracellular dialysis of the G-protein activator GTP $\gamma$ S (I-GTP $\gamma$ S) and the bath application of the specific GIRK1/2 activator ML-297 were smaller throughout the LHb of MS mice (Supplementary Fig. 2c, d)<sup>16,17</sup>. These results indicate that early-life stress, similarly to foot-shocks<sup>10,18</sup>, reduces GABA<sub>B</sub>-GIRK function within the LHb.

Activation of the GABA<sub>B</sub>-GIRK signaling requires GABA spillover from the presynaptic terminal<sup>19</sup>. A major input source of GABA onto LHb neurons arises from the entopeduncular nucleus (EPN). Furthermore, the reduction of EPN-originating inhibitory transmission within the LHb contributes to depressive-like symptoms<sup>14,20,21</sup>. We therefore set out to provide proof of principle that MS reduces, not only agonist-evoked GABA<sub>B</sub>R responses, but more precisely synaptically-relevant GABA<sub>B</sub>R function. To probe synaptically-activated GABA<sub>B</sub>Rs, we transduced EPN neurons with a rAAV2-hSyn-CoChR-eGFP allowing for the expression of the excitatory opsin from *Chloromonas oogama* (CoChR; Fig. 2e)<sup>22</sup>. CoChR-expressing EPN terminals received trains of light-pulses (20 Hz), which elicited fast-GABA<sub>A</sub>R and slow-GABA<sub>B</sub>R outward currents (I-GABA<sub>A</sub> and I-GABA<sub>B-slow</sub> respectively), the latter likely mediated by GABA spillover diffusing to perisynaptic GABA<sub>B</sub>-Rs (Fig. 2f). We then computed the I-GABA<sub>B-slow</sub>/I-GABA<sub>A</sub> ratios as a measure of the postsynaptic strength of inhibitory transmission. MS diminished the I-GABA<sub>B-slow</sub>/I-GABA<sub>A</sub> ratios without significant alterations in miniature EPSCs or IPSCs, nor on presynaptic GABA<sub>B</sub>R function (Fig. 2f, Supplementary Fig. 3a–d). Altogether, MS diminishes postsynaptic GABA<sub>B</sub>-GIRK signaling in LHb.

Thus, we predicted that MS-dependent LHb hyperexcitability results from the above-described GABA<sub>B</sub>-GIRK reduction. Blocking GABA<sub>A</sub>Rs, AMPARs and NMDARs left MS hyperexcitability unaffected. However, MS occluded GABA<sub>B</sub>Rs antagonism-driven increased neuronal excitability observed in control slices (Fig. 1e, Fig. 3a, b; (Ctrl, aCSF/CGP54626,  $F_{(10;410)}=2.3$   $p<0.05$ ; MS, aCSF/CGP54626,  $F_{(10;410)}=0.37$   $p > 0.05$ ; two-way ANOVA RM, interaction). This suggests that MS leads to LHb hyperexcitability via GABA<sub>B</sub>-GIRK plasticity.

### Limiting habenular activity ameliorates depressive-like symptoms

Is LHb hyperexcitability necessary for MS depressive-like phenotypes? MS-driven adaptations occur throughout the LHb (Fig. 2b–d). Therefore, we sought to limit hyperactivity of a large LHb neuronal population. Thus, we virally expressed the inhibitory designer receptors exclusively-activated by designer drugs (rAAV8-hSyn-HA-hM4D-mCherry; Gi-DREADD) in the LHb (Fig. 4a, Supplementary Fig. 4a). *Ex-vivo*, bath application of the specific DREADDi ligand clozapine-N-oxide (CNO) generated a K<sup>+</sup>-dependent outward current (I-CNO) and abolished neuronal firing (Supplementary Fig. 4b, c). MS reduced I-CNO, supporting a diminished GIRK function<sup>23</sup>. We next examined baseline neuronal activity using single unit recordings in anesthetized mice. The baseline firing rate of MS mice was higher than Control animals, an observation in line with the increased excitability reported in acute slices. The systemic injection of CNO diminished LHb neuronal firing in Gi-DREADD-expressing mice, and reduced the activity of MS-LHb neurons to values not statistically different from Control animals (Supplementary Fig. 4d, e). This validates this strategy to limit hyperexcitability in behaving mice. When exposed to escapable foot-shocks (shuttle box), in absence of CNO MS mice (YFP/Gi-DREADD) expressed high failure rates (Fig. 4b). After a recovery period of three days, mice of all experimental groups received a single systemic injection of CNO ~15 minutes prior the test. CNO reduced the failure rate in the shuttle box only in Gi-DREADD-expressing MS mice. However, five days later, after complete clearance of CNO from the animal body, MS mice displayed the depressive state (Fig. 4b). Accordingly, in different sets of mice treated with CNO (see Methods), TST immobility and sucrose preference were comparable between Gi-DREADD-expressing MS mice and Controls (Fig. 4c, Supplementary Fig. 4f). In contrast, CNO treatment did not affect locomotor activity measured in the open field, arguing against compromised motor function (Supplementary Fig. 4f). Therefore, the chemogenetic reduction of LHb activity is sufficient to ameliorate MS-driven depressive-like symptoms.

Individuals presenting symptoms of depression following early-life stress poorly respond to antidepressants<sup>24</sup>, heightening the need of alternative treatments. Deep brain stimulation (DBS) of the LHb ameliorates depressive symptoms, but its efficiency in the context of MS is unknown<sup>11,25</sup>. When applied *ex-vivo* within the LHb, DBS-like stimulation (130 Hz)<sup>11</sup> reduced glutamate release, diminished neuronal firing, hyperpolarized neurons and

decreased input resistance (Fig. 4d, e). Accordingly, in anesthetized mice, DBS lowered LHb activity (Fig. 2f, g and Supplementary Fig. 4g). Therefore, DBS reduces neuronal activity by engaging both presynaptic and postsynaptic mechanisms. We then unilaterally implanted DBS electrodes in LHb (Fig. 4f), and examined its efficacy on MS-induced depressive behavior. DBS reduced the number of failures in the shuttle box (Fig. 4h). This highlights DBS as a strategy, complementary to pharmacology, to compensate for MS-driven LHb hyperexcitability and ameliorate depressive states.

## Discussion

Here we demonstrate that MS promotes LHb neuronal hyperactivity by reducing GABA<sub>B</sub>-GIRK function. This hyperexcitability ultimately triggers depressive-like symptoms.

The GABA<sub>B</sub>-GIRK signaling in the LHb tightly controls neuronal activity<sup>10</sup> and GABA<sub>B</sub>-R internalization often occurs along with GIRK trafficking<sup>10,26,27</sup>. Consistently, we report that MS-driven reduced GABA<sub>B</sub>-Rs function occurs along with diminished GIRK channels either expression or function. Internalization of GABA<sub>B</sub>-Rs and GIRKs requires the activity of phosphatases including PP2A, and a PP2A inhibitor presents antidepressant properties<sup>10,26,27</sup>. However, whether PP2A contributes to MS-driven GABA<sub>B</sub>-GIRK plasticity in the LHb remains to be established.

In line with a reduction of I-Baclofen, we observed a diminished I-GABA<sub>B-slow</sub>/I-GABA<sub>A</sub> ratios at EPN-to-LHb synapses. These findings provide new insights on *i.* physiological patterns of presynaptic activity to elicit synaptic GABA<sub>B</sub>-Rs in the LHb *ii.* MS-mediated plasticity of synaptically-evoked GABA<sub>B</sub>-Rs. However MS-driven GABA<sub>B</sub>-Rs reduction may also occur at synaptic inputs other than the EPN.

Our data indicate that MS does not significantly affect mIPSCs, however these events stem from unidentified inputs, leaving open the possibility that MS also engages input-specific changes of fast inhibitory transmission<sup>14,20</sup>. In addition, the learned helplessness depressive state potentiated fast excitatory transmission onto LHb<sup>VTA</sup> neurons<sup>11</sup>. We cannot completely rule out that a similar adaptation also occur in MS mice. The detection threshold for MS plasticity of mEPSCs might be lowered by the different animal model of depression employed or, alternatively, by circuit-specific adaptations yet to be identified. Overall, plasticity of GABA<sub>B</sub>-GIRKs in the LHb emerges as a general cellular substrate underlying stressor-driven depressive phenotypes as it is common to acute traumatic events and chronic stressful conditions such as MS<sup>10,18</sup>.

Reduced GABA<sub>B</sub>-GIRK signaling mediates LHb neuronal hyperactivity<sup>10</sup>. Considering that MS-driven plasticity occurs in VTA and RMTg-projecting LHb neurons, MS cellular adaptations may remodel target midbrain circuits highlighting LHb-to-midbrain relevance in mood disorders<sup>3,7,11</sup>. The habenular output connectivity is however complex indicating that LHb-receiving structures other than the midbrain may contribute to the MS-driven behavioral phenotypes. This is indeed likely, as the inactivation of the LHb fails to rescue aberrant dopamine neurons activity in the chronic mild stress model of depression<sup>28</sup>. Altogether, stress-driven depressive-like symptoms emerge from the dysfunction of complex and parallel neuronal circuits (i.e. LHb-related and midbrain-related)<sup>10,28-30</sup>.

MS-dependent hyperactivity can be limited by chemogenetic and DBS approaches, which in turn are efficient to ameliorate MS-mediated depressive-like phenotypes.

Our data provide an extensive description of Gi-DREADD efficiency at the single cell level *ex-vivo* and *in-vivo* within the LHb. We report that Gi-DREADD activation *in vivo* in the LHb reduces, but does not silence, neuronal activity. This highlights Gi-DREADD efficacy in rescuing aberrant activity, without abruptly altering the physiology of neural systems. These properties may differ according to neuronal populations, viral vector properties or promoter employed.

In addition to a chemogenetic-based strategy we also investigated the use of DBS approaches to reduce MS hyperactivity in the LHb. The high frequency DBS protocol reported in our work was previously shown to also ameliorate depressive symptoms emerging in congenital learned helplessness rats<sup>11</sup>. Our data suggest that DBS efficiency not only relies on reduced presynaptic release<sup>11</sup> but also on postsynaptic mechanisms. The DBS-

mediated modulation of LHb activity is however transient, suggesting that the MS depressive-like phenotypes can recover after the intervention<sup>11</sup>. This indicates that DBS efficacy stems from its pre/postsynaptic-mediated reduction in LHb neuronal activity rather than on the MS-driven plasticity expression mechanisms (i.e. GABA<sub>B</sub>-GIRK plasticity).

Altogether, this study provides mechanistic insights underlying MS-induced adaptations in the LHb. Moreover, limiting LHb neuronal activity has potential therapeutic relevance in alleviating affective symptoms of neuropsychiatric disorders.

### **Contributions**

**A.T. performed and analyzed in vitro recordings together with K.V. and M.M.. S.L. performed in vivo recordings. A.T. performed behavioral experiments with M.M. and S.L.. M.M. and A.T. designed the study and wrote the manuscript.**

### **Acknowledgements**

**This work was supported by the European Research Council (Starting grant Saliensy 335333) to M.M.. We are grateful to M. Creed and C. Luscher for support on DBS approach. We thank C. Bellone, M. Creed, C. Lüscher, and the Mameli Laboratory for feedback on the manuscript. M.M. is a member of the Fens-Kavli Network of Excellence.**

### **Competing financial interests**

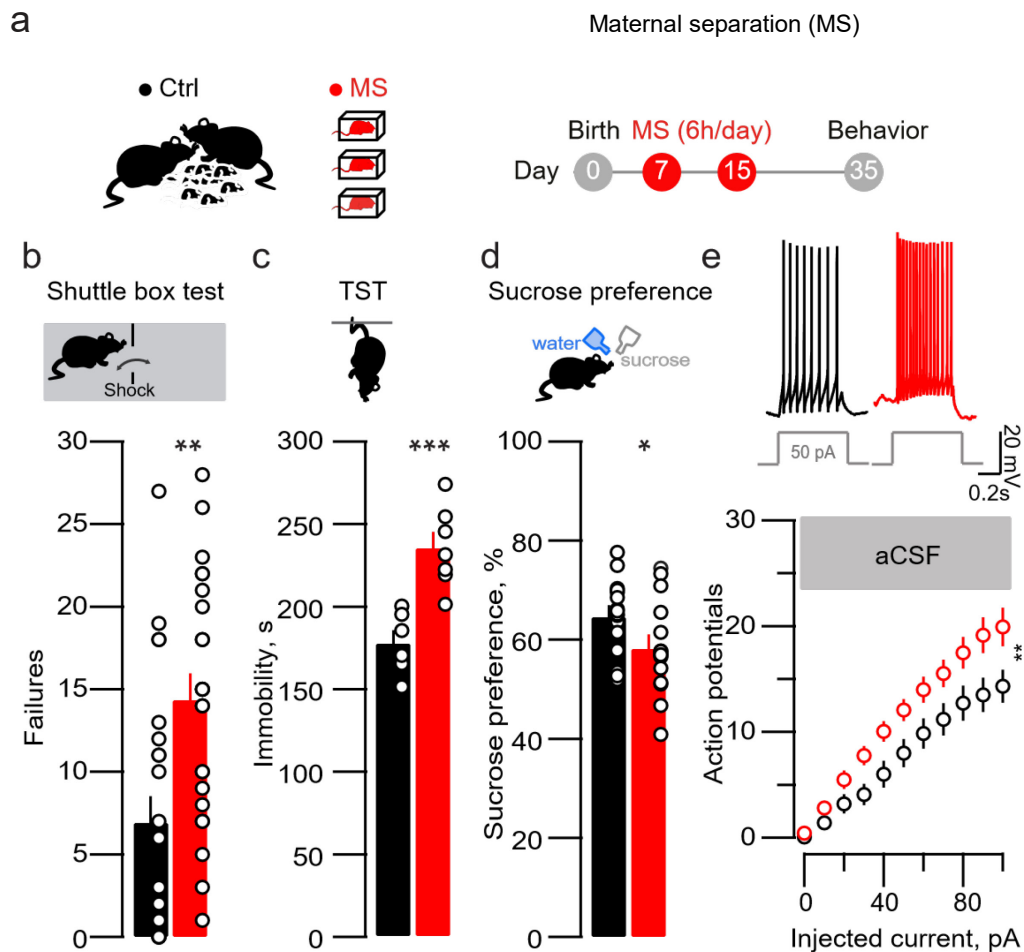
**The authors declare no competing financial interests.**

## References

1. Norman, R. E. *et al.* The long-term health consequences of child physical abuse, emotional abuse, and neglect: a systematic review and meta-analysis. *PLoS Med* **9**, e1001349 (2012).
2. Tractenberg, S. G. *et al.* An overview of maternal separation effects on behavioural outcomes in mice: Evidence from a four-stage methodological systematic review. *Neurosci Biobehav Rev* **68**, 489-503 (2016).
3. Authement, M. E. *et al.* Histone Deacetylase Inhibition Rescues Maternal Deprivation-Induced GABAergic Metaplasticity through Restoration of AKAP Signaling. *Neuron* **86**, 1240-1252 (2015).
4. Marco, E. M., Adriani, W., Llorente, R., Laviola, G. & Viveros, M. P. Detrimental psychophysiological effects of early maternal deprivation in adolescent and adult rodents: altered responses to cannabinoid exposure. *Neurosci Biobehav Rev* **33**, 498-507 (2009).
5. Nishi, M., Horii-Hayashi, N. & Sasagawa, T. Effects of early life adverse experiences on the brain: implications from maternal separation models in rodents. *Front Neurosci* **8**, 166 (2014).
6. Matsumoto, M. & Hikosaka, O. Representation of negative motivational value in the primate lateral habenula. *Nat Neurosci* **12**, 77-84 (2009).
7. Meye, F. J. *et al.* Cocaine-evoked negative symptoms require AMPA receptor trafficking in the lateral habenula. *Nat Neurosci* **18**, 376-378 (2015).
8. Proulx, C. D., Hikosaka, O. & Malinow, R. Reward processing by the lateral habenula in normal and depressive behaviors. *Nat Neurosci* **17**, 1146-1152 (2014).
9. Stamatakis, A. M. & Stuber, G. D. Activation of lateral habenula inputs to the ventral midbrain promotes behavioral avoidance. *Nat Neurosci* **15**, 1105-1107 (2012).
10. Lecca, S. *et al.* Rescue of GABAB and GIRK function in the lateral habenula by protein phosphatase 2A inhibition ameliorates depression-like phenotypes in mice. *Nat Med* **22**, 254-261 (2016).
11. Li, B. *et al.* Synaptic potentiation onto habenula neurons in the learned helplessness model of depression. *Nature* **470**, 535-539 (2011).
12. Wilcox, K. S., Christoph, G. R., Double, B. A. & Leonzio, R. J. Kainate and electrolytic lesions of the lateral habenula: effect on avoidance responses. *Physiol Behav* **36**, 413-417 (1986).
13. Li, K. *et al.*  $\beta$ CaMKII in lateral habenula mediates core symptoms of depression. *Science* **341**, 1016-1020 (2013).
14. Shabel, S. J., Proulx, C. D., Piriz, J. & Malinow, R. Mood regulation. GABA/glutamate co-release controls habenula output and is modified by antidepressant treatment. *Science* **345**, 1494-1498 (2014).
15. George, E. D., Bordner, K. A., Elwafi, H. M. & Simen, A. A. Maternal separation with early weaning: a novel mouse model of early life neglect. *BMC Neurosci* **11**, 123 (2010).
16. Kaufmann, K. *et al.* ML297 (VU0456810), the first potent and selective activator of the GIRK potassium channel, displays antiepileptic properties in mice. *ACS Chem Neurosci* **4**, 1278-1286 (2013).
17. Logothetis, D. E., Kurachi, Y., Galper, J., Neer, E. J. & Clapham, D. E. The beta gamma subunits of GTP-binding proteins activate the muscarinic K<sup>+</sup> channel in heart. *Nature* **325**, 321-326 (1987).
18. Lecca, S., Trusel, M. & Mameli, M. Footshock-induced plasticity of GABAB signalling in the lateral habenula requires dopamine and glucocorticoid receptors. *Synapse* **71**, (2017).
19. Lüscher, C., Jan, L. Y., Stoffel, M., Malenka, R. C. & Nicoll, R. A. G protein-coupled inwardly rectifying K<sup>+</sup> channels (GIRKs) mediate postsynaptic but not presynaptic transmitter actions in hippocampal neurons. *Neuron* **19**, 687-695 (1997).
20. Meye, F. J. *et al.* Shifted pallidal co-release of GABA and glutamate in habenula drives cocaine withdrawal and relapse. *Nat Neurosci* **19**, 1019-1024 (2016).
21. Shabel, S. J., Proulx, C. D., Trias, A., Murphy, R. T. & Malinow, R. Input to the lateral habenula from the basal ganglia is excitatory, aversive, and suppressed by serotonin. *Neuron* **74**, 475-481 (2012).
22. Klapoetke, N. C. *et al.* Independent optical excitation of distinct neural populations. *Nat Methods* **11**, 338-346 (2014).
23. Pascoli, V., Terrier, J., Hiver, A. & Lüscher, C. Sufficiency of Mesolimbic Dopamine Neuron Stimulation for the Progression to Addiction. *Neuron* **88**, 1054-1066 (2015).
24. Williams, L. M., Debattista, C., Duchemin, A. M., Schatzberg, A. F. & Nemeroff, C. B. Childhood trauma predicts antidepressant response in adults with major depression: data from the randomized international

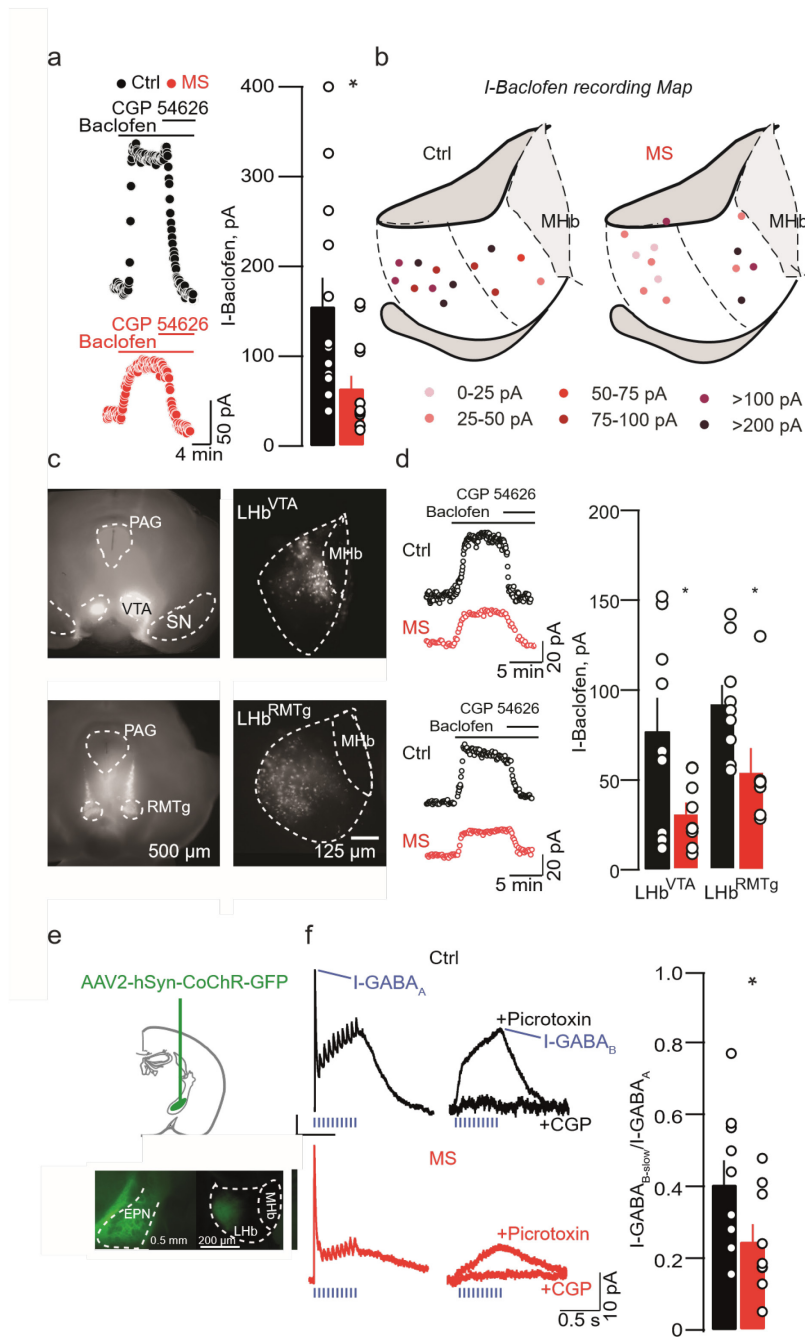


- study to predict optimized treatment for depression. *Transl Psychiatry* **6**, e799 (2016).
25. Sartorius, A. *et al.* Remission of major depression under deep brain stimulation of the lateral habenula in a therapy-refractory patient. *Biol Psychiatry* **67**, e9-e11 (2010).
  26. Hearing, M. *et al.* Repeated cocaine weakens GABA(B)-Girk signaling in layer 5/6 pyramidal neurons in the prelimbic cortex. *Neuron* **80**, 159-170 (2013).
  27. Padgett, C. L. *et al.* Methamphetamine-evoked depression of GABA(B) receptor signaling in GABA neurons of the VTA. *Neuron* **73**, 978-989 (2012).
  28. Moreines, J. L., Owrutsky, Z. L. & Grace, A. A. Involvement of Infralimbic Prefrontal Cortex but not Lateral Habenula in Dopamine Attenuation After Chronic Mild Stress. *Neuropsychopharmacology* **42**, 904-913 (2017).
  29. Tye, K. M. *et al.* Dopamine neurons modulate neural encoding and expression of depression-related behaviour. *Nature* **493**, 537-541 (2013).
  30. Yang, L. M., Hu, B., Xia, Y. H., Zhang, B. L. & Zhao, H. Lateral habenula lesions improve the behavioral response in depressed rats via increasing the serotonin level in dorsal raphe nucleus. *Behav Brain Res* **188**, 84-90 (2008).



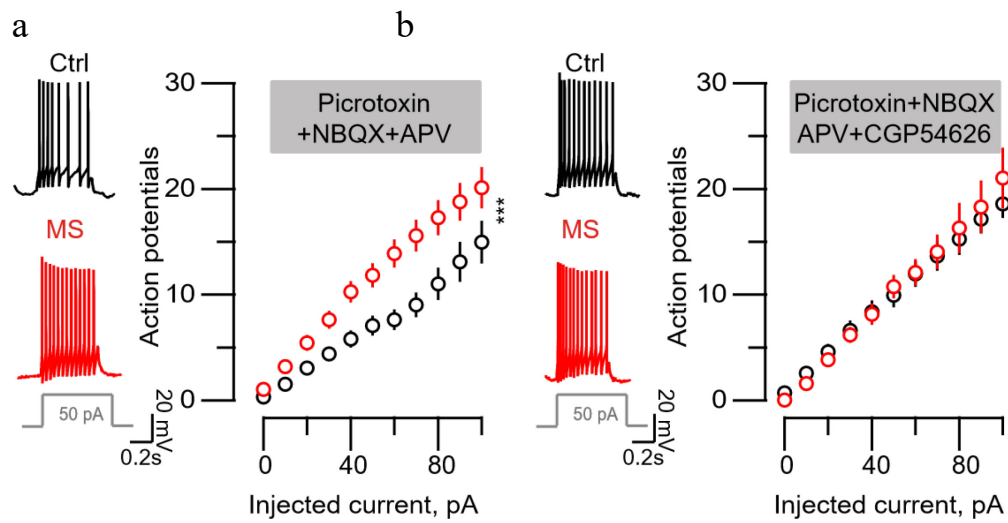
**Figure 1 MS-induced depressive-like symptoms and hyperexcitability**

(a) MS protocol (all schematics are original drawing made by authors). (b) Bar graph and scatter plot of failures in the shuttle box for control (Ctrl) and MS mice (Ctrl vs MS;  $n_{\text{mice}}=24$ , unpaired t-test,  $t_{45}=3.36^{**}p<0.01$ ). (c) Same as b for TST immobility (Ctrl vs MS;  $n_{\text{mice}}=6-7$ ; unpaired t-test,  $t_{11}=4.63$ ;  $^{***}p<0.001$ ). (d) Same as b but for sucrose preference (Ctrl vs MS;  $n_{\text{mice}}=16$ ; unpaired t-test,  $t_{30}=32.12$ ;  $*p<0.05$ ). (e) Top, sample traces from Ctrl and MS mice of current-evoked firing (50pA step). Bottom, action potentials versus injected current (0 to 100pA, steps of 10pA) in all experimental groups (Ctrl vs MS; aCSF,  $n_{\text{mice}}=6/\text{group}$ ;  $n_{\text{cells}}=23/\text{group}$ ; two-way ANOVA-RM, interaction,  $F(10;440)=2.74$ ;  $^{**}p<0.01$ ). Scale bars, 0.2 s and 20 mV.



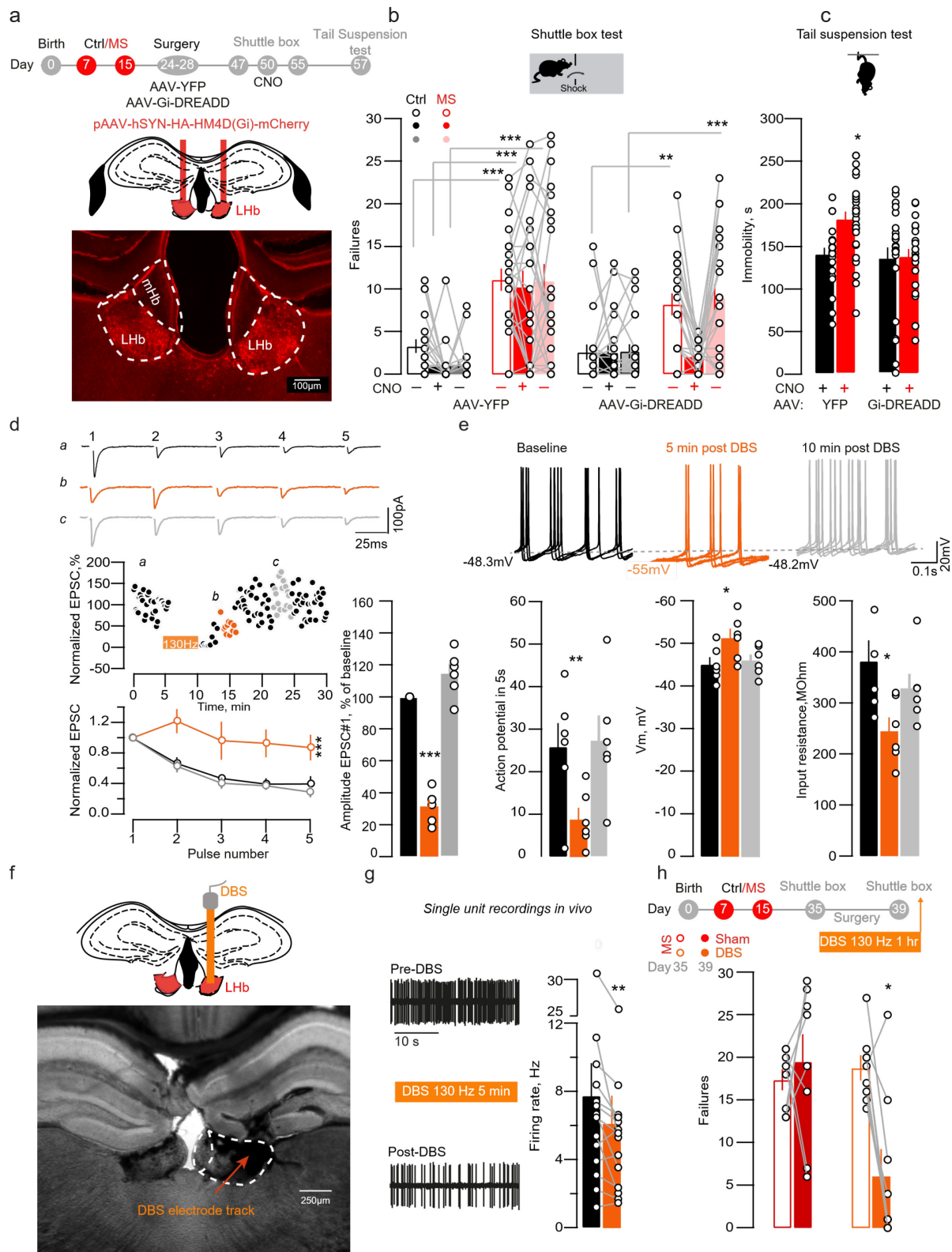
### Figure 2 MS drives GABA<sub>B</sub>-GIRK plasticity in Lhb.

**(a)** Sample traces, bar graph and scatter plots depicting CGP54626-sensitive I-Baclofen (I-Baclofen Ctrl vs MS;  $n_{mice}=5/6$ ;  $n_{cells}=13$ ; unpaired t-test,  $t_{24}=2.67$  \* $p<0.05$ ). I-Baclofen was measured at steady state. **(b)** Territorial distribution of I-Baclofen showing MS-dependent reduction of GABA<sub>B</sub>-GIRK signaling throughout the Lhb. **(c)** Examples of the injection site of red retrobeads infused in the VTA (top) and in the RMTg (bottom). Right, retrogradely labeled Lhb neurons projecting to VTA or RMTg. **(d)** Sample traces, bar graph and scatter plots depicting CGP54626-sensitive I-Baclofen in Lhb<sup>VTA</sup> and Lhb<sup>RMTg</sup> neurons (Lhb<sup>VTA</sup>: I-Baclofen Ctrl vs MS;  $n_{mice}=2$ ;  $n_{cells}=9$ ; unpaired t-test,  $t_{16}=2.37$  \* $p<0.05$ ; Lhb<sup>RMTg</sup>: I-Baclofen Ctrl vs MS;  $n_{mice}=2$ ;  $n_{cells}=9$  vs 7; unpaired t-test,  $t_{14}=2.35$  \* $p<0.05$ ). **(e)** Stereotactic infusion of AAV2-hSyn-CoChR-GFP within the EPN, and opsin expression in terminals within the Lhb **(f)** Opto-GABA<sub>A</sub>-IPSCs and opto-GABA<sub>B</sub>-IPSC sample traces and summary plot (Ctrl vs MS;  $n_{mice}=6/3$ ;  $n_{cells}=9$ /group; unpaired t-test,  $t_{16}=2.21$ ; \* $p<0.05$ ). Values for opto-GABA<sub>A</sub>-IPSC and opto-GABA<sub>B</sub>-IPSC were taken at the maximal peak as indicated. Scale bars, 4 min and 50 pA (a), 500 μm and 125 μm (c), 5 min and 20 pA (d), 0.5 mm and 200 μm (e), 0.5 s and 10 pA



**Figure 3 MS-induced Lhb neurons hyperexcitability requires reduced GABA<sub>B</sub>-GIRK signaling**

(a) Left, sample traces for recordings in Ctrl and MS mice of a current-evoked firing (for a 50pA step) in presence of picrotoxin/NBQX. Graph representing the action potentials versus injected current in all experimental groups. (picrotoxin/NBQX,  $n_{mice}=4/6$ ;  $n_{cells}=20/group$ ; two-way ANOVA-RM, interaction  $F_{(10;380)}=3.52$ ;  $***p<0.001$ ) (b) Same than (a) but in presence of picrotoxin/NBQX/CGP54626,  $n_{mice}=5/6$ ;  $n_{cells}=20/group$ ; two-way ANOVA-RM, interaction  $F_{(10;380)}=0.32$ ). Scale bars, 0.2 s and 20 mV.

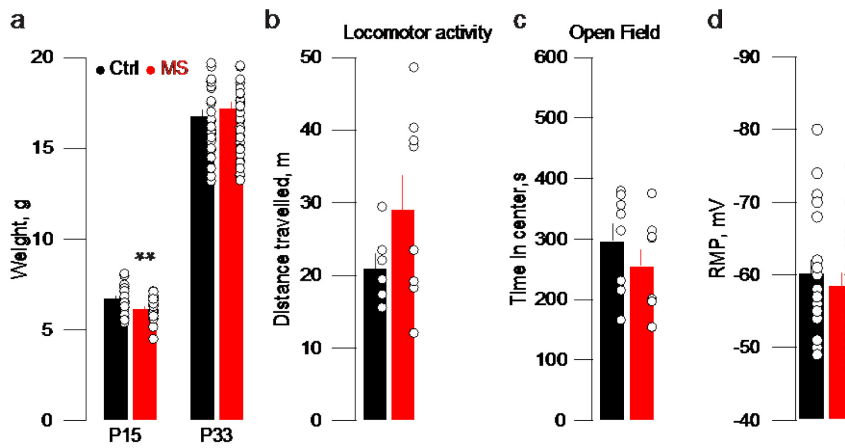


**Figure 4 Chemogenetic and DBS approaches reduce LHb activity and ameliorate MS-dependent depressive-like symptoms.**

**(a)** Schematic and image for Gi-DREADD LHb expression. **(b)** CNO effects on failures in the shuttle box (AAV-YFP, Ctrl vs MS and AAV-Gi-DREADD, Ctrl vs MS;  $n_{\text{mice}}=21/22/23/26$ ; two-way ANOVA RM, interaction,  $F_{(6,176)}=3.29$ ,  $**p<0.01$ ). **(c)** Bar graph and scatter plot for TST immobility (AAV-YFP and AAV-Gi-

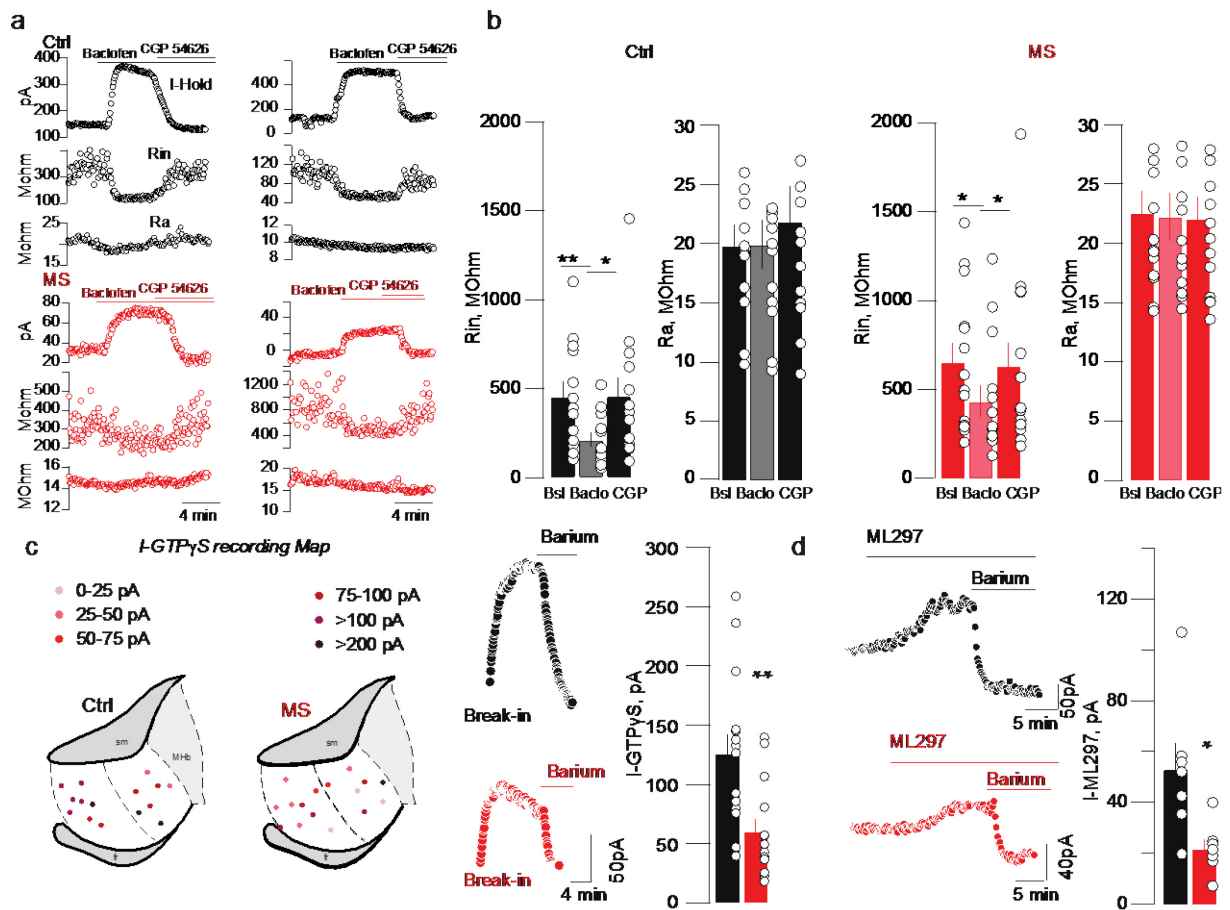
DREADD, Ctrl vs MS:  $n_{\text{mice}}=23/25/25/25$ ; two-way ANOVA, interaction,  $F_{(1,94)}=4$ ,  $*p<0.05$ ). **(d)** DBS effect on 1<sup>st</sup> EPSC and PPR (5 pulses, 20Hz. Normalized eEPSC post-DBS,  $n_{\text{mice}}=2$ ;  $n_{\text{cells}}=6$ ; One-way ANOVA RM;  $F_{(1.23,6.13)}=99.65$ ,  $***p<0.001$ ; Normalized EPSCs,  $n_{\text{mice}}=2$ ;  $n_{\text{cells}}=6$ ; Two-way ANOVA RM; DBS effect,  $F_{(2,50)}=25.1$ ,  $***p<0.001$ ). **(e)** Sample I-clamp recordings (5 superimposed-sweeps), and DBS effects on action potentials, resting membrane potential and input resistance (Before vs 5min post-DBS vs 10min post-DBS,  $n_{\text{mice}}=2$ ;  $n_{\text{cells}}=6$ : Action potential:  $F_{(1.29,6.49)}=13.5$ ,  $**p<0.01$ ;  $V_m$ :  $F_{(1.15,5.77)}=6.3$ ,  $*p<0.05$ ;  $R_i$ :  $F_{(1.06,5.30)}=8.3$ ,  $*p<0.05$ ; One-way ANOVA-RM) **(f)** DBS-electrode placement in LHb. **(g)** DBS-induced (130Hz, 150 $\mu$ A) reduction of activity in vivo (Firing before vs post-DBS,  $n_{\text{mice}}=4$ ;  $n_{\text{cells}}=14$ ; paired t-test,  $t_6=3.1$ ;  $**p<0.01$ ) **(h)** DBS-driven reduction of failures in the shuttle on MS mice (Sham vs DBS;  $n_{\text{mice}}=8/9$ ; Two-way ANOVA RM, interaction,  $F_{(1,15)}=9.476$ ,  $**p<0.01$ ). Scale bars, 100  $\mu$ m (a), 25 ms and 100 pA (d), 0.1 s and 20 mV (e), 250  $\mu$ m (f), 10 s (g).

## Supplemental information



### Supplementary Figure 1 Behavioral analysis of MS mice.

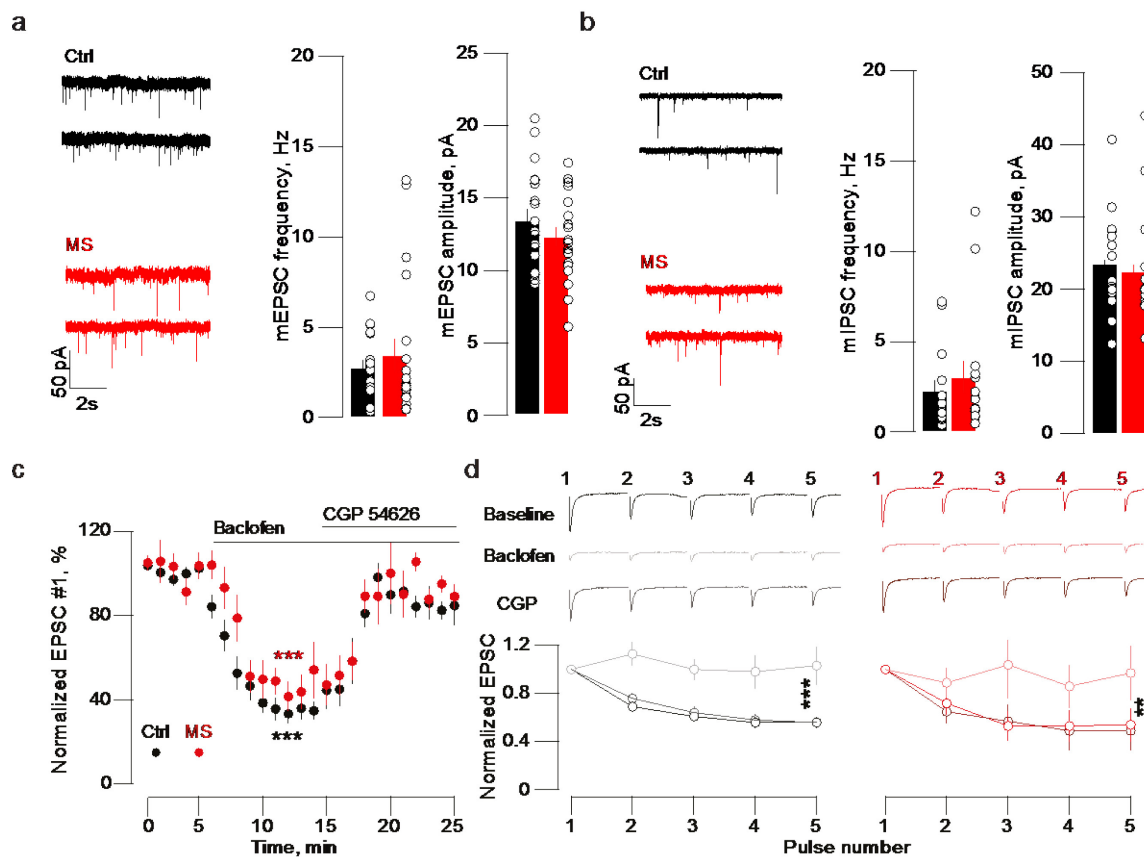
(a) Bar graphs and scatter plots depicting weight of mice at P15 and P33 (Ctrl vs MS,  $n_{\text{mice}} = 26$  vs 28, P15: unpaired t-test  $t_{52}=2.98$ ; \*\* $p < 0.01$ , P33; unpaired t-test  $t_{50}=1.024$ ;  $p > 0.05$ ). (b) Same as a but for locomotor activity at P33 (Ctrl vs MS,  $n_{\text{mice}} = 6/8$ ; distance travelled in 20 min, unpaired t-test  $t_{12}=1.50$ ;  $p > 0.05$ ). (c) Same as b but for activity in the open field (Ctrl vs MS,  $n_{\text{mice}} = 8$ ; time in center, unpaired t-test;  $t_{14}=1.045$   $p > 0.05$ ). (d) Comparison of resting membrane potential of Lhb neurons recorded in Fig. 1e (Ctrl vs MS; aCSF,  $n_{\text{mice}}=6/\text{group}$ ;  $n_{\text{cells}}=23/\text{group}$ ; unpaired t-test,  $t_{44}=0.74$ ;  $p > 0.05$ ).



### Supplementary Figure 2 MS reduces GABA<sub>B</sub>-GIRK signaling

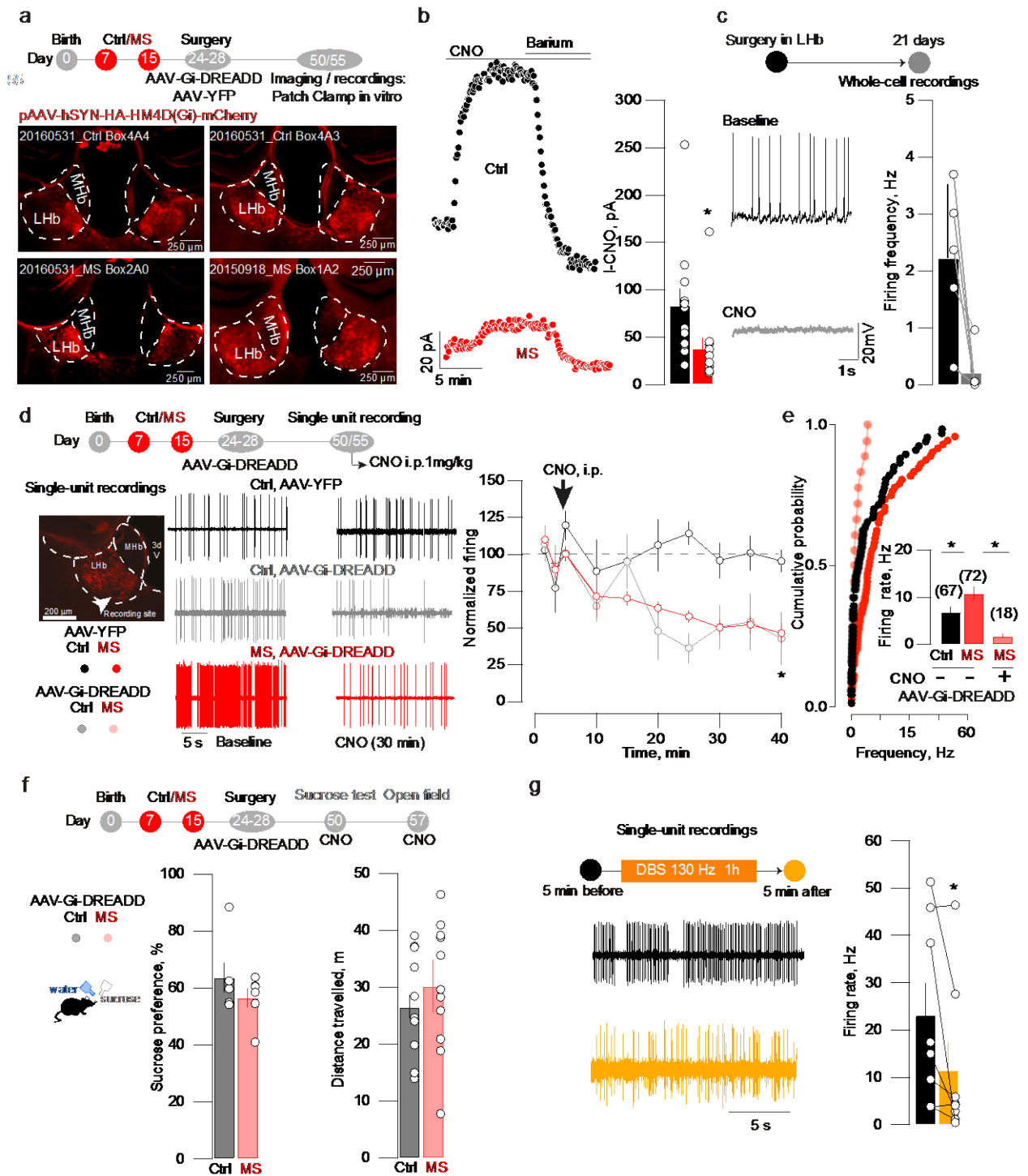
**(a)** Sample traces depicting CGP54626-sensitive I-Baclofen input resistance and access resistance in both experimental groups. **(b)** Bar graph representing Baclofen-mediated changes in input and access resistance in all the experimental groups. (Input resistance: Ctrl mice, baseline vs after baclofen vs CGP54626:  $n_{\text{mice}} = 5$ ;  $n_{\text{cells}} = 13$ ; One-way ANOVA RM; Treatment effect,  $F_{(1.532, 18.38)} = 11.44$ ,  $**p < 0.01$ ; MS mice: One-way ANOVA RM; Treatment effect,  $F_{(1.929, 25.08)} = 7.895$ ,  $**p < 0.01$ ) (Access resistance Ctrl mice, baseline vs after baclofen vs CGP54626:  $n_{\text{mice}} = 5$ ;  $n_{\text{cells}} = 13$ ; One-way ANOVA RM; Treatment effect  $F_{(2, 36)} = 0.239$ ,  $p > 0.05$ ; MS mice: One-way ANOVA RM; Treatment effect,  $F_{(2, 39)} = 0.017$ ,  $p > 0.05$ ) **(c)** Left, territorial distribution of I-GTP $\gamma$ S (100  $\mu$ M) showing MS-dependent reduction of GIRK signaling throughout the LHb. Right, sample traces, bar graph and scatter plots depicting I-GTP $\gamma$ S in Ctrl and MS mice (I-GTP $\gamma$ S Ctrl vs MS;  $n_{\text{mice}} = 5$ ;  $n_{\text{cells}} = 15$ ; unpaired t-test,  $t_{28} = 3.35$ ;  $**p < 0.01$ ). **(d)** Sample traces, bar graph and scatter plots depicting I-ML297 (50  $\mu$ M) in Ctrl and MS mice (I-ML297 Ctrl vs MS;  $n_{\text{mice}} = 2$ ;  $n_{\text{cells}} = 7$ ; unpaired t-test;  $t_{12} = 2.84$ ,  $*p < 0.05$ ).





### Supplementary Figure 3 MS does not alter synaptic neurotransmission

**(a)** Sample traces of mEPSCs from Lhb neuron of a Ctrl and a MS mice. Bar graphs and scatter plots showing frequency and amplitude of mEPSC for Ctrl and MS mice (Ctrl vs MS,  $n_{\text{mice}} = 8$  vs  $9$ ,  $n_{\text{cells}} = 20$  /group; frequency mEPSC; Kolmogorov-smirnov test,  $p > 0.05$ ; amplitude mEPSC Ctrl vs MS; unpaired t-test,  $p > 0.05$ ). **(b)** Same as **a** but for mIPSCs ( $n_{\text{mice}} = 7$  /group  $n_{\text{cells}} = 15$  /group; frequency mIPSC, Ctrl vs MS; Kolmogorov-smirnov test,  $p > 0.05$ ; amplitude mIPSC, Ctrl vs MS; unpaired t-test,  $p > 0.05$ ). **(c)** Timeline showing the baclofen-mediated reduction of evoked EPSC in Ctrl and MS mice (Ctrl vs MS:  $n_{\text{mice}} = 4$  and  $5$ ;  $n_{\text{cells}} = 7$  and  $6$ ; two-way ANOVA RM, interaction,  $F_{(24,264)} = 0.79$ ). **(d)** PPR of EPSCs before, and during baclofen application and subsequent CGP54626 (Normalized EPSC: Ctrl mice, baseline vs after baclofen vs subsequent CGP application for each pulses  $n_{\text{mice}} = 4$ ;  $n_{\text{cells}} = 6$ ; Two-way ANOVA RM; Treatment effect,  $F_{(2,50)} = 44.6$ ,  $***p < 0.001$ ; same for MS mice,  $n_{\text{mice}} = 5$ ;  $n_{\text{cells}} = 6$ ; Two-way ANOVA RM  $F_{(2,50)} = 15$ ,  $***p < 0.001$ ).



**Supplementary Figure 4 Gi-DREADD activation hyperpolarizes neurons and reduces LHB neuronal activity *in vitro* and *in vivo*.**

(a) Experimental timeline and representative images (4 different mice) for the site of injection in a coronal slice expressing the Gi-DREADD-mCherry in the LHB. (b) Sample traces depicting the CNO-induced current in LHB neurons of Ctrl and MS mice and its reversal by barium (1mM). Bar graph and scatter plot of the CNO-evoked current amplitude ( $n_{mice} = 3$ /group,  $n_{cells} = 12$  cells /group Ctrl vs MS; unpaired t-test,  $t_{22}=2.118$ ,  $*p < 0.05$ ). (c) Sample traces depicting the CNO-induced effect on neuronal firing in acute slices in naive mice (Baseline vs post CNO,  $n_{mice} = 3$ ;  $n_{cells} = 5$ ; paired t-test,  $t_4=3.1$ ,  $*p < 0.05$ ). (d) Representative image for Gi-DREADD expression and the site of *in vivo* recording labeled with pontamine sky blue. Sample traces and time course of CNO effect in Ctrl mice expressing AAV-YFP and Ctrl/MS mice expressing AAV-Gi-DREADD. ( $n_{mice} = 3$  vs 4 vs 4,  $n_{cells} = 3$  vs 4 vs 4, Two-way ANOVA, interaction,  $F_{(18,72)} = 2.15$ ,  $*p < 0.05$ ). (e) Cumulative probability plot

depicting the non-normal distribution of baseline firing of LHb neurons recorded in vivo from Gi-DREADD expressing Control (without CNO;  $n_{mice/cells} = 7/67$ ), MS (without CNO;  $n_{mice/cells} = 9/72$ ) and MS with CNO (i.p. 1mg/kg;  $n_{mice/cells} = 4/18$ ) (Kolmogorov-Smirnov test; Control vs MS,  $D=0.28$ ,  $**p<0.008$ ; MS vs  $MS_{CNO}$   $D=0.56$   $***p<0.0003$ ; Control vs  $MS_{CNO}$ ,  $D=0.35$ ,  $p>0.05$ ). **(f)** Left, effect on sucrose preference in Gi-DREADD Control and MS mice (MS vs Ctrl at baseline  $n_{mice} = 6$  vs  $6$ ,  $t_{10}=1.17$  unpaired t-test,  $p>0.05$ ). Right, same for locomotor activity (MS vs Ctrl at baseline  $n_{mice} = 11$  vs  $11$ ,  $t_{20}=0.82$  unpaired t-test,  $p>0.05$ ). **(g)** Effect of DBS (1h duration, 130Hz, 150 $\mu$ A) on baseline firing recorded in anesthetized mice ( $n_{mice}=5$ ;  $n_{cells}=7$ ; paired t-test,  $t_7=2.412$ ,  $*p<0.05$ ).

## Methods

### Experimental subjects and MS paradigm

All procedures were used in accordance with the guidelines of the French Agriculture and Forestry Ministry for handling animals (Committee Charles Darwin #5, University Pierre et Marie Curie, Paris). Part of the current study was carried out in the Department of Fundamental Neuroscience (Lausanne, Switzerland) under license and according to regulations of the Cantonal Veterinary Offices of Vaud and Zurich (Switzerland). Pregnant dams C57Bl/6J were received at the gestational stage E13-18 (Janvier laboratories, France). Mothers were housed 2 per cages with access of food and water at libitum. After birth, pups of either sex remained untouched until postnatal day (P) 7. At P7, litters were randomly divided in 2 groups. The maternal separation group consisted of pups removed from their litter and isolated in small compartments for 6 hours per day (light phase 8:19h) repeated from P7 to P15 and followed by an early weaning at P17. During the separation, animals were maintained in heating plate and water was provided, maintaining constant temperature and humidity. The control group consisted of mice from independent litters, which were not manipulated until the regular weaning at P21 except during cage changing. During cage changing some old bedding and nest were transferred into the new cage in order to limit novelty stress. After weaning, mice were separated by sex and housed 6 per cage. Experiments were performed in mice aged 4-8 weeks.

### Surgery

Animals, aged at least 24 days were anesthetized with Ketamine (150 mg kg<sup>-1</sup>)/Xylazine (100 mg kg<sup>-1</sup> i.p.) before bilateral injection of rAAV8-Hsyn-Gi-DREADD-mCherry (University of Pennsylvania, US) in the LHb at the following coordinates (from bregma, in mm): A-P: -1.45; M-L: ±0.45; D-V: -3.1. After three weeks, mice were subjected to CNO i.p injection (1mg/kg) for the DREADD activation. For optogenetic experiments rAAV2.1-hSyn-CoChr-eGFP (University of North Carolina, US) was infused in the entopeduncular nucleus (from bregma, in mm: A-P: -1.25; M-L: ±1.8; D-V: -4.65). Recordings were performed 3 weeks after surgery. The injection sites were carefully examined and only animals with correct injections were kept for behavioral and electrophysiological analysis. DBS electrodes were unilaterally implanted using similar procedures and coordinates in the LHb. DBS electrodes were chronically implanted using a Superbond resin cements (Sun medical, Japan). For the experiment analyzing the output specificity of I-Baclofen, mice were bilaterally injected with a mixture of herpes simplex virus (McGovern Institute, US) expressing enhanced GFP and red retrobeads (Lumafuor, US) into the RMTg or the VTA. The following coordinates were used (RMTg: from bregma, in mm: A-P: -2.9; M-L: ±0.5; D-V: -4.3; VTA: from bregma, in mm: A-P: -2.4; M-L: ±0.65; D-V: -4.9). Recordings from fluorescent LHb neurons were performed ±12 days following the surgery, and injection site were verified using the retrobeads labelling.

### Behavioral paradigm

All experimental behaviors were performed during the light phase and experimenters were blind of their experimental group.

The shuttle box test was performed in a shuttle box (13 × 18 × 30 cm) equipped with an electrified grid floor and a door separating the two compartments. The test session consisted of 30 trials of escapable foot-shocks (10 sec

at 0.1–0.3 mA) separated by an interval of 30s. The shock terminated any time that the animal shuttled in the other compartment. Failure is defined as the absence of shuttling to the other compartment within the 10 sec shock delivery.

The tail suspension test was performed with mice being suspended by their tails with adhesive tape for a single session of 6 min. Immobility time of each animal was scored online by the experimenter. Mice were considered immobile only when they suspended passively and motionless.

The sucrose test preference was performed with mice being single-housed and habituated with two bottles of 1% sucrose for 2 days. At day 3 (test day) mice were exposed to two bottles filled with either 1% sucrose or water for 24 h. The sucrose preference was defined as the ratio of the consumption of sucrose solution vs total intake (sucrose + water) during the test day and expressed as a percent.

Behavioral experiments in DREADD-injected animals were performed three weeks after viral infusion. For the shuttle Box, the tail suspension test, and the locomotor activity all the groups (YFP or DREADDi injected animals) were injected 15 minutes with CNO i.p. (1mg kg<sup>-1</sup>). For sucrose preference experiments, all groups were injected with CNO i.p. (1mg kg<sup>-1</sup>) every 3h for the extent of the preference session (24h) to maintain a constant DREADD-mediated inhibition.

### **Electrophysiology**

For in vitro recordings, animals were anesthetized with ketamine and xylazine (i.p. 150 mg kg<sup>-1</sup> and 100 mg kg<sup>-1</sup>, respectively). Coronal brain slices (250  $\mu$ m) containing the LHb were prepared in bubble ice-cold 95% O<sub>2</sub>/5% CO<sub>2</sub>-equilibrated solution containing: 110 mM choline chloride; 25 mM glucose; 25 mM NaHCO<sub>3</sub>; 7 mM MgCl<sub>2</sub>; 11.6 mM ascorbic acid; 3.1 mM sodium pyruvate; 2.5 mM KCl; 1.25 mM NaH<sub>2</sub>PO<sub>4</sub>; 0.5 mM CaCl<sub>2</sub>. Slices were then stored at room temperature in 95% O<sub>2</sub>/5% CO<sub>2</sub>-equilibrated artificial cerebrospinal fluid (ACSF) containing: 124 mM NaCl; 26.2 mM NaHCO<sub>3</sub>; 11 mM glucose; 2.5 mM KCl; 2.5 mM CaCl<sub>2</sub>; 1.3 mM MgCl<sub>2</sub>; 1 mM NaH<sub>2</sub>PO<sub>4</sub>. Recordings (flow rate of 2.5 ml/min) were made under an Olympus-BX51 microscope (Olympus, France) at 30 °C. Currents were amplified, filtered at 5 kHz and digitized at 20 kHz. Access resistance and input resistance were monitored by a step of -4 mV (0.1 Hz). Experiments were discarded if the access resistance increased more than 20%.

The internal solution used to examine GABA<sub>B</sub> and/or GIRK currents and neuronal excitability contained: 140 mM potassium gluconate, 4 mM NaCl, 2 mM MgCl<sub>2</sub>, 1.1 mM EGTA, 5 mM HEPES, 2 mM Na<sub>2</sub>ATP, 5 mM sodium creatine phosphate, and 0.6 mM Na<sub>3</sub>GTP (pH 7.3 with KOH). The liquid junction potential was ~12 mV. When we measured the synaptic inhibitory or excitatory release, the internal solution contained: 130 mM CsCl; 4 mM NaCl; 2 mM MgCl<sub>2</sub>; 1.1 mM EGTA; 5 mM HEPES; 2 mM Na<sub>2</sub>ATP; 5 mM sodium creatine phosphate; 0.6 mM Na<sub>3</sub>GTP; and 0.1 mM spermine. The liquid junction potential was -3 mV. Whole-cell voltage clamp recordings were achieved to measure GABA<sub>B</sub>-GIRK currents in aCSF only. For agonist-induced currents, changes in holding currents in response to bath application of baclofen (100  $\mu$ M) were measured (at -50 mV every 5-10 s). The plotted values correspond to the difference between the baseline and the plateau (for the baclofen and ML297 experiments) or the difference between the plateau and the value of holding current after barium (for the I-GTP- $\gamma$ S) GABA<sub>B</sub>-GIRK currents were confirmed by antagonism with 10  $\mu$ M of CGP54626. When stated, 100  $\mu$ M of GTP- $\gamma$ S was added to the internal solution in place of Na<sub>3</sub>GTP. Plateau currents were then reversed by 1 mM Barium application, a selective inhibitor of K<sup>+</sup> channels. Changes in

holding currents in response to GIRK agonist were measured (at  $-50$  mV every 5-10 s) by bath application of ML-297 ( $50$   $\mu$ M), a Selective GIRK1/2 channel activator then reversed by  $1$  mM Barium application. Synaptic GABA<sub>B</sub> slow IPSCs were optically evoked by trains of 10 pulses delivered at  $20$  Hz through a  $470$  nm LED. The fast GABA amplitude correspond to the amplitude of the first pic of the train, the slow GABA current instead were measured after picrotoxin bath application, and correspond to the I-max. Miniature excitatory postsynaptic currents (mEPSCs) were recorded in voltage-clamp mode at  $-60$  mV in presence of bicuculline ( $10$   $\mu$ M), AP5 ( $50$   $\mu$ M) and tetrodotoxin (TTX,  $1$   $\mu$ M). Miniature inhibitory postsynaptic currents (mIPSCs) were recorded ( $-60$  mV) in presence of NBQX ( $20$   $\mu$ M) AP5 ( $50$   $\mu$ M) and TTX ( $1$   $\mu$ M). EPSCs were evoked through an ACSF-filled monopolar glass electrode placed in the LHb. For the experiments in which high-frequency stimulation trains were used to determine presynaptic release probability ( $5$  pulses at  $20$  Hz), QX314 ( $5$  mM) was included in the internal solution to prevent the generation of sodium spikes.

Current-clamp experiments were performed using a series of current steps (from  $-80$  pA to  $100$  pA or when the cell reached a depolarization block) injected to induce action potentials ( $10$ -pA injection current per step, duration of  $500$  ms). Cells were maintained at  $-55$ mV throughout the experiment. When testing changes in tonic firing, cells were depolarized to obtain stable firing activity in current clamp mode.

When in vivo single unit recordings were performed, mice were anesthetized with isoflurane (induction:  $2\%$ ; maintenance:  $1$ - $1.5\%$ ) using an anaesthesia device for small animals (Univentor 410, Malta). We placed the mice in the stereotaxic apparatus (Kopf, Germany) and their body temperature was maintained at  $36\pm 1$  °C using a feedback-controlled heating pad (CMA 450 Temperature Controller, USA). The scalp was retracted and one burr hole was drilled above the LHb (A-P:  $-1.3$ / $-1.6$ ; M-L:  $\pm 0.4$ / $0.5$ ) for the placement of a recording electrode. Single unit activity of neurons located in the LHb (Ventral  $2.3$ – $3.2$  mm to cortical surface) was recorded extracellularly by glass micropipettes filled with  $2\%$  pontamine sky blue dissolved in  $0.5$  M sodium acetate (impedance  $3$ – $6$  M $\Omega$ ). Signal was pre-amplified (DAM80, WPI, Germany), filtered (band-pass  $500$ – $5000$  Hz) amplified (Neurolog System, Digitimer, UK), displayed on a digital storage oscilloscope (OX 530, Metrix, USA), and digitally recorded. Experiments were sampled on- and off-line by a computer connected to CED Power 1401 laboratory interface (Cambridge Electronic Design, Cambridge, UK) running the Spike2 software (Cambridge Electronic Design). Single units were isolated and identified according to previously described electrophysiological characteristics (Meyer et al 2015) including a broad triphasic extracellular spike ( $>3$  ms), and a tonic regular, tonic irregular or bursting spontaneous activity.

Isolated LHb neurons were recorded for  $5$  min to establish the basal spontaneous firing rate. CNO was administered i.p. ( $1$  mg  $\text{kg}^{-1}$ ) and the firing activity of the neuron was monitoring every  $5$ m for total  $40$ m. When CNO was administered, only one cell was recorded per mouse.

DBS experiments were performed with a modified double barrel system allowing to stimulate in close proximity of the recording site: the stimulating electrode was attached to the recording one by using glass barrels (the 2 electrodes form an angle of  $\pm 30^\circ$ ). The stimulating tip was glued above the recording tip ( $<300$  $\mu$ m). A stable spontaneous firing rate was recorded for  $5$ min before to start the DBS protocol (total duration:  $2$ - $5$ m; Train pulses:  $7$ ; ITI:  $40$ ms; Frequency:  $130$ Hz; Intensity:  $150$  $\mu$ A). The firing activity recorded immediately after the protocol was compared with the respective baseline.

At the end of each experiment, the electrode placement was marked with an iontophoretic deposit of pontamine sky blue dye ( $-80$   $\mu$ A, continuous current for  $35$  min). Brains were then rapidly removed and fixed in  $4\%$

paraformaldehyde solution. The position of the electrodes was microscopically identified on serial sections (60  $\mu\text{m}$ ).

### **Deep brain stimulation**

MS mice for DBS experiments were first preselected on the basis of their failure rate in the Shuttle box test (A cutoff of 12 failures was used for the preselection). 50 mice were tested, and 17 of these animals met the criteria. Standard surgical procedures were used to implant bipolar concentric electrodes unilaterally into the LHb (coordinates  $-1.45$  mm AP,  $\pm 0.45$  mm ML and  $-3.1$  mm DV). After 5 days recovery from surgery, DBS or no (Sham) stimulation was applied for 1h (seven stimulus trains of 130 Hz, separated by 40 ms intervals; 150  $\mu\text{A}$  intensity) prior testing each mouse in the shuttle box test.

### **Analysis and drugs.**

All drugs were obtained from Abcam (Cambridge, UK) and Hello Bio, and Tocris (Bristol, UK) and dissolved in water, except for TTX (citric acid 1%), ML297 and CNO (DMSO). Online/offline analysis were performed using IGOR-6 (Wavemetrics, US) and Prism (Graphpad, US). Data analysis for *in vivo* electrophysiology was performed off-line using Spike2 (CED, UK) software. Sample size required for the experiment was empirically tested by running pilots experiments in the laboratory. While behavioral experiments were run in a single-to-triple trial, electrophysiological experiments were replicated at least 5 times. Experiments were replicated in the laboratory at least twice. Animals were randomly assigned to experimental groups. Data distribution was assumed to be normal, and single data points are always plotted. Compiled data are expressed as mean  $\pm$  s.e.m. All groups were tested with Grubbs exclusion test (limit set at 0.05) to determine outliers. Significance was set at  $p < 0.05$  using Student's t-test two-sided, Kolmogorov-smirnov test, one-way, two-way or three-way Anova with multiple comparison when applicable.

### **Data availability.**

All relevant data are available from the authors upon request.

## Discussion

---

The two articles presented in this thesis work showed that different types of stress can trigger GABA<sub>B</sub>R-dependent hyperexcitability of the lateral habenula (LHb) that is, in turn, instrumental in the emergence of depressive-like symptoms. Indeed, reversal strategies aiming to restore the neuronal activity directly acting on the excitability (DREADD/DBS) or indirectly through the restoring/upregulation of the postsynaptic GABA<sub>B</sub>R function (LB-100, GIRK overexpression) could ameliorate depressive symptoms in two different rodent models of depression (LHp and MS). The work of this thesis establishes a causal relationship between stress-driven LHb hyperexcitability and subsequent depressive-like symptoms. Altogether, these data suggest that LHb hyperactivity could be a general substrate underlying features of depressive-like states. However, several questions remain to be addressed, and different consideration will be discussed in the next paragraphs.

### I. Stress-driven mechanisms underlying GABA<sub>B</sub> receptor plasticity in the LHb

From our data, we can extract two important aspects regarding the GABA<sub>B</sub>R-dependent regulation of LHb neuron's function in aversive states: first, the GABA<sub>B</sub>R internalization occurs rapidly following acute unpredictable aversive stimuli; second, GABA<sub>B</sub>R functional reduction represents a long-term adaptation for the establishment of MS-driven depressive-like states. These findings highlight the reduction of LHb GABA<sub>B</sub>Rs as a common marker of depression. However, we are still lacking fundamental knowledge in terms of the molecular machinery that could underlie GABA<sub>B</sub>R plasticity in the LHb. Thus, an essential point to address in future studies is first to identify the potential modulators of GABA<sub>B</sub>R-GIRK signaling in the LHb. This will set the stage to understand how such mechanisms are regulated in physiological and pathological conditions to eventually open a new window toward potential pharmacological targets to treat depressive symptoms. In line with that our data provide insights about a GABA<sub>B</sub>R intracellular modulator important for LHb neuronal function: the PP2A.

Previous results obtained in midbrain and cortical neurons revealed that intracellular infusion of okadaic acid, protein phosphatase type 1 (PP1) and protein phosphatase type 2 (PP2A) inhibitor can rescue psychostimulant-driven GABA<sub>B</sub>R internalization (Hearing et al., 2013; Padgett et al., 2012). Similarly, in our study, following inescapable foot-shock (FS), GABA<sub>B</sub>R signaling down-regulation in the LHb neurons also involves PP2A increased



activity as measured by enzyme assay. Moreover, we took advantage of a new compound, the LB-100 that present the advantage to have a higher affinity for PP2A than PP1, differently then okadaic acid (Lu et al., 2009) and importantly is cell permeable and passes the blood brain barrier, permitting its use in vivo. This allowed us to test the efficacy of PP2A inhibition in reversing GABA<sub>B</sub>R plasticity in vivo and to causally link the PP2A upregulation to the emergence of the depressive phenotype.

Mechanistically, the increase in PP2A activity following FS involved GABA<sub>B</sub>R-GIRK internalization and their retention in the internal compartments. In contrast, studies in cell culture preparations have reported a PP2A-dependent degradation of the GABA<sub>B</sub>Rs (Terunuma et al., 2010a). Whether a shift toward lysosomal degradation occurs at later time points in our and other studies remains however matter of future investigations. Importantly, a potential degradation of the receptor at a later stage could compromise the efficiency of the LB-100 in reverting the GABA<sub>B</sub>R plasticity, if LB-100 will be provided long time after the FS.

Another aspect to address involves the mechanism underlying GABA<sub>B</sub>R-GIRK plasticity following MS. Indeed, while we provide substantial information showing functional down-regulation of the GABA<sub>B</sub>R-GIRK, we did not provide evidence regarding the location of these proteins following MS. Whether the receptor is internalized, and/or directed to lysosomal degradation is not known. Further experiments such as western blot analysis, or ultrastructure electron microscopy will allow respectively to assess the total protein level as well as to decipher if internalization or degradation of the GABA<sub>B</sub>Rs also occurs in this case. Moreover, whether MS model presents an increased PP2A activity and if in this case, LB-100 could be efficient to ameliorate depressive phenotype remains an open question.

Undeniably, PP2A is only one of the molecular determinants governing GABA<sub>B</sub>R trafficking, and could explain the GABA<sub>B</sub>R down-regulation following stress. As example, CaMKII-dependent phosphorylation have also been implicated in the stabilization of GABA<sub>B</sub>Rs on the plasma membrane (Couve et al., 2002; Guetg et al., 2010). Notably,  $\beta$ -CaMKII is upregulated in the LHb in different models of depression (Li et al., 2013). Despite that CaMKII inhibition was not able to restore the I-baclofen current in the FS model, we did not test its action in the MS. In addition to this, the four K<sup>+</sup> channel tetramerization domain-containing (KCTD)12 is also known to stabilize GABA<sub>B</sub>Rs at the cell surface and to regulate kinetic properties of the receptor response (Fritzius et al., 2017; Metz et al., 2011; Schwenk et al., 2010). The KCTD8, 12, and 12b transcripts expression have been reported in the LHb (Metz et al., 2011). Moreover, in another region of the brain (amygdala), a translational microarray study

identified KCTD12 as one of the genes with an upregulated expression in major depression disorder patients and in mice exposed to unpredictable chronic mild stress (Sibille et al., 2009). The analysis of the GABA<sub>B</sub>R-GIRK Baclofen-evoked currents in LHb reveals a very low, almost absent desensitization, which is instead characterized in cells expressing KCTD12. If these proteins can be expressed in a specific cell subpopulations and how they are regulated in physiological and pathological conditions will require future investigations in order to establish their potential implication in GABA<sub>B</sub>R signaling in the LHb.

Additionally, GABA<sub>B</sub>R-GIRK signaling decrease may rely not only on reduced GABA<sub>B</sub>R function and expression but also on a direct regulation of the GIRK surface expression. Our data support a functional reduction of GIRKs following FS and MS, as well as a GIRK internalization following FS. As described elsewhere, one possibility is that both GABA<sub>B</sub>Rs and GIRKs channels are physically interacting, forming functional macro-complexes (Ciruela et al., 2010; Fowler et al., 2007; Lavine et al., 2002; Riven et al., 2006) that may traffic together to the intracellular compartments (Clancy et al., 2007). However, a direct and independent regulation of GIRK channels cannot be excluded. For instance, after methamphetamine treatment, the loss of sorting nexin 27 (SNX27) contributes to GABA<sub>B</sub>R-GIRK signaling reduction in VTA DA neurons via its interaction with GIRK3 subunit (Munoz et al., 2016). Currently, no data are available concerning the expression of such proteins in the LHb. Furthermore, unlike certain regions such as the VTA (Labouèbe et al., 2007) information concerning the GIRK subunits composition are critically missing in the LHb. RT-PCR suggests the expression of all the subunits of GIRK(1-4) within the LHb. Yet, only GIRK2 surface expression have been established as measured by electron microscopy. Moreover, this subunit is downregulated following FS while GIRK2 overexpression within the LHb is able to restore both I-baclofen response and ameliorate the depressive state in the FS animal suggesting for an important functional role of the GIRK2 subunit. In the VTA neurons, the heterogeneity of GIRK responses has been associated with the different subunit composition. While DA neurons express only GIRK2,3 subunits and present large baclofen-evoked currents and large desensitization, GABA neurons instead express GIRK1-3 contributing to a non-desensitizing somewhat smaller I-Baclofen currents (Labouèbe et al., 2007). Our data suggest that I-baclofen current and I-GTP $\gamma$ S in LHb neurons present low desensitization suggesting for at least a functional GIRK1-2. In addition, considering the important role of GIRK3 for the trafficking of the channel (Lalivè et al., 2014; Lunn et al., 2007), it will be interesting to see if also in the LHb such regulation exists and can underlie GABA<sub>B</sub>R plasticity. Future studies employing GIRKs knock-out (KO) mice could help to

better clarify the LHb-GIRK subunit composition and the functional relevance of GABA<sub>B</sub>R-GIRK signaling.

Altogether, although our study provides evidence for a crucial role of PP2A for GABA<sub>B</sub>R plasticity within the LHb in the context of depression, the complexity of the GABA<sub>B</sub>R signaling keeps open the possibility of a more complex scenario where other partners can have a role. Especially, a better understanding of the mechanism underlying GABA<sub>B</sub>R regulation hold the promise to unravel alternative targets for GABA<sub>B</sub>R signaling.

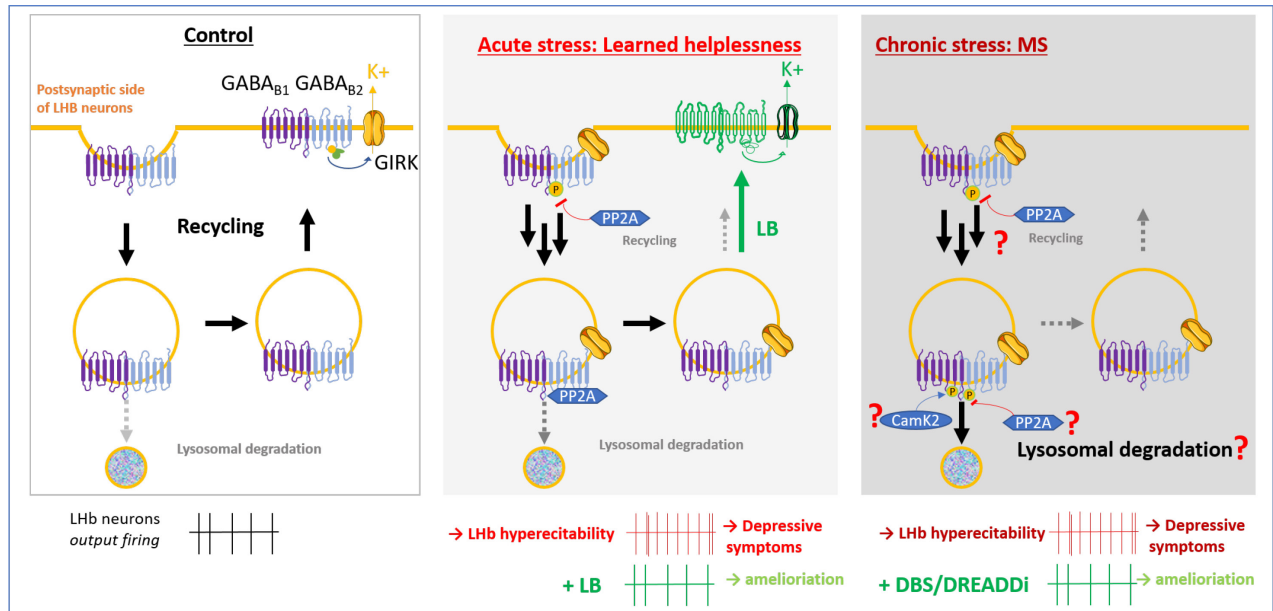
## II. Induction mechanism of GABA<sub>B</sub> receptor plasticity following different kind of stress

In both studies, one question that remains non-addressed is the lack of information regarding the induction mechanism triggering the down-regulation of GABA<sub>B</sub>Rs following stress exposure. Chronic stress has been shown to increase the function of the HPA axis and glucocorticoids activity subsequently triggering behavioral impairments (de Kloet et al., 2005). Neuroendocrine markers of elevated stress reactivity have notably been reported in human depressed patient (Carroll, 1982; Nemeroff et al., 1984) as well as in rodent models such as maternal separation (MS) (Anisman et al., 1998; Ladd et al., 2000) and after an inescapable stress in rats (Kant et al., 1987). A recent study from our laboratory reported that both the activation of glucocorticoid receptors or DA receptors are required for LHb GABA<sub>B</sub>R plasticity since systemic injection of specific antagonists can prevent it (Lecca et al., 2017). However, the local application of corticosterone or DA was not sufficient to trigger the plasticity. One explanation could be that the activation of glucocorticoid receptors or DA receptors may occur in structures different than the LHb and the plasticity will require a circuit re-adaptation.

Alternatively, N-methyl-D-aspartate receptors (NMDAR) activation can similarly regulate GABA<sub>B</sub>R function. Studies in primary neuronal culture described a NMDA-dependent calcium increase that allows the activation of CaMKII (Guettg et al., 2010) or PP2A (Terunuma et al., 2010a) that respectively act at the S867 of the GABA<sub>B1</sub> and the S783 of the GABA<sub>B2</sub> subunit to ultimately trigger the internalization/degradation of the receptor. Furthermore, a recent study performed in acute brain slices unravels a role of NMDA receptor in dampening GABA<sub>B</sub>R signals in paraventricular hypothalamic neurons after unpredictable aversive stimuli exposure (Gao et al., 2017). Altogether, these studies pointed out for a crucial role of intracellular calcium increase (via NMDA activation) as a trigger for the induction of GABA<sub>B</sub>R internalization/degradation. The synaptic transmission onto LHb neurons have the

property to display a very small NMDA receptor component (Li et al., 2011; Maroteaux and Mameli, 2012). However, the  $\alpha$ -amino-3-hydroxy-5methyl-4-isoxazolepropionic acid (AMPA) receptor component in the LHb shows strong inward rectification, suggesting the presence of the GluA2-lacking calcium permeable AMPA receptors. Thus, a hypothetical scenario is that GluA1 type AMPAR in the LHb could play a similar role as the NMDA in other synapses and be sufficient to increase the calcium ( $\text{Ca}^{2+}$ ) levels sufficient to trigger  $\text{GABA}_{\text{B}}\text{R}$  down regulation.

If we were to consider that glutamate is a requirement for  $\text{GABA}_{\text{B}}\text{R}$  plasticity, we can think about a special organization of the glutamatergic and GABAergic presynaptic components that will promote this interaction. Interestingly, different studies pointed out a particular feature of certain LHb synapses: inputs from the EPN and from the VTA to LHb display a co-release of glutamate and GABA from a single neuron (Root et al., 2014b; Shabel et al., 2014). This property could represent a perfect setting for the expression of the above-mentioned plasticity. Notably, in the second study, we revealed that the synaptically relevant  $\text{GABA}_{\text{B}}\text{R}$  signaling from the EPN was altered after MS. If other inputs are able to elicit a postsynaptic  $\text{GABA}_{\text{B}}\text{R}$  response, and whether it is modified following stress is an object of future investigations.



**Figure 10: Potential mechanisms underlying LHb  $\text{GABA}_{\text{B}}\text{R}$ -GIRK reduction in rodent model of depression**

In the learned helplessness, PP2A-dependant  $\text{GABA}_{\text{B}}\text{R}$ -GIRK internalization is responsible of an increased LHb neuronal activity underlying depressive-like symptoms. In the MS, decrease in  $\text{GABA}_{\text{B}}\text{R}$ -GIRK signaling also triggers LHb neuronal excitability and depressive-like symptoms. However, the underlying mechanism of such adaptation remains more elusive. One hypothesis is that it could involve an increase in endocytosis and/or degradation. The subsequent decrease surface expression of  $\text{GABA}_{\text{B}}\text{R}$ -GIRK leads also in this case in LHb hyperactivity that can be rescue by interventions dampening LHb activity such as DREADDi or DBS.

### III. Circuit specificity of GABA<sub>B</sub> receptor regulation in the LHb

In the first study, GABA<sub>B</sub>R responses were evoked by applying a saturating concentration of the selective agonist baclofen (I-baclofen). This experiment allows the quantification of the total GABA<sub>B</sub>R-GIRK current in the cell but remains however non-physiological because it engages the activation of all the potential available receptors in a given LHb cell, not necessarily recruited in physiological condition. This raises questions about the physiological and behavioral relevance of GABA<sub>B</sub>R activation in the LHb, a question that remains quite open in the field of neuroscience. Moreover, agonist evoked current cannot provide information about circuit specificity of the GABA<sub>B</sub>R signaling. In my second study, I have tried to refine this approach in order to specifically activate synaptically relevant GABA<sub>B</sub>Rs. Using 20 Hz opto-stimulation, I was able to promote GABA release from EPN terminals, likely inducing GABA spillover and to evoke a synaptically-relevant GABA<sub>B</sub>R slow current. This range of activity is physiologically more relevant, as it is likely to happen in vivo (Scanziani, 2000; Stephenson-Jones et al., 2016), although the behavioral relevance of such slow inhibition remains in the entire field still enigmatic.

Despite the data provided, several questions remain unanswered and are the object of interest of my following study: (1) the EPN is only one of the GABAergic sources in the LHb. Could specific activation of other GABAergic inputs trigger a GABA<sub>B</sub>R postsynaptic currents? (2) Does stress modulate these responses in a circuit specific manner? (3) Could it be possible that inducing LTP/LTD protocol by stimulation of specific inputs, can mimic or reverse the depressive-like symptoms?

In this context, a previous study highlighted a plasticity of GABA<sub>B</sub>R-GIRK signaling in the VTA DA cells: somatic low frequency stimulation of DA neurons induced NMDA-dependent decrease of GABA<sub>B</sub>R-GIRK signaling (Lalivie et al., 2014). If such protocol could be applied at LHb to modulate the slow inhibition, potentially at specific inputs such as VTA, VP or lateral hypothalamus (LH) (all described to present both GABAergic and glutamatergic component) remains a very interesting question to be addressed (Root et al., 2014b; Knowland et al., 2017; Stamatakis et al., 2016).

Notably, to date we have no indication of the input instrumental for the expression of the depressive symptoms. In light of a new study from our laboratory describing the involvement of the LH in conveying aversive information to the LHb (Lecca et al., 2017), we can speculate that the recruitment of this input during stressful event is necessary and sufficient to trigger

LHb aberrant plasticity (i.e. AMPA transmission potentiation and/or GABA<sub>B</sub>R decrease), and potentially drive behaviors reminiscent of depression.

#### IV. What is the functional relevance of GABA<sub>B</sub> receptor dependent hyperexcitability for the emergence of depressive like symptoms

In both studies, we showed that GABA<sub>B</sub>R-GIRK signaling decreases throughout the LHb leading to a widespread increased neuronal excitability and triggers depressive like symptoms. But, is there any linear relationship between LHb excitability and depressive symptoms? Notably, whether the emergence of the depressive symptoms requires a progressive increase in excitability in a given LHb neuronal population or a progressive engagement of diverse neuronal ensembles is still an open issue. The analysis of ensemble of neurons, using for example calcium imaging approaches in awake mice (via a GRIN-lens implantation and microendoscope) may allow to visualize online the LHb single neurons dynamic during the establishment of depressive states and to assess which of these two scenarios hold true. Alternatively, optogenetic or chemogenetic modulation of the LHb, can be employed to selectively activate and recruit a growing number of neuronal population. By injecting ChR2 (channel rhodopsin 2) or DREADDs (Designer Receptor Exclusively Activated by Designer Drugs excitatory) at different virus dilution, we could assess the threshold for minimal neuronal ensemble sufficient to trigger a depressive phenotype. Furthermore, to gain knowledge at the level of the circuit, we can study defined LHb output specific populations, employing retrograde expression of ChR2 or DREADDs in different subpopulation (LHb to raphe, VTA and/or RMTg). Such sophisticated experiments are not trivial to be set but will probe the need of the recruitment of one or more pathways in triggering depressive phenotypes.

Now, would it be possible that GABA<sub>B</sub>R plasticity is the only neurobiological substrate underlying LHb hyperexcitability and depressive like symptoms? In our study, we did not provide proof for the sufficiency of GABA<sub>B</sub>R dysregulation in inducing depressive-like symptoms. Moreover, other mechanisms have been described to be dysregulated in the LHb in the context of depression. Indeed, electrophysiology recording in the Learned Helplessness (LHp) rat, a decrease of the fast GABAergic transmission has been reported at EPN to LHb synapses (Shabel et al., 2014). In the same model of depression, an increase in presynaptic glutamatergic transmission in VTA-projecting LHb neurons occurs together with an increase of LHb neuronal activity (Li et al., 2011). Moreover, a study by Li and colleagues (2013)

identifies an increased  $\beta$ CaMKII activity as a potential upstream mechanism for this AMPAR changes. Given this data, we also recorded excitatory miniature activity in MS and FS mice without finding overall changes. However, this discrepancy could be explained at least by three factors: the animal model (rat versus mice and stress protocol), the fact that we did not preselect the depressed animal and the lack of cell specificity to assess fast synaptic transmission in our studies.

Taking altogether these studies we can imagine two hypothetical scenarios. The rapid GABA<sub>B</sub>R-GIRK reduction-dependent increase in excitability following acute unpredictable stress could represent a permissive initial cellular trigger for consequent adaptations, such as  $\beta$ -CaMKII-mediated synaptic modifications. Alternatively, these changes can occur as parallel cellular processes that contribute in synergy to LHB hyperactivity and depressive phenotype.

## V. Targeting LHB hyperexcitability to treat depression?

Convergent studies in the last decade showed substantial agreement regarding the instrumental role of LHB hyperactivity in depressive-symptoms (Boulos et al., 2017; Lecca et al., 2014; Proulx et al., 2014). Indeed, different kind of stressors, including acute stress, chronic-stress or drug withdrawal, all trigger depressive-like symptoms associated with LHB hyperactivity (i.e. (Li et al., 2011; Meye et al., 2015; Seo et al., 2017; Shumake et al., 2003). Importantly, successful attempts to causally link LHB hyperactivity and depressive symptoms were also made (Li et al., 2011; Li et al., 2013; Meye et al., 2015). Employing acute stressors and two different models of depression (LHp and MS) we demonstrate a causal link between LHB hyperexcitability and discrete depressive phenotypes, since manipulating the LHB hyperactivity was sufficient to ameliorate the phenotype. In particular, in these studies, we used two potential therapeutically relevant strategies to reverse the depressive like symptoms via a selective dampening of LHB activity. However, several considerations need to be taken into account when thinking about the translational aspect.

### A. *Caveat of DBS intervention:*

#### i. *A controversial effect of DBS on neuronal activity*

DBS is an intervention widely used in the clinics to treat diverse neuropathologies including mood disorders (Delaloye and Holtzheimer, 2014; Fitzgerald and Segrave, 2015; Funkiewiez et al., 2004; Holtzheimer and Mayberg, 2011b; Lüscher and Pollak, 2016; Naesström et al., 2016; Narang et al., 2016; Salling and Martinez, 2016). Notably, a seminal study reported the potential interest of LHB DBS in a treatment-resistant depressed patient (Sartorius et al.,

2010). However, the mechanism underlying its effect were poorly understood (Mcintyre et al., 2004; Vitek, 2002). In the MS model, we observed that DBS in the LHb was able to reduce the excitatory glutamatergic drive as well as to hyperpolarize the postsynaptic neurons potentially by opening potassium conductance as suggested by the decrease in the resting membrane potential and in the cell input resistance. Moreover, in vivo recording indicated that the global effect of the stimulation reduces LHb neuronal firing activity. However, DBS could inhibit postsynaptically but could have the opposite effect in downstream structures (Vitek, 2002). Although further experiments to verify the effect in downstream targets would be interesting per se, we did not directly control for that. However, to overcome these caveats, we employed the selective chemogenetic inhibition of LHb in the MS model that led to similar physiological (postsynaptic) effect and behavioral rescue suggesting that the antidepressant effect of DBS seems, at least in part, to rely on a local inhibition of LHb.

#### *ii. Temporal limitation of DBS*

Another general feature of DBS treatment is its chronicity. Patients under treatment need a continuous stimulation. Indeed, the depressed patient treated with LHb-DBS showed a rapid relapse when the pacer malfunctioned (within 1 week) (Kiening and Sartorius, 2013; Sartorius et al., 2010). In the MS model, we also observed a transient effect of the stimulation in reducing LHb neuronal activity, however we did not assess for the long term effects of DBS in the behavioral outcome leaving this question still opened. One caveat of this experiment, is that DBS ameliorates the pathological phenotype engaging many mechanism (presynaptic excitatory decrease and potentially opening of potassium channels) without however targeting the expression mechanism (i.e. GABA<sub>B</sub>R-GIRK reduction). Taking advantage of the advanced knowledge we acquired on the underlying molecular mechanisms, we could think to refine the protocol, trying to target specific plasticity such as the GABA<sub>B</sub>Rs.

The DBS shows a good efficacy but it is still an invasive intervention. Therefore, researcher are looking for novel drug compounds that will improve the efficacy especially in treatment-resistant patients.

#### ***B. PP2A inhibitors as potential antidepressant drugs***

In our study, the PP2A inhibitor LB-100 revealed to be efficient in ameliorating depressive symptoms, rescuing GABA<sub>B</sub>R signaling, and LHb activity. Notably, we showed comparable results acting systemically and locally, restoring the GABA<sub>B</sub>R surface expression in LHb and its neuronal activity, highlighting a causal link between LHb GABA<sub>B</sub>R downregulation and depressive symptoms. However we tested LB-100 only immediately (within few days) after a



traumatic experience, such as FS, whether inhibiting PP2A activity can be a valid strategy to reverse the depressive phenotype in a later time point and for different models needs to be determined.

Importantly, central and peripheral effects have to be taken into account. In this context, one could ask if LB-100 is able to modulate GABA<sub>B</sub>R expression in brain regions other than the LHb, and consequently have side effects. In our study, we show that LB-100 treatment let unaltered the food and water intake, the weight, the locomotion and the maintenance of contextual fear memory in mice. Nevertheless, further experiments looking at the physiological consequences in other brain areas and more elaborate behavioral paradigms should be determined. Furthermore, PP2A have many other downstream targets: it has been reported to play a role in cell proliferation and apoptosis (Seshacharyulu et al., 2013). Yet the use of LB-100 for translational studies is a reality as this compound was recently approved by the Food and Drug Administration for Phase I study in patients with advanced cancers (Lixte, biotechnology), and its potential toxicity was also tested in humans (Chung et al., 2016).

Aside from PP2A, functional responsiveness of GABA<sub>B</sub>R is dependent on GABA<sub>B1</sub> and GABA<sub>B2</sub> synthesis, their coupling with G proteins, the phosphorylation state of the receptor, scaffolding proteins such as RGS and cytosolic proteins such as KTCD (see paragraphs A. and introduction). This provides evidence for possible pharmacological heterogeneity among GABA<sub>B</sub>Rs. A better understanding of the different partner depending of the brain region and cell-type specificity can be essential for customizing compounds to selectively interact with subsets of GABA<sub>B</sub>Rs in developing new therapies for the treatment of CNS disorders, including major depression.

Overall, although both strategies (DBS/LB-100) are efficient in rodent models to restore the depressive phenotype, lack of information concerning potential off targets could compromise their use in therapy, precise dissection of their circuit level effects and more precise dissection of their molecular action should be the object of further investigation

### ***C. Consequences of LHb hyperexcitability on downstream circuitries***

LHb neurons exert a tight control on diverse downstream targets (Pollak Dorocic et al., 2014; Weissbourd et al., 2014; Stamatakis and Stuber, 2012; Lammel et al., 2012; Yang et al., 2016). Specific LHb projections to the midbrain, mainly innervate GABAergic cells in the RMTg and the VTA (Balcita-Pedicino et al., 2011; Omelchenko et al., 2009). Yet, a minor subpopulation of LHb neurons, located in the medial division has been described monosynaptically innervate dopaminergic neurons (Meye et al., 2016). Notably, LHb neurons

preferentially synapse on dopamine neurons projecting to the mPFC and the activation of this pathway encodes aversion (Lammel et al., 2012). Despite this compelling segregation, LHB cell-type specific studies in the context of depression are at date missing. Notably, based on morphological and cytochemical analysis, ten subnuclei have been identified in the LHB (Geisler et al., 2003). However, the significance of each LHB neuronal subpopulation remains obscure. This is partly due to the lack of genetic profiling that limits the development of tools such as mice CRE-lines to assess cell type specific function of the LHB subpopulation. Single-cell resolution transcription analysis could be a way to discriminate and eventually test the significance of each individual LHB neuronal subtype to refine our knowledge on LHB function.

Regarding the need to have a better insight of the specific LHB output, we can consider the possibility to use different cre-line mice (such as the DAT-cre, SERT-cre and GAD-cre) combined with rabies virus strategies in downstream structures, to identify specific LHB populations and to gain knowledge about the circuit specific adaptations. This will ultimately provide better insights on how LHB hyperexcitability can translate into functional changes into one or more LHB output (DA cells of the VTA or 5HT cells in the raphe or GABAergic cells of either VTA or RMTg). Yet, few attempts have been made to determine population-specific effects in the LHB in the context of depression. In the LHp model, using cholera toxin to allow retrograde labelling of LHB projecting to the VTA, Li and colleagues provide insight of presynaptic potentiation in this subpopulation along with an increase potentiation (Li et al., 2011). However, they did not provide information regarding other LHB population, leaving open the possibility that other populations such as the RMTg projecting neurons were also altered. In cocaine withdrawal for example depressive symptoms are associated with drug-evoked plasticity specifically in LHB neurons projecting to the RMTg (Meye et al., 2015). In our study, we show that in the MS model the GABA<sub>B</sub>R reductions occur in both subpopulations. But, whether and how these changes are regulating the activity of downstream regions remains unknown.

A previous study reported that acute unpredictable FS, the same protocol used as well in our first study, enhances LHB-RMTg presynaptic glutamatergic release (Stamatakis and Stuber, 2012). Considering that RMTg, in turn, has been reported to exert a strong inhibitory control in the VTA DA neurons (Lecca et al., 2011; Stamatakis and Stuber, 2012), it is possible that the increased excitability of LHB, in the context of depression would decrease the activity of DA neurons. Accordingly, CMS paradigm induced a decreased burst firing activity of VTA DA cells, which in turn is instrumental for the expression of depressive-symptoms (Chang

and Grace, 2014; Tye et al., 2013). Nonetheless, another line of elegant studies, using the social defeat model (SD) showed surprisingly an increased activity of the DA neurons leading to similar depressive-like symptoms (Cao et al., 2010; Chaudhury et al., 2013; Friedman et al., 2014; Krishnan et al., 2007). Altogether, despite this dichotomy, these data suggest alterations of the DA systems along with specific symptoms of depression. Given the heterogeneity of the DA neurons, the difference in the VTA DA neurons modulation after these different stress (SD vs. CMS) might stem in part from cell-type specificity, engaging different circuits (Lammel et al., 2014).

A hint of LHb hyperactivity in the CMS is suggested by the reported increased metabolic activity (Caldecott-Hazard et al., 1988), and the fact that inhibition of this area by DBS reverses the behavioral sequelae of CMS (Lim et al., 2015; Meng et al., 2011). Instead, regardless of one paper mentioning hyperexcitability of LHb-projecting pallidal glutamatergic neurons following SD, whether LHb activity is affected in such rodent model remains unknown (Knowland et al., 2017). Notably, other inputs have been described to regulate DA neurons independently of LHb activity and may play a role in depression (Moreines et al., 2017). This information is extremely relevant as a complex disorder such as depression that impairs several behavioral aspects, and as well engages the dysfunction of complex interactive circuits. This renders the quest for treatment an extremely difficult challenge. One hypothesis could be that discrete phenotypes would depend on the modulation of specific circuits but the current depressive tests do not permit to decipher subtle aspect of particular behavior. A new computational method, “*syllables*” permits to microdissect patterns of action during a particular behavioral task (Wiltschko et al., 2015). Such a tool associated with precise circuit manipulation would help to characterize the precise role of different circuits in different animal models of depression.

Another point to take under consideration is that LHb do not only impinge DA system but also exert a tonic direct and indirect control on 5HT neurons of the raphe. These other LHb pathways could also be involved in the emergence of discrete depressive like symptoms. Initial anatomical studies and rabies virus tracing strategies in combination with cell-type specific (5HT versus GABA) cre-driver mouse lines led to the identification of a projection from LHb to 5HT neurons of the medial and dorsal raphe as well as to GABAergic neurons of the dorsal raphe (Bernard and Veh, 2012; Lecca et al., 2017; Pollak Dorocic et al., 2014; Quina et al., 2015; Wang and Aghajanian, 1977; Weissbourd et al., 2014). Remarkably, electrical stimulation of the LHb results in powerful suppression of putative dorsal raphe neurons (Varga et al., 2003; Wang and Aghajanian, 1977). However, optogenetic inhibition of

the LHb terminal in the dorsal raphe during inescapable shocks was also able to attenuate the increase in extracellular 5-HT level in the amygdala (Amat et al., 2001; Dolzani et al., 2016). Even if the net inhibitory effect on dorsal raphe 5-HT neurons is still poorly investigated, one possible explanation is that LHb axons primarily contact local circuit GABA dorsal raphe neurons, which in turn inhibit the activity of 5-HT neurons (Varga et al., 2003; Weissbourd et al., 2014) or indirectly via RMTg (Jhou et al., 2009a; Segó et al., 2014). Importantly, a decrease of 5HT level in the brain is widely accepted to be associated with depression and current antidepressants are primarily targeting the serotonergic machinery (Middlemiss et al., 2002; Sharp and Cowen, 2011). However, whether the LHb-raphe pathway is dysregulated in the context of depression is still neglected. A general prediction is that the LHb hyperactivity reported in depression could exert a tonic inhibition on the 5HT neuronal activity. In support of this idea, CMS rats present a low 5HT level in the DR. Using this same model, LHb lesions have been shown to reduce immobility in the FST in depressed rats, along with an increase of 5-HT levels in the dorsal raphe (Yang et al., 2008). These observations remain at the moment correlative and do not yet provide a causal link between the implication of this pathway and the depressive phenotype.

## Conclusion

---

In this thesis, I provide an overview of the well-established role of the LHb in aversive-related stimuli encoding and its importance in motivated behaviors via its connection to monoaminergic systems. In this context, LHb has been suggested to play a major role in the etiology of depression. Nevertheless, studies looking at precise molecular and cellular mechanisms underlying LHb dysfunction in the context of depression are still limited.

In the two sets of data I have presented in this thesis, we identify the downregulation of the GABA<sub>B</sub>R-GIRK as an early adaptation following an acute traumatic experience, responsible for the subsequent increase of LHb neuronal activity and the emergence of depressive-like symptoms. Moreover, this GABA<sub>B</sub>R-GIRK dependent LHb hyperexcitability was also observed as long-term adaptation following MS paradigm, highlighting this mechanism as a shared marker of depressive like state. Finally using different reversal strategies aiming to limit LHb neuronal activity we were able to ameliorate certain depressive like symptoms unraveling a causal relationship between LHb hyperexcitability and depressive state. Overall, our study, and others, point to LHb hyperactivity as a common substrate underlying depressive like symptoms highlighting the role of the LHb in the etiology of depression and

opening new insights for potential targets in the treatment of mood disorders, such as PP2A inhibitors.

However, depression is not a single disease, but rather a constellation of symptoms that is not necessary similar from one patient to another. This could explain why no single mechanistic approach, such as enhancement of monoaminergic transmission, would be effective in all the depressed patients because of the variable nature of the underlying cause. Although our study and others give potential relevant information in terms of precise molecular alterations, underlying depressive-like symptoms, temporal information regarding when these changes occur and how they influence discrete circuit responsible for precise behavior maladaptation are missing. Taking advantage of the new cutting edge technology in the field of neuroscience will help to answer many of these questions. Indeed, optogenetic techniques as well as molecular genetics and viral engineering can allow cell-type specific targeting improving our knowledge about the role of precise neural circuits in discrete behaviors affected in depression (Deisseroth, 2014; Huang and Zeng, 2013; Luo et al., 2008). Moreover, the development of wireless miniaturized implants to record or image brain activity combined with optomodulation and drug local delivery can provide a mean to interrogate the neuronal basis of discrete behaviors in an animal free to move in a more naturalistic fashion (Shin et al., 2017). Translating in my field of interest, a clear advantage in using such technology is the possibility to perform accurate longitudinal studies to monitor the dynamic modifications of given circuits when challenged over time with particular stressors. Concisely, in an animal model of depression, this will allow a real-time analysis of the development of the pathophysiological adaptations. Despite the exciting and promising implication that these new technologies can offer to the basic research, it is imperative to align and integrate them in a broader framework aiming to fill the gap between basic science and clinical translational research in human.

## Publications and contributions

---

1. **Tchenio A.**, Lecca, S., Valentinova, K. and Mameli, M. Limiting habenular hyperactivity ameliorates maternal separation-driven depressive-like symptoms. Accepted at Nat.Comm.
2. Lecca, S., Meye, F.J., Trusel, M., **Tchenio, A.**, Harris, J., Schwarz, M.K., Burdakov, D., Georges, F., and Mameli, M. (2017). Aversive stimuli drive hypothalamus-to-habenula excitation to promote escape behavior. *eLife* 6, e30697.
3. Lecca, S., Pelosi, A., **Tchenio, A.**, Moutkine, I., Lujan, R., Hervé, D., and Mameli, M. (2016). Rescue of GABAB and GIRK function in the lateral habenula by protein phosphatase 2A inhibition ameliorates depression-like phenotypes in mice. *Nat. Med.* 22, 254–261.
4. **Tchenio, A.**, Valentinova, K., and Mameli, M. (2016). Can the Lateral Habenula Crack the Serotonin Code? *Front. Synaptic Neurosci.* 8.
5. Valentinova, K., **Tchenio, A.**, Meye, F.J., Lecca, S., and Mameli, M. (2015). [Hell after the pleasure: drug-induced negative symptoms involve lateral habenula]. *Med. Sci. MS* 31, 478–481.

## References

---

- Abramson, L.Y., Seligman, M.E., and Teasdale, J.D. (1978). Learned helplessness in humans: critique and reformulation. *J. Abnorm. Psychol.* *87*, 49–74.
- Adrien, J., Dugovic, C., and Martin, P. (1991). Sleep-wakefulness patterns in the helpless rat. *Physiol. Behav.* *49*, 257–262.
- Agid, O., Shapira, B., Zislin, J., Ritsner, M., Hanin, B., Murad, H., Troudart, T., Bloch, M., Heresco-Levy, U., and Lerer, B. (1999). Environment and vulnerability to major psychiatric illness: a case control study of early parental loss in major depression, bipolar disorder and schizophrenia. *Mol. Psychiatry* *4*, 163–172.
- Aisa, B., Tordera, R., Lasheras, B., Del Río, J., and Ramírez, M.J. (2007). Cognitive impairment associated to HPA axis hyperactivity after maternal separation in rats. *Psychoneuroendocrinology* *32*, 256–266.
- Aizawa, H., Amo, R., and Okamoto, H. (2011). Phylogeny and Ontogeny of the Habenular Structure. *Front. Neurosci.* *5*.
- Aizawa, H., Kobayashi, M., Tanaka, S., Fukai, T., and Okamoto, H. (2012). Molecular characterization of the subnuclei in rat habenula. *J. Comp. Neurol.* *520*, 4051–4066.
- Al-Harbi, K.S. (2012). Treatment-resistant depression: therapeutic trends, challenges, and future directions. *Patient Prefer. Adherence* *6*, 369–388.
- Amat, J., Sparks, P.D., Matus-Amat, P., Griggs, J., Watkins, L.R., and Maier, S.F. (2001). The role of the habenular complex in the elevation of dorsal raphe nucleus serotonin and the changes in the behavioral responses produced by uncontrollable stress. *Brain Res.* *917*, 118–126.
- Andres, K.H., Düring, M.V., and Veh, R.W. (1999). Subnuclear organization of the rat habenular complexes. *J. Comp. Neurol.* *407*, 130–150.
- Anisman, H., and Matheson, K. (2005). Stress, depression, and anhedonia: Caveats concerning animal models. *Neurosci. Biobehav. Rev.* *29*, 525–546.
- Anisman, H., Zaharia, M.D., Meaney, M.J., and Merali, Z. (1998). Do early-life events permanently alter behavioral and hormonal responses to stressors? *Int. J. Dev. Neurosci. Off. J. Int. Soc. Dev. Neurosci.* *16*, 149–164.
- Baghai, T.C., Blier, P., Baldwin, D.S., Bauer, M., Goodwin, G.M., Fountoulakis, K.N., Kasper, S., Leonard, B.E., Malt, U.F., Stein, D., et al. (2011). General and comparative efficacy and effectiveness of antidepressants in the acute treatment of depressive disorders: a report by the WPA section of pharmacopsychiatry. *Eur. Arch. Psychiatry Clin. Neurosci.* *261*, 207–245.
- Balana, B., Maslennikov, I., Kwiatkowski, W., Stern, K.M., Bahima, L., Choe, S., and Slesinger, P.A. (2011). Mechanism underlying selective regulation of G protein-gated inwardly rectifying potassium channels by the psychostimulant-sensitive sorting nexin 27. *Proc. Natl. Acad. Sci. U. S. A.* *108*, 5831–5836.
- Balcita-Pedicino, J.J., Omelchenko, N., Bell, R., and Sesack, S.R. (2011). The inhibitory influence of the lateral habenula on midbrain dopamine cells: ultrastructural evidence for indirect mediation via the rostromedial mesopontine tegmental nucleus. *J. Comp. Neurol.* *519*, 1143–1164.
- Beck, A.T. (2008). The evolution of the cognitive model of depression and its neurobiological correlates. *Am. J. Psychiatry* *165*, 969–977.
- Benke, D. (2010). Mechanisms of GABAB Receptor Exocytosis, Endocytosis, and Degradation. *Adv. Pharmacol.* *58*, 93–111.
- Benke, D. (2013). GABAB receptor trafficking and interacting proteins: Targets for the development of highly specific therapeutic strategies to treat neurological disorders? *Biochem. Pharmacol.* *86*, 1525–1530.

- Bernard, R., and Veh, R.W. (2012). Individual neurons in the rat lateral habenular complex project mostly to the dopaminergic ventral tegmental area or to the serotonergic raphe nuclei. *J. Comp. Neurol.* *520*, 2545–2558.
- Berton, O., McClung, C.A., DiLeone, R.J., Krishnan, V., Renthal, W., Russo, S.J., Graham, D., Tsankova, N.M., Bolanos, C.A., Rios, M., et al. (2006). Essential Role of BDNF in the Mesolimbic Dopamine Pathway in Social Defeat Stress. *Science* *311*, 864–868.
- Bettler, B., and Fakler, B. (2017). Ionotropic AMPA-type glutamate and metabotropic GABAB receptors: determining cellular physiology by proteomes. *Curr. Opin. Neurobiol.* *45*, 16–23.
- Bettler, B., Kaupmann, K., Mosbacher, J., and Gassmann, M. (2004). Molecular Structure and Physiological Functions of GABAB Receptors. *Physiol. Rev.* *84*, 835–867.
- Bewernick, B.H., Hurlmann, R., Matusch, A., Kayser, S., Grubert, C., Hadrysiewicz, B., Axmacher, N., Lemke, M., Cooper-Mahkorn, D., Cohen, M.X., et al. (2010). Nucleus Accumbens Deep Brain Stimulation Decreases Ratings of Depression and Anxiety in Treatment-Resistant Depression. *Biol. Psychiatry* *67*, 110–116.
- Bianco, I.H., and Wilson, S.W. (2009). The habenular nuclei: a conserved asymmetric relay station in the vertebrate brain. *Philos. Trans. R. Soc. B Biol. Sci.* *364*, 1005–1020.
- Biermann, B., Ivankova-Susankova, K., Bradaia, A., Aziz, S.A., Besseyrias, V., Kapfhammer, J.P., Missler, M., Gassmann, M., and Bettler, B. (2010). The Sushi Domains of GABAB Receptors Function as Axonal Targeting Signals. *J. Neurosci.* *30*, 1385–1394.
- Billinton, A., Upton, N., and Bowery, N.G. (1999). GABAB receptor isoforms GBR1a and GBR1b, appear to be associated with pre- and post-synaptic elements respectively in rat and human cerebellum. *Br. J. Pharmacol.* *126*, 1387–1392.
- Bolwig, T.G. (2011). How Does Electroconvulsive Therapy Work? Theories on its Mechanism. *Can. J. Psychiatry* *56*, 13–18.
- Boulos, L.-J., Darceq, E., and Kieffer, B.L. (2017). Translating the Habenula-From Rodents to Humans. *Biol. Psychiatry* *81*, 296–305.
- Bowery, N.G. (2006). GABAB receptor: a site of therapeutic benefit. *Curr. Opin. Pharmacol.* *6*, 37–43.
- Bowery, N.G., Doble, A., Hill, D.R., Hudson, A.L., Turnbull, M.J., and Warrington, R. (1981). Structure/activity studies at a baclofen-sensitive, bicuculline-insensitive GABA receptor. *Adv. Biochem. Psychopharmacol.* *29*, 333–341.
- Brischoux, F., Chakraborty, S., Brierley, D.I., and Ungless, M.A. (2009). Phasic excitation of dopamine neurons in ventral VTA by noxious stimuli. *Proc. Natl. Acad. Sci.* *106*, 4894–4899.
- Brown, G.W., and Harris, T. (1978). Social origins of depression: a reply. *Psychol. Med.* *8*, 577–588.
- Bunney, W.E., and Davis, J.M. (1965). Norepinephrine in depressive reactions. A review. *Arch. Gen. Psychiatry* *13*, 483–494.
- Caldecott-Hazard, S., Mazziotta, J., and Phelps, M. (1988). Cerebral correlates of depressed behavior in rats, visualized using <sup>14</sup>C- 2-deoxyglucose autoradiography. *J. Neurosci.* *8*, 1951–1961.
- Calver, A.R., Robbins, M.J., Cosio, C., Rice, S.Q., Babbs, A.J., Hirst, W.D., Boyfield, I., Wood, M.D., Russell, R.B., Price, G.W., et al. (2001). The C-terminal domains of the GABA(b) receptor subunits mediate intracellular trafficking but are not required for receptor signaling. *J. Neurosci. Off. J. Soc. Neurosci.* *21*, 1203–1210.
- Cao, J.-L., Covington, H.E., Friedman, A.K., Wilkinson, M.B., Walsh, J.J., Cooper, D.C., Nestler, E.J., and Han, M.-H. (2010). Mesolimbic Dopamine Neurons in the Brain Reward Circuit Mediate Susceptibility to Social Defeat and Antidepressant Action. *J. Neurosci.* *30*, 16453–16458.
- Carceller-Sindreu, M., de Diego-Adeliño, J., Serra-Blasco, M., Vives-Gilabert, Y., Martí;n-Blanco, A., Puigdemont, D., Álvarez, E., Pérez, V., and Portella, M.J. (2015). Volumetric MRI study of the habenula in first episode, recurrent and chronic major depression. *Eur. Neuropsychopharmacol.* *25*, 2015–2021.



- Carroll, B.J. (1982). Clinical applications of the dexamethasone suppression test for endogenous depression. *Pharmacopsychiatry* 15, 19–25.
- Chalifoux, J.R., and Carter, A.G. (2011). GABAB receptor modulation of synaptic function. *Curr. Opin. Neurobiol.* 21, 339–344.
- Chang, C., and Grace, A.A. (2014). Amygdala-Ventral Pallidum Pathway Decreases Dopamine Activity After Chronic Mild Stress in Rats. *Biol. Psychiatry* 76, 223–230.
- Charles, K.J., Evans, M.L., Robbins, M.J., Calver, A.R., Leslie, R.A., and Pangalos, M.N. (2001). Comparative immunohistochemical localisation of GABAB1a, GABAB1b and GABAB2 subunits in rat brain, spinal cord and dorsal root ganglion. *Neuroscience* 106, 447–467.
- Chattarji, S., Tomar, A., Suvrathan, A., Ghosh, S., and Rahman, M.M. (2015). Neighborhood matters: divergent patterns of stress-induced plasticity across the brain. *Nat. Neurosci.* 18, 1364–1375.
- Chaudhury, D., Walsh, J.J., Friedman, A.K., Juarez, B., Ku, S.M., Koo, J.W., Ferguson, D., Tsai, H.-C., Pomeranz, L., Christoffel, D.J., et al. (2013). Rapid regulation of depression-related behaviours by control of midbrain dopamine neurons. *Nature* 493, 532–536.
- Chourbaji, S., Zacher, C., Sanchis-Segura, C., Dormann, C., Vollmayr, B., and Gass, P. (2005). Learned helplessness: Validity and reliability of depressive-like states in mice. *Brain Res. Protoc.* 16, 70–78.
- Christianson, J.P., Paul, E.D., Irani, M., Thompson, B.M., Kubala, K.H., Yirmiya, R., Watkins, L.R., and Maier, S.F. (2008). The role of prior stressor controllability and the dorsal raphe nucleus in sucrose preference and social exploration. *Behav. Brain Res.* 193, 87–93.
- Christoph, G.R., Leonzio, R.J., and Wilcox, K.S. (1986). Stimulation of the lateral habenula inhibits dopamine-containing neurons in the substantia nigra and ventral tegmental area of the rat. *J. Neurosci. Off. J. Soc. Neurosci.* 6, 613–619.
- Chung, V., Mansfield, A.S., Braiteh, F., Richards, D., Durivage, H., Ungerleider, R.S., Johnson, F., and Kovach, J.S. (2016). Safety, Tolerability, and Preliminary Activity of LB-100, an Inhibitor of Protein Phosphatase 2A, in Patients with Relapsed Solid Tumors: An Open-Label, Dose Escalation, First-in-Human, Phase I Trial. *Clin. Cancer Res.*
- Ciruela, F., Fernández-Dueñas, V., Sahlholm, K., Fernández-Alacid, L., Nicolau, J.C., Watanabe, M., and Luján, R. (2010). Evidence for oligomerization between GABAB receptors and GIRK channels containing the GIRK1 and GIRK3 subunits. *Eur. J. Neurosci.* 32, 1265–1277.
- Clancy, S.M., Boyer, S.B., and Slesinger, P.A. (2007). Coregulation of natively expressed pertussis toxin-sensitive muscarinic receptors with G-protein-activated potassium channels. *J. Neurosci. Off. J. Soc. Neurosci.* 27, 6388–6399.
- Cohen, J.Y., Amoroso, M.W., and Uchida, N. (2015). Serotonergic neurons signal reward and punishment on multiple timescales. *ELife* 4, e06346.
- Couto, F.S. do, Batalha, V.L., Valadas, J.S., Data-Franca, J., Ribeiro, J.A., and Lopes, L.V. (2012). Escitalopram improves memory deficits induced by maternal separation in the rat. *Eur. J. Pharmacol.* 695, 71–75.
- Couve, A., Moss, S.J., and Pangalos, M.N. (2000). GABAB Receptors: A New Paradigm in G Protein Signaling. *Mol. Cell. Neurosci.* 16, 296–312.
- Couve, A., Thomas, P., Calver, A.R., Hirst, W.D., Pangalos, M.N., Walsh, F.S., Smart, T.G., and Moss, S.J. (2002). Cyclic AMP-dependent protein kinase phosphorylation facilitates GABA(B) receptor-effector coupling. *Nat. Neurosci.* 5, 415–424.
- Couve, A., Calver, A.R., Fairfax, B., Moss, S.J., and Pangalos, M.N. (2004). Unravelling the unusual signalling properties of the GABAB receptor. *Biochem. Pharmacol.* 68, 1527–1536.

- Covington, H.E., Lobo, M.K., Maze, I., Vialou, V., Hyman, J.M., Zaman, S., LaPlant, Q., Mouzon, E., Ghose, S., Tamminga, C.A., et al. (2010). Antidepressant Effect of Optogenetic Stimulation of the Medial Prefrontal Cortex. *J. Neurosci.* *30*, 16082–16090.
- Crockett, M.J., Clark, L., and Robbins, T.W. (2009). Reconciling the role of serotonin in behavioral inhibition and aversion: acute tryptophan depletion abolishes punishment-induced inhibition in humans. *J. Neurosci. Off. J. Soc. Neurosci.* *29*, 11993–11999.
- Cruz, H.G., Ivanova, T., Lunn, M.-L., Stoffel, M., Slesinger, P.A., and Lüscher, C. (2004). Bi-directional effects of GABA(B) receptor agonists on the mesolimbic dopamine system. *Nat. Neurosci.* *7*, 153–159.
- Cryan, J.F., and Slattery, D.A. (2010). GABAB receptors and depression. Current status. *Adv. Pharmacol. San Diego Calif* *58*, 427–451.
- Dalley, J.W., Cardinal, R.N., and Robbins, T.W. (2004). Prefrontal executive and cognitive functions in rodents: neural and neurochemical substrates. *Neurosci. Biobehav. Rev.* *28*, 771–784.
- Deakin, J.F.W., and Graeff, F.G. (1991). 5-HT and mechanisms of defence. *J. Psychopharmacol. (Oxf.)* *5*, 305–315.
- Deisseroth, K. (2014). Circuit dynamics of adaptive and maladaptive behaviour. *Nature* *505*, 309–317.
- Delaloye, S., and Holtzheimer, P.E. (2014). Deep brain stimulation in the treatment of depression. *Dialogues Clin. Neurosci.* *16*, 83–91.
- Delgado, P.L. (2000). Depression: the case for a monoamine deficiency. *J. Clin. Psychiatry* *61 Suppl 6*, 7–11.
- Dess, N.K., Raizer, J., Chapman, C.D., and Garcia, J. (1988). Stressors in the learned helplessness paradigm: Effects on body weight and conditioned taste aversion in rats. *Physiol. Behav.* *44*, 483–490.
- Di Chiara, G., Loddo, P., and Tanda, G. (1999). Reciprocal changes in prefrontal and limbic dopamine responsiveness to aversive and rewarding stimuli after chronic mild stress: implications for the psychobiology of depression. *Biol. Psychiatry* *46*, 1624–1633.
- Dolzani, S.D., Baratta, M.V., Amat, J., Agster, K.L., Sadoris, M.P., Watkins, L.R., and Maier, S.F. (2016). Activation of a Habenulo-Raphe Circuit Is Critical for the Behavioral and Neurochemical Consequences of Uncontrollable Stress in the Male Rat. *ENeuro* *3*.
- Douppnik, C.A. (2015). RGS Redundancy and Implications in GPCR–GIRK Signaling. *Int. Rev. Neurobiol.* *123*, 87–116.
- Dunn, E.C., Brown, R.C., Dai, Y., Rosand, J., Nugent, N.R., Amstadter, A.B., and Smoller, J.W. (2015). Genetic determinants of depression: Recent findings and future directions. *Harv. Rev. Psychiatry* *23*, 1–18.
- Edwards, N.J., Tejada, H.A., Pignatelli, M., Zhang, S., McDevitt, R.A., Wu, J., Bass, C.E., Bettler, B., Morales, M., and Bonci, A. (2017). Circuit specificity in the inhibitory architecture of the VTA regulates cocaine-induced behavior. *Nat. Neurosci.* *20*, 438–448.
- Elliott, R., Sahakian, B.J., McKay, A.P., Herrod, J.J., Robbins, T.W., and Paykel, E.S. (1996). Neuropsychological impairments in unipolar depression: the influence of perceived failure on subsequent performance. *Psychol. Med.* *26*, 975–989.
- Enkel, T., Spanagel, R., Vollmayr, B., and Schneider, M. (2010). Stress triggers anhedonia in rats bred for learned helplessness. *Behav. Brain Res.* *209*, 183–186.
- Erburu, M., Cajaleon, L., Guruceaga, E., Venzala, E., Muñoz-Cobo, I., Beltrán, E., Puerta, E., and Tordera, R.M. (2015). Chronic mild stress and imipramine treatment elicit opposite changes in behavior and in gene expression in the mouse prefrontal cortex. *Pharmacol. Biochem. Behav.* *135*, 227–236.
- Fairfax, B.P., Pitcher, J.A., Scott, M.G.H., Calver, A.R., Pangalos, M.N., Moss, S.J., and Couve, A. (2004). Phosphorylation and chronic agonist treatment atypically modulate GABAB receptor cell surface stability. *J. Biol. Chem.* *279*, 12565–12573.

- Fales, C.L., Barch, D.M., Rundle, M.M., Mintun, M.A., Snyder, A.Z., Cohen, J.D., Mathews, J., and Sheline, Y.I. (2008). Altered emotional interference processing in affective and cognitive-control brain circuitry in major depression. *Biol. Psychiatry* *63*, 377–384.
- Farmer, A.E., and McGuffin, P. (2003). Humiliation, loss and other types of life events and difficulties: a comparison of depressed subjects, healthy controls and their siblings. *Psychol. Med.* *33*, 1169–1175.
- Ferrari, A.J., Charlson, F.J., Norman, R.E., Patten, S.B., Freedman, G., Murray, C.J.L., Vos, T., and Whiteford, H.A. (2013). Burden of Depressive Disorders by Country, Sex, Age, and Year: Findings from the Global Burden of Disease Study 2010. *PLOS Med.* *10*, e1001547.
- Fitzgerald, P.B., and Segrave, R.A. (2015). Deep brain stimulation in mental health: Review of evidence for clinical efficacy. *Aust. N. Z. J. Psychiatry* *49*, 979–993.
- Fowler, C.E., Aryal, P., Suen, K.F., and Slesinger, P.A. (2007). Evidence for association of GABAB receptors with Kir3 channels and regulators of G protein signalling (RGS4) proteins. *J. Physiol.* *580*, 51–65.
- Frader, M.A. (1987). **Melancholia and Depression: From Hippocratic Times to Modern Times** —by Stanley W. Jackson, M.D.; Yale University Press, New Haven, Connecticut, 1986, 439 pages, \$35. *Psychiatr. Serv.* *38*, 1121–1122.
- Franklin, T.B., Russig, H., Weiss, I.C., Gräff, J., Linder, N., Michalon, A., Vizi, S., and Mansuy, I.M. (2010). Epigenetic Transmission of the Impact of Early Stress Across Generations. *Biol. Psychiatry* *68*, 408–415.
- Friedman, A., Friedman, Y., Dremencov, E., and Yadid, G. (2008). VTA Dopamine Neuron Bursting is Altered in an Animal Model of Depression and Corrected by Desipramine. *J. Mol. Neurosci.* *34*, 201–209.
- Friedman, A.K., Walsh, J.J., Juarez, B., Ku, S.M., Chaudhury, D., Wang, J., Li, X., Dietz, D.M., Pan, N., Vialou, V.F., et al. (2014). Enhancing Depression Mechanisms in Midbrain Dopamine Neurons Achieves Homeostatic Resilience. *Science* *344*, 313–319.
- Fritzius, T., Turecek, R., Seddik, R., Kobayashi, H., Tiao, J., Rem, P.D., Metz, M., Kralikova, M., Bouvier, M., Gassmann, M., et al. (2017). KCTD Hetero-oligomers Confer Unique Kinetic Properties on Hippocampal GABAB Receptor-Induced K<sup>+</sup> Currents. *J. Neurosci.* *37*, 1162–1175.
- Funkiewiez, A., Ardouin, C., Caputo, E., Krack, P., Fraix, V., Klingner, H., Chabardes, S., Foote, K., Benabid, A.-L., and Pollak, P. (2004). Long term effects of bilateral subthalamic nucleus stimulation on cognitive function, mood, and behaviour in Parkinson's disease. *J. Neurol. Neurosurg. Psychiatry* *75*, 834–839.
- Gainetdinov, R.R., Premont, R.T., Bohn, L.M., Lefkowitz, R.J., and Caron, M.G. (2004). Desensitization of G protein-coupled receptors and neuronal functions. *Annu. Rev. Neurosci.* *27*, 107–144.
- Galvez, T., Parmentier, M.-L., Joly, C., Malitschek, B., Kaupmann, K., Kuhn, R., Bittiger, H., Froestl, W., Bettler, B., and Pin, J.-P. (1999). Mutagenesis and Modeling of the GABAB Receptor Extracellular Domain Support a Venus Flytrap Mechanism for Ligand Binding. *J. Biol. Chem.* *274*, 13362–13369.
- Gao, Y., Zhou, J.-J., Zhu, Y., Wang, L., Kosten, T.A., Zhang, X., and Li, D.-P. (2017). Neuroadaptations of presynaptic and postsynaptic GABAB receptor function in the paraventricular nucleus in response to chronic unpredictable stress. *Br. J. Pharmacol.* *174*, 2929–2940.
- Garcia, L.S.B., Comim, C.M., Valvassori, S.S., Réus, G.Z., Stertz, L., Kapczinski, F., Gavioli, E.C., and Quevedo, J. (2009). Ketamine treatment reverses behavioral and physiological alterations induced by chronic mild stress in rats. *Prog. Neuropsychopharmacol. Biol. Psychiatry* *33*, 450–455.
- Gassmann, M., Haller, C., Stoll, Y., Aziz, S.A., Biermann, B., Mosbacher, J., Kaupmann, K., and Bettler, B. (2005). The RXR-Type Endoplasmic Reticulum-Retention/Retrieval Signal of GABAB1 Requires Distant Spacing from the Membrane to Function. *Mol. Pharmacol.* *68*, 137–144.
- Geisler, S., Andres, K.H., and Veh, R.W. (2003). Morphologic and cytochemical criteria for the identification and delineation of individual subnuclei within the lateral habenular complex of the rat. *J. Comp. Neurol.* *458*, 78–97.

- Gracia-Rubio, I., Moscoso-Castro, M., Pozo, O.J., Marcos, J., Nadal, R., and Valverde, O. (2016). Maternal separation induces neuroinflammation and long-lasting emotional alterations in mice. *Prog. Neuropsychopharmacol. Biol. Psychiatry* *65*, 104–117.
- Grampp, T., Sauter, K., Markovic, B., and Benke, D. (2007).  $\gamma$ -Aminobutyric Acid Type B Receptors Are Constitutively Internalized via the Clathrin-dependent Pathway and Targeted to Lysosomes for Degradation. *J. Biol. Chem.* *282*, 24157–24165.
- Grampp, T., Notz, V., Broll, I., Fischer, N., and Benke, D. (2008). Constitutive, agonist-accelerated, recycling and lysosomal degradation of GABAB receptors in cortical neurons. *Mol. Cell. Neurosci.* *39*, 628–637.
- Greenberg, L., Edwards, E., and Henn, F.A. (1989). Dexamethasone suppression test in helpless rats. *Biol. Psychiatry* *26*, 530–532.
- Greenberg, P.E., Fournier, A.-A., Sisitsky, T., Pike, C.T., and Kessler, R.C. (2015). The economic burden of adults with major depressive disorder in the United States (2005 and 2010). *J. Clin. Psychiatry* *76*, 155–162.
- Grønli, J., Murison, R., Bjorvatn, B., Sørensen, E., Portas, C.M., and Ursin, R. (2004). Chronic mild stress affects sucrose intake and sleep in rats. *Behav. Brain Res.* *150*, 139–147.
- Grønli, J., Murison, R., Fiske, E., Bjorvatn, B., Sørensen, E., Portas, C.M., and Ursin, R. (2005). Effects of chronic mild stress on sexual behavior, locomotor activity and consumption of sucrose and saccharine solutions. *Physiol. Behav.* *84*, 571–577.
- Guetg, N., Seddik, R., Vigot, R., Turecek, R., Gassmann, M., Vogt, K.E., Bräuner-Osborne, H., Shigemoto, R., Kretz, O., Frotscher, M., et al. (2009). The GABAB1a Isoform Mediates Heterosynaptic Depression at Hippocampal Mossy Fiber Synapses. *J. Neurosci.* *29*, 1414–1423.
- Guetg, N., Aziz, S.A., Holbro, N., Turecek, R., Rose, T., Seddik, R., Gassmann, M., Moes, S., Jenoe, P., Oertner, T.G., et al. (2010). NMDA receptor-dependent GABAB receptor internalization via CaMKII phosphorylation of serine 867 in GABAB1. *Proc. Natl. Acad. Sci.* *107*, 13924–13929.
- Hammen, C., Kim, E.Y., Eberhart, N.K., and Brennan, P.A. (2009). Chronic and acute stress and the prediction of major depression in women. *Depress. Anxiety* *26*, 718–723.
- Harayama, N., Shibuya, I., Tanaka, K., Kabashima, N., Ueta, Y., and Yamashita, H. (1998). Inhibition of N- and P/Q-type calcium channels by postsynaptic GABAB receptor activation in rat supraoptic neurones. *J. Physiol.* *509*, 371–383.
- Hayes, D.J., Duncan, N.W., Xu, J., and Northoff, G. (2014). A comparison of neural responses to appetitive and aversive stimuli in humans and other mammals. *Neurosci. Biobehav. Rev.* *45*, 350–368.
- Hearing, M., Kotecki, L., de Velasco, E.M.F., Fajardo-Serrano, A., Luján, R., and Wickman, K. (2013). Repeated cocaine weakens GABAB-Girk signaling in Layer 5/6 pyramidal neurons in the prelimbic cortex. *Neuron* *80*, 159–170.
- Heim, C., Newport, D.J., Mletzko, T., Miller, A.H., and Nemeroff, C.B. (2008). The link between childhood trauma and depression: Insights from HPA axis studies in humans. *Psychoneuroendocrinology* *33*, 693–710.
- Henn, F.A., and Vollmayr, B. (2005). Stress models of depression: Forming genetically vulnerable strains. *Neurosci. Biobehav. Rev.* *29*, 799–804.
- Hill, D.R., and Bowery, N.G. (1981). 3H-baclofen and 3H-GABA bind to bicuculline-insensitive GABA B sites in rat brain. *Nature* *290*, 149–152.
- Hindmarch, I. (2002). Beyond the monoamine hypothesis: mechanisms, molecules and methods! To be presented at ECNP Barcelona, 5-9 October 2002, during the symposium “A new pharmacology of depression: the concept of synaptic plasticity.” *Eur. Psychiatry* *17*, 294–299.
- Hirschfeld, R.M.A. (2000). History and Evolution of the Monoamine Hypothesis of Depression. *J. Clin. Psychiatry* *61*, 4–6.

- Holmes, A., le Guisquet, A.M., Vogel, E., Millstein, R.A., Leman, S., and Belzung, C. (2005). Early life genetic, epigenetic and environmental factors shaping emotionality in rodents. *Neurosci. Biobehav. Rev.* *29*, 1335–1346.
- Holtzheimer, P.E., and Mayberg, H.S. (2011a). Stuck in a rut: rethinking depression and its treatment. *Trends Neurosci.* *34*, 1–9.
- Holtzheimer, P.E., and Mayberg, H.S. (2011b). Deep Brain Stimulation for Psychiatric Disorders. *Annu. Rev. Neurosci.* *34*, 289–307.
- Hong, S., Jhou, T.C., Smith, M., Saleem, K.S., and Hikosaka, O. (2011). Negative Reward Signals from the Lateral Habenula to Dopamine Neurons Are Mediated by Rostromedial Tegmental Nucleus in Primates. *J. Neurosci.* *31*, 11457–11471.
- Huang, Z.J., and Zeng, H. (2013). Genetic Approaches to Neural Circuits in the Mouse. *Annu. Rev. Neurosci.* *36*, 183–215.
- Ingram, A., Saling, M.M., and Schweitzer, I. (2008). Cognitive Side Effects of Brief Pulse Electroconvulsive Therapy: A Review. *J. ECT* *24*, 3–9.
- Ivankova, K., Turecek, R., Fritzius, T., Seddik, R., Prezeau, L., Comps-Agrar, L., Pin, J.-P., Fakler, B., Besseyrias, V., Gassmann, M., et al. (2013). Up-regulation of GABAB Receptor Signaling by Constitutive Assembly with the K<sup>+</sup> Channel Tetramerization Domain-containing Protein 12 (KCTD12). *J. Biol. Chem.* *288*, 24848–24856.
- Jhou, T.C., Geisler, S., Marinelli, M., Degarmo, B.A., and Zahm, D.S. (2009a). The mesopontine rostromedial tegmental nucleus: A structure targeted by the lateral habenula that projects to the ventral tegmental area of Tsai and substantia nigra compacta. *J. Comp. Neurol.* *513*, 566–596.
- Jhou, T.C., Fields, H.L., Baxter, M.G., Saper, C.B., and Holland, P.C. (2009b). The rostromedial tegmental nucleus (RMTg), a major GABAergic afferent to midbrain dopamine neurons, selectively encodes aversive stimuli and promotes behavioral inhibition. *Neuron* *61*, 786–800.
- Ji, H., and Shepard, P.D. (2007). Lateral Habenula Stimulation Inhibits Rat Midbrain Dopamine Neurons through a GABA<sub>A</sub> Receptor-Mediated Mechanism. *J. Neurosci.* *27*, 6923–6930.
- Johnston, B.A., Steele, J.D., Tolomeo, S., Christmas, D., and Matthews, K. (2015). Structural MRI-Based Predictions in Patients with Treatment-Refractory Depression (TRD). *PLOS ONE* *10*, e0132958.
- Jones, K.A., Borowsky, B., Tamm, J.A., Craig, D.A., Durkin, M.M., Dai, M., Yao, W.J., Johnson, M., Gunwaldsen, C., Huang, L.Y., et al. (1998). GABA(B) receptors function as a heteromeric assembly of the subunits GABA(B)R1 and GABA(B)R2. *Nature* *396*, 674–679.
- Kant, G.J., Leu, J.R., Anderson, S.M., and Mougey, E.H. (1987). Effects of chronic stress on plasma corticosterone, ACTH and prolactin. *Physiol. Behav.* *40*, 775–779.
- Kantamneni, S., González-González, I.M., Luo, J., Cimarosti, H., Jacobs, S.C., Jaafari, N., and Henley, J.M. (2014). Differential Regulation of GABAB Receptor Trafficking by Different Modes of N-methyl-d-aspartate (NMDA) Receptor Signaling. *J. Biol. Chem.* *289*, 6681–6694.
- Katz, R.J. (1982). Animal model of depression: Pharmacological sensitivity of a hedonic deficit. *Pharmacol. Biochem. Behav.* *16*, 965–968.
- Kaufling, J., Veinante, P., Pawlowski, S.A., Freund-Mercier, M.-J., and Barrot, M. (2009). Afferents to the GABAergic tail of the ventral tegmental area in the rat. *J. Comp. Neurol.* *513*, 597–621.
- Kaupmann, K., Huggel, K., Heid, J., Flor, P.J., Bischoff, S., Mickel, S.J., McMaster, G., Angst, C., Bittiger, H., Froestl, W., et al. (1997). Expression cloning of GABA(B) receptors uncovers similarity to metabotropic glutamate receptors. *Nature* *386*, 239–246.
- Kendler, K.S., Karkowski, L.M., and Prescott, C.A. (1999). Causal Relationship Between Stressful Life Events and the Onset of Major Depression. *Am. J. Psychiatry* *156*, 837–841.

- Kendler, K.S., Gardner, C.O., and Prescott, C.A. (2002). Toward a comprehensive developmental model for major depression in women. *Am. J. Psychiatry* 159, 1133–1145.
- Kessler, R.C. (1997). The Effects of Stressful Life Events on Depression. *Annu. Rev. Psychol.* 48, 191–214.
- Kiening, K., and Sartorius, A. (2013). A new translational target for deep brain stimulation to treat depression. *EMBO Mol. Med.* 5, 1151–1153.
- Kim, J.J., and Diamond, D.M. (2002). The stressed hippocampus, synaptic plasticity and lost memories. *Nat. Rev. Neurosci.* 3, 453–462.
- de Kloet, E.R., Joëls, M., and Holsboer, F. (2005). Stress and the brain: from adaptation to disease. *Nat. Rev. Neurosci.* 6, 463–475.
- Knowland, D., Lilascharoen, V., Pacia, C.P., Shin, S., Wang, E.H.-J., and Lim, B.K. (2017). Distinct Ventral Pallidal Neural Populations Mediate Separate Symptoms of Depression. *Cell* 0.
- Krach, S., Paulus, F.M., Bodden, M., and Kircher, T. (2010). The Rewarding Nature of Social Interactions. *Front. Behav. Neurosci.* 4.
- Krishnan, V., Han, M.-H., Graham, D.L., Berton, O., Renthal, W., Russo, S.J., LaPlant, Q., Graham, A., Lutter, M., Lagace, D.C., et al. (2007). Molecular Adaptations Underlying Susceptibility and Resistance to Social Defeat in Brain Reward Regions. *Cell* 131, 391–404.
- Kudryavtseva, N.N., Bakshtanovskaya, I.V., and Koryakina, L.A. (1991). Social model of depression in mice of C57BL/6J strain. *Pharmacol. Biochem. Behav.* 38, 315–320.
- Kuhn, R. (1957). [Treatment of depressive states with an iminodibenzyl derivative (G 22355)]. *Schweiz. Med. Wochenschr.* 87, 1135–1140.
- Kuner, R., Köhr, G., Grünewald, S., Eisenhardt, G., Bach, A., and Kornau, H.-C. (1999). Role of Heteromer Formation in GABAB Receptor Function. *Science* 283, 74–77.
- Kuramoto, N., Wilkins, M.E., Fairfax, B.P., Revilla-Sanchez, R., Terunuma, M., Tamaki, K., Iemata, M., Warren, N., Couve, A., Calver, A., et al. (2007). Phospho-Dependent Functional Modulation of GABAB Receptors by the Metabolic Sensor AMP-Dependent Protein Kinase. *Neuron* 53, 233–247.
- Labouèbe, G., Lomazzi, M., Cruz, H.G., Creton, C., Luján, R., Li, M., Yanagawa, Y., Obata, K., Watanabe, M., Wickman, K., et al. (2007). RGS2 modulates coupling between GABAB receptors and GIRK channels in dopamine neurons of the ventral tegmental area. *Nat. Neurosci.* 10, 1559–1568.
- Ladd, C.O., Huot, R.L., Thiruvikraman, K.V., Nemeroff, C.B., Meaney, M.J., and Plotsky, P.M. (2000). Long-term behavioral and neuroendocrine adaptations to adverse early experience. *Prog. Brain Res.* 122, 81–103.
- Lajud, N., Roque, A., Cajero, M., Gutiérrez-Ospina, G., and Torner, L. (2012). Periodic maternal separation decreases hippocampal neurogenesis without affecting basal corticosterone during the stress hypo-responsive period, but alters HPA axis and coping behavior in adulthood. *Psychoneuroendocrinology* 37, 410–420.
- Lalivè, A.L., Muñoz, M.B., Bellone, C., Slesinger, P.A., Lüscher, C., and Tan, K.R. (2014). Firing Modes of Dopamine Neurons Drive Bidirectional GIRK Channel Plasticity. *J. Neurosci.* 34, 5107–5114.
- Lammel, S., Lim, B.K., Ran, C., Huang, K.W., Betley, M.J., Tye, K.M., Deisseroth, K., and Malenka, R.C. (2012). Input-specific control of reward and aversion in the ventral tegmental area. *Nature* 491, 212–217.
- Lammel, S., Tye, K.M., and Warden, M.R. (2014). Progress in understanding mood disorders: optogenetic dissection of neural circuits. *Genes Brain Behav.* 13, 38–51.
- Lammel, S., Steinberg, E.E., Földy, C., Wall, N.R., Beier, K., Luo, L., and Malenka, R.C. (2015). Diversity of Transgenic Mouse Models for Selective Targeting of Midbrain Dopamine Neurons. *Neuron* 85, 429–438.
- Lauffer, B.E.L., Melero, C., Temkin, P., Lei, C., Hong, W., Kortemme, T., and von Zastrow, M. (2010). SNX27 mediates PDZ-directed sorting from endosomes to the plasma membrane. *J. Cell Biol.* 190, 565–574.

- Lavine, N., Ethier, N., Oak, J.N., Pei, L., Liu, F., Trieu, P., Rebois, R.V., Bouvier, M., Hébert, T.E., and Tol, H.H.M.V. (2002). G Protein-coupled Receptors Form Stable Complexes with Inwardly Rectifying Potassium Channels and Adenylyl Cyclase. *J. Biol. Chem.* *277*, 46010–46019.
- Lecca, S., Melis, M., Luchicchi, A., Ennas, M.G., Castelli, M.P., Muntoni, A.L., and Pistis, M. (2011). Effects of Drugs of Abuse on Putative Rostromedial Tegmental Neurons, Inhibitory Afferents to Midbrain Dopamine Cells. *Neuropsychopharmacology* *36*, 589–602.
- Lecca, S., Meye, F.J., and Mameli, M. (2014). The lateral habenula in addiction and depression: an anatomical, synaptic and behavioral overview. *Eur. J. Neurosci.* *39*, 1170–1178.
- Lecca, S., Trusel, M., and Mameli, M. (2017). Footshock-induced plasticity of GABAB signalling in the lateral habenula requires dopamine and glucocorticoid receptors. *Synapse* *71*, n/a-n/a.
- Lecca, S., Meye, F.J., Trusel, M., Tchenio, A., Harris, J., Schwarz, M.K., Burdakov, D., Georges, F., and Mameli, M. (2017). Aversive stimuli drive hypothalamus-to-habenula excitation to promote escape behavior. *ELife* *6*, e30697.
- Lecourtier, L., DeFrancesco, A., and Moghaddam, B. (2008). Differential tonic influence of lateral habenula on prefrontal cortex and nucleus accumbens dopamine release. *Eur. J. Neurosci.* *27*, 1755–1762.
- Lee, J.-H., Kim, H.J., Kim, J.G., Ryu, V., Kim, B.-T., Kang, D.-W., and Jahng, J.W. (2007). Depressive behaviors and decreased expression of serotonin reuptake transporter in rats that experienced neonatal maternal separation. *Neurosci. Res.* *58*, 32–39.
- Li, B., Piriz, J., Mirrione, M., Chung, C., Proulx, C.D., Schulz, D., Henn, F., and Malinow, R. (2011). Synaptic potentiation onto habenula neurons in the learned helplessness model of depression. *Nature* *470*, 535–539.
- Li, K., Zhou, T., Liao, L., Yang, Z., Wong, C., Henn, F., Malinow, R., Yates, J.R., and Hu, H. (2013).  $\beta$ CaMKII in Lateral Habenula Mediates Core Symptoms of Depression. *Science* *341*, 1016–1020.
- Lim, L.W., Prickaerts, J., Huguet, G., Kadar, E., Hartung, H., Sharp, T., and Temel, Y. (2015). Electrical stimulation alleviates depressive-like behaviors of rats: investigation of brain targets and potential mechanisms. *Transl. Psychiatry* *5*, e535.
- Llorente, R., Miguel-Blanco, C., Aisa, B., Lachize, S., Borcel, E., Meijer, O.C., Ramirez, M.J., De Kloet, E.R., and Viveros, M.P. (2011). Long Term Sex-Dependent Psychoneuroendocrine Effects of Maternal Deprivation and Juvenile Unpredictable Stress in Rats. *J. Neuroendocrinol.* *23*, 329–344.
- Loomer, H.P., Saunders, J.C., and Kline, N.S. (1957). A clinical and pharmacodynamic evaluation of iproniazid as a psychic energizer. *Psychiatr. Res. Rep. Am. Psychiatr. Assoc.* *8*, 129–141.
- Lu, J., Kovach, J.S., Johnson, F., Chiang, J., Hodes, R., Lonsler, R., and Zhuang, Z. (2009). Inhibition of serine/threonine phosphatase PP2A enhances cancer chemotherapy by blocking DNA damage induced defense mechanisms. *Proc. Natl. Acad. Sci. U. S. A.* *106*, 11697–11702.
- Lujan, R., and Ciruela, F. (2012). GABAB receptors-associated proteins: potential drug targets in neurological disorders? *Curr. Drug Targets* *13*, 129–144.
- Luján, R., de Velasco, E.M.F., Aguado, C., and Wickman, K. (2014). New insights into the therapeutic potential of Girk channels. *Trends Neurosci.* *37*.
- Lukkes, J.L., Meda, S., Thompson, B.S., Freund, N., and Andersen, S.L. (2017). Early life stress and later peer distress on depressive behavior in adolescent female rats: Effects of a novel intervention on GABA and D2 receptors. *Behav. Brain Res.* *330*, 37–45.
- Lunn, M.-L., Nassirpour, R., Arrabit, C., Tan, J., McLeod, I., Arias, C.M., Sawchenko, P.E., Yates, J.R., and Slesinger, P.A. (2007). A unique sorting nexin regulates trafficking of potassium channels via a PDZ domain interaction. *Nat. Neurosci.* *10*, 1249–1259.
- Luo, L., Callaway, E.M., and Svoboda, K. (2008). Genetic Dissection of Neural Circuits. *Neuron* *57*, 634–660.

- Lüscher, C., and Pollak, P. (2016). Optogenetically inspired deep brain stimulation: linking basic with clinical research. *Swiss Med. Wkly.* *146*, w14278.
- Lüscher, C., and Slesinger, P.A. (2010). Emerging concepts for G protein-gated inwardly rectifying potassium (GIRK) channels in health and disease. *Nat. Rev. Neurosci.* *11*, 301–315.
- MacQueen, G.M., Ramakrishnan, K., Ratnasingan, R., Chen, B., and Young, L.T. (2003). Desipramine treatment reduces the long-term behavioural and neurochemical sequelae of early-life maternal separation. *Int. J. Neuropsychopharmacol.* *6*, 391–396.
- Maier, S.F., and Seligman, M.E. (1976). Learned helplessness: Theory and evidence. *J. Exp. Psychol. Gen.* *105*, 3–46.
- Maier, P.J., Marin, I., Grampp, T., Sommer, A., and Benke, D. (2010). Sustained Glutamate Receptor Activation Down-regulates GABAB Receptors by Shifting the Balance from Recycling to Lysosomal Degradation. *J. Biol. Chem.* *285*, 35606–35614.
- Maks, C.B., Butson, C.R., Walter, B.L., Vitek, J.L., and McIntyre, C.C. (2009). Deep brain stimulation activation volumes and their association with neurophysiological mapping and therapeutic outcomes. *J. Neurol. Neurosurg. Psychiatry* *80*, 659–666.
- Malitschek, B., Schweizer, C., Keir, M., Heid, J., Froestl, W., Mosbacher, J., Kuhn, R., Henley, J., Joly, C., Pin, J.-P., et al. (1999). The N-Terminal Domain of  $\gamma$ -Aminobutyric AcidBReceptors Is Sufficient to Specify Agonist and Antagonist Binding. *Mol. Pharmacol.* *56*, 448–454.
- Manji, H.K., Drevets, W.C., and Charney, D.S. (2001). The cellular neurobiology of depression. *Nat. Med.* *7*, 541–547.
- Margeta-Mitrovic, M., Jan, Y.N., and Jan, L.Y. (2000). A Trafficking Checkpoint Controls GABAB Receptor Heterodimerization. *Neuron* *27*, 97–106.
- Maroteaux, M., and Mameli, M. (2012). Cocaine Evokes Projection-Specific Synaptic Plasticity of Lateral Habenula Neurons. *J. Neurosci.* *32*, 12641–12646.
- Marvel, C.L., and Paradiso, S. (2004). Cognitive and neurological impairment in mood disorders. *Psychiatr. Clin.* *27*, 19–36.
- Massart, R., Mongeau, R., and Lanfumey, L. (2012). Beyond the monoaminergic hypothesis: neuroplasticity and epigenetic changes in a transgenic mouse model of depression. *Phil Trans R Soc B* *367*, 2485–2494.
- Matsumoto, M., and Hikosaka, O. (2007). Lateral habenula as a source of negative reward signals in dopamine neurons. *Nature* *447*, 1111–1115.
- Matsumoto, M., and Hikosaka, O. (2009a). Two types of dopamine neuron distinctly convey positive and negative motivational signals. *Nature* *459*, 837–841.
- Matsumoto, M., and Hikosaka, O. (2009b). Representation of negative motivational value in the primate lateral habenula. *Nat. Neurosci.* *12*, 77–84.
- Mayberg, H.S., Lozano, A.M., Voon, V., McNeely, H.E., Seminowicz, D., Hamani, C., Schwalb, J.M., and Kennedy, S.H. (2005). Deep Brain Stimulation for Treatment-Resistant Depression. *Neuron* *45*, 651–660.
- McCutcheon, J.E., Ebner, S.R., Loriaux, A.L., and Roitman, M.F. (2012). Encoding of Aversion by Dopamine and the Nucleus Accumbens. *Front. Neurosci.* *6*.
- Mcintyre, C.C., Savasta, M., Walter, B.L., and Vitek, J.L. (2004). How Does Deep Brain Stimulation Work? Present Understanding and Future Questions. *J. Clin. Neurophysiol.* *21*, 40–50.
- Meng, H., Wang, Y., Huang, M., Lin, W., Wang, S., and Zhang, B. (2011). Chronic deep brain stimulation of the lateral habenula nucleus in a rat model of depression. *Brain Res.* *1422*, 32–38.
- Metz, M., Gassmann, M., Fakler, B., Schaeren-Wiemers, N., and Bettler, B. (2011). Distribution of the auxiliary GABAB receptor subunits KCTD8, 12, 12b, and 16 in the mouse brain. *J. Comp. Neurol.* *519*, 1435–1454.



- Meye, F.J., Valentinova, K., Lecca, S., Marion-Poll, L., Maroteaux, M.J., Musardo, S., Moutkine, I., Gardoni, F., Haganir, R.L., Georges, F., et al. (2015). Cocaine-evoked negative symptoms require AMPA receptor trafficking in the lateral habenula. *Nat. Neurosci.* *18*, 376–378.
- Meye, F.J., Soiza-Reilly, M., Smit, T., Diana, M.A., Schwarz, M.K., and Mameli, M. (2016). Shifted pallidal co-release of GABA and glutamate in habenula drives cocaine withdrawal and relapse. *Nat. Neurosci.* *19*, 1019–1024.
- Middlemiss, D.N., Price, G.W., and Watson, J.M. (2002). Serotonergic targets in depression. *Curr. Opin. Pharmacol.* *2*, 18–22.
- Mirrione, M.M., Schulz, D., Lapidus, K., Zhang, S., Goodman, W., and Henn, F.A. (2014). Increased metabolic activity in the septum and habenula during stress is linked to subsequent expression of learned helplessness behavior. *Front. Hum. Neurosci.* *8*.
- Monteggia, L.M., Malenka, R.C., and Deisseroth, K. (2014). Depression: The best way forward. *Nature* *515*, 200–201.
- Moreau, J.-L. (2002). Simulating the anhedonia symptom of depression in animals. *Dialogues Clin. Neurosci.* *4*, 351–360.
- Moreines, J.L., Owrutsky, Z.L., and Grace, A.A. (2017). Involvement of Infralimbic Prefrontal Cortex but not Lateral Habenula in Dopamine Attenuation After Chronic Mild Stress. *Neuropsychopharmacology* *42*, 904–913.
- Morris, J.S., Smith, K.A., Cowen, P.J., Friston, K.J., and Dolan, R.J. (1999). Covariation of Activity in Habenula and Dorsal Raphé Nuclei Following Tryptophan Depletion. *NeuroImage* *10*, 163–172.
- Muller, J.C., Pryor, W.W., Gibbons, J.E., and Orgain, E.S. (1955). Depression and anxiety occurring during Rauwolfia therapy. *J. Am. Med. Assoc.* *159*, 836–839.
- Munoz, M.B., and Slesinger, P.A. (2014a). Sorting nexin 27 regulation of G protein-gated inwardly rectifying K<sup>+</sup> channels attenuates in vivo cocaine response. *Neuron* *82*, 659–669.
- Munoz, M.B., and Slesinger, P.A. (2014b). SNX27 regulation of GIRK channels in VTA dopamine neurons attenuates in vivo cocaine response. *Neuron* *82*, 659–669.
- Munoz, M.B., Padgett, C.L., Rifkin, R., Terunuma, M., Wickman, K., Contet, C., Moss, S.J., and Slesinger, P.A. (2016). A Role for the GIRK3 Subunit in Methamphetamine-Induced Attenuation of GABAB Receptor-Activated GIRK Currents in VTA Dopamine Neurons. *J. Neurosci.* *36*, 3106–3114.
- Naesström, M., Blomstedt, P., and Bodlund, O. (2016). A systematic review of psychiatric indications for deep brain stimulation, with focus on major depressive and obsessive-compulsive disorder. *Nord. J. Psychiatry* *70*, 483–491.
- Namboodiri, V.M.K., Rodriguez-Romaguera, J., and Stuber, G.D. (2016). The habenula. *Curr. Biol.* *26*, R873–R877.
- Narang, P., Retzlaff, A., Brar, K., and Lippmann, S. (2016). Deep Brain Stimulation for Treatment-Refractory Depression. *South. Med. J.* *109*, 700–703.
- Nemeroff, C.B., Widerlov, E., Bissette, G., Walleus, H., Karlsson, I., Eklund, K., Kilts, C.D., Loosen, P.T., and Vale, W. (1984). Elevated concentrations of CSF corticotropin-releasing factor-like immunoreactivity in depressed patients. *Science* *226*, 1342–1344.
- Nestler, E.J., and Carlezon Jr, W.A. (2006). The Mesolimbic Dopamine Reward Circuit in Depression. *Biol. Psychiatry* *59*, 1151–1159.
- Nestler, E.J., and Hyman, S.E. (2010). Animal models of neuropsychiatric disorders. *Nat. Neurosci.* *13*, 1161–1169.
- Nestler, E.J., Barrot, M., DiLeone, R.J., Eisch, A.J., Gold, S.J., and Monteggia, L.M. (2002). Neurobiology of Depression. *Neuron* *34*, 13–25.

- Norman, R.E., Byambaa, M., De, R., Butchart, A., Scott, J., and Vos, T. (2012). The Long-Term Health Consequences of Child Physical Abuse, Emotional Abuse, and Neglect: A Systematic Review and Meta-Analysis. *PLoS Med.* *9*.
- Ogawa, S.K., Cohen, J.Y., Hwang, D., Uchida, N., and Watabe-Uchida, M. (2014). Organization of Monosynaptic Inputs to the Serotonin and Dopamine Neuromodulatory Systems. *Cell Rep.* *8*, 1105–1118.
- O’Leary, O.F., and Cryan, J.F. (2013). Towards translational rodent models of depression. *Cell Tissue Res.* *354*, 141–153.
- O’Leary, O.F., O’Brien, F.E., O’Connor, R.M., and Cryan, J.F. (2014). Drugs, genes and the blues: Pharmacogenetics of the antidepressant response from mouse to man. *Pharmacol. Biochem. Behav.* *123*, 55–76.
- O’Leary, O.F., Dinan, T.G., and Cryan, J.F. (2015). Faster, better, stronger: Towards new antidepressant therapeutic strategies. *Eur. J. Pharmacol.* *753*, 32–50.
- Omelchenko, N., Bell, R., and Sesack, S.R. (2009). Lateral habenula projections to dopamine and GABA neurons in the rat ventral tegmental area. *Eur. J. Neurosci.* *30*, 1239–1250.
- Owens, M.J., and Nemeroff, C.B. (1994). Role of serotonin in the pathophysiology of depression: focus on the serotonin transporter. *Clin. Chem.* *40*, 288–295.
- P, S., B, J., J, A., and C, R. (2006). Cost of depression in Europe. *J. Ment. Health Policy Econ.* *9*, 87–98.
- Padgett, C.L., and Slesinger, P.A. (2010). GABAB Receptor Coupling to G-proteins and Ion Channels. *Adv. Pharmacol.* *58*, 123–147.
- Padgett, C.L., Lalive, A.L., Tan, K.R., Terunuma, M., Munoz, M.B., Pangalos, M.N., Martínez-Hernández, J., Watanabe, M., Moss, S.J., Luján, R., et al. (2012). Methamphetamine-evoked depression of GABA(B) receptor signaling in GABA neurons of the VTA. *Neuron* *73*, 978–989.
- Pagano, A., Rovelli, G., Mosbacher, J., Lohmann, T., Duthey, B., Stauffer, D., Ristig, D., Schuler, V., Meigel, I., Lampert, C., et al. (2001). C-Terminal Interaction Is Essential for Surface Trafficking But Not for Heteromeric Assembly of GABAB Receptors. *J. Neurosci.* *21*, 1189–1202.
- Paykel, E.S. (2003). Life events and affective disorders. *Acta Psychiatr. Scand. Suppl.* 61–66.
- Pérez-Garci, E., Gassmann, M., Bettler, B., and Larkum, M.E. (2006). The GABAB1b Isoform Mediates Long-Lasting Inhibition of Dendritic Ca<sup>2+</sup> Spikes in Layer 5 Somatosensory Pyramidal Neurons. *Neuron* *50*, 603–616.
- Pfau, M.L., and Russo, S.J. (2014). Peripheral and central mechanisms of stress resilience. *Neurobiol. Stress* *1*, 66–79.
- Pinard, A., Seddik, R., and Bettler, B. (2010). GABAB Receptors: Physiological Functions and Mechanisms of Diversity. *Adv. Pharmacol.* *58*, 231–255.
- Pizzagalli, D.A. (2014). Depression, Stress, and Anhedonia: Toward a Synthesis and Integrated Model. *Annu. Rev. Clin. Psychol.* *10*, 393–423.
- Pollak Dorocic, I., Fürth, D., Xuan, Y., Johansson, Y., Pozzi, L., Silberberg, G., Carlén, M., and Meletis, K. (2014). A Whole-Brain Atlas of Inputs to Serotonergic Neurons of the Dorsal and Median Raphe Nuclei. *Neuron* *83*, 663–678.
- Pontier, S.M., Lahaie, N., Gingham, R., St-Gelais, F., Bonin, H., Bell, D.J., Flynn, H., Trudeau, L.-E., McIlhinney, J., White, J.H., et al. (2006). Coordinated action of NSF and PKC regulates GABAB receptor signaling efficacy. *EMBO J.* *25*, 2698–2709.
- Pooler, A.M., Gray, A.G., and McIlhinney, R. a. J. (2009). Identification of a novel region of the GABA(B)2 C-terminus that regulates surface expression and neuronal targeting of the GABA(B) receptor. *Eur. J. Neurosci.* *29*, 869–878.

- Porsolt, R.D., Le Pichon, M., and Jalfre, M. (1977). Depression: a new animal model sensitive to antidepressant treatments. *Nature* 266, 730–732.
- Proulx, C.D., Hikosaka, O., and Malinow, R. (2014). Reward processing by the lateral habenula in normal and depressive behaviors. *Nat. Neurosci.* 17, 1146–1152.
- Puglisi-Allegra, S., and Andolina, D. (2015). Serotonin and stress coping. *Behav. Brain Res.* 277, 58–67.
- Quina, L.A., Tempest, L., Ng, L., Harris, J.A., Ferguson, S., Jhou, T.C., and Turner, E.E. (2015). Efferent pathways of the mouse lateral habenula. *J. Comp. Neurol.* 523, 32–60.
- Ramirez, S., Liu, X., MacDonald, C.J., Moffa, A., Zhou, J., Redondo, R.L., and Tonegawa, S. (2015). Activating positive memory engrams suppresses depression-like behaviour. *Nature* 522, 335–339.
- Ranft, K., Dobrowolny, H., Krell, D., Bielau, H., Bogerts, B., and Bernstein, H.-G. (2010). Evidence for structural abnormalities of the human habenular complex in affective disorders but not in schizophrenia. *Psychol. Med.* 40, 557–567.
- Restituto, S., Couve, A., Bawagan, H., Jourdain, S., Pangalos, M.N., Calver, A.R., Freeman, K.B., and Moss, S.J. (2005). Multiple motifs regulate the trafficking of GABAB receptors at distinct checkpoints within the secretory pathway. *Mol. Cell. Neurosci.* 28, 747–756.
- Riven, I., Iwanir, S., and Reuveny, E. (2006). GIRK channel activation involves a local rearrangement of a preformed G protein channel complex. *Neuron* 51, 561–573.
- Robbins, M.J., Calver, A.R., Filippov, A.K., Hirst, W.D., Russell, R.B., Wood, M.D., Nasir, S., Couve, A., Brown, D.A., Moss, S.J., et al. (2001). GABA(B2) is essential for g-protein coupling of the GABA(B) receptor heterodimer. *J. Neurosci. Off. J. Soc. Neurosci.* 21, 8043–8052.
- Root, D.H., Mejias-Aponte, C.A., Qi, J., and Morales, M. (2014a). Role of Glutamatergic Projections from Ventral Tegmental Area to Lateral Habenula in Aversive Conditioning. *J. Neurosci.* 34, 13906–13910.
- Root, D.H., Mejias-Aponte, C.A., Zhang, S., Wang, H.-L., Hoffman, A.F., Lupica, C.R., and Morales, M. (2014b). Single rodent mesohabenular axons release glutamate and GABA. *Nat. Neurosci.* 17, 1543–1551.
- Russo, S.J., and Nestler, E.J. (2013). The brain reward circuitry in mood disorders. *Nat. Rev. Neurosci.* 14, 609–625.
- Salling, M.C., and Martinez, D. (2016). Brain Stimulation in Addiction. *Neuropsychopharmacology* 41, 2798–2809.
- Sartorius, A., Kiening, K.L., Kirsch, P., von Gall, C.C., Haberkorn, U., Unterberg, A.W., Henn, F.A., and Meyer-Lindenberg, A. (2010). Remission of Major Depression Under Deep Brain Stimulation of the Lateral Habenula in a Therapy-Refractory Patient. *Biol. Psychiatry* 67, e9–e11.
- Sauter, K., Grampp, T., Fritschy, J.-M., Kaupmann, K., Bettler, B., Mohler, H., and Benke, D. (2005). Subtype-selective Interaction with the Transcription Factor CCAAT/Enhancer-binding Protein (C/EBP) Homologous Protein (CHOP) Regulates Cell Surface Expression of GABAB Receptors. *J. Biol. Chem.* 280, 33566–33572.
- Scanziani, M. (2000). GABA Spillover Activates Postsynaptic GABAB Receptors to Control Rhythmic Hippocampal Activity. *Neuron* 25, 673–681.
- Schildkraut, J.J. (1965). The catecholamine hypothesis of affective disorders: a review of supporting evidence. *Am. J. Psychiatry* 122, 509–522.
- Schlaepfer, T.E., Cohen, M.X., Frick, C., Kosel, M., Brodesser, D., Axmacher, N., Joe, A.Y., Kreft, M., Lenartz, D., and Sturm, V. (2007). Deep Brain Stimulation to Reward Circuitry Alleviates Anhedonia in Refractory Major Depression. *Neuropsychopharmacology* 33, 368–377.
- Schmidt, F.M., Schindler, S., Adamidis, M., Strauß, M., Tränkner, A., Trampel, R., Walter, M., Hegerl, U., Turner, R., Geyer, S., et al. (2017). Habenula volume increases with disease severity in unmedicated major depressive disorder as revealed by 7T MRI. *Eur. Arch. Psychiatry Clin. Neurosci.* 267, 107–115.

- Schultz, W. (2007). Behavioral dopamine signals. *Trends Neurosci.* *30*, 203–210.
- Schultz, W., Dayan, P., and Montague, P.R. (1997). A Neural Substrate of Prediction and Reward. *Science* *275*, 1593–1599.
- Schweimer, J.V., and Ungless, M.A. (2010). Phasic responses in dorsal raphe serotonin neurons to noxious stimuli. *Neuroscience* *171*, 1209–1215.
- Schwenk, J., Metz, M., Zolles, G., Turecek, R., Fritzius, T., Bildl, W., Tarusawa, E., Kulik, A., Unger, A., Ivankova, K., et al. (2010). Native GABA(B) receptors are heteromultimers with a family of auxiliary subunits. *Nature* *465*, 231–235.
- Sego, C., Gonçalves, L., Lima, L., Furigo, I.C., Donato, J., and Metzger, M. (2014). Lateral habenula and the rostromedial tegmental nucleus innervate neurochemically distinct subdivisions of the dorsal raphe nucleus in the rat. *J. Comp. Neurol.* *522*, 1454–1484.
- Seo, J.-S., Zhong, P., Liu, A., Yan, Z., and Greengard, P. (2017). Elevation of p11 in lateral habenula mediates depression-like behavior. *Mol. Psychiatry*.
- Seshacharyulu, P., Pandey, P., Datta, K., and Batra, S.K. (2013). Phosphatase: PP2A structural importance, regulation and its aberrant expression in cancer. *Cancer Lett.* *335*, 9–18.
- Shaban, H., Humeau, Y., Herry, C., Cassasus, G., Shigemoto, R., Ciocchi, S., Barbieri, S., van der Putten, H., Kaupmann, K., Bettler, B., et al. (2006). Generalization of amygdala LTP and conditioned fear in the absence of presynaptic inhibition. *Nat. Neurosci.* *9*, 1028–1035.
- Shabel, S.J., Proulx, C.D., Trias, A., Murphy, R.T., and Malinow, R. (2012). Input to the Lateral Habenula from the Basal Ganglia Is Excitatory, Aversive, and Suppressed by Serotonin. *Neuron* *74*, 475–481.
- Shabel, S.J., Proulx, C.D., Piriz, J., and Malinow, R. (2014). GABA/glutamate co-release controls habenula output and is modified by antidepressant treatment. *Science* *345*, 1494–1498.
- Sharp, T., and Cowen, P.J. (2011). 5-HT and depression: is the glass half-full? *Curr. Opin. Pharmacol.* *11*, 45–51.
- Sherman, A.D., Sacquitne, J.L., and Petty, F. (1982). Specificity of the learned helplessness model of depression. *Pharmacol. Biochem. Behav.* *16*, 449–454.
- Shin, G., Gomez, A.M., Al-Hasani, R., Jeong, Y.R., Kim, J., Xie, Z., Banks, A., Lee, S.M., Han, S.Y., Yoo, C.J., et al. (2017). Flexible Near-Field Wireless Optoelectronics as Subdermal Implants for Broad Applications in Optogenetics. *Neuron* *93*, 509–521.e3.
- Short, K.R., and Maier, S.F. (1993). Stressor controllability, social interaction, and benzodiazepine systems. *Pharmacol. Biochem. Behav.* *45*, 827–835.
- Shumake, J., Edwards, E., and Gonzalez-Lima, F. (2003). Opposite metabolic changes in the habenula and ventral tegmental area of a genetic model of helpless behavior. *Brain Res.* *963*, 274–281.
- Sibille, E., Wang, Y., Joeyen-Waldorf, J., Gaiteri, C., Surget, A., Oh, S., Belzung, C., Tseng, G.C., and Lewis, D.A. (2009). A Molecular Signature of Depression in the Amygdala. *Am. J. Psychiatry* *166*, 1011–1024.
- Sienaert, P. (2011). What We Have Learned about Electroconvulsive Therapy and its Relevance for the Practising Psychiatrist. *Can. J. Psychiatry* *56*, 5–12.
- Sjögren, B. (2011). Regulator of G protein signaling proteins as drug targets: current state and future possibilities. *Adv. Pharmacol. San Diego Calif* *62*, 315–347.
- Slavich, G.M., O'Donovan, A., Epel, E.S., and Kemeny, M.E. (2010). Black sheep get the blues: A psychobiological model of social rejection and depression. *Neurosci. Biobehav. Rev.* *35*, 39–45.
- Smith, Y., Séguéla, P., and Parent, A. (1987). Distribution of gaba-immunoreactive neurons in the thalamus of the squirrel monkey (*Saimiri sciureus*). *Neuroscience* *22*, 579–591.

- Song, L., Che, W., Min-wei, W., Murakami, Y., and Matsumoto, K. (2006). Impairment of the spatial learning and memory induced by learned helplessness and chronic mild stress. *Pharmacol. Biochem. Behav.* *83*, 186–193.
- Stamatakis, A.M., and Stuber, G.D. (2012). Activation of lateral habenula inputs to the ventral midbrain promotes behavioral avoidance. *Nat. Neurosci.* *15*, 1105–1107.
- Stamatakis, A.M., Van Swieten, M., Basiri, M.L., Blair, G.A., Kantak, P., and Stuber, G.D. (2016). Lateral Hypothalamic Area Glutamatergic Neurons and Their Projections to the Lateral Habenula Regulate Feeding and Reward. *J. Neurosci. Off. J. Soc. Neurosci.* *36*, 302–311.
- Stephenson-Jones, M., Yu, K., Ahrens, S., Tucciarone, J.M., Huijstee, A.N. van, Mejia, L.A., Penzo, M.A., Tai, L.-H., Wilbrecht, L., and Li, B. (2016). A basal ganglia circuit for evaluating action outcomes. *Nature* *539*, 289–293.
- Steru, L., Chermat, R., Thierry, B., and Simon, P. (1985). The tail suspension test: A new method for screening antidepressants in mice. *Psychopharmacology (Berl.)* *85*, 367–370.
- Strekalova, T., Spanagel, R., Bartsch, D., Henn, F.A., and Gass, P. (2004). Stress-Induced Anhedonia in Mice is Associated with Deficits in Forced Swimming and Exploration. *Neuropsychopharmacology* *29*, 2007–2017.
- Sullivan, P.F., Neale, M.C., and Kendler, K.S. (2000). Genetic Epidemiology of Major Depression: Review and Meta-Analysis. *Am. J. Psychiatry* *157*, 1552–1562.
- Temkin, P., Lauffer, B., Jager, S., Cimermancic, P., Krogan, N.J., and von Zastrow, M. (2011). SNX27 mediates retromer tubule entry and endosome-to-plasma membrane trafficking of signaling receptors. *Nat. Cell Biol.* *13*, 715–721.
- Terunuma, M., Vargas, K.J., Wilkins, M.E., Ramírez, O.A., Jaureguiberry-Bravo, M., Pangalos, M.N., Smart, T.G., Moss, S.J., and Couve, A. (2010a). Prolonged activation of NMDA receptors promotes dephosphorylation and alters postendocytic sorting of GABAB receptors. *Proc. Natl. Acad. Sci.* *107*, 13918–13923.
- Terunuma, M., Pangalos, M.N., and Moss, S.J. (2010b). Functional Modulation of GABAB Receptors by Protein Kinases and Receptor Trafficking. *Adv. Pharmacol.* *58*, 113–122.
- Tractenberg, S.G., Levandowski, M.L., de Azeredo, L.A., Orso, R., Roithmann, L.G., Hoffmann, E.S., Brenhouse, H., and Grassi-Oliveira, R. (2016). An overview of maternal separation effects on behavioural outcomes in mice: Evidence from a four-stage methodological systematic review. *Neurosci. Biobehav. Rev.* *68*, 489–503.
- Trezza, V., Campolongo, P., and Vanderschuren, L.J.M.J. (2011). Evaluating the rewarding nature of social interactions in laboratory animals. *Dev. Cogn. Neurosci.* *1*, 444–458.
- Trivedi, M.H., Rush, A.J., Wisniewski, S.R., Nierenberg, A.A., Warden, D., Ritz, L., Norquist, G., Howland, R.H., Lebowitz, B., McGrath, P.J., et al. (2006). Evaluation of Outcomes With Citalopram for Depression Using Measurement-Based Care in STAR\*D: Implications for Clinical Practice. *Am. J. Psychiatry* *163*, 28–40.
- Tye, K.M., Mirzabekov, J.J., Warden, M.R., Ferenczi, E.A., Tsai, H.-C., Finkelstein, J., Kim, S.-Y., Adhikari, A., Thompson, K.R., Andalman, A.S., et al. (2013). Dopamine neurons modulate neural encoding and expression of depression-related behaviour. *Nature* *493*, 537–541.
- Ulrich, D., Besseyrias, V., and Bettler, B. (2007). Functional Mapping of GABAB-Receptor Subtypes in the Thalamus. *J. Neurophysiol.* *98*, 3791–3795.
- Ungless, M.A., Magill, P.J., and Bolam, J.P. (2004). Uniform Inhibition of Dopamine Neurons in the Ventral Tegmental Area by Aversive Stimuli. *Science* *303*, 2040–2042.
- Ungless, M.A., Argilli, E., and Bonci, A. (2010). Effects of stress and aversion on dopamine neurons: Implications for addiction. *Neurosci. Biobehav. Rev.* *35*, 151–156.
- Varga, V., Kocsis, B., and Sharp, T. (2003). Electrophysiological evidence for convergence of inputs from the medial prefrontal cortex and lateral habenula on single neurons in the dorsal raphe nucleus. *Eur. J. Neurosci.* *17*, 280–286.

- Vargas, K.J., Terunuma, M., Tello, J.A., Pangalos, M.N., Moss, S.J., and Couve, A. (2008). The Availability of Surface GABAB Receptors Is Independent of  $\gamma$ -Aminobutyric Acid but Controlled by Glutamate in Central Neurons. *J. Biol. Chem.* *283*, 24641–24648.
- Venzala, E., García-García, A.L., Elizalde, N., and Tordera, R.M. (2013). Social vs. environmental stress models of depression from a behavioural and neurochemical approach. *Eur. Neuropsychopharmacol.* *23*, 697–708.
- Vetulani, J. (2013). Early maternal separation: a rodent model of depression and a prevailing human condition. *Pharmacol. Rep.* *PR 65*, 1451–1461.
- Vigot, R., Barbieri, S., Bräuner-Osborne, H., Turecek, R., Shigemoto, R., Zhang, Y.-P., Luján, R., Jacobson, L.H., Biermann, B., Fritschy, J.-M., et al. (2006). Differential Compartmentalization and Distinct Functions of GABAB Receptor Variants. *Neuron* *50*, 589–601.
- Vitek, J.L. (2002). Mechanisms of deep brain stimulation: excitation or inhibition. *Mov. Disord. Off. J. Mov. Disord. Soc.* *17 Suppl 3*, S69-72.
- Vollmayr, B., and Henn, F.A. (2001). Learned helplessness in the rat: improvements in validity and reliability. *Brain Res. Protoc.* *8*, 1–7.
- Vollmayr, B., Bachteler, D., Vengeliene, V., Gass, P., Spanagel, R., and Henn, F. (2004). Rats with congenital learned helplessness respond less to sucrose but show no deficits in activity or learning. *Behav. Brain Res.* *150*, 217–221.
- Von Frijtag, J.C., Reijmers, L.G.J.E., Van der Harst, J.E., Leus, I.E., Van den Bos, R., and Spruijt, B.M. (2000). Defeat followed by individual housing results in long-term impaired reward- and cognition-related behaviours in rats. *Behav. Brain Res.* *117*, 137–146.
- Wang, R.Y., and Aghajanian, G.K. (1977). Physiological evidence for habenula as major link between forebrain and midbrain raphe. *Science* *197*, 89–91.
- Wang, H.-Y., Kuo, Z.-C., Fu, Y.-S., Chen, R.-F., Min, M.-Y., and Yang, H.-W. (2015). GABAB receptor-mediated tonic inhibition regulates the spontaneous firing of locus coeruleus neurons in developing rats and in citalopram-treated rats. *J. Physiol.* *593*, 161–180.
- Wang, L., LaBar, K.S., Smoski, M., Rosenthal, M.Z., Dolcos, F., Lynch, T.R., Krishnan, R.R., and McCarthy, G. (2008). Prefrontal mechanisms for executive control over emotional distraction are altered in major depression. *Psychiatry Res.* *163*, 143–155.
- Warden, M.R., Selimbeyoglu, A., Mirzabekov, J.J., Lo, M., Thompson, K.R., Kim, S.-Y., Adhikari, A., Tye, K.M., Frank, L.M., and Deisseroth, K. (2012). A prefrontal cortex-brainstem neuronal projection that controls response to behavioural challenge. *Nature* *492*, 428–432.
- Weiss, J.M. (1968). Effects of coping responses on stress. *J. Comp. Physiol. Psychol.* *65*, 251.
- Weiss, T., and Veh, R.W. (2011). Morphological and electrophysiological characteristics of neurons within identified subnuclei of the lateral habenula in rat brain slices. *Neuroscience* *172*, 74–93.
- Weissbourd, B., Ren, J., DeLoach, K.E., Guenther, C.J., Miyamichi, K., and Luo, L. (2014). Presynaptic Partners of Dorsal Raphe Serotonergic and GABAergic Neurons. *Neuron* *83*, 645–662.
- White, J.H., Wise, A., Main, M.J., Green, A., Fraser, N.J., Disney, G.H., Barnes, A.A., Emson, P., Foord, S.M., and Marshall, F.H. (1998). Heterodimerization is required for the formation of a functional GABA(B) receptor. *Nature* *396*, 679–682.
- Wilkins, M.E., Li, X., and Smart, T.G. (2008). Tracking Cell Surface GABAB Receptors Using an  $\alpha$ -Bungarotoxin Tag. *J. Biol. Chem.* *283*, 34745–34752.
- Willner, P. (1984). The validity of animal models of depression. *Psychopharmacology (Berl.)* *83*, 1–16.
- Willner, P. (2017). The chronic mild stress (CMS) model of depression: History, evaluation and usage. *Neurobiol. Stress* *6*, 78–93.

- Willner, P., Towell, A., Sampson, D., Sophokleous, S., and Muscat, R. (1987). Reduction of sucrose preference by chronic unpredictable mild stress, and its restoration by a tricyclic antidepressant. *Psychopharmacology (Berl.)* 93, 358–364.
- Wiltchko, A.B., Johnson, M.J., Iurilli, G., Peterson, R.E., Katon, J.M., Pashkovski, S.L., Abaira, V.E., Adams, R.P., and Datta, S.R. (2015). Mapping Sub-Second Structure in Mouse Behavior. *Neuron* 88, 1121–1135.
- Wise, R.A. (2004). Dopamine, learning and motivation. *Nat. Rev. Neurosci.* 5, 483–494.
- Xu, C., Zhang, W., Rondard, P., Pin, J.-P., and Liu, J. (2014). Complex GABAB receptor complexes: how to generate multiple functionally distinct units from a single receptor. *Front. Pharmacol.* 5.
- Yang, H., Yang, J., Xi, W., Hao, S., Luo, B., He, X., Zhu, L., Lou, H., Yu, Y., Xu, F., et al. (2016). Laterodorsal tegmentum interneuron subtypes oppositely regulate olfactory cue-induced innate fear. *Nat. Neurosci.* 19, 283–289.
- Yang, L.-M., Hu, B., Xia, Y.-H., Zhang, B.-L., and Zhao, H. (2008). Lateral habenula lesions improve the behavioral response in depressed rats via increasing the serotonin level in dorsal raphe nucleus. *Behav. Brain Res.* 188, 84–90.
- Zacharko, R.M., Bowers, W.J., Kokkinidis, L., and Anisman, H. (1983). Region-specific reductions of intracranial self-stimulation after uncontrollable stress: Possible effects on reward processes. *Behav. Brain Res.* 9, 129–141.
- Zhang, J., Tan, L., Ren, Y., Liang, J., Lin, R., Feng, Q., Zhou, J., Hu, F., Ren, J., Wei, C., et al. (2016a). Presynaptic Excitation via GABAB Receptors in Habenula Cholinergic Neurons Regulates Fear Memory Expression. *Cell* 166, 716–728.
- Zhang, L., Hernández, V.S., Vázquez-Juárez, E., Chay, F.K., and Barrio, R.A. (2016b). Thirst Is Associated with Suppression of Habenula Output and Active Stress Coping: Is there a Role for a Non-canonical Vasopressin-Glutamate Pathway? *Front. Neural Circuits* 10.